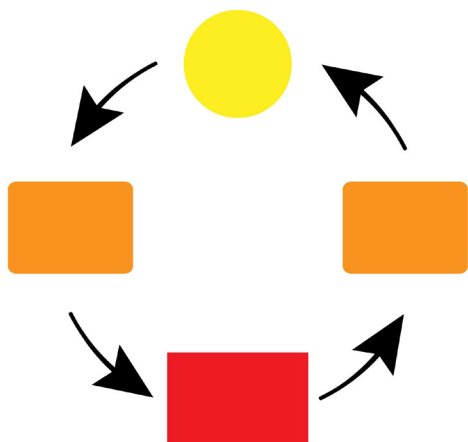
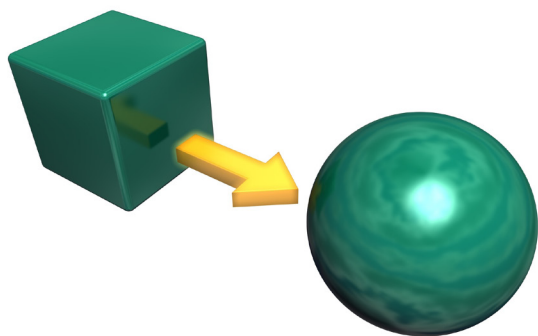


# Shape Memory Polymers: Fundamentals, Advances and Applications

Jinlian Hu



# Shape Memory Polymers: Fundamentals, Advances and Applications

Jinlian Hu



A Smithers Group Company

Shawbury, Shrewsbury, Shropshire, SY4 4NR, United Kingdom  
Telephone: +44 (0)1939 250383 Fax: +44 (0)1939 251118  
<http://www.polymer-books.com>



First Published in 2014 by

**Smithers Rapra Technology Ltd**

Shawbury, Shrewsbury, Shropshire, SY4 4NR, UK

©Smithers Information Ltd., 2014

All rights reserved. Except as permitted under current legislation no part of this publication may be photocopied, reproduced or distributed in any form or by any means or stored in a database or retrieval system, without the prior permission from the copyright holder.

A catalogue record for this book is available from the British Library.

Every effort has been made to contact copyright holders of any material reproduced within the text and the author and publishers apologise if any have been overlooked.

ISBN: 978-1-90903-032-9 (hardback)

978-1-90903-050-3 (softback)

978-1-90903-033-6 (ebook)

Typeset by Argil Services

# Acknowledgments

I would like to express my sincere appreciation to the people who have helped to prepare the chapters in this book. In particular, my gratitude goes to Dr Bipin Kumar, whose careful and pertinent assistance were instrumental in accomplishing this work. Moreover, I would like to thank Mr Wang Yifu, Ms Gao Chang and Mr Chen Jianming for their co-operation in the editing of this book, specifically:

- Dr Bipin Kumar helped with the editing of **Chapters 1, 3, 5, 6, 7, 8 and 9.**
- Ms Gao Chang and Mr Wang Yifu edited the final versions of **Chapters 2 and 4.**
- Mr Chen Jianming helped to format the chapters, figures, tables and all copyright permissions.

I am deeply indebted to my research students, postdoctoral fellows and research assistants. They have undertaken a considerable amount of research over the past decade that has contributed a major part of this book. I would like to acknowledge the doctoral work of Hongsheng Luo, Qinghao Meng and Shaojun Chen. Some reviews published with my team members (especially Doctors Qinghao Meng, Zhu Yong, Huang Huahua, Lu Jing and Mr Wu You) have supplemented the latest knowledge in shape-memory polymers.

I wish to acknowledge the generous support of the textile and apparel industry in Hong Kong as well as the Governments of Mainland China and Hong Kong for funding support. In particular, I acknowledge grants from the Shenzhen Large Scale Incubating Project (grant number JC201104210132A), Chinese Mainland National 12-Plan Scheme Project (2012BAI17B00), University Grant Council (PolyU 5161/11E and PolyU 5182/09E) and the Innovation and Technology Commission (ITP/012/12TP, ITP/046/09TP, ITP/010/07TP, GHS/088/04 and ITS/098/02) over the past many years.

I would like to acknowledge all the people who have offered help and support (directly or indirectly) in the completion of this book.

*Shape Memory Polymers: Fundamentals, Advances and Applications*

In addition, I would like to thank Smithers Rapra for giving me the opportunity to publish this book.

**Jinlian Hu**

2014

# Preface

Shape-memory polymers (SMP) have undergone rapid growth over the previous decade. They have received considerable attention from researchers, scientists and engineers worldwide. SMP have made a significant breakthrough in the development of novel smart materials for various engineering applications and have influenced methods of product design. SMP have become leading members of the fantastic world of shape-memory materials.

SMP are a unique branch of the smart-materials family that can change shape upon exposure to an external stimulus. SMP have the common advantages of polymers: high elastic deformation, low cost, low density, as well as potential biocompatibility and biodegradability. Furthermore, they are easy to process, having tuneable stiffness and application temperatures in broad ranges. Because of these advantages, SMP have great potential in various application areas such as smart products, transportation, biomedical devices and electronics.

This book provides a systematic review on SMP. It covers several research dimensions of SMP, from their novel molecular architectures and structure–property relationships to their broad application domains and associated challenges. This information provides a foundation for understanding the various aspects of SMP. Such information will enlighten readers to the achievements and numerous possibilities for the further growth of SMP.

There have been significant developments in shape-memory technology in recent years. It is beyond the scope of this book to cover all aspects of the chemistry and technology of SMP in different fields. Instead, several topics have been chosen to enlighten readers of the ongoing research fields of SMP over the past decade. This book also provides thorough understanding of the basic concepts and principles of using SMP in terms of their structure, synthesis, and underlying shape-memory mechanisms. I hope that, after reading this book, readers will be more familiar with several new research areas of SMP, and that the book will guide them to undertake their own research.

**Chapter 1** introduces shape-memory effects (SME), the mechanisms of SME, as well as the structural characterisation and classification of SMP. This will help readers

to become familiar with the basic concepts, which will help them to understand the subsequent chapters of this book. **Chapter 2** presents an overview of the development of SMP in shape-memory switches, shape-memory functionalities and shape-memory programming. **Chapter 3** focuses on SMP composites, their properties and recent achievements in this field. **Chapter 4** is about SMP blends, their importance, and potential in SMP applications. **Chapter 5** details several breakthroughs that have been made in developing SMP with novel stimulus-active mechanisms, and explains their shape-memory mechanisms and fabrication strategies. **Chapter 6** explains the theoretical modelling of SMP to understand new polymer systems, functionalities, applications, and various SME mechanisms. **Chapter 7** exposes readers to supramolecular SMP (a new research direction of shape-memory materials). It reveals useful information regarding supramolecular chemistry, characterization of supramolecular SMP, their structure–property relationships, and potential applications. **Chapter 8** unveils the enormous applications of SMP in industrial, biological, textile, consumer, transport, actuation, and filtration areas. **Chapter 9** discloses the future research directions for SMP.

This book is best suited to any academic, R&D manager, researcher, scientist or engineer interested in SMP research. Such individuals could exploit current knowledge to overcome application problems by finding more innovative solutions. Some topics in this book could be used for teaching undergraduate and postgraduate students. Some advanced topics could be studied by doctoral students and experienced researchers. I hope that this book will prove to be very useful and informative to readers. I welcome comments and suggestions from readers that will help me in drafting the second edition of this book.

**Jinlian Hu**

2013

# C

## ontents

1	Shape-memory Polymers .....	1
1.1	Introduction.....	1
1.2	Shape-memory Effect .....	4
1.2.1	Shape-memory Effect in Shape-memory Polymers.....	5
1.2.2	Shape-memory Effect in Shape-memory Polymers and Shape-memory Alloys .....	7
1.3	Structure of Shape-memory Polymers.....	9
1.3.1	Thermally Induced Shape-memory Polymers.....	10
1.3.2	Athermal Shape-memory Polymers .....	13
1.4	Classification of Shape-memory Polymers .....	15
1.5	Conclusions .....	17
2	Shape-memory Polymers: Molecular Design, Shape-memory Functionality and Programming.....	23
2.1	Introduction.....	23
2.2	Molecular Design of Shape-memory Polymers .....	23
2.2.1	Thermally Sensitive Shape-memory Polymers.....	24
2.2.1.1	Shape-memory Polymers based on the Amorphous Phase .....	24
2.2.1.2	Shape-memory Polymers based on Semi-crystalline Phase .....	25
2.2.1.3	Shape-memory Polymers based on Liquid Crystalline Phase.....	26
2.2.2	Photosensitive Shape-memory Polymers.....	26
2.2.3	Other Molecular Architectures of Shape-memory Polymers .....	28

2.3	Shape-memory Programming.....	30
2.3.1	Processing One-way Shape-memory Effects .....	30
2.3.1.1	Dual-shape Creation Process for One-way Dual-shape Shape-memory Effects .....	31
2.3.1.2	Programming for One-way Triple-shape Shape-memory Effects.....	33
2.3.2	Processing Two-way Shape-memory Effects .....	34
2.3.2.1	Programming for Two-way Dual-shape Shape-memory Effects.....	35
2.3.2.2	Programming for Two-way Triple-shape Shape-memory Effects.....	35
2.3.3	Multiple Shape-memory Effects Programming .....	38
2.4	Shape-memory Functionality.....	38
2.4.1	One-way Shape-memory Effects.....	38
2.4.2	Two-way Shape-memory Effects .....	40
2.4.2.1	Liquid Crystalline Elastomers .....	41
2.4.2.2	Shape-memory Polymers having a Semi-crystalline Phase under Constant Stress .....	42
2.4.2.3	Shape-memory Polymer Laminated Composites .....	43
2.4.3	Triple/Multiple Shape-memory Effects .....	44
2.4.4	Temperature-memory Effects .....	48
2.5	Conclusions .....	48
3	Shape-memory Polymer Composites .....	57
3.1	Introduction.....	57
3.2	Nanowhisker/Shape-memory Polymer Composites .....	61
3.2.1	Cellulose Nanowhiskers.....	61
3.2.2	Integration of Cellulose Nanowhiskers .....	62
3.3	Carbon/Shape-memory Polymer Composites .....	65
3.3.1	Carbon Nanotube and Carbon Nanofibre/Shape-memory Polymer Composites .....	66

3.3.2	Carbon Black/Shape-memory Polymer Composites.....	67
3.3.3	Electrically Sensitive Shape-memory Polymer Nanocomposites .....	68
3.3.4	Light-sensitive Shape-memory Polymer Nanocomposites .	70
3.3.5	Enhanced General Shape-memory Effect.....	71
3.4	Fibre/Fabric-reinforced Shape-memory Polymer Composites .....	71
3.4.1	Microfibre or Fabric/Shape-memory Polymer Composites	71
3.4.2	Electrospun Nanofibre Shape-memory Polymer Nanocomposites .....	74
3.5	Metal and Metal Oxides/Shape-memory Polymer Composites .....	75
3.6	Other Shape-memory Polymer Composites .....	76
3.6.1	Nanoclay/Shape-memory Polymer Composites .....	76
3.6.2	Other Inorganic Filler/Shape-memory Polymer Composites .....	78
3.6.3	Organic Filler/Shape-memory Polymer Composites.....	78
3.6.4	Shape-memory Polymer Composites with Special Functions .....	79
3.7	Conclusions .....	81
4	Shape-memory Polymer Blends .....	89
4.1	Introduction.....	89
4.2	Miscible Polymer Blends .....	90
4.2.1	Shape-memory Polymer/Polymer Blends .....	90
4.2.2	Amorphous Polymer/Crystalline Polymer Blends .....	95
4.3	Immiscible Polymer Blends.....	97
4.3.1	Elastomer/Polymer Blends.....	97
4.3.2	Other Types of Immiscible Blends .....	100
4.4	Blending and Post-crosslinking Polymers Networks.....	106
4.4.1	Interpenetrating Polymer Networks .....	106
4.4.2	Crosslinked Polymer Blends.....	108
4.5	Conclusions .....	112



5	Shape-memory Polymers Sensitive to Different Stimuli.....	117
5.1	Introduction.....	117
5.2	Thermally sensitive Shape-memory Polymers.....	117
5.2.1	Shape-memory Effect based on Conventional Glass or Melting Transition .....	118
5.2.2	Shape-memory Effect by Indirect Heating.....	120
5.2.3	Shape-memory Effect based on a Thermally Reversible Reaction .....	122
5.2.4	Shape-memory Effect based on Supramolecular Structure .....	123
5.2.5	Two-way Shape-memory Effect based on Change in the Conformation of Anisotropic Chains .....	125
5.2.6	Two-way Shape-memory Effect based on Cooling-induced Crystallisation Elongation .....	126
5.2.7	Two-way Shape-memory Effect based on Shape-memory Polymer/Carbon Nanotube Composites .....	127
5.2.8	Multiple Shape-memory Effect based on Combined Switches.....	128
5.2.9	Thermally active and pH-active Polymeric Hydrogels....	131
5.3	Light-sensitive Shape-memory Polymers.....	132
5.3.1	Photodeformability Induced by Photoisomerisation.....	132
5.3.2	Photodeformability induced by Photoreactive Molecules	134
5.3.3	Photoactive Effect from the Addition–fragmentation Chain Transfer Reaction .....	134
5.3.4	Light-active Polymeric Hydrogels .....	136
5.4	Magnetic-sensitive Shape-memory Polymers .....	139
5.4.1	Shape-memory Polymer Matrices filled with Magnetic Particles .....	139
5.4.2	Magnetic-active polymeric gels .....	140
5.5	Water/solvent-sensitive Shape-memory Polymers .....	141
5.6	Electric-sensitive Shape-memory Polymers .....	144
5.7	Conclusions .....	148

6	Modelling of Shape-memory Polymers .....	157
6.1	Introduction.....	157
6.2	Macroscale Constitutive Modelling.....	158
6.2.1	Stress–strain Characteristics .....	160
6.2.2	Shape-memory Properties .....	162
6.3	Mesoscale Modelling .....	166
6.4	Microscale Modelling .....	170
6.5	Molecular Dynamics and Monte Carlo Simulations.....	173
6.5.1	Reaction Characteristics .....	173
6.5.2	Physical Properties .....	173
6.5.3	Microstructure.....	174
6.5.4	Hydrogen bonding Interactions .....	176
6.5.5	Mechanical Properties.....	177
6.6	Mathematical Modelling.....	178
6.7	Modelling of Device Structures .....	178
6.8	Modelling for Light-sensitive Shape-memory Polymers .....	179
6.8.1	Three-dimensional Finite Deformation Modelling.....	179
6.8.2	Multiple Natural Configurations Modelling .....	181
6.8.3	Multi-scale Modelling.....	182
6.9	Conclusions .....	183
7	Supramolecular Shape-memory Polymers.....	189
7.1	Introduction.....	189
7.2	Supramolecular Chemistry .....	190
7.2.1	Hydrogen Bonding.....	192
7.2.2	Relationship between Shape-memory Polymers and Supramolecular Polymer Networks.....	192
7.3	Polymers Containing Pyridine Moieties: a Pathway to Achieve Supramolecular Networks .....	194
7.3.1	Function of Pyridine Moieties in Supramolecular Chemistry .....	194

7.3.2	Supramolecular Pyridine-containing Polymers .....	195
7.3.3	Supramolecular Liquid Crystalline Polymer-containing Pyridine Moieties .....	196
7.4	Supramolecular Shape-memory Polymers based on Pyridine Moieties .....	197
7.4.1	Synthesis .....	197
7.4.2	Structure and Morphology .....	198
7.4.3	Thermally induced Shape-memory Effect .....	204
7.4.4	Moisture-sensitive Shape-memory Effect .....	206
7.5	Supramolecular Shape-memory Polymers based on Cyclodextrins .....	208
7.5.1	Cyclodextrins .....	208
7.5.2	Thermally induced Shape-memory Effect .....	209
7.5.3	Non-thermally Induced Shape-memory Effects .....	211
7.6	Potential Applications .....	215
7.6.1	Reshape Applications .....	215
7.6.2	Shape-memory Effect for Hairstyles in Beauty Care .....	215
7.6.3	Two-way Shape-memory Polymer Laminates .....	215
7.6.4	Medical Application: Antibacterial .....	216
7.6.5	Intelligent Windows for Smart Textile Applications .....	216
7.7	Conclusions .....	218
8	Applications of Shape-memory Polymers .....	223
8.1	Introduction .....	223
8.2	Applications of Bulk Shape-memory Polymers .....	223
8.2.1	Fixation .....	224
8.2.1.1	Orthodontic Wires .....	225
8.2.1.2	Medical Casts .....	226
8.2.2	Actuation .....	226
8.2.2.1	Actuation Realised by Combining Shape- memory Polymers with Specific Structures .....	226

8.2.2.2	Actuation arising from a Two-way Shape-memory Effect .....	228
8.2.3	Deployment .....	228
8.2.3.1	Cold Hibernated Elastic Memory of Shape-memory Polymer Foams .....	229
8.2.3.2	Expandable Stents.....	229
8.2.3.3	Deployable Dialysis Needles, Coils and Neuronal Electrodes .....	229
8.2.4	Self-healing .....	231
8.2.4.1	Confined Shape-recovery Self-healing .....	232
8.2.5	Fitting .....	233
8.3	Applications in Surface Wrinkling and Patterning.....	234
8.3.1	Principle of Surface Wrinkling .....	234
8.3.2	Wetting and Spreading.....	236
8.3.3	Adaptable Biological Devices for Modulating Cellular-substrate Interactions.....	236
8.3.4	Biosensor and Micro-systems.....	238
8.3.5	Programmable Surface Pattern.....	239
8.3.6	No-programming Reversible Shape-memory Surface Patterns.....	239
8.4	Applications in Textiles.....	239
8.4.1	Shape-memory Polymer Fibres.....	239
8.4.2	Shape-memory Polymer Yarns and Fabrics .....	242
8.4.3	Shape-memory Polymer Solutions for Finishing Fabrics.	243
8.4.4	Shape-memory Polymer Nanofibres and their Nonwovens.....	245
8.4.5	Shape-memory Polymer Film/Foam and Laminated Textiles .....	247
8.5	Engineering Applications .....	249
8.5.1	Transportation.....	249
8.5.2	Sensors and Actuators.....	249
8.5.3	Filtration.....	251

8.5.4	Insulation.....	251
8.6	Conclusions .....	252
9	Future Outlook .....	261
9.1	Introduction.....	261
9.2	New Shape-memory Polymers with Novel Structures and Diversified Functionalities.....	261
9.2.1	New Stimulus Switches .....	262
9.2.2	Intrinsic Athermal Switches .....	262
9.2.3	Multi-responsive and Multi-functional Switches .....	263
9.3	Development Trends of Shape-memory Polymer Composites and Blends .....	263
9.3.1	Electric-Sensitive Shape-memory Effect.....	264
9.3.2	Light-Sensitive Shape-memory Effect .....	265
9.3.3	Magnetic-Sensitive Shape-memory Effect.....	265
9.3.4	Water/Solvent-Sensitive Shape-memory Effect.....	265
9.3.5	Shape-memory Effect based on Non-thermal Phase Transitions.....	266
9.4	Versatile Shape-memory Effects by Novel Programming Protocols.....	266
9.4.1	Programmability .....	266
9.4.2	Imperfection or a New Shape-memory Effect.....	267
9.5	Fundamental Understanding .....	268
9.6	Comprehensive Study of Structure–property Relationships .....	268
9.7	Modelling .....	269
9.8	Application in Textiles .....	269
9.9	Biomedical Applications .....	271
9.10	Applications toward Commercial Success .....	274
9.10.1	Maturing and Broadening of Applications .....	274
9.10.1.1	Existing Widely Researched Areas .....	274
9.10.1.2	Broadening Areas.....	275

9.10.1.3 Untouched Areas .....	275
9.10.2 Integrated Approaches .....	275
9.10.3 Challenging Issues in Applications .....	276
9.11 Supramolecular Shape-memory Polymers.....	277
9.12 Conclusions .....	279
Abbreviations.....	285
Index .....	295



# 1 Shape-memory Polymers

## 1.1 Introduction

Shape-memory materials (SMM) have stimulated research interest from academia and industry to solve problems related to aerospace [1], biomedical [2, 3], transport [4], construction [5], electronic [6], textile [7] and consumer products [8, 9]. The term ‘shape-memory’ was first proposed by Vernon in 1941 [10] to describe a unique feature of a special class of material. SMM are smart materials that can respond to various external stimuli (e.g., heat [11], light [12], and electric or magnetic fields [13–15]) by changing some of their properties (e.g., stiffness, colour and shape). Such smart functions provided by SMM are distinct from smart systems or facilities because they do not rely on the complicated sense–response structure of a feedback system. Instead, they can be intrinsically sensitive to changes in their ambient environment. For materials to have shape-memory, their shape change must be rapid and finish within a narrow band (Figure 1.1) [16]. These materials have been developed rapidly in past few decades, and include shape-memory alloys (SMA), shape-memory ceramics (SMC) and shape-memory polymers (SMP) (Figure 1.2).

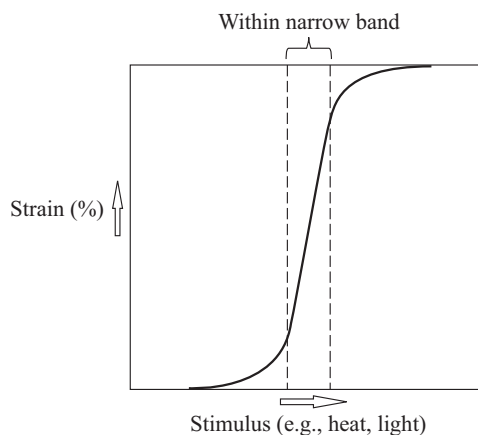
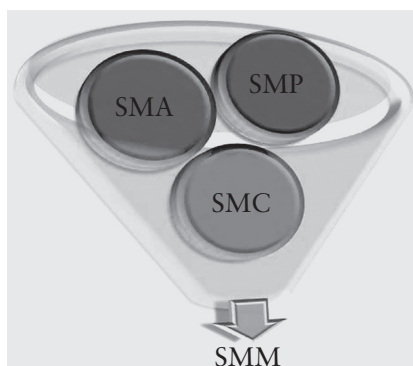


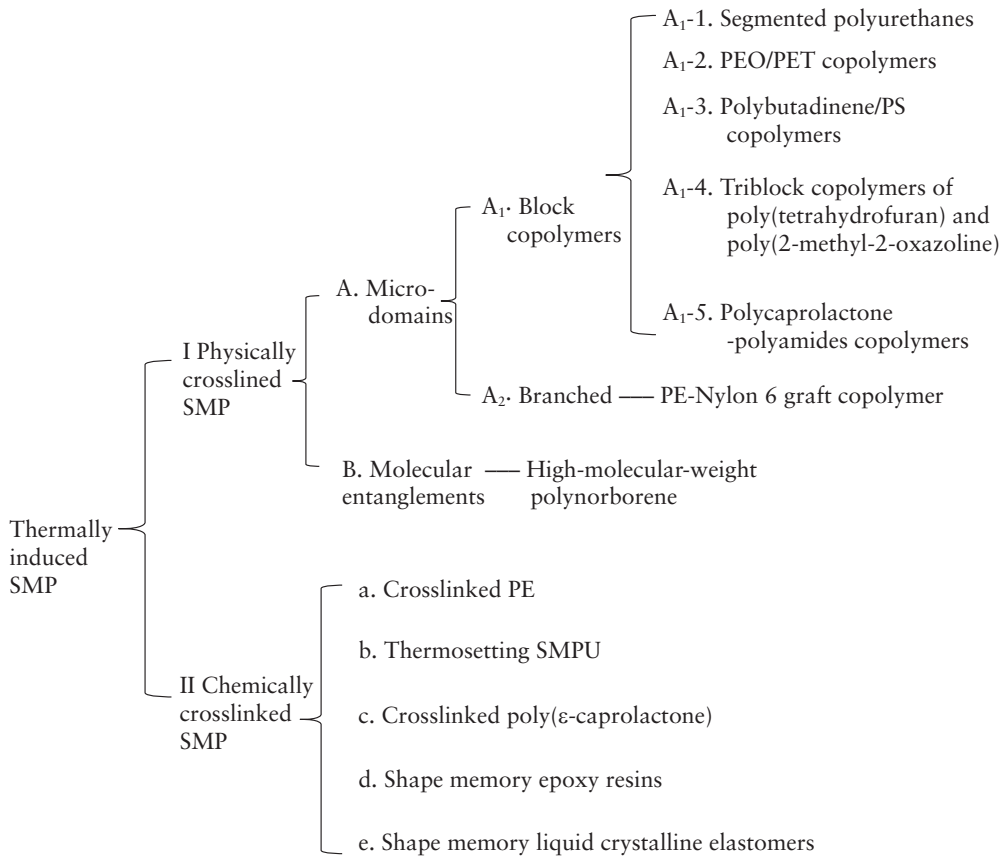
Figure 1.1 Stimuli-responsive shape-memory effects (SME) (schematic)





**Figure 1.2** Family of SMM

SMP, one of the unique members of SMM, have drawn increasing attention because of their scientific and technological significance [16]. However, the importance of SMP was not recognised until the 1960s, when crosslinked polyethylene (PE) was used for making heat-shrinkable tubes and films [17]. Further efforts to develop SMP began in the late-1980s, accelerated in the 1990s, but made significant progress only in the past 5–10 years. Polymeric materials are called SMP if they can change to a temporary shape and recover their original shape upon application of an external stimulus. This unique property of SMP is also called shape-memory effects (SME). Various types of polymers, such as polyacrylate copolymers [18], polynorbornene [19], segmented polyurethanes [20], segmented polyurethane ionomers [21], epoxy-based polymers [22], thio-ene-based polymers [23], crosslinked polycyclooctene [24], crosslinked ethylene-vinyl acetate copolymer [25] and styrene-based polymers [26] can demonstrate SME. Most of them are thermally induced SMP that can use heat as a triggering environment. **Figure 1.3** shows different thermally induced SMP.



**Figure 1.3** Thermally induced SMP and their structural categorisation. PEO: Polyethylene oxide; PET: polyethylene terephthalate; PS; polystyrene and SMPU: shape-memory polyurethanes

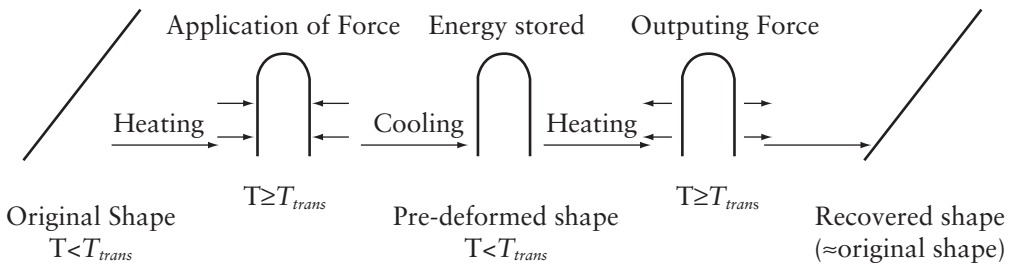
SMP can ‘sense’ the environment and/or their own state, make a ‘judgment’, and then change their functions according to the predetermined purpose. With the rapid development and wide investigation of SMP, their features are becoming increasingly prominent, particularly compared with SMA. SMP have several advantages [16], as detailed below:

- They can use diverse external stimuli and triggers: in addition to heating, there are many alternative ways to trigger shape recovery (e.g., light, magnetic field, chemicals and electricity) which can co-exist, leading to multi-sensitive materials.

- They show highly flexible programming: the programming can be done with different stimuli through single and multi-step processes.
- They have a broad range of structural designs: there is an abundance of approaches for designing netpoints and switches for various types of SMP. Additionally, different polymers and foreign materials can be used to construct different SME.
- They possess tunable properties: the properties of SMP can be engineered very easily and tuned accurately using composites, blending and synthetic methods.
- They are well-suited for responses to human senses/tissues and biodegradability: SMP are made from polymers, which are soft materials that provide an abundant array of choices for making highly biodegradable, biocompatible and comfortable devices to interfere with our bodies, thereby offering unique opportunities for smart medical, biological, and garment-integrated devices.
- They can be very light and can occupy a large volume (foam): these properties are extremely important for applications such as aerospace devices, air-force items and airplane components. For example, deployable SMP devices are preferred by the National Aeronautics and Space Administration as well as the United States Air Force Research Laboratory over their SMA peers due to their light weight [27].

## **1.2 Shape-memory Effect**

SME represent the capability of SMM to ‘memorise’ the original shape and allow the materials to recover the original shape from a temporary deformed shape under appropriate stimuli. SME involves two features: fixability and recoverability. Fixability refers to the capability of the SMM to change from the original undeformed shape to a temporary deformed shape through a suitable programming process (i.e., shape fixing). Recoverability indicates its ability to recover the original shape. In the programming process, SMM are deformed mechanically and the deformed shape fixed temporarily. The most important characteristic of SME is the stability of this temporarily deformed shape, which does not change in the absence of suitable stimuli. The temporary shape is triggered actively to recover the original permanent shape by exposure to an appropriate stimulus. **Figure 1.4** shows a schematic representation of SME. In general, heat [28], light [12, 29] and electricity [14, 15] can be used for triggering. There are reports on SMP triggered from other stimuli, such as magnetic-induced SME [13] and water-driven SME [30]. Among them, thermally induced SME are more common, and in which shape recovery takes place with respect to a certain critical temperature [31].



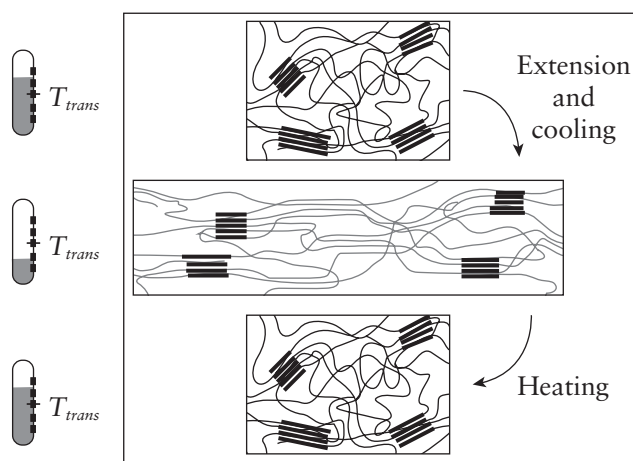
**Figure 1.4** Shape-memory effect during a typical thermomechanical cycle (schematic).  $T$ : temperature and  $T_{trans}$ : transition temperature. Reproduced with permission from J. Leng, X. Lan, Y. Liu and S. Du, *Progress in Materials Science*, 2011, 56, 7, 1077. ©2011, Elsevier [32]

### 1.2.1 Shape-memory Effect in Shape-memory Polymers

The SME of SMP is not a specific property of a single polymer. It results from the structure and morphology of the polymer, and is influenced by the programmed testing conditions. The prerequisite to achieve a SME involves two aspects: netpoint (hard segment) and switch (soft segment) [33]. The former provides entropic elasticity and is responsible for shape recovery. The latter is reversibly sensitive to certain external stimuli and responsible for shape fixing. In general, in the permanent shape, the internal stress is zero or very low. If the SMP is subjected to deformation, the internal stress can be ‘stored’ in the polymer structure by following a suitable programming process. By exposing the polymer to a suitable stimulus, the SMP recovers its permanent shape as a result of releasing the internal stress stored in the crosslinking structure.

Let us consider a SME in a thermally induced SMP. The elastic networks (i.e., hard segments) in the SMP can be created by chemical/physical crosslinking, as well as interpenetrating or any other approaches. The hard segments in the polymer network play the part of network conjunctions that can stabilise the network all along in the series of thermomechanical processes. The polymeric network chains have the role of ‘switching domains’ whose thermal transition temperature ( $T_{trans}$ ) essentially serves as the  $T_{trans}$  for triggering SME. The molecular mobility of switching domains changes greatly above and below the  $T_{trans}$ , and the modulus of materials can thus change by  $\geq 1$ –2 orders of magnitude in a narrow temperature range around the  $T_{trans}$ . The network chain segments are flexible at temperatures above the  $T_{trans}$  but rigid at temperatures below the  $T_{trans}$ , where the mobility of the chains is frozen (or

at least limited). The polymer materials, therefore, can develop large deformations at temperatures above the  $T_{trans}$  and afterwards can fix into a temporary shape at temperatures below the  $T_{trans}$ . **Figure 1.5** shows the molecular mechanism of SME in a thermally induced SMP. According to the mechanism, the reversible phase, having a melting transition temperature of the soft segments as the  $T_{trans}$  is used to hold the temporary deformation. The fixed phase is referred to the hard segments, which are linked to the soft segments *via* physical crosslinks. Hence, the fixed phase inhibits the plastic slip of the molecular chains by physical crosslinkage points among them, and can be responsible for memorising the permanent shape.



**Figure 1.5** Molecular mechanism of SME of thermally induced SMP (schematic). Reproduced with permission from A. Lendlein and S. Kelch, *Angewandte Chemie International Edition*, 2002, **41**, 12, 2034. ©2002, John Wiley & Sons [34]

It is worth clarifying the SME of polymers and SMP. Liu and co-workers [24] stated in their investigation that polymers intrinsically show SME on the basis of rubber elasticity, but with varied shape-memory performance. There is no reason for excluding the shape fixing and shape recovery occurring under any condition from the term ‘SME’. It is also unreasonable to define ‘SME’ in a quantitative manner and remove some low extent of shape fixity and shape recovery from the scope of SME. If one polymer is deformed and cooled down to a frozen state quickly so that stress relaxation is effectively avoided, the elastic stress generated in the deformation can mostly be preserved. If the material is reheated to a high temperature, the stored

stress is released, resulting in its original shape being recovered more or less. Hence, all polymers (even those having no apparent network structure) may tend to exhibit more or less shape fixity and shape recovery, namely, SME.

However, SMP should have polymeric networks to effectively memorise their original shape. The major difference between ‘traditional’ polymeric elastomers and SMP lies in the different  $T_{trans}$  of their polymeric network chains. It can be readily envisaged that a traditional polymeric elastomer can also be fixed in a temporary shape if it is cooled down to a sufficiently low temperature. That is, traditional polymeric elastomers can also show SME under ‘particular conditions’. However, from the view of applications, the SME under these ‘particular conditions’ is un-meaningful practically. Hayashi and co-workers [35, 36] developed a series of polyurethane SMP whose  $T_{trans}$  was from  $-30\text{ }^{\circ}\text{C}$  to  $65\text{ }^{\circ}\text{C}$ . Nevertheless, the SMP that can hold a temporary shape around room temperature will be more useful for practical applications. Therefore, the  $T_{trans}$  of SMP is most often above room temperature. It can be concluded that SMP represent only a small section of the ‘polymer family’ and demonstrate SME under ambient conditions (Figure 1.6).

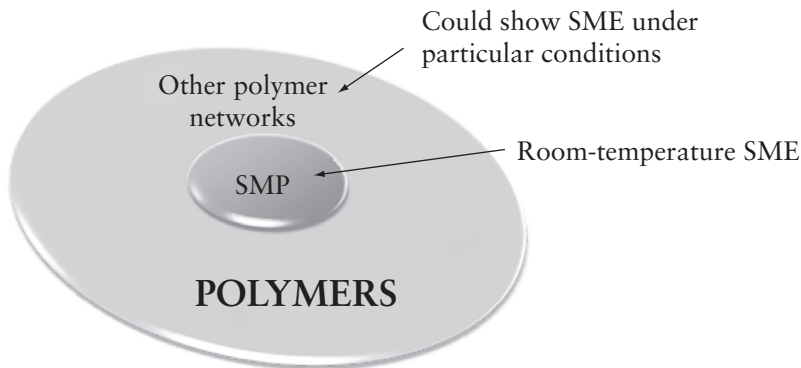


Figure 1.6 Relationship between SMP and traditional polymers

### 1.2.2 Shape-memory Effect in Shape-memory Polymers and Shape-memory Alloys

Different from SMP, the shape-memory properties of SMA arise from the change in crystal lattice of a specific martensite variant to the parent single crystal phase [34].

Nickel-titanium (NiTi), copper-aluminium-nickel and copper-zinc-aluminium-nickel alloys are the three main types of SMA. During shape recovery cycles, SMA show two phases: (i) an austenite phase with a body-centred cubic structure at high temperature, and (ii) a martensite phase with tetragonal, orthorhombic or monoclinic crystal lattice at low temperature. NiTi alloys change from austenite to martensite upon cooling and change from martensite to austenite upon heating. The phase transformation from austenite to martensite upon cooling is not by diffusion of atoms but by shear lattice distortion. Upon cooling, the austenite transforms to martensite, which results in the formation of several martensitic variants ( $\leq 24$  for NiTi). At a temperature below the martensite transformation finish temperature, deformation stress alters the variants of the other martensite phases into a specific variant of the martensite phase, which leads to a macroscopic shape change of the SMA. If the SMA is heated to a temperature above the start temperature of the austenite phase, the specific martensite variant transforms to the lattice of original austenite phase, leading to a one-way shape recovery of SMA. Figure 1.7 shows the SME for a SMA based on a martensitic phase transformation.

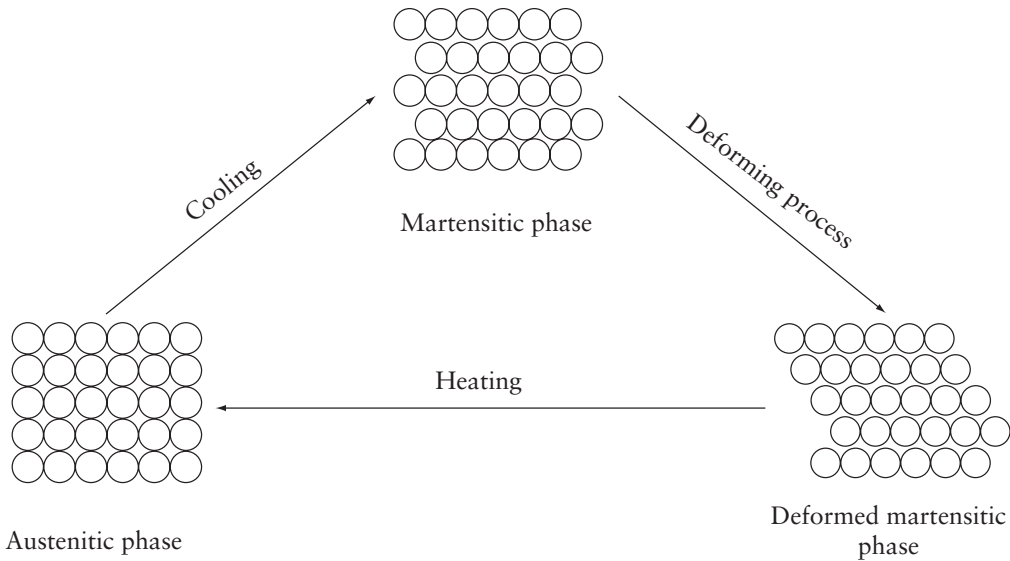


Figure 1.7 SME for a SMA (schematic)

SMA can generate tremendous recovery forces during their transformation, usually in the range of 50 to 500 MPa. Hence, they have been found to be more suitable for

medical, military, robotics and safety applications. However, the major limitation of SMA is their poor transformation strain [32]. The recoverable deformation strain of SMA is usually <10%, otherwise the deformation causes slippage of the lattice, which is unrecoverable. The poor transformation strain in SMA limits their application, especially if a large strain is required. SMP have advantages over SMA: light weight, low cost, good processability, high deformability, high shape recoverability, soft handle, and tailor-able switching temperature. SMP exhibiting deformation  $\leq 200\%$  have been reported. The main drawback of SMP is their poor recovery stress, which is much lower than that for SMA. As an illustration, **Table 1.1** shows comparisons of the shape-memory and mechanical properties of NiTi SMA and polystyrene SMP.

Table 1.1 Properties of typical SMP and SMA		
Thermomechanical properties	Polystyrene SMP	NiTi-SMA
$T_{trans}$ , °C	62	$\approx 40-100$
Transformation strain, %	50-100	Maximum 8
Actuation stress, MPa	2-10	$\approx 100$
Young's Modulus above the $T_{trans}$ , GPa	1.24	$\approx 83$
Young's Modulus below the $T_{trans}$ , MPa	2-10	$\approx 28-41$
Density, g/cm <sup>3</sup>	0.92	6.45
Reproduced with permission from J. Leng, X. Lan, Y. Liu and S. Du, <i>Progress in Materials Science</i> , 2011, <b>56</b> , 7, 1077. ©2011, John Wiley & Sons [32]		

### 1.3 Structure of Shape-memory Polymers

Researchers have used polymer chemistry to experiment with different networks or architectures of polymers. The molecular design for the polymer networks of SMP is consistent with that of traditional polymer networks. Similar to conventional polymers, the polymer network in SMP can be constructed *via* chemical crosslinking or physical crosslinking (which corresponds to thermosetting SMP and thermoplastic SMP). The advantage of physical crosslinked SMP is that they exhibit a reversible nature (i.e., their primary shape can be reshaped). Covalently crosslinked SMP show an irreversible nature and do not offer the easy possibility to change the primary shape once processed through casting or moulding. Individual primary chains are



connected by covalent or chemical bonds, so their structures are more stable than the physical crosslinked network. Today, several polymer networks demonstrate SME, but the most researched group of SMP were thermally induced SMP. This section details some of the structural characteristics of different SMP.

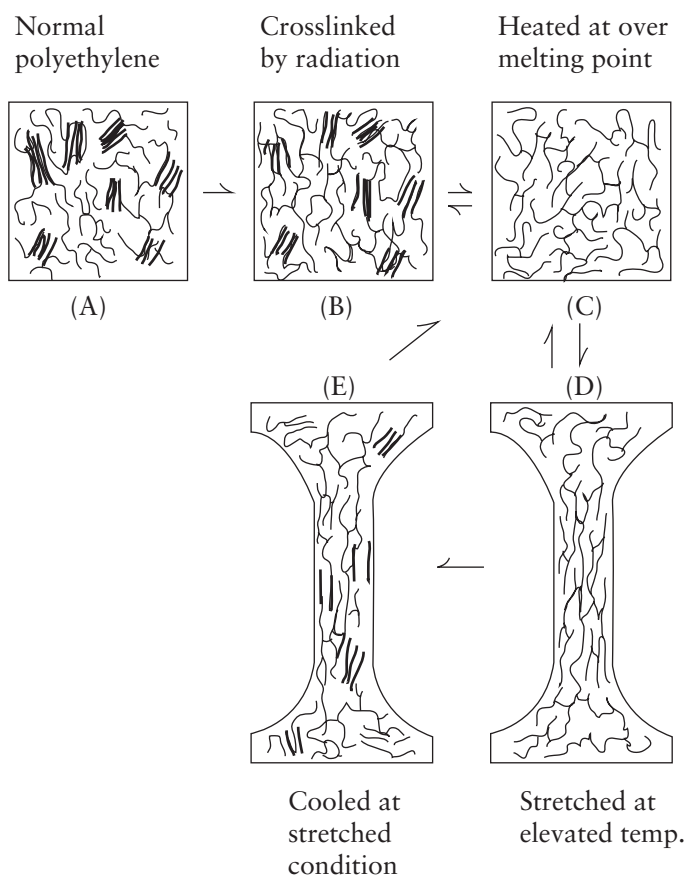
### **1.3.1 Thermally Induced Shape-memory Polymers**

Netpoints and molecular switches are the two basic structural requirements of SMP. Here, the netpoints in the polymer network are connected by chain segments which determine the permanent shape. The chain segments between the netpoints offer flexibility to the structure of SMP to be deformed upon application of external stress, and hence allow shape fixing to complete. For thermoplastics and thermosetting SMP, these netpoints in the polymer network are constructed with physical crosslinks and chemical crosslinks, respectively. For physically crosslinked structures, the phase separation between the two components of the polymer network (i.e., hard and soft segments) is the important criteria to demonstrate SME. The dissimilarity in the structure and thermodynamic incompatibility of the hard and soft segments often leads to phase segregations of these components in the polymer network.

SMP can have more than one type of chain segments in the structure where each of the used chain segment types can carry out different functions. That is, some segment chains can act as switching domains essential for thermally induced SME, whereas other segment chains can form hard segments. (Multi)block copolymers are commonly used in such cases, where different domains are formed due to phase separation, resulting in a certain polymer morphology [37]. For such phase-segregated morphology, the domains providing the highest  $T_{trans}$  act as netpoints (i.e., hard domains) whereas the polymer segments having the second highest  $T_{trans}$  behave like switching domains. The switching domains can form additional reversible crosslinks to fix the deformed shape temporarily. They can generate reversible crosslinks by solidification or by functional groups, which can reversibly form and cleave crosslinks based on a suitable programming process. Lendlein and colleagues have proposed the general molecular mechanism of thermally induced SMP, in which the network structure is chemically or physically crosslinked and the switch units are made from a semi-crystalline or amorphous soft phase [34]. As an example, **Figure 1.5** shows the molecular shape-memory mechanism of thermally induced SMP based on a physically crosslinked structure with a  $T_{trans}$  as the melting temperature of soft segments.

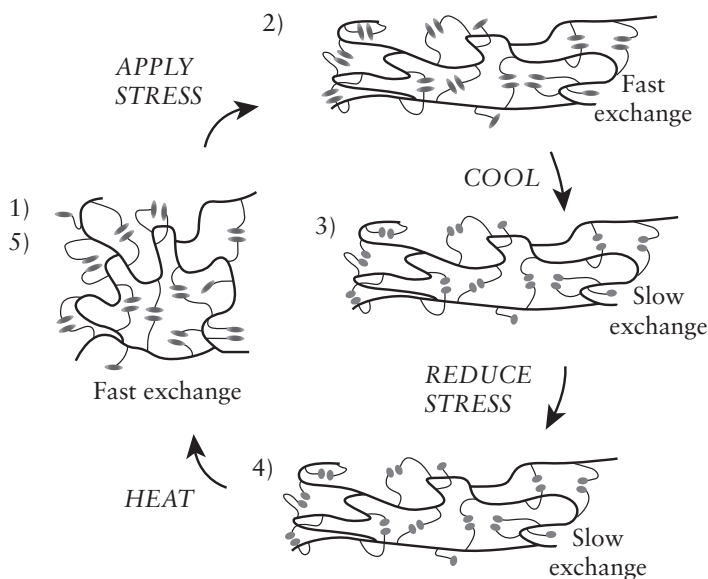
Thermally induced SMP can also be produced from one type of chain segments. In general, covalent crosslinks in the polymer networks can generate SME in the same type of polymer chains. This can be realised during synthesis starting from low-molecular-weight (co)monomers or by post-processing methods to create the

netpoints of the covalent SMP networks. Several polymer types, such as acrylate [18], poly( $\epsilon$ -caprolactone) [38], ethylene-vinyl acetate [25], polycyclooctene [24] and polyvinyl ethers [39, 40] have been tried to realise SME using covalent crosslinks in their structure. As an example, **Figure 1.8** demonstrates the progress of representative models developed for thermally sensitive SMP. In chemically crosslinked semi-crystalline PE, the crystalline phase with a crystal melting temperature ( $T_m$ ) is used as a switch unit to provide the shape fixity capacity. The chemically crosslinked PE network ‘memorises’ the permanent shape after deformation upon heating [41].

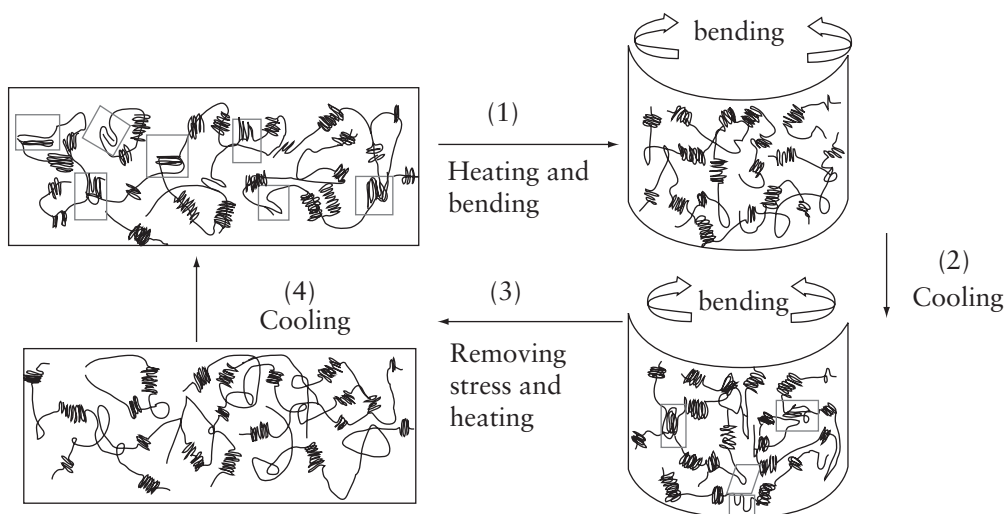


**Figure 1.8** Molecular model of thermally induced SME in crosslinked PE. Reproduced with permission from S. Ota, *Radiation Physics Chemistry*, 1981, 18, 1-2, 81. ©1981, Elsevier [41]

Apart from using single or (multi)block copolymers to design SMP, another possibility to derive SMP are from a combination of (multi)block copolymers and covalent polymer networks. Here, the blends form multimaterial systems in which the first blend component (i.e., (multi)block copolymer) can provide the SMP matrix whereas the second blend component is used for modification of the properties of one or both domains [37]. The other structural possibility is the incorporation of linear or branched multifunctional molecules which can be equipped with functional groups to deliver multifunctionality. For example, the supramolecular system tends to adapt its architecture in response to environmental conditions (e.g., temperature change) due to the labile nature of non-covalent interactions [42]. This phenomenon led to a novel shape-memory mechanism involving thermo-reversible quadruple hydrogen-bonding side groups in an elastic polymer network for supramolecular SMP (**Figure 1.9**) [43]. Another supramolecular SMP system is based on a partial cyclodextrin-polyethylene glycol (CD-PEG) inclusion complex in which CD-PEG inclusion crystallites serve as the fixing phase and naked PEG crystallites function as the reversible phase. A corresponding molecular model of supramolecular SMP was established in 2008 by Zhang and co-workers (**Figure 1.10**) [44]. **Figure 1.3** details structural characterisation of different thermally induced SMP.



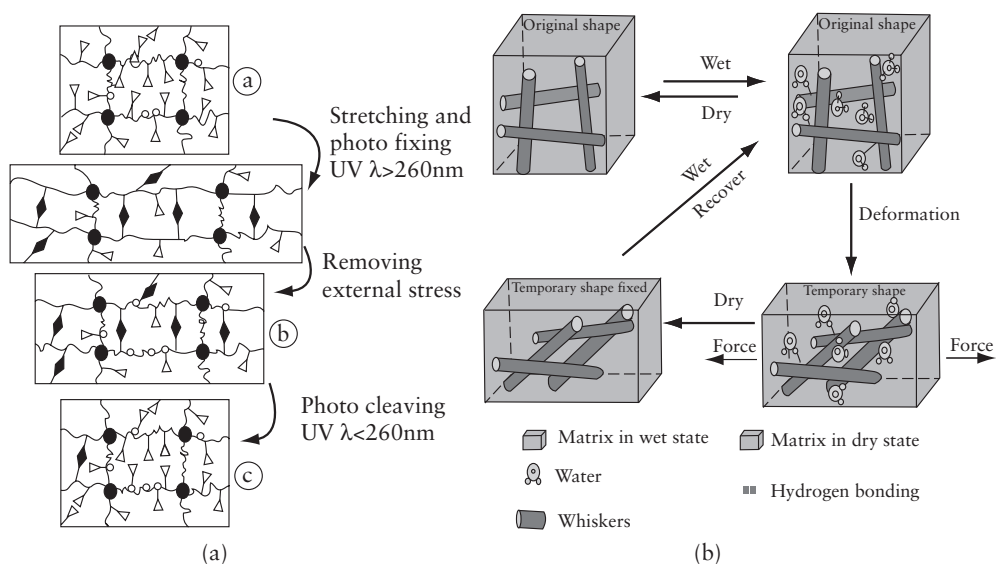
**Figure 1.9** Molecular model of SME involving thermally reversible supramolecular switches. Reproduced with permission from J.H. Li, J.A. Viveros, M.H. Wrue and M. Anthamatten, *Advanced Materials*, 2007, 19, 19, 2851. ©2007, John Wiley & Sons [43]



**Figure 1.10** Molecular model of SME involving partial  $\alpha$ -CD-PEG inclusion as switches. Reproduced with permission from S. Zhang, Z.J. Yu, T. Govender, H.Y. Luo and B.J. Li, *Polymer*, 2008, 49, 15, 3205. ©2008, Elsevier [44]

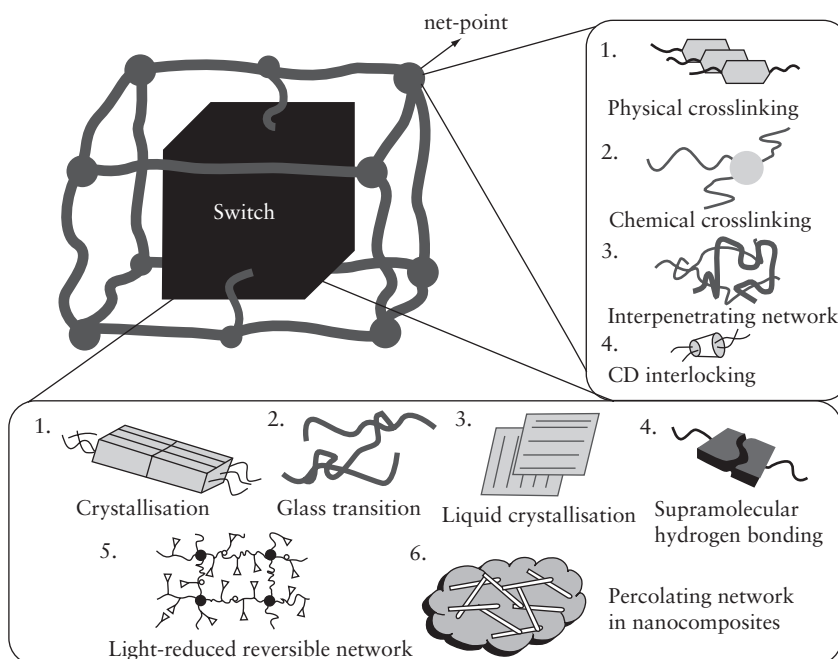
### 1.3.2 Athermal Shape-memory Polymers

All of the SMP models mentioned above contribute substantially to determination of the theoretical configuration of thermally sensitive SMP, whereas diversification of the molecular structure design provides the opportunity to develop SMP with stimulus sensitivities other than thermal induction. As shown in **Figure 1.11**, two types of structures and programming models have been proposed for athermally sensitive SMP. One model is designed to create a SME of light-sensitive SMP in which chromophores are grafted covalently onto a crosslinked polymer network. Light-sensitive SME can be achieved through efficient, photoreversible (2+2) cycloaddition reactions between chromophore molecules (i.e., cinnamic acid-type molecules) [29]. Another athermal water-sensitive SMP system has been made from a nanocomposite containing nano-cellulose whiskers dispersed in an elastomer matrix. The reversible formation and disruption of a percolation network of nano-cellulose whiskers in an elastomer matrix features an unprecedentedly fast switching SME that is sensitive to water [45].



**Figure 1.11** (a) Molecular models of athermal light-sensitive SME. UV: ultraviolet. Reproduced with permission from A. Lendlein, H.Y. Jiang, O. Junger and R. Langer, *Nature*, 2005, 434, 7035, 879. ©2005, Nature Publishing Group [29], and (b) molecular models of athermal water-sensitive SME

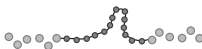

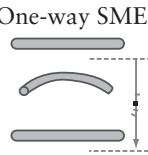



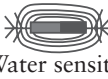




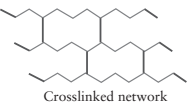
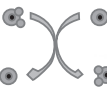

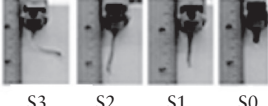

Hu and Chen proposed an overall three-dimensional SMP architecture based on the development of molecular mechanisms [46], which looks simple but is reasonable and comprehensive (Figure 1.12). This model is not limited to certain types of SMP, but can describe any SMP polymer. In this model, SMP consist of switch units and netpoints. The latter determine the permanent shape and can be made of chemical or physical crosslinks, with an interpenetrated or interlocked supramolecular complex. The driving force for strain recovery in SMP is the entropic elasticity of the polymer network. Similarly, the switch unit is responsible for controlling the shape fixity and recovery upon a specific and predetermined external stimulus. Until now, the amorphous, crystalline and liquid crystalline phases, supramolecular entities, light-reversible coupling groups and newly utilised percolating cellulose-whisker networks have served as the switches in SMP. In all of these systems, the entropic elastic force results from the polymer networks. Thus, physical or chemical netpoints *via* intermolecular forces and/or covalent bonding are usually required.



**Figure 1.12** Overall architecture of SMP. Reproduced with permission from J.L. Hu, Y. Zhu, H.H. Huang and J. Lu, *Progress in Polymer Science*, 2012, 37, 12, 1720. ©2012, Elsevier [16]

## 1.4 Classification of Shape-memory Polymers

The classifications of SMP have been discussed widely. SMP have been reported to be thermally induced, light-induced, electro-active, water/moisture/solvent-induced, pH-sensitive and magnetic-sensitive based on their external stimulus. Ratna and Karger-Kocsis [47] as well as Liu and co-workers [48] divided SMP into physically crosslinked and chemically crosslinked SMP according to the nature of their netpoints. Even biodegradable SMP are regarded as special types of SMP [47]. Sometimes, SMP can be subdivided based on their switch type into glass transition temperature-type SMP with an amorphous phase or  $T_m$ -type SMP with a crystalline phase [47]. However, Behl and Lendlein used actively moving polymers to classify them into shape-memory and shape-changing polymers [49]. These classifications may not be uniformly accepted because they only partially show the principle of SMP.

Composition & structure	Stimulus	Shape memory function
Block-copolymer 	Temperature 	One-way SME  Two-way SME 
Supramolecular polymer 	Electricity  Magnetic 	
Polymer blend/composite 	Water sensitive 	2) Water sensitive
Polymer IPN/semi-IPN 	Light/radiation 	3) Light sensitive
Crosslinked homopolymer 	Oxidation-reduction 	4) Redox sensitive
		Triple-shape SME  Multi-shape SME  Multi-functionality 

**Figure 1.13** Integrated insight into SMP based on structure, stimulus, and shape-memory function. IPN: interpenetrating polymer networks. Reproduced with permission from J.L. Hu, Y. Zhu, H.H. Huang and J. Lu, *Progress in Polymer Science*, 2012, 37, 12, 1720. ©2012, Elsevier [16]

**Figure 1.13** presents an integrated insight into the classification of SMP by polymerisation, structure, stimuli and shape-memory functionality. The composition and structure of SMP encompasses block/segmented copolymers [50–53], chemically crosslinked polymers [24, 54–56], polymer interpenetrating [57]/semi-interpenetrating [58–60], polymer blends [61–63], polymer composites [64–67] and even supramolecular polymer networks [43]. Thus, practically all polymerisation methods can be used to synthesise SMP: addition [68], condensation [69], free-radical [43] and photochemical polymerisation [54], radiation reaction [38], acyclic diene metathesis

polymerisation [70] and even ring-opening polymerisation [71]. SMPU and ethylene oxide-ethylene terephthalate segmented copolymers are, in general, synthesised *via* condensation polymerisation [69]. Crosslinked PE is prepared through a radiation reaction. Moreover, some SMP materials can be prepared by blending two polymers [61] or fabricating non-woven fabric composites into an elastomer matrix [72].

Diverse shape-memory functions (including SME and other functions) can be achieved by controlling the composition and chemistry/polymerisation of SMP. The SME of SMP have been developed from conventional one-way SME to two-way, triple and even multiple SME. Additionally, multi-functionality (e.g., permeable, optical, biodegradable, and thermal-chromic properties) can be achieved in SMP, as discussed by Behl and co-workers [37]. To achieve SME, an external stimulus (e.g., Joule heating, light or moisture) is currently used to trigger strain recovery after deformation. Joule heating can be achieved by direct or indirect heating, just like electric-induced [6, 73], magnetic-induced [74, 75] and infrared light-induced [76] heating. Additionally, SME can be triggered by redox conditions [77]. Thus, SMP can be categorised by their stimulus into four groups: (1) thermally induced; (2) athermal water (molecule)-sensitive; (3) athermal light-sensitive; and (4) redox-sensitive.

## 1.5 Conclusions

SMP are stimuli-responsive polymers capable of changing their properties (i.e., moduli and shapes) upon exposure to external stimuli (e.g., heat, water and light). They have been the focus of research for several decades. Some of the important advantages of SMP are detailed and highlight their tremendous potential for many engineering applications. The concepts of SME in SMP, in addition to their differences in SME with respect to conventional polymers and SMA, are introduced. A systematic review is described to cover various aspects of SMP, including fundamental concepts, different mechanisms of SME in SMP, structural characterisation of SMP, and classification of SMP. This format will help readers to familiarise themselves with SMP and the basic concepts that will guide them to understand subsequent chapters of this book.

## References

1. W.M. Sokolowski and S.C. Tan, *Journal of Spacecraft and Rockets*, 2007, **44**, 4, 750.
2. W. Small, P. Singhal, T.S. Wilson and D.J. Maitland, *Journal of Materials Chemistry*, 2010, **20**, 17, 3356.



3. A. Lendlein and M. Behl, *Advances in Science and Technology*, 2009, **54**, 96.
4. Y. Gonzalez-Garcia, J. M. C. Mol, T. Muselle, I. De Graeve, G. Van Assche, G. Scheltjens, B. Van Mele and H. Terryn, *Electrochimica Acta*, 2011, **56**, 26, 9619.
5. P.J. Hood, S. Garrigan and F. Auffinger, inventors; Cornerstone Research Group, Inc., assignee; US 7981229 B2, 2011.
6. N.G. Sahoo, Y.C. Jung, N.S. Goo and J.W. Cho, *Macromolecular Materials and Engineering*, 2005, **290**, 11, 1049.
7. J. L. Hu, H.P. Meng, G.Q. Li and S.I. Ibekwe, *Smart Materials & Structures*, 2012, **21**, 5.
8. C.C. Mock, inventor; no assignee; US 8359677 B1, 2013.
9. T. Kikutani, S. Kondo, S. Hayashi, K. Sugihara, T. Haguri and K. Akimoto, inventors; Sunstar Inc., Mitsubishi Heavy Industries, Ltd., and Aoyoshi Co. Ltd., assignees; US 6173477, 2001.
10. L.B. Vernon, Beaver and H.M. Vernon, inventors; Vernon Benshoff Company, assignee; US 2234993, 1941.
11. S.J. Chen, J.L. Hu, Y.Q. Liu, H.M. Liem, Y. Zhu and Q.H. Meng, *Polymer International*, 2007, **56**, 9, 1128.
12. H. Koerner, G. Price, N.A. Pearce, M. Alexander and R.A. Vaia, *Nature Materials*, 2004, **3**, 2, 115.
13. T. Weigel, R. Mohr and A. Lendlein, *Smart Materials & Structures*, 2009, **18**, 2.
14. W. Choi, I. Lahiri, R. Seelaboyina and Y.S. Kang, *Critical Reviews in Solid State and Materials Sciences*, 2010, **35**, 1, 52.
15. H. Kim, A.A. Abdala and C.W. Macosko, *Macromolecules*, 2010, **43**, 16, 6515.
16. J.L. Hu, Y. Zhu, H.H. Huang and J. Lu, *Progress in Polymer Science*, 2012, **37**, 12, 1720.
17. W.C. Rainer, R.I. Barrington, E.M. Redding, I. Winnetka, J.J. Hitov, P. Levittown, A.W. Slaon, D.C. Washington and W. D. Stewart, inventors; Grace W R & Co., assignee; US 3144398, 1964.

18. Y. Kagami, J.P. Gong and Y. Osada, *Macromolecular Rapid Communications*, 1996, **17**, 8, 539.
19. K. Sakurai, T. Kashiwagi and T. Takahashi, *Journal of Applied Polymer Science*, 1993, **47**, 5, 937.
20. J.L. Hu and S. Mondal, *Polymer International*, 2005, **54**, 5, 764.
21. Y. Zhu, J. Hu, K.W. Yeung, K.F. Choi, Y.Q. Liu and H.M. Liem, *Journal of Applied Polymer Science*, 2007, **103**, 1, 545.
22. T. Xie and I.A. Rousseau, *Polymer*, 2009, **50**, 8, 1852.
23. D.P. Nair, N.B. Cramer, T.F. Scott, C.N. Bowman and R. Shandas, *Polymer*, 2010, **51**, 19, 4383.
24. C.D. Liu, S.B. Chun, P.T. Mather, L. Zheng, E.H. Haley and E.B. Coughlin, *Macromolecules*, 2002, **35**, 27, 9868.
25. F.K. Li, W. Zhu, X. Zhang, C.T. Zhao and M. Xu, *Journal of Applied Polymer Science*, 1999, **71**, 7, 1063.
26. K. Sakurai, H. Tanaka, N. Ogawa and T. Takahashi, *Journal of Macromolecular Science: Physics*, 1997, **36**, 6, 703.
27. W.M. Sokolowski, A.B. Chmielewski, S. Hayashi and T. Yamada, *P Soc Photo-Opt Ins*, 1999, **3669**, 179.
28. Q. Meng, J. Hu, Y. Zhu, J. Lu and Y. Liu, *Journal of Applied Polymer Science*, 2007, **106**, 2515.
29. A. Lendlein, H.Y. Jiang, O. Junger and R. Langer, *Nature*, 2005, **434**, 7035, 879.
30. S.J. Chen, J.L. Hu and S.G. Chen, *Polym International*, 2012, **61**, 2, 314.
31. P.T. Mather, X.F. Luo and I.A. Rousseau, *Annual Review of Materials Research*, 2009, **39**, 445.
32. J. Leng, X. Lan, Y. Liu and S. Du, *Progress in Materials Science*, 2011, **56**, 7, 1077.
33. J. Hu in *Advances in Shape Memory Polymers*, Woodhead Publishing Ltd., Cambridge, UK, 2013.

34. A. Lendlein and S. Kelch, *Angewandte Chemie International Edition*, 2002, **41**, 12, 2034.
35. C. Liang, C.A. Rogers and E. Malafeev, *Journal of Intelligent Material Systems and Structures*, 1997, **8**, 4, 380.
36. S. Hayashi, S. Kondo, P. Kapadia and E. Ushioda, *Plastics Engineering*, 1995, **51**, 2, 29.
37. M. Behl, M.Y. Razzaq and A. Lendlein, *Advanced Materials*, 2010, **22**, 31, 3388.
38. G. Zhu, G. Liang, Q. Xu and Q. Yu, *Journal of Applied Polymer Science*, 2003, **90**, 6, 1589.
39. E. J. Goethals, W. Reyntjens and S. Lievens, *Macromolecular Symposia*, 1998, **132**, 57.
40. W.G. Reyntjens, F.E. Du Prez and E.J. Goethals, *Macromolecular Rapid Communications*, 1999, **20**, 5, 251.
41. S. Ota, *Radiation Physics and Chemistry*, 1981, **18**, 1-2, 81.
42. J. M. Lehn, *Chemical Society Reviews*, 2007, **36**, 2, 151.
43. J.H. Li, J.A. Viveros, M.H. Wrue and M. Anthamatten, *Advanced Materials*, 2007, **19**, 19, 2851.
44. S. Zhang, Z.J. Yu, T. Govender, H.Y. Luo and B.J. Li, *Polymer*, 2008, **49**, 15, 3205.
45. Y. Zhu, J.L. Hu, H.S. Luo, R.J. Young, L.B. Deng, S. Zhang, Y. Fan and G.D. Ye, *Soft Matter*, 2012, **8**, 8, 2509.
46. J.L. Hu and S.J. Chen, *Journal of Materials Chemistry*, 2010, **20**, 17, 3346.
47. D. Ratna and J. Karger-Kocsis, *Journal of Materials Science*, 2008, **43**, 1, 254.
48. C. Liu, H. Qin and P.T. Mather, *Journal of Materials Chemistry*, 2007, **17**, 16, 1543.
49. M. Behl and A. Lendlein, *Soft Matter*, 2007, **3**, 1, 58.

50. L.T.J. Korley, B.D. Pate, E.L. Thomas and P.T. Hammond, *Polymer*, 2006, **47**, 9, 3073.
51. F.L. Ji, J.L. Hu and J.P. Han, *High Performance Polymers*, 2011, **23**, 3, 177.
52. F.L. Ji, J.L. Hu, T.C. Li and Y.W. Wong, *Polymer*, 2007, **48**, 17, 5133.
53. S.J. Chen, J.L. Hu, Y.Q. Liu, H.M. Liem, Y. Zhu and Y.J. Liu, *Journal of Polymer Science, Part B: Polymer Physics Edition*, 2007, **45**, 4, 444.
54. A. Lendlein, A.M. Schmidt and R. Langer, *Proceedings of the National Academy of Sciences USA*, 2001, **98**, 3, 842.
55. C.M. Yakacki, R. Shandas, D. Safranski, A.M. Ortega, K. Sassaman and K. Gall, *Advanced Functional Materials*, 2008, **18**, 16, 2428.
56. D.L. Safranski and K. Gall, *Polymer*, 2008, **49**, 20, 4446.
57. S.F. Zhang, Y.K. Feng, L. Zhang, J.F. Sun, X.K. Xu and Y.S. Xu, *Journal of Polymer Science, Part A: Polymer Chemistry Edition*, 2007, **45**, 5, 768.
58. G.Q. Liu, X.B. Ding, Y.P. Cao, Z.H. Zheng and Y.X. Peng, *Macromolecular Rapid Communications*, 2005, **26**, 8, 649.
59. D. Ratna and J. Karger-Kocsis, *Polymer*, 2011, **52**, 4, 1063.
60. E.D. Rodriguez, X.F. Luo and P.T. Mather, *ACS Applied Materials & Interfaces*, 2011, **3**, 2, 152.
61. H. Zhang, H.T. Wang, W. Zhong and Q.G. Du, *Polymer*, 2009, **50**, 6, 1596.
62. E. Kurahashi, H. Sugimoto, E. Nakanishi, K. Nagata and K. Inomata, *Soft Matter*, 2012, **8**, 2, 496.
63. S.C. Li and L. Tao, *Polymer-Plastics Technology and Engineering*, 2010, **49**, 2, 218.
64. X.T. Zheng, S.B. Zhou, X.H. Li and H. Weng, *Biomaterials*, 2006, **27**, 24, 4288.
65. M.K. Jang, A. Hartwig and B.K. Kim, *Journal of Materials Chemistry*, 2009, **19**, 8, 1166.
66. J. Ivens, M. Urbanus and C. De Smet, *eXPRESS Polymer Letters*, 2011, **5**, 3, 254.

67. K. Fan, W.M. Huang, C.C. Wang, Z. Ding, Y. Zhao, H. Purnawali, K.C. Liew and L.X. Zheng, *eXPRESS Polymer Letters*, 2011, **5**, 5, 409.
68. F.L. Ji and J.L. Hu, *High Performance Polymers*, 2011, **23**, 4, 314.
69. X.L. Luo, X.Y. Zhang, M.T. Wang, D.H. Ma, M. Xu and F.K. Li, *Journal of Applied Polymer Science*, 1997, **64**, 12, 2433.
70. E. del Rio, G. Lligadas, J.C. Ronda, M. Galia, V. Cadiz and M.A.R. Meier, *Macromolecular Chemistry and Physics*, 2011, **212**, 13, 1392.
71. D. Yang, W. Huang, J.H. Yu, J.S. Jiang, L.Y. Zhang and M.R. Xie, *Polymer*, 2010, **51**, 22, 5100.
72. X.F. Luo and P.T. Mather, *Advanced Functional Materials*, 2010, **20**, 16, 2649.
73. J.W. Cho, J.W. Kim, Y.C. Jung and N.S. Goo, *Macromolecular Rapid Communications*, 2005, **26**, 5, 412.
74. A.M. Schmidt, *Macromolecular Rapid Communications*, 2006, **27**, 14, 1168.
75. R. Mohr, K. Kratz, T. Weigel, M. Lucka-Gabor, M. Moneke and A. Lendlein, *Proceedings of the National Academy of Sciences USA*, 2006, **103**, 10, 3540.
76. J.S. Leng, D.W. Zhang, Y. Liu, K. Yu and X. Lan, *Applied Physics Letters*, 2010, **96**, 11.
77. D. Aoki, Y. Teramoto and Y. Nishio, *Biomacromolecules*, 2007, **8**, 12, 3749.

# 2 Shape-memory Polymers: Molecular Design, Shape-memory Functionality and Programming

## 2.1 Introduction

In recent years, the development of shape-memory materials (SMM) has been rapid. This has led to shape-memory alloys (SMA), shape-memory ceramics and shape-memory polymers (SMP). Compared with the other two types of materials, SMP have attracted more interest due to their prominent advantages. First, SMP have a broad range of structural designs. There are an abundance of approaches for designing the hard and soft domains of SMP. By utilising biocompatible and biodegradable raw materials, the obtained SMP could be better suited for biomedical applications. Therefore, studying the molecular design of SMP is important to obtain the appropriate shape-memory effects (SME) according to application requirements. Second, SMP could use diverse external stimuli and triggers. Adoption of different types of switches could make the SMP sensitive to stimuli other than heating, such as light [1] and moisture [2]. Third, highly flexible programming procedures can be done to achieve SMP with various functionalities. The same SMP could show distinct shape-memory behaviours after different programming methods.

The molecular design of SMP, programming methods, and functionalities of SMP are reviewed in this chapter. They will provide guidance for the design of novel SMP and widen their applications in different fields.

## 2.2 Molecular Design of Shape-memory Polymers

Various polymers and foreign materials can be used to construct different SMP to meet the requirements of applications. As mentioned in **Chapter 1**, SMP comprise netpoints and switch units. The netpoints (made of chemical or physical crosslinks) determine the permanent shape of a SMP. The chain segments should be sufficiently long and flexible to allow a certain orientation for required deformability. The recoiling of the chain segments enables the recovery of the permanent shape. The switch units (which are sensitive to the stimuli) are used to fix the temporary shapes of SMP. Various types of switches have been utilised for designing SMP: amorphous, semi-crystalline, liquid crystalline phases, and some functional units. The molecular

design of thermally sensitive, photosensitive and other types of SMP will be introduced in subsequent sections.

### **2.2.1 Thermally Sensitive Shape-memory Polymers**

Polymers are, in general, intrinsically viscoelastic materials with at least one thermally reversible phase transition (glass transition temperature ( $T_g$ ) or melting temperature ( $T_m$ )). In thermally sensitive SMP, the domains related to the highest transition temperature act as netpoints and the chain segments associated with the second highest transition temperature ( $T_{trans}$ ) act as switches. An amorphous phase with a  $T_g$ , a semi-crystalline phase with a  $T_m$ , and even an liquid crystalline (LC) phase with an isotropic temperature ( $T_i$ ) can be used as switches to construct SMP. SMP can be divided into three types based on the different phases of the switch:  $T_g$ -type,  $T_m$ -type and LC-type SMP. Among them, the crystallised phase, in general, provides the greatest mobility to the entire polymer chain above the  $T_m$ . With respect to the  $T_g$ -type SMP, a large rubber modulus can usually be maintained above the  $T_g$ . Thus,  $T_g$ -type SMP require a larger recovery force and have higher strength at low and high temperatures. LC-type SMP are accompanied by a significantly reversible change in orientation of the polymer chain, allowing the formation of reversible shape changes or two-way SME.

#### **2.2.1.1 Shape-memory Polymers based on the Amorphous Phase**

Various  $T_g$ -type polymers have been investigated due to their diversified amorphous switching segments, such as epoxy [3], polyether ether ketone [4], acrylate-type polymers [5, 6], polynorbornene [7], poly(lactic-co-glycolic) acid (PLGA) [8, 9] and poly(glycerol-co-dodecanoate) [10].  $T_g$ -type SMP exhibit relatively slow shape recovery compared with  $T_m$ - or LC-type SMP due to their broader glass transition interval, which hinders their application if immediate shape recovery is required. However,  $T_g$ -type SMP have become more attractive with the current widespread applications of SMP in biomedical areas [11]. Slow shape recovery of SMP is required not only for certain special clinical purposes (e.g., orthodontic applications) but also for avoiding insertion-induced tissue damage. For example, a self-deploying neuronal electrode made of a  $T_g$ -type SMP has been reported by Sharp and co-workers and a suitable slow recovery rate attained [12].

Another advantage of  $T_g$ -type SMP is that their shape recovery can be triggered by a solvent, such as water or organic solvents [13, 14], rather than the conventional heating stimulus. This phenomenon was first discovered by Huang and co-workers in 2004, and the proposed mechanism of sensitivity in shape-memory polyurethanes (SMPU) was due to the absorbed water weakening the H-bonding of the material.

Consequently, water/moisture reduced the  $T_g$  of the SMPU and triggered shape recovery at room temperature [15–17]. Inspired by their work, Du and Zhang [18] studied 13 types of organic solvents as stimuli in polyvinyl alcohol-based SMP systems. However, only four of those solvents triggered shape recovery. Their results showed that the solubility parameter and polarity of solvents determined the shape recovery.

Solvent-sensitive SME can be achieved by using a solvent as the plasticiser in  $T_g$ -type SMP, but the recovery stress is often very small. Additionally, solvent-induced recovery is strongly dependent upon sample size. Thus, bulky materials made of  $T_g$ -type SMP are not suitable for solvent-sensitive materials.

### **2.2.1.2 Shape-memory Polymers based on Semi-crystalline Phase**

Crosslinked polyethylene (PE) is thought to be the first type of SMP based on semi-crystalline phase switches. Since then, most synthesised polymers with a suitable  $T_m$  of  $\approx 20$ – $100$  °C have been used as switches in a physically or chemically crosslinked structure to prepare various  $T_m$ -type SMP. Current polymeric segments used as semi-crystalline-phase switches for SMP can be classified into three types: (i) polyolefins (e.g., PE) [19], poly(ethylene-co-1-octene) [20], *trans*-polyisoprene [21], *trans*-polycyclooctene (TPCO) [22] and poly(1,4-butadiene) [23]; (ii) polyethers (e.g., polyethylene oxide [24], polyethylene glycol (PEG) [25] and polytetramethylene ether glycol (PTMEG) [26]); (iii) polyesters (e.g., poly( $\epsilon$ -caprolactone) (PCL) [27–29], polybutylene adipate (PBA) [30] and poly(3-hydroxyalkanoates) [31]). Polyolefin-based SMP have few H-bonds between the switches and netpoints due to the inherently non-polar nature of polyolefin. Consequently, they often form a more complete micro-phase separation structure compared with polyether- or polyester-based SMP [21]. Thus, polyolefin-based SMP are good model compounds for theoretical studies of structure–property relationships due to the negligible effect of thermodynamic interactions [32].

Polyether- or polyester-based SMP usually have strong molecular interactions not only among the switches but also between the switches and netpoints. Therefore, considerable efforts have been devoted to enhancing the micro-phase separation of SMP (especially segmented SMP) to optimise their shape-memory properties [33, 34]. Researchers have used various strategies, such as introducing ionic groups [30, 35], mesogenic segments [36, 37] and aramid units [38, 39] into the hard segments of SMP. The ionic groups are meant to localise inter-molecular ionic interactions among the hard segments, whereas the mesogenic and aramid units should enhance the molecular-chain rigidity of the hard segments. Interestingly, the effects of the ionic and aramid units on the SME are quite complicated according to an in-depth investigation by Hu and co-workers [40, 41]. These units have a positive influence



on the shape-memory properties under a certain hard-segment content (HSC) range of SMP. Additionally, D'Hollander and co-workers introduced flexible polymeric segments such as polypropylene oxide between the hard and soft segments of PCL-based SMPU to enhance micro-phase separation [42]. As a result, the melting enthalpy of PCL segments increased, and the  $T_m$  region became narrower, indicating that the SME of SMPU can be improved by incorporating a suitable flexible segment.

### **2.2.1.3 Shape-memory Polymers based on Liquid Crystalline Phase**

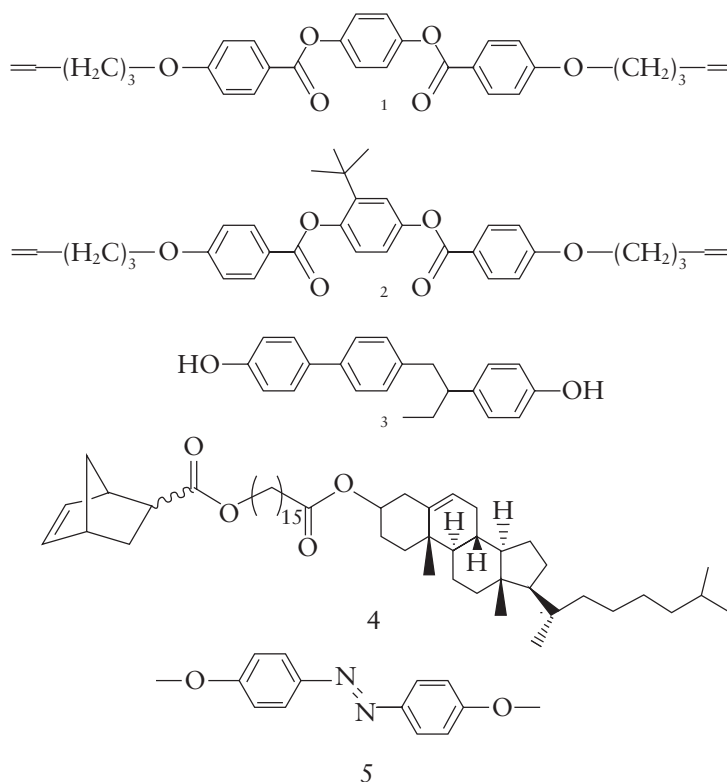
Liquid crystalline elastomers (LCE) show a first-order phase transition with an endothermic peak on heating curves, which shows the material's transition from an anisotropic to an isotropic phase. Similar to  $T_g$ - and  $T_m$ -type SMP, chemical or physical crosslinks are also required in  $T_i$ -type SMP made of LCE to exhibit SME.

Currently, the LC phase that serves as the shape-memory switch can be a nematic phase [43] or smectic phase [44]. Many types of LCE, including main-chain and side-chain, have been designed and prepared for use in SME by introducing various LC monomers into the elastomers [45]. Some typical LC monomers for constructing SMP are presented in **Figure 2.1**. For example, Rousseau and Mather [44] synthesised main-chain smectic-C LCE using two distinct mesogenic monomers. Monomer 1 (**Figure 2.1**) melted into a nematic phase at 136.6 °C and transitioned to an isotropic phase at 229.0 °C, whereas Monomer 2 possessed two similar transitions at lower temperatures (80.6 °C and 91.4 °C). Thus, the  $T_i$  of the final LCE is expected to vary depending on the ratio of the two types of monomers. Additionally, Ahn and co-workers [46, 47] thoroughly investigated the shape-memory behaviour of side-chain LCE based on Monomer 4. They demonstrated three one-way SME using two transition temperatures ( $T_g$  (22.5 °C) and  $T_i$  (103.5 °C)) and a combination of  $T_g$  and  $T_i$  as shape-memory  $T_{trans}$ , respectively. Notably, most of the LCE showed two-way SME [48, 49]. Moreover, these materials can be developed to show triple SME that memorise more than one shape because LCE, in general, possess a low  $T_g$  or  $T_m$ , in addition to the  $T_i$  mentioned above. LCE with two-way or triple SME will be introduced in the following section on functionality [46].

### **2.2.2 Photosensitive Shape-memory Polymers**

Photosensitive units are the most popular molecular switch. Light is a clean energy and can be controlled rapidly, precisely and remotely. Therefore, photo-deformable polymers have attracted increasing attention. Lendlein and co-workers [51] developed the first light-sensitive SMP (LSMP) by introducing photosensitive cinnamic groups into polymer networks to serve as molecular switches. In this way, SME could

be induced completely independently of any temperature effects using only light. Cinnamic groups form covalently crosslinked bonds under ultraviolet (UV)-light of  $\lambda > 260$  nm, whereas these bonds are cleaved under UV-light irradiations of  $< 260$  nm [52]. These LSMP exhibited a high shape recovery ratio ( $R_r$ ) but a low shape fixity ratio ( $R_f$ ). The maximal  $R_f$  of the graft polymers was only 52% when the strain was 20%. The low  $R_f$  of LSMP was due to the low efficiency of crosslinked bond formation from cinnamic groups *via* irradiation. After this research, a biodegradable LSMP comprising *N,N*-bis(2-hydroxyethyl) cinnamamide, poly(L-lactic acid) and PCL was synthesised by Wu and co-workers [1]. Compared with thermally induced SMP, the strain fixity of light-induced SMP was much lower. However, the unique characteristics of LSMP enabled shape recovery at room temperature using remote activation, which is more attractive for SMP in medical uses and other applications that require temperature constraints.



**Figure 2.1** Typical LC monomers or units for the synthesis of LCE with SME. Reproduced with permission from J.L. Hu, Y. Zhu, H.H. Huang and J. Lu, *Progress in Polymer Science*, 2012, 37, 12, 1720. ©2012, Elsevier [50]

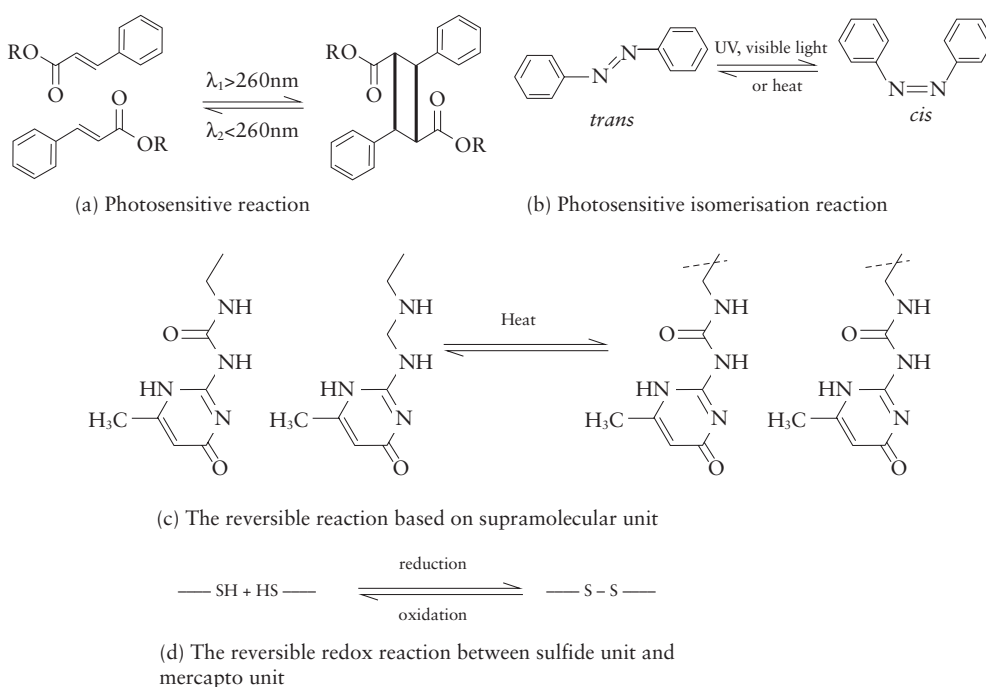
Photo-induced SME, like photo-induced contraction or bending, can also be achieved using LCE. In contrast to the LC monomers of thermally induced SME, the LC monomers of photo-induced SME usually contain photo-responsive moieties, like the structure of unit 5 in **Figure 2.1**. For example, films made of LCEs bend toward the direction of light irradiation, with the bending occurring parallel to the direction of light polarisation after exposure to light at 366 nm. When the bent film is exposed to visible light with a wavelength longer than 540 nm, it reverts back completely to its initial flat state. Moreover, the bending–unbending cycle of this mode can be repeated without apparent fatigue [53]. The molecular mechanisms of light-induced LCE and thermally induced shape-memory LCE are different, but both of their SME result from the LC phase transition.

### **2.2.3 Other Molecular Architectures of Shape-memory Polymers**

Besides the molecular design of SMP mentioned above, there are many other types of SMP design. In chemistry, there are many reactions that can be conducted readily in a reversible manner under special conditions, and the corresponding reversible units can be used as the molecular switches of smart polymers. Inspired by the first example of a reversible photosensitive unit as a shape-memory switch in 2005, researchers have been looking to exploit more reversible units to create new SMP. **Figure 2.2** shows three main types of reversible units (supramolecular, mercapto and photosensitive) which have been used successfully as switches to exhibit SME.

Mercapto units have been developed as molecular switches in SMP. In 2007, Aoki and co-workers [54] demonstrated shape-memory behaviour in cellulose acetate derivatives with a crosslinkable mercapto group (CA-MA). In this system, the on–off switching of the CA-MA was achieved through redox treatments. However, the recovery time for these films required  $\leq 96$  h. The SME ability of the CA-MA film decayed progressively with repeated redox treatments. Additionally, Yoshi and Ishida reported reversible networks that consisted of furyl-telechelic poly(1,4-butylene succinate-*co*-1,3-propylene succinate) prepolymer (PBPSF2) reacted by a Diels–Alder (DA) addition with a tri-maleimide linker. DA reactions with the linker above or below the  $T_m$  of PBPSF2 gave network polymers with soft or hard properties, respectively. The shape-memory characteristics of these materials were not discussed, but this chemistry represents a different mechanism to achieve  $T_m$ -triggered SME compared with conventional  $T_m$ -type SMP [55]. These results show that DA reactions can also be used to trigger the shape recovery of polymers.

*Shape-memory Polymers: Molecular Design, Shape-memory Functionality and Programming*



**Figure 2.2** Reversible reactions/interactions based on three types of units as shape-memory switches. Reproduced with permission from J.L. Hu, Y. Zhu, H.H. Huang and J. Lu, *Progress in Polymer Science*, 2012, 37, 12, 1720. ©2012, Elsevier [50]

In the past 5 years, reversible supramolecular units have been utilised in SMP to fix the temporary shape. Non-covalent H-bonding interactions (the most common supramolecular interaction) can dissociate at elevated temperatures, making the materials readily deformable. However, the association of H-bonds at low temperatures can stabilise a deformed strain. Based on this mechanism, Anthamatten and co-workers as well as Hu and co-workers fabricated shape-memory elastomers that contained an H-bonding moiety, ureidopyridinone (UPy), as the side-group. In these elastomers, the thermally sensitive UPy moieties were used to attain reversible fixing of the temporary shape [56, 57]. Similarly, Guan and co-workers synthesised a biomimetic modular polymer composed of a tandem array of cyclic UPy modules that closely mimicked the architecture of the protein titin. This novel polymer possesses excellent thermally sensitive SME, along with a high Young's modulus ( $\approx 200$  MPa) and high toughness [58].

Chen and co-workers also exploited another H-bonding system formed by pyridine moieties as H-acceptors [59] to synthesise PU supramolecular networks using a

pyridine derivative: (Py-SMPU). Interestingly, the SME of Py-SMPU were triggered not only by heat [60] but also by moisture [2]. Moreover, the moisture-sensitive SME of Py-SMPU were controlled easily by humidity and temperature. Subsequently, the SME mechanism, structure and morphology of this supramolecular network were also investigated [60, 61], confirming that the H-bonds present in the urethane group and pyridine ring played an important part in movement of the polymer chain. The detailed reports are detailed further in **Chapter 8**.

More recently, another special supramolecular reversible crosslinking moiety, in the form of metal–ligand coordination bonds, was also used to fix and release a temporary shape by Kumpfer and Rowan [62]. Because of a metal–ligand hard phase as the switch, three different types of stimuli (heat, light, solvents) that result in softening of the hard phase and increased decomplexation or rate of exchange of the metal–ligand complexes can be used to attain shape-memory function of the polymer networks. Additionally, this material could selectively target a localised shape-memory response of the temporary shapes triggered by light, due to their low thermal conductivity.

Supramolecular units as shape-memory switches can offer a great opportunity to create diversified shape-memory performances and unexpected properties in the resultant SMP. Therefore, exploiting and studying SMP with supramolecular switches are valuable investigation directions for SMP.

## **2.3 Shape-memory Programming**

Time-delayed viscoelastic recovery and rubber elasticity are typical features of polymeric materials, and are the basis of the shape-memory behaviour of SMP. However, the shape-memory behaviour of a given polymer is the result of an appropriate combination of the molecular design of the material and programming rather than an intrinsic property. Under different programming methods, SMP show various SME, including one-way, two-way, triple SME and multiple SME.

### **2.3.1 Processing One-way Shape-memory Effects**

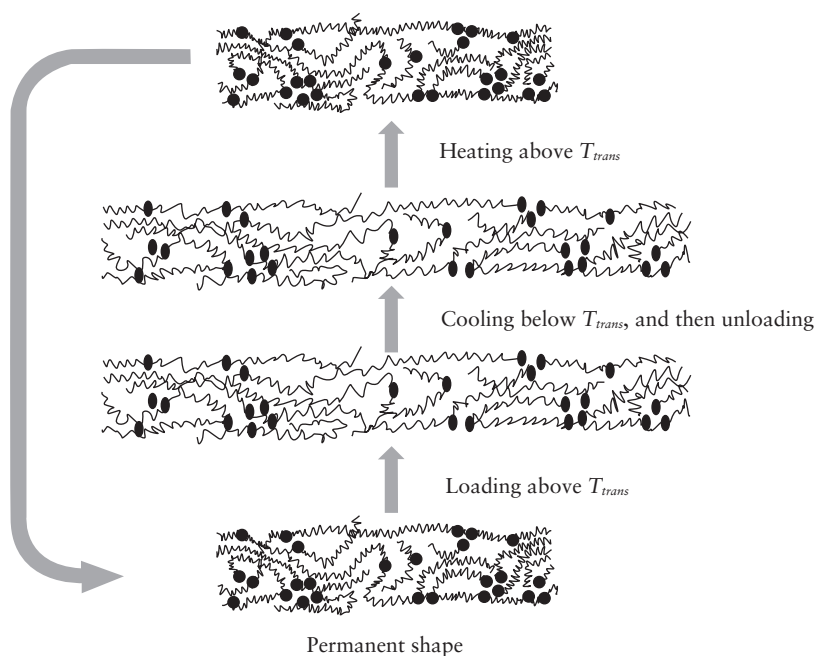
One-way SMP can retain a temporary shape once the stimulus is terminated. As increasing numbers of programming protocols are devised and reported, one-way SMP seemed to be much more flexible, versatile and applicable than two-way SMP because of easy programming. The programming step was carried out by deforming the specimens above the  $T_m$  and cooling the deformed specimens under fixed-strain conditions below the crystallisation temperature. The deformed specimen could recover to its initial shape when heated above the  $T_m$ .

### **2.3.1.1 Dual-shape Creation Process for One-way Dual-shape Shape-memory Effects**

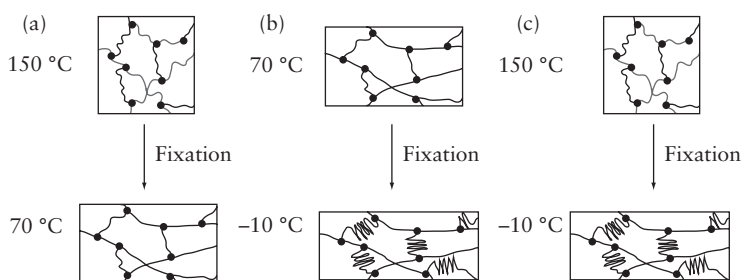
The tailored processing and programming technology used for one-way dual-shape SME is also termed as the ‘dual-shape creation process’ (DSCP). Conventional dual-shape SMP contain one switching domain with a related  $T_{trans}$ , which can be the  $T_m$  or  $T_g$ . The dual-shape effect is triggered by heating the material above the switching temperature ( $T_{sw}$ ).

As an example, a dual SME was imparted to the fibre in the work of Meng and co-workers [63]. The shape-memory fibre was prepared by wet spinning using polycaprolactone diol as the soft segment. The  $T_{sw}$  was the  $T_m$  of the soft segment phase. During programming, the fibres were heated to 70 °C and stretched to 100% strain at 10 mm/min, after which the fibres were cooled to ambient temperature whereas the same strain was maintained for 15 min. Afterwards, clamps were unloaded so that they returned to their original position at 40 mm/min. The SME of the fibre is illustrated in **Figure 2.3**. When the fibre is heated above the  $T_{trans}$ , the soft segment phases melt. If they are stretched, the soft segment phases are extended. When the temperature is cooled below the  $T_{trans}$  and the fibre is maintained at constant strain, and the soft segment phases crystallise. The internal stress is stored in the fibre and the associated deformation fixed temporally. When it is reheated to above the  $T_{trans}$ , its soft segment phase becomes flexible. It returns to a folded configuration because of the internal stress stored between hard segments. As a result, the fibre recovers to its original length.

The dual-shape capability can also be obtained from a multiphase polymer by dual-shape programming. Marc and co-workers investigated three temperature ranges for the programming of a graft-polymer network from PCL-dimethacrylates as macro-crosslinkers and PEG monomethyl ether-monomethacrylate to form grafted side chains having a ‘dangling’ end [64]. These temperature ranges allowed for use of the crystallisable PCL phase or crystallisable PEG phase individually or simultaneously to fix a temporary shape. If only one phase was used for fixation of the temporary shape, the materials showed dual-shape recovery behaviour in which the  $T_{sw}$  was closely related to the  $T_{trans}$  of the domains used for temporary fixation. Different switching phases can be used for fixation of a temporary shape by a dual-shape programming mechanism (**Figure 2.4**). By adjustment of the temperature range in which the experiment is carried out, the different switching phases can be selected.



**Figure 2.3** Molecular mechanism of SME of SMF (schematic). The zig-zag represents the coiled or folded chains of polyols, and circles represent isocyanate groups. SMF: shape-memory fibre . Reproduced with permission from Q. Meng, J. Hu, Y. Zhu, J. Lu and Y. Liu, *Journal of Applied Polymer Science*, 2007, 106, 4, 2515. ©2007, John Wiley & Sons [63]

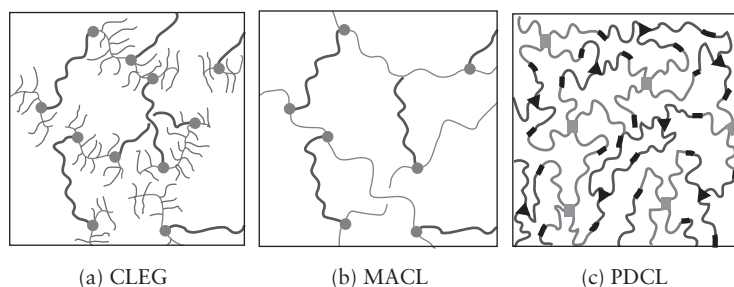


**Figure 2.4** Molecular mechanism for three methods of one-step dual-shape programming for AB polymer networks: (a) fixation by vitrification of the PCHMA phase; (b) fixation by crystallisation of PCL segments; and (c) fixation by PCHMA and PCL phases. PCHMA: polycyclohexyl methacrylate. Reproduced with permission from M. Behl, I. Bellin, S. Kelch, W. Wagermaier and A. Lendlein, *Advanced Functional Materials*, 2009, 19, 1, 102. ©2009, John Wiley & Sons [64]

### 2.3.1.2 Programming for One-way Triple-shape Shape-memory Effects

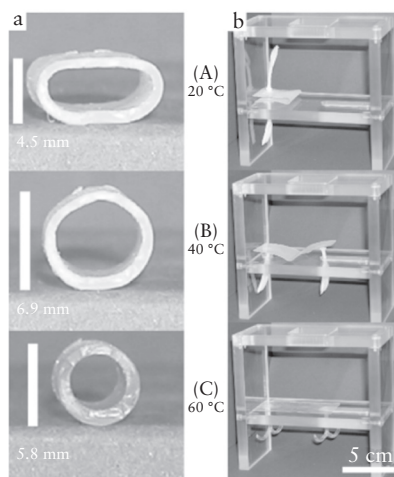
Triple-shape polymers can switch from the first temporary shape (A) to the second temporary shape (B) and from there to the permanent shape (C) when stimulated by subsequent temperature increases. In triple-shape polymer networks shape (C) is determined by covalent netpoints. Shapes (A) and (B) are fixed temporarily by a respective switching domain which is assigned to a corresponding  $T_{\text{trans}}$ .

Commonly, two-step programming is necessary to achieve triple-shape functionality, which allows stepwise creation of the two independent shapes (A) and (B). Bellin and co-workers developed three polymer networks with triple SME (**Figure 2.5**) through two-step programming [65]. In the creation of temporary shapes A and B, the polymer network is heated to higher order transition temperature ( $T_{\text{high}}$ ), at which point the material is in an elastic state, and is deformed. When the material is cooled to the lower order transition temperature ( $T_{\text{low}} < T < T_{\text{high}}$ ) and external stress is maintained, and physical crosslinks established. In molecular networks consisting of PCL (MACL) and polycyclohexyl methacrylate (PCHMA) segments, crosslinks are formed by freezing the PCHMA domains; in molecular networks consisting of PEG and PCL (CLEG), the crosslinks are formed by partially crystallising the PCL segments. Finally, shape B results after release of external stress. In the second step, shape A is created. The sample, which presently is in shape B, is deformed further at  $T_{\text{low}} < T < T_{\text{high}}$ . Cooling under external stress to  $T_{\text{low}}$  leads to a second set of physical netpoints; crystalline domains are formed by PCL segments in MACL networks and by PEG segments in CLEG networks. These new physical crosslinks stabilise shape A, which the material takes when the external stress is released. Reheating to  $T_{\text{high}}$  recovers shapes B and C sequentially (**Figure 2.6**).



**Figure 2.5** The polymer network architecture of (a) CLEG; (b) MACL; and (c) PDCL networks. PDCL: PCL dimethacrylate. Reproduced with permission from J. Zotzmann, M. Behl, D. Hofmann and A. Lendlein, *Advanced Materials*, 2010, 22, 31, 3424. ©2010, John Wiley & Sons [66]





**Figure 2.6** Photographs illustrating the triple-shape effect. Two different demonstration objects prepared from CLEG: (a) tube; and (b) fastener consisting of a plate with anchors. Reproduced with permission from I. Bellin, S. Kelch, R. Langer and A. Lendlein, *Proceedings of the National Academy of Sciences*, 2006, **103**, 48, 18043. ©2006, United States National Academy of Sciences [65]

More importantly, a triple-shape capability could also be created by one-step programming. Marc and co-workers selected AB polymer networks based on PCL and PCHMA to generate triple SME [64]. The results showed that the triple-shape behaviour is influenced by the PCL content of the AB polymer network and the mechanical deformation applied during programming. The PCHMA phase and PCL phase contribute to fixation of the temporary shape for materials with PCL content of 35–60 wt%. Therefore, a triple SME could be obtained utilising one-step dual-shape programming because these two types of polymer chain segments forming different switching phases were covalently linked with both chain ends to the polymer network.

### **2.3.2 Processing Two-way Shape-memory Effects**

One-way SMP can satisfy the requirements of a wide variety of applications when these require only a single cycle to be carried out. By contrast, development of polymers featuring reversible shape-memory behaviour may fulfill the requirements of applications such as sensors and actuators. For two-way SME, the temporary shapes can be recovered to the initial shape when the stimulus is terminated. Reversible behaviour occurs during heating and cooling in the presence or absence of external stress.

### **2.3.2.1 Programming for Two-way Dual-shape Shape-memory Effects**

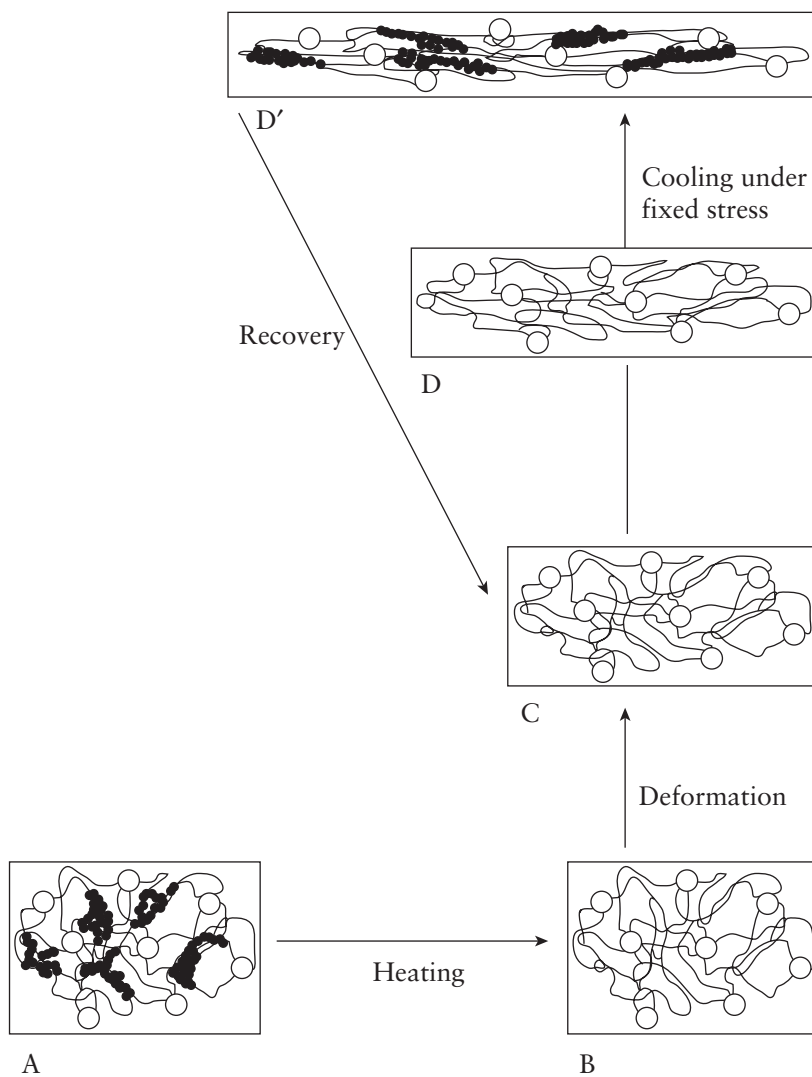
As mentioned in **Section 2.2.1.3**, LCE are commonly used as two-way SMP because they can undergo cyclic elongation–contraction when subjected to a cooling–heating cycle across the isotropic–nematic transition under a non-zero applied stress [49]. Semi-crystalline networks (in which covalent crosslinks are combined with crystalline regions that act as thermal switches) are usually employed as one-way SMP. Recently, a further advantage of this type of polymer was reported, i.e., the ability to display a two-way SME under specific thermo-mechanical conditions [67]. It could undergo similar elongation–contraction cycles when under an applied stress, was cooled, heated, and cooled again on a thermal region ranging from above the  $T_m$  to below the crystallisation temperature. Due to their easier and cheaper preparation, and the possibility to readily tailor elongation capabilities by changing the molecular architecture, semi-crystalline networks have gained popularity over LCE.

Pandini and co-workers studied the two-way SME of semi-crystalline networks based on sol-gel crosslinked PCL [68]. **Figure 2.7** displays the two-way shape-memory cycle of the networks. The semi-crystalline material (A) is heated above the  $T_m$  (B), deformed at a given stress (C) and by cooling under fixed stress undergoes an entropy- and crystallisation-driven elongation (D and D', respectively) to finally recover the pre-stretch shape when heated above the  $T_m$ . This two-way property was achieved by applying similar thermo-mechanical heating–cooling histories while maintaining specimens under a constant non-zero load (rather than under constant strain as in one-way programming).

Imai and co-workers developed a novel actuator of two-way behaviour by using two types of SMP with different  $T_g$  values ( $T_{g1} < T_{g2}$ ) [69]. During programming, a memory shape relating to  $T_{g1}$  is formed, canceled by the memory shape relating to  $T_{g2}$  at  $T_{g2}$  (i.e., the memory shape of  $T_{g2}$  is set to the reverse shape of the memory shape of  $T_{g1}$ ). This method needs only the temperature cycle of heating and cooling to operate the actuator. This simple operating method is suitable for small-sized actuators.

### **2.3.2.2 Programming for Two-way Triple-shape Shape-memory Effects**

Reversible triple SME have attracted much attention because of their potential applications in various fields. Zotzmann and co-workers created two-way multiphase polymer networks containing two crystallisable segments [66]. Their  $T_m$  and crystallisation temperatures were well separated and they exhibited sufficient elasticity at  $T_{high}$ . The network containing polypentadecalactone- and PCL-segments was prepared and showed reversible triple shape-memory behaviour (**Figure 2.8**).

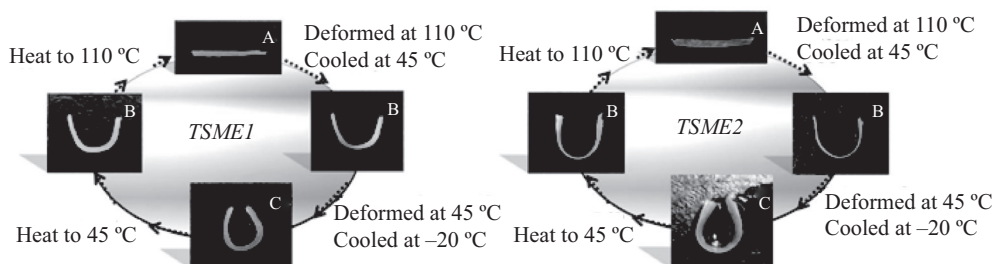


**Figure 2.7** Structural evolution during a two-way shape-memory cycle (schematic). Reproduced with permission from S. Pandini, F. Baldi, K. Paderni, M. Messori, M. Toselli, F. Pilati, A. Gianoncelli, M. Brisotto, E. Bontempi and T. Riccò, *Polymer*, 2013, 54, 16, 4253. ©2013, Elsevier [68]



**Figure 2.8** Examples of reversible shape-memory behaviour. Reproduced with permission from J. Zotzmann, M. Behl, D. Hofmann and A. Lendlein, *Advanced Materials*, 2010, **22**, 31, 3424. ©2010, John Wiley & Sons [66]

Zhang and co-workers designed and developed a novel triple-shape network based on thermally reversible chemical crosslinking through a Diels–Alder reaction [70]. The obtained poly(*p*-dioxanone) (PPDO)-PTMEG co-network possessed two independent SME based on the  $T_m$  of the PPDO-bisfuranic (BF) and PTMEG-BF segments, and permanent shape was maintained by thermo-reversible chemical crosslinking. The Diels–Alder reaction was carried out under mild conditions (75 °C) without a catalyst. The thermo-reversible character of the Diels–Alder adduct allowed netpoint cleavage under thermal treatment at 150 °C, which was accelerated by dimethyl formamide. For the SME, the first and recovered semi-crystalline crosslinked triple-shape co-network exhibited excellent triple-shape-memory properties (**Figure 2.9**).



**Figure 2.9** Triple-SME of the initial Diels–Alder co-network (TSME1) and recovered Diels–Alder co-network (TSME2). Reproduced with permission from J. Zhang, Y. Niu, C. Huang, L. Xiao, Z. Chen, K. Yang and Y. Wang, *Polymer Chemistry*, 2012, **3**, 6, 1390. ©2012, RSC Publishing [70]

### **2.3.3 Multiple Shape-memory Effects Programming**

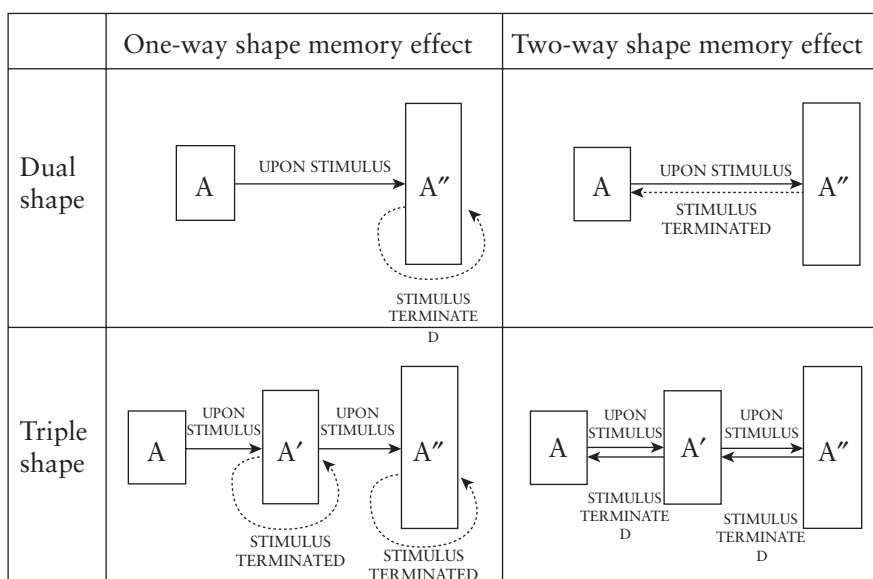
Xie and co-workers used perfluorosulfonic acid (PFSA), which has only one broad reversible phase transition, to achieve a multiple SMP through programming [71]. The permanent shape for PFSA was defined by the equilibrium length after annealing. In a typical thermally activated dual-shape memory cycle, a SMP is deformed at an elevated temperature (deformation temperature) and the deformed temporary shape is fixed upon cooling. When heated to a recovery temperature, the permanent shape is recovered. The results suggested that the polymer memorised not just the strain, but also the thermo-mechanical history. The simple one-step programming for this multiple SME shows great potential in practical applications.

## **2.4 Shape-memory Functionality**

The approaches to designing different shape-memory functions have become more abundant as scientists better understand the SME mechanism of SMP and as the types of SMP materials diversify. The development of shape-memory functions of SMP is growing rapidly (Figure 2.10). Apart from one-way SME, two-way, triple, multiple SME and even temperature-memory effects have been investigated widely in SMP. Moreover, two and even three types of shape-memory functions can be achieved simultaneously in the same SMP material [49, 63]. An example of this is an SMP network composed mainly of star-shaped hydroxy-telechelic poly( $\omega$ -pentadecalactone) (PPD) and PCL, herein named the PDCL network, that shows one-way, two-way and triple SME under different programming [66].

### **2.4.1 One-way Shape-memory Effects**

Scientists once thought that one-way SME were not good enough for many applications because they were the most simple and common SME of SMP, so they began to explore two-way SME of polymers. However, as increasing numbers of programming protocols are devised and reported, one-way SMP have been found to be much more flexible, versatile and applicable than two-way SMP because two-way SME are difficult to programme or do not require programming. One-way SME have their original shapes predefined in the manufacturing process, whereas temporary shapes can be varied based on different shape-memory programming processes. There are several evaluation methods for characterising one-way SME: cyclic tensile investigation [72], strain recovery process [73], bending tests [74, 75] and shrinkage determination [76].



**Figure 2.10** Shape-memory functionality of SMP. Reproduced with permission from J.L. Hu, Y. Zhu, H.H. Huang and J. Lu, *Progress in Polymer Science*, 2012, 37, 12, 1720. ©2012, Elsevier [50]

Considerable effort has been devoted to determining the factors that influence the shape-memory performance of SMP of one-way SME. Different factors have been studied using common one-way SME systems (SMPU and SMPU ionomers), including the segment contents [26, 31, 77], molecular weight and crystallisation of soft segments [27, 77], ionic group contents [41], thermo-mechanical cyclic conditions (i.e., deformation and fixing speed [78] and maximum strain [72]), and processing conditions [79]. In 2008, Ratna and Karger-Kocsis wrote a comprehensive review on the shape-memory properties of SMPU with different structures, and focused particularly on the  $R_r$  and  $R_f$  of SMPU [33]. The segment contents and molecular weight of soft segments have a vital role on shape-memory properties, particularly  $R_r$ ,  $R_f$  and shape recovery stress [26–28, 38].

**Figure 2.11** illustrates the dependency of the  $R_r$  and recovery stress on the temperature of SMPU with various HSC. The SMPU with 10 wt% HSC had no hard-segment domains, while those with 15 wt% HSC had more or less hard-segment domains. The SMPU with 15 wt%  $\leq$  HSC  $\leq$  40 wt% exhibited good shape recovery (over 90%), while the shape recovery dramatically dropped as the HSC increased above 45 wt% [27] due to the hard-segment domains changing from isolated states into

interconnected states (Figure 2.12). The crystallinity of the soft segment phase decreased and the interdomain spacing reduced, while the number and size of the hard-segment domains rose with increasing HSC. The recovery stress can be adjusted by varying the HSC. Specifically, the presence of rigid chain extenders can result in higher recovery stress [38]. Thus, achieving good one-way SME requires a microdomain morphological structure with isolated hard domains. Additionally, the adequate molecular weight of the soft segments, particularly in  $T_m$ -type SMPU, are a prerequisite for achieving good shape-memory properties, and their optimum molecular weight is generally 4,000-6,000 g/mol [72]. Therefore, by varying the content of the soft or hard segments, the molecular weight of the soft segments and the preparation process, we can adjust the morphologies of SMPU and thus control the shape-memory properties.

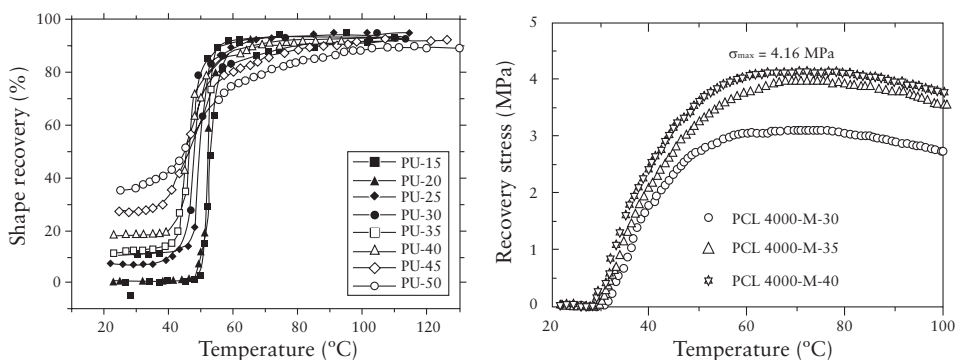
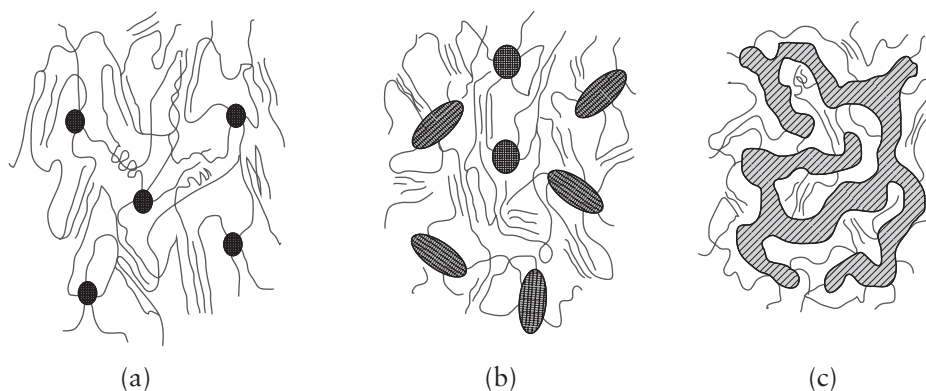


Figure 2.11 Shape recovery and recovery stress of SMPU with various HSC. Reproduced with permission from F.L. Ji and J.L. Hu, *High Performance Polymers*, 2011, 23, 4, 314. ©2011, SAGE Publications [38]

## 2.4.2 Two-way Shape-memory Effects

Research on smart materials with two-way SME has attracted considerable attention because these materials can change their geometries provided that they are exposed to an external stimulus. In addition to classical approaches such as SMA, many polymeric materials and approaches are under active investigation, including LCE, SMP under constant stress, and laminated polymer composites.



**Figure 2.12** Model of microdomain formation in SMPU with different HSC (a) 15% and 20% HSC; (b) 25%, 35% and 40% HSC; and (c) 45% and 50% HSC. Reproduced with permission from F.L. Ji, J.L. Hu, T.C. Li and Y.W. Wong, *Polymer*, 2007, 48, 17, 5133. ©2007, Elsevier [27]

### 2.4.2.1 Liquid Crystalline Elastomers

As mentioned in Section 2.2.1.3, the most interesting property of LCE is their ability to change their shape reversibly after applying a defined external stimulus, such as heat [80], light [81], electric field [82] and humidity [83]. This feature was predicted by de Gennes in 1975 and realised by Finkelmann and co-workers in 1981 [84]. This phenomenon is commonly referred to as ‘reversible contraction/extension’ in the LCE field, while recently, with the rapid development of SMP, more authors prefer the term ‘SME’ [45] or ‘two-way SME’ [49]. During the past three decades, LCE have attracted scientific and industrial interests as a result of their reversible strain actuation and potential applications (e.g., artificial muscles, soft actuators and nonlinear optical devices). They have been the subject of several reviews [81, 85–87]. The main aim of this section is to focus on the basic mechanisms of thermo-sensitive and light-sensitive two-way SME in LCE and current technological advances.

Thermo-sensitivity in two-way LCE results from a coupling between the liquid crystalline ordering of mesogenic moieties and the elastic properties of the polymer. When a LCE film is heated toward the anisotropic–isotropic phase-transition temperature, the mesogens become disordered, and the film, in general, contracts. When the temperature is lowered below the phase-transition temperature, the LCE film expands back to its original size [88]. However, to observe the unique properties of LCE on a macroscopic scale, the mesogens must be aligned uniformly over the whole



sample, yielding a liquid crystalline monodomain, which is an important prerequisite. Thus, producing LCE with two-way SME, in general, includes two procedures: the synthesis of LCE materials and the formation of the liquid crystalline monodomain [85, 89]. Currently, a maximum spontaneous elongation  $\leq 500\%$  has been achieved in LCE fibres by Ahir and co-workers [43]. Such large elongation occurred because the nematic ordering and telechelic crosslinking occurred simultaneously, resulting in a high degree of alignment and uniformity during the high shear of fibre drawing. Obviously, the requirement of the liquid crystalline monodomain has restricted the broader application of two-way LCE as smart materials. However, in 2009, Qin and Mather reported that a glass-forming polydomain nematic network also exhibited quite a large two-way SME comparable with monodomain LCE [49]. This phenomenon was associated with a polydomain–monodomain transition at relatively low temperatures. Thus, the polydomain LCE may offer an efficient and simple alternative to their monodomain counterparts because they do not require alignment procedures during processing.

LCE containing azobenzene units are the most widely investigated photomechanical polymers for two-way light-sensitive SME [90, 91]. In those systems, the driving force for deformation arises from the variation in the alignment order. Upon UV-light irradiation, the azobenzene-containing LCE show reduced alignment order and even an isotropisation phase transition. Usually, the rod-like trans-azobenzene moieties stabilise the LC alignment, whereas the bent *cis* forms reduce the LC order parameter. Thus, on a macroscopic level, reversible shape changes such as bending and unbending are achieved in the azobenzene-containing LCE. The research team of Ikeda has conducted extensive research in this field, producing a film [52] and fibre [92] that can repeatedly and precisely bend along any chosen direction using linearly polarised light. They also studied the effect of the concentration and location of azobenzene units on the photomechanical properties of LCE, and found that the photoisomerisation of azobenzene units at the crosslinks has more pronounced effects than at the side chains [93]. Recently, Ikeda and co-workers wrote a comprehensive review on the photomechanical effects of LCE and other polymers [81], which concluded that LCE are the most promising materials for constructing artificial muscles driven by light. However, there are many problems, such as fatigue resistance and the biocompatibility of LCE, which need further investigation.

#### **2.4.2.2 Shape-memory Polymers having a Semi-crystalline Phase under Constant Stress**

Another category of two-way SMP is based on the principle of the crystallisation-induced elongation (CIE) that occurs during cooling and melting-induced contraction (MIC) upon heating under constant stress based on  $T_m$ -type SMP systems. During

cooling to  $T_{\text{low}}$  under constant stress, CIE was attributed to the formation of crystallites in the load direction. When heated from  $T_{\text{low}}$  to  $T_{\text{high}}$ , the increased elongation caused by the CIE can be reversed by the MIC. Thus, by applying a constant stress, crystals are formed along a single preferred orientation in these systems, and the semi-crystalline phase shows reversible shape changing. Therefore, one-way, two-way and even triple SME can be achieved in semi-crystalline polymer networks. Two-way SME under constant stress was first reported by Chung and co-workers in 2008 [94]. They found that a simple one-way SMP, crosslinked polycyclooctene, could exhibit tensile elongation ( $\approx 25\%$ ) upon cooling and complete tensile contraction on heating under a constant stress of 600 kPa. The mechanism of CIE was investigated by wide-angle X-ray diffraction (WAXD) methods. The results suggested that, by increasing the stress, crystallisation was promoted increasingly along the uniaxial axis, thereby leading to greater elongation. Subsequently, a series of systems based on semi-crystalline PCL segment, such as the polyhedral oligomeric silsesquioxanes (POSS)/PCL networks [95], SMPU [96], and chemically crosslinked PCL [97], have been shown to exhibit two-way SME under an appropriate constant tensile load. Among these systems, the chemically crosslinked PCL possesses the best two-way shape-memory properties: the maximum strain increment is 44% with a recovery ratio of 85% under a stress of 0.4 MPa. In addition, a detailed investigation of SME of chemically crosslinked semi-crystalline poly(ethylene-co-vinyl acetate) was reported by Xie and co-workers [98, 99]. Their results suggested that a high gel fraction of the system ( $>75\%$ ) was required for good two-way SME. Research on two-way SME under constant stress is not yet sufficient. However, recent results suggest an opportunity to exploit all the common  $T_m$ -type SMP to exhibit two-way SME under special conditions and certain constant stress with CIE and MIC mechanisms.

#### **2.4.2.3 Shape-memory Polymer Laminated Composites**

Much research has concentrated on developing two-way SME using composite technologies. Previous two-way SMP laminated composites focused mainly on SMA/polymer composites. Research teams led by Winzek and Tobushi developed thin SMA/polymer composites [100] and SMA/SMP composites [101], respectively. In the SMA/SMP composite, two-way bending deformation with an angle of  $56^\circ$  was observed. In fact, the two-way SME of the SMA/polymers or SMA/SMP composites resulted from the SME and the super-elasticity of the SMA during heating and cooling.

Two-way SMP composites based on pure polymeric materials by layer methods (similar to bimetal) were not reported until 2008 [102]. Hu and co-workers achieved reversible bending/unbending behaviour in pure SMP composites prepared using two types of one-way SMP films [102, 103]. The driving force of the two-way SME resulted from a combination of the recovery force in the SMP layers during

heating and elasticity or stiffness of the other polymer layers. Two repeatable two-way SME cycles are shown in **Figure 2.13**, and the results of dynamic mechanical analyses suggested that >5 cycles could be repeated. Subsequently, Tamagawa used the mismatch in the thermal expansion and contraction coefficients between a pure epoxy resin and a fibre-reinforced resin to fabricate another polymeric laminate with two-way SME behaviour [104]. Most recently, Qi and co-workers developed a pure two-way SMP laminated composite by embedding pre-stretched SMP into an elastomeric matrix. This resultant composite could show two-way SME in response to changes in temperature without a constant external load. A transversal actuation of 10% in actuator length was achieved [105]. This work suggests that two-way SME can be undertaken more simply in SMP.

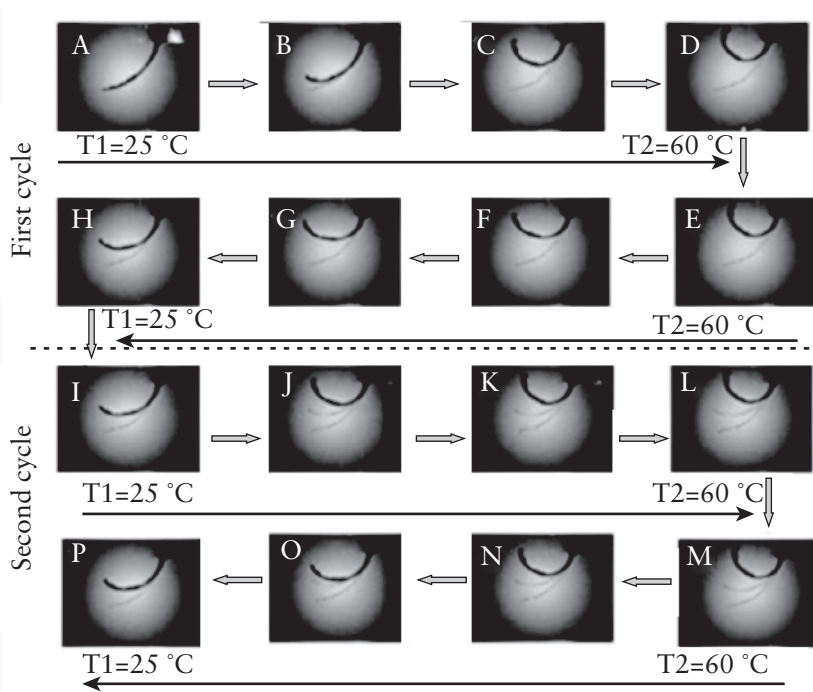
Compared with two-way SMA or SMA/polymer laminated composites, these SMP composites are capable of much larger recoverable strains, and their reversible deformation is controlled easily by the hardness, thickness and deformation ratio of the SMP layers. Moreover, their two-way SME can be achieved readily without external stress. Thus, composite technologies based on SMP have great promise for future applications due to their diverse advantages: easy fabrication, easy application, as well as tunable mechanical and shape-memory properties. More SMP composite systems will be studied as highly attractive actuator materials.

### **2.4.3 Triple/Multiple Shape-memory Effects**

Unlike traditional one-way SMP, triple SMP can fix two temporary shapes and recover sequentially from the first temporary shape (shape A') to the second temporary shape (shape A''), and eventually to the permanent shape (shape A) upon a certain stimulus (**Figure 2.10**). In general, a triple SMP is ascribed to a multiphase polymer network that contains  $\geq 2$  separated domains, which are associated with individual transition temperatures. Triple SME have been achieved in chemically [64] or physically [106] crosslinked networks, LCE [107] and even in a system with a bilayer structure [108].

Behl and Lendlein fabricated three types of chemically crosslinked networks with triple SME [11]. The first was a CLEG network obtained by incorporating PEG segments as side chains with one end 'dangling' into a PCL network. The second was a MACL network consisting of polycyclohexyl methacrylate chains crosslinked by PCL segments. The third was a network of crosslinked star-shaped hydroxy-telechelic PPD and PCL, i.e., a PDCL network (**Figure 2.5**) [11, 65]. The triple SME of these three networks can be observed through a general two-step programme. More importantly, a single-step process (similar to a conventional dual-shape programme) can also generate triple SME for the latter two types of networks [64]. This single-step process facilitates triple-shape technology. Subsequently, based on the PDCL

network, they developed reversible triple SME by using the CIE and MIC capabilities of PPD and PCL segments [66]. Similarly, Kolesov and Radusch also studied the triple SME of chemically crosslinked blends from poly(ethylene-co-1-octene) that had different degrees of branching and/or linear PE. Only the crosslinked system of 50% PE/50% poly(ethylene-co-1-octene) 30 demonstrated a pronounced triple SME due to its distinctly segregated phase morphology [109]. Most recently, a novel triple SMP system was reported by Voit and co-workers. Its triple SME resulted from the combination of the  $T_g$  of acrylate-based segments and the dissociation of UPy supramolecular units in a chemically crosslinked network [110].



**Figure 2.13** Two-way SME observed in SMPU laminated composites. Reproduced with permission from S. Chen, J. Hu and H. Zhuo, *Composites Science and Technology*, 2010, 70, 10, 1437. ©2010, Elsevier [103]

The 4 types of systems mentioned above are chemically crosslinked networks that determine the permanent shape of triple SMP. Recently, Hu and co-workers created triple SME in physically crosslinked SMPU with multiple crystalline phases. In this

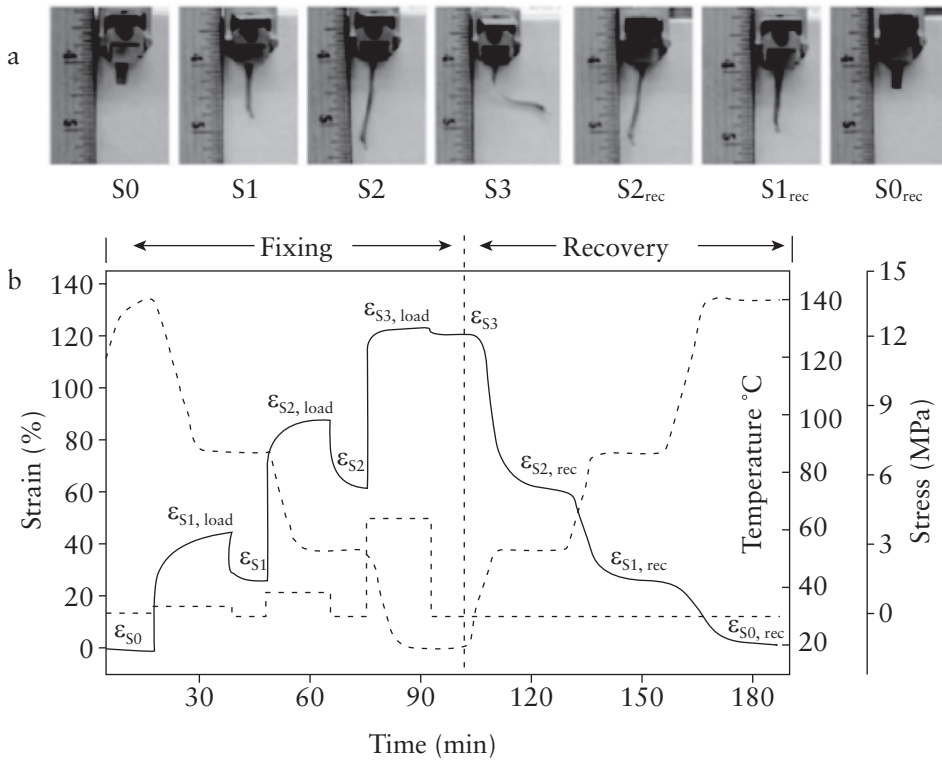
system, the triple SMPU consisted of two soft segments, PCL and PTMG, with a different  $T_m$ . A two-step programme for shape recovery was achieved when the mass proportion of PCL to PTMG reached a balanced value (e.g., 3:5). In addition, Pretsch studied the triple SME of a polyester urethane with semi-crystalline PBA as the soft segment [111, 112] and star-shaped POSS-PCL networks [113]. In these two systems, the very low  $T_g$  of PBA and PCL were also used as the  $T_{trans}$  of the triple SME. Therefore, this triple-shape-memory behaviour may not be attractive.

Mather and co-workers reported a side-chain liquid crystalline network (SCLCN) that can fix two temporary shapes through the first isotropic–nematic transition ( $\approx 150$  °C) and then through the glass transition ( $\approx 80$  °C). Heating the fixed sample led to complete and sequential recovery of two temporary shapes [49]. More recently, another type of SCLCN system exhibiting triple SME has been investigated by Ahn and Kasi [107]. They demonstrated that a sufficient extent of motional decoupling between mesogen-rich and backbone-rich domains is a key factor in creating a triple SME in the SCLCN system.

In 2009, Xie and co-workers synthesised triple SMP with a bilayer structure consisting of two epoxy dual-SMP of well-separated  $T_g$  [108]. The triple SME of those bilayer epoxy samples could be explained by a stress-balancing mechanism. The epoxy liquid mixture with a high  $T_g$  was first cured in a mould to produce the first layer, and then a mixture with a low  $T_g$  was poured on top of the first layer and cured. The final product showed a strong interface due to the reaction among the residual epoxy or amine groups on the surface of the two layers (which is a key factor for the triple SME behaviour of the bilayer). Another cohesive bilayer of two films composed of epoxy-silica nanocomposites with different components also demonstrated triple SME with shape fixation. This material showed a recovery rate  $>80\%$  as well as synergistic mechanical properties such as the modulus and strength [114].

After investigations of triple SMP, Xie and co-workers used the broad glass transition of  $T_g$ -type polymers to demonstrate multiple SME, which can remember more than two temporary shapes. Quadruple SME have been created through only one broad glass transition (from  $\approx 55$  to  $\approx 130$  °C) of commercial PFSA ionomer in 2010. **Figure 2.14** shows the quadruple shape-memory properties of PFSA [71]. They also systematically investigated the influence of thermo-mechanical conditions on these multiple SME of PFSA. The results suggested that the programming and recovery heating methods significantly affect multiple shape-memory properties when constructing multiple shape-memory cycles [115]. More recently, the Xie research team exploited new multiple SME systems based on multi-composite SMP made of a  $Fe_3O_4$ -SMP region and a carbon nanotube (CNT)-SMP region separated by a neat  $T_g$ -type SMP region. The two nanofillers ( $Fe_3O_4$  and CNT) can induce heat at two distinctively different radiofrequency ranges (296 kHz and 13.56 MHz), so the multi-composite

demonstrated well-controlled multiple shape recoveries [116]. Additionally, Li and co-workers [117] created a quintuple-SME using polymethyl methacrylate (PMMA)/PEG semi-interpenetrating polymer network (IPN) systems with a broad  $T_g$  range (45–125 °C) and an additional  $T_m$  ( $\approx 30$  °C) from PEG crystallites as total transition temperatures. The broad  $T_g$  range was attributed to the formation of semi-IPN, which led to the partial miscibility of amorphous PMMA with PEG. These publications on triple SME and multiple SME not only meet the requirements of increasingly complex applications but also further stimulate development of the shape-memory functions of SMP.



**Figure 2.14** Quadruple-shape memory properties of PFSA. Reproduced with permission from T. Xie, *Nature*, 2010, **464**, 7286, 267. ©2010, Nature Publishing Group [71]

#### **2.4.4 Temperature-memory Effects**

The temperature-memory effect in SMP (which refers to the capability of a polymer to memorise temperatures instead of shapes) is being studied increasingly often. In 2007, Miaudet and co-workers reported the shape and temperature memory in SMP/CNT nanocomposites [118]. The SMP nanocomposites could revert to their original shapes if reheated. The nanoparticles broadened the  $T_g$  and showed temperature memory with a peak recovery stress at the initial deformation temperature. The stress generated by shape recovery was a growing function of the energy absorbed during deformation at a high temperature. Thus, a high failure energy is necessary for strong shape-memory materials. Most recently, Xie and co-workers also developed a strain-based temperature-memory effect for Nafion. In this work, under carefully selected strain-controlled experimental conditions, the temperature at which a maximum strain recovery speed occurred was found to be quantitatively related to the deformation temperature. Interestingly, the polymer could memorise more than one deformation temperature (i.e., multi-temperature memory effect) [119]. Additionally, Mather and co-workers fabricated another functionally graded SMP that encompassed a range of  $T_g$  values distributed in a gradient fashion by post-curing the material in a linear temperature gradient. The gradient recovery properties of the material were achieved using indentation-based surface shape-memory. This new class of SMP offers great potential for material-based temperature sensors [120]. Temperature-memory effects have been studied widely in research on SMA, whereas these effects are being studied on SMP only now. The temperature-memory effect in SMP will be investigated further.

## **2.5 Conclusions**

The present chapter introduced the fundamental studies (including the molecular design, programming processes and functionalities) of SMP. Work on shape-memory switches has greatly increased the flexibility for the design of SMP and development of new applications. More shape-memory functionalities have been developed in SMP using molecular designs. The shape-memory behaviour of a given polymer is the result of an appropriate combination of the molecular design of the material and programming rather than an intrinsic property. In this regard, SME prepared by various programming processes have also been covered in this chapter. In general, research on SMP is expected to continue for further development of applications. A better understanding of the molecular design, functionalities and programming methods of SMP will help in developing better engineered products with more efficient designs and desired shape-memory products.



## References

1. L. Wu, C. Jin and X. Sun, *Biomacromolecules*, 2010, **12**, 1, 235.
2. S. Chen, J. Hu, C-W. Yuen and L. Chan, *Polymer*, 2009, **50**, 19, 4424.
3. I. A. Rousseau and T. Xie, *Journal of Materials Chemistry*, 2010, **20**, 17, 3431.
4. C.H. Chen, G.D. Dang, J.P. Gao, C.Q. Zhang, X.C. He, H.Y. Ma, X.F. An and X.S. Yi, *Advanced Materials Research*, 2011, **152**, 530.
5. L. Song, W. Hu, G. Wang, G. Niu, H. Zhang, H. Cao, K. Wang, H. Yang and S. Zhu, *Macromolecular Bioscience*, 2010, **10**, 1194.
6. K. Inomata, K. Nakagawa, C. Fukuda, Y. Nakada, H. Sugimoto and E. Nakanishi, *Polymer*, 2010, **51**, 3, 793.
7. H.G. Jeon, P.T. Mather and T.S. Haddad, *Polymer International*, 2000, **49**, 5, 453.
8. A. Alteheld, Y. Feng, S. Kelch and A. Lendlein, *Angewandte Chemie International Edition*, 2005, **44**, 8, 1188.
9. P.T. Knight, K.M. Lee, T. Chung and P.T. Mather, *Macromolecules*, 2009, **42**, 17, 6596.
10. F. Migneco, Y-C. Huang, R.K. Birla and S.J. Hollister, *Biomaterials*, 2009, **30**, 33, 6479.
11. M. Behl and A. Lendlein, *Journal of Materials Chemistry*, 2010, **20**, 17, 3335.
12. A.A. Sharp, H.V. Panchawagh, A. Ortega, R. Artale, S. Richardson-Burns, D.S. Finch, K. Gall, R.L. Mahajan and D. Restrepo, *Journal of Neural Engineering*, 2006, **3**, 4, L23.
13. H. Lv, J. Leng, Y. Liu and S. Du, *Advanced Engineering Materials*, 2008, **10**, 6, 592.
14. H. Lu, Y. Liu, J. Leng and S. Du, *Smart Materials & Structures*, 2009, **18**, 8, 085003.
15. B. Yang, W. Huang, C. Li, C. Lee and L. Li, *Smart Materials & Structures*, 2004, **13**, 1, 191.



16. B. Yang, W. Huang, C. Li and L. Li, *Polymer*, 2006, **47**, 4, 1348.
17. W. Huang, B. Yang, L. An, C. Li and Y. Chan, *Applied Physics Letters*, 2005, **86**, 11, 114105.
18. H. Du and J. Zhang, *Soft Matter*, 2010, **6**, 14, 3370.
19. J. Morshedien, H. Khonakdar, M. Mehrabzadeh and H. Eslami, *Advances in Polymer Technology*, 2003, **22**, 2, 112.
20. I.S. Kolesov, K. Kratz, A. Lendlein and H-J. Radusch, *Polymer*, 2009, **50**, 23, 5490.
21. X. Sun and X. Ni, *Journal of Applied Polymer Science*, 2004, **94**, 6, 2286.
22. C. Liu, S.B. Chun, P.T. Mather, L. Zheng, E.H. Haley and E.B. Coughlin, *Macromolecules*, 2002, **35**, 27, 9868.
23. K. Sakurai, Y. Shirakawa, T. Kashiwagi and T. Takahashi, *Polymer*, 1994, **35**, 19, 4238.
24. X. Luo, X. Zhang, M. Wang, D. Ma, M. Xu and F. Li, *Journal of Applied Polymer Science*, 1997, **64**, 12, 2433.
25. Q. Meng and J. Hu, *Solar Energy Materials and Solar Cells*, 2008, **92**, 10, 1260.
26. B.S. Lee, B.C. Chun, Y-C. Chung, K.I. Sul and J.W. Cho, *Macromolecules*, 2001, **34**, 18, 6431.
27. F.L. Ji, J.L. Hu, T.C. Li and Y.W. Wong, *Polymer*, 2007, **48**, 17, 5133.
28. D. Rickert, A. Lendlein, A. Schmidt, S. Kelch, W. Roehlke, R. Fuhrmann and R. Franke, *Journal of Biomedical Materials Research, Part B: Applied Biomaterials*, 2003, **67**, 2, 722.
29. J. Hu, Z. Yang, L. Yeung, F. Ji and Y. Liu, *Polymer International*, 2005, **54**, 5, 854.
30. S-I. Han, B.H. Gu, K.H. Nam, S.J. Im, S.C. Kim and S.S. Im, *Polymer*, 2007, **48**, 7, 1830.
31. S. Chen, J. Hu, Y. Liu, H. Liem, Y. Zhu and Y. Liu, *Journal of Polymer Science, Part B: Polymer Physics Edition*, 2007, **45**, 4, 444.

32. H.A. Khonakdar, S.H. Jafari, S. Rasouli, J. Morshedian and H. Abedini, *Macromolecular Theory and Simulations*, 2007, **16**, 1, 43.
33. D. Ratna and J. Karger-Kocsis, *Journal of Materials Science*, 2008, **43**, 1, 254.
34. A. Lendlein and S. Kelch, *Angewandte Chemie International Edition*, 2002, **41**, 12, 2034.
35. B.K. Kim, S.Y. Lee, J.S. Lee, S.H. Baek, Y.J. Choi, J.O. Lee and M. Xu, *Polymer*, 1998, **39**, 13, 2803.
36. H. Jeong, J. Lee, S. Lee and B. Kim, *Journal of Materials Science*, 2000, **35**, 2, 279.
37. Y. Zhang, C. Wang, X. Pei, Q. Wang and T. Wang, *Journal of Materials Chemistry*, 2010, **20**, 44, 9976.
38. F.L. Ji and J.L. Hu, *High Performance Polymers*, 2011, **23**, 4, 314.
39. G. Rabani, H. Luftmann and A. Kraft, *Polymer*, 2006, **47**, 12, 4251.
40. Y. Zhu, J-L. Hu, K-W. Yeung, H-J. Fan and Y-Q. Liu, *Chinese Journal of Polymer Science*, 2006, **24**, 02, 173.
41. Y. Zhu, J. Hu, K.W. Yeung, K.F. Choi, Y. Liu and H. Liem, *Journal of Applied Polymer Science*, 2007, **103**, 1, 545.
42. S. D'hollander, G. Van Assche, B. Van Mele and F. Du Prez, *Polymer*, 2009, **50**, 19, 4447.
43. S.V. Ahir, A.R. Tajbakhsh and E.M. Terentjev, *Advanced Functional Materials*, 2006, **16**, 4, 556.
44. I.A. Rousseau and P.T. Mather, *Journal of the American Chemical Society*, 2003, **125**, 50, 15300.
45. K. Hiraoka, W. Sagano, T. Nose and H. Finkelmann, *Macromolecules*, 2005, **38**, 17, 7352.
46. S-K. Ahn, P. Deshmukh and R.M. Kasi, *Macromolecules*, 2010, **43**, 17, 7330.
47. S-K. Ahn, P. Deshmukh, M. Gopinadhan, C.O. Osuji and R.M. Kasi, *ACS Nano*, 2011, **5**, 4, 3085.

48. Y. Yu and T. Ikeda, *Angewandte Chemie International Edition*, 2006, **45**, 33, 5416.
49. H. Qin and P.T. Mather, *Macromolecules*, 2008, **42**, 1, 273.
50. J.L. Hu, Y. Zhu, H.H. Huang and J. Lu, *Progress in Polymer Science*, 2012, **37**, 12, 1720.
51. H. Jiang, S. Kelch and A. Lendlein, *Advanced Materials*, 2006, **18**, 11, 1471.
52. G. Zhu, G. Liang, Q. Xu and Q. Yu, *Journal of Applied Polymer Science*, 2003, **90**, 6, 1589.
53. M.H. Li, P. Keller, B. Li, X. Wang and M. Brunet, *Advanced Materials*, 2003, **15**, 7-8, 569.
54. D. Aoki, Y. Teramoto and Y. Nishio, *Biomacromolecules*, 2007, **8**, 12, 3749.
55. K. Ishida and N. Yoshie, *Macromolecules*, 2008, **41**, 13, 4753.
56. S.J. Chen, J.L. Hu, Y.Q. Liu, H.M. Liem, Y. Zhu and Y.J. Liu, *Journal of Polymer Science, Part B: Polymer Physics Edition*, 2007, **45**, 4, 444.
57. Y. Zhu, J. Hu and Y. Liu, *The European Physical Journal E*, 2009, **28**, 1, 3.
58. A.M. Kushner, J.D. Vossler, G.A. Williams and Z. Guan, *Journal of the American Chemical Society*, 2009, **131**, 25, 8766.
59. S. Chen, J. Hu, C.W. Yuen and L. Chan, *Materials Letters*, 2009, **63**, 17, 1462.
60. S. Chen, J. Hu, C.W. Yuen and L. Chan, *Polymer International*, 2010, **59**, 4, 529.
61. S. Chen, J. Hu, S. Chen and C. Zhang, *Smart Materials & Structures*, 2011, **20**, 6, 065003.
62. J.R. Kumpfer and S.J. Rowan, *Journal of the American Chemical Society*, 2011, **133**, 32, 12866.
63. Q. Meng, J. Hu, Y. Zhu, J. Lu and Y. Liu, *Journal of Applied Polymer Science*, 2007, **106**, 4, 2515.
64. M. Behl, I. Bellin, S. Kelch, W. Wagermaier and A. Lendlein, *Advanced Functional Materials*, 2009, **19**, 1, 102.

65. I. Bellin, S. Kelch, R. Langer and A. Lendlein, *Proceedings of the National Academy of Sciences*, 2006, **103**, 48, 18043.
66. J. Zotzmann, M. Behl, D. Hofmann and A. Lendlein, *Advanced Materials*, 2010, **22**, 31, 3424.
67. J-S. Ahn, W-R. Yu, J.H. Youk and H.Y. Ryu, *Smart Materials & Structures*, 2011, **20**, 10, 105024.
68. S. Pandini, F. Baldi, K. Paderni, M. Messori, M. Toselli, F. Pilati, A. Gianoncelli, M. Brisotto, E. Bontempi and T. Riccò, *Polymer*, 2013, **54**, 16, 4253.
69. S. Imai and K. Sakurai, *Precision Engineering*, 2013, **37**, 3, 572.
70. J. Zhang, Y. Niu, C. Huang, L. Xiao, Z. Chen, K. Yang and Y. Wang, *Polymer Chemistry*, 2012, **3**, 6, 1390.
71. T. Xie, *Nature*, 2010, **464**, 7286, 267.
72. B.K. Kim, S.Y. Lee and M. Xu, *Polymer*, 1996, **37**, 26, 5781.
73. F. Li, X. Zhang, J. Hou, M. Xu, X. Luo, D. Ma and B.K. Kim, *Journal of Applied Polymer Science*, 1997, **64**, 8, 1511.
74. J. Lin and L. Chen, *Journal of Applied Polymer Science*, 1998, **69**, 8, 1563.
75. J. Lin and L. Chen, *Journal of Applied Polymer Science*, 1998, **69**, 8, 1575.
76. S. Kumar and M. Pandya, *Journal of Applied Polymer Science*, 1997, **64**, 5, 823.
77. S. Chen, J. Hu, Y. Liu, H. Liem, Y. Zhu and Q. Meng, *Polymer International*, 2007, **56**, 9, 1128.
78. J.L. Hu, F.L. Ji and Y.W. Wong, *Polymer International*, 2005, **54**, 3, 600.
79. J. Hu, Y. Zeng and H. Yan, *Textile Research Journal*, 2003, **73**, 2, 172.
80. P. Beyer, E.M. Terentjev and R. Zentel, *Macromolecular Rapid Communications*, 2007, **28**, 14, 1485.
81. T. Ikeda, J.I. Mamiya and Y. Yu, *Angewandte Chemie International Edition*, 2007, **46**, 4, 506.

82. W. Lehmann, H. Skupin, C. Tolksdorf, E. Gebhard, R. Zentel, P. Krüger, M. Lösche and F. Kremer, *Nature*, 2001, **410**, 6827, 447.
83. K.D. Harris, C.W. Bastiaansen, J. Lub and D.J. Broer, *Nano letters*, 2005, **5**, 9, 1857.
84. T. Ikeda and T. Ube, *Materials Today*, 2011, **14**, 10, 480.
85. M. Yamada, M. Kondo, R. Miyasato, Y. Naka, J-I. Mamiya, M. Kinoshita, A. Shishido, Y. Yu, C.J. Barrett and T. Ikeda, *Journal of Materials Chemistry*, 2008, **19**, 1, 60.
86. P. Xie and R. Zhang, *Journal of Materials Chemistry*, 2005, **15**, 26, 2529.
87. K. Urayama, *Macromolecules*, 2007, **40**, 7, 2277.
88. D.L. Thomsen, P. Keller, J. Naciri, R. Pink, H. Jeon, D. Shenoy and B.R. Ratna, *Macromolecules*, 2001, **34**, 17, 5868.
89. K. Hiraoka, N. Tagawa and K. Baba, *Macromolecular Chemistry and Physics*, 2008, **209**, 3, 298.
90. K.M. Lee, H. Koerner, R.A. Vaia, T.J. Bunning and T.J. White, *Soft Matter*, 2011, **7**, 9, 4318.
91. L. Cui, X. Tong, X. Yan, G. Liu and Y. Zhao, *Macromolecules*, 2004, **37**, 19, 7097.
92. T. Yoshino, M. Kondo, J.I. Mamiya, M. Kinoshita, Y. Yu and T. Ikeda, *Advanced Materials*, 2010, **22**, 12, 1361.
93. M. Kondo, M. Sugimoto, M. Yamada, Y. Naka, J-I. Mamiya, M. Kinoshita, A. Shishido, Y. Yu and T. Ikeda, *Journal of Materials Chemistry*, 2010, **20**, 1, 117.
94. T. Chung, A. Romo-Uribe and P.T. Mather, *Macromolecules*, 2008, **41**, 1, 184.
95. K.M. Lee, P.T. Knight, T. Chung and P.T. Mather, *Macromolecules*, 2008, **41**, 13, 4730.
96. S.J. Hong, W-R. Yu and J.H. Youk, *Smart Materials & Structures*, 2010, **19**, 3, 035022.

97. J.M. Raquez, S. Vanderstappen, F. Meyer, P. Verge, M. Alexandre, J.M. Thomassin, C. Jérôme and P. Dubois, *Chemistry-A European Journal*, 2011, **17**, 36, 10135.
98. H. Zhuo, J. Hu and S. Chen, *Journal of Materials Science*, 2011, **46**, 10, 3464.
99. J. Li, W.R. Rodgers and T. Xie, *Polymer*, 2011, **52**, 23, 5320.
100. B. Winzek, S. Schmitz, H. Rumpf, T. Sterzl, R. Hassdorf, S. Thienhaus, J. Feydt, M. Moske and E. Quandt, *Materials Science and Engineering: A*, 2004, **378**, 1, 40.
101. H. Tobushi, S. Hayashi and Y. Sugimoto, *Materials Science Forum*, 2010, **638**, 218.
102. S. Chen, J. Hu, H. Zhuo and Y. Zhu, *Materials Letters*, 2008, **62**, 25, 4088.
103. S. Chen, J. Hu and H. Zhuo, *Composites Science and Technology*, 2010, **70**, 10, 1437.
104. H. Tamagawa, *Materials Letters*, 2010, **64**, 6, 749.
105. K.K. Westbrook, P.T. Mather, V. Parakh, M.L. Dunn, Q. Ge, B.M. Lee and H.J. Qi, *Smart Materials & Structures*, 2011, **20**, 6, 065010.
106. S. Chen, J. Hu, C.W. Yuen, L. Chan and H. Zhuo, *Polymers for Advanced Technologies*, 2010, **21**, 5, 377.
107. S.K. Ahn and R.M. Kasi, *Advanced Functional Materials*, 2011, **21**, 23, 4543.
108. T. Xie, X. Xiao and Y.T. Cheng, *Macromolecular Rapid Communications*, 2009, **30**, 21, 1823.
109. I. Kolesov and H. Radusch, *eXPRESS Polymer Letters*, 2008, **2**, 461.
110. T. Ware, K. Hearon, A. Lonneckner, K.L. Wooley, D.J. Maitland and W. Voit, *Macromolecules*, 2012, **45**, 2, 1062.
111. T. Pretsch, *Smart Materials & Structures*, 2010, **19**, 1, 015006.
112. T. Pretsch, *Polymer Degradation and Stability*, 2010, **95**, 12, 2515.

113. M. Bothe, K.Y. Mya, E.M.J. Lin, C.C. Yeo, X. Lu, C. He and T. Pretsch, *Soft Matter*, 2012, **8**, 4, 965.
114. C. Bae, J. Park, E. Kim, Y. Kang and B. Kim, *Journal of Materials Chemistry*, 2011, **21**, 30, 11288.
115. J. Li and T. Xie, *Macromolecules*, 2010, **44**, 1, 175.
116. Z. He, N. Satarkar, T. Xie, Y.T. Cheng and J.Z. Hilt, *Advanced Materials*, 2011, **23**, 28, 3192.
117. J. Li, T. Liu, S. Xia, Y. Pan, Z. Zheng, X. Ding and Y. Peng, *Journal of Materials Chemistry*, 2011, **21**, 33, 12213.
118. P. Miaudet, A. Derré, M. Maugey, C. Zakri, P.M. Piccione, R. Inoubli and P. Poulin, *Science*, 2007, **318**, 5854, 1294.
119. T. Xie, K.A. Page and S.A. Eastman, *Advanced Functional Materials*, 2011, **21**, 11, 2057.
120. A.M. DiOrio, X. Luo, K.M. Lee and P.T. Mather, *Soft Matter*, 2011, **7**, 1, 68.

# 3 Shape-memory Polymer Composites

## 3.1 Introduction

The development of shape-memory polymers (SMP), particularly thermally sensitive SMP, with more elaborate molecular designs accompanied by specific thermomechanical programming allows them to exhibit triple-, multiple- or two-way shape-memory effects (SME). However, there are two weaknesses for this type of chemistry approach in SMP: (i) the molecular design is usually complex and is not readily accessible and (ii) the type of SMP responsiveness to external stimuli is limited and based on polymer segments. Thus, research attempts are exploring other approaches to extend SME and SMP capacities, particularly with regard to responsiveness to athermal stimuli.

An efficient method to enhance mechanical properties or incorporate new functionalities is to introduce fillers in the SMP matrix to develop SMP composites. Composite materials refer to a special class of materials comprising  $\geq 2$  constituents with significantly different physical or chemical properties. If these constituents are combined together, they form a material with characteristics different from their individual components. These components are classified as the ‘matrix’ (‘binder’) and ‘reinforcement’. The latter is usually much stronger and stiffer than the matrix, and gives the composite its advantageous properties. The matrix holds the reinforcements in an orderly pattern.

Similar to other composite materials, SMP composites also have different components in their structure (usually polymer matrices) which act as binders and fillers that enhance mechanical properties or provide additional functionalities to the system. The physical combination of a ‘switching’ element with another material allows the composite to behave like two-phase copolymers in appropriate shape-memory cycles [1]. These composites (i.e., SMP composites) are another branch of the SMP family. The preparation of SMP composites can serve the following functions [2]:

- Improve shape recovery stress and mechanical properties.
- Decrease the induction time of shape recovery by increasing thermal conductivity.



- Create new modes of SME (e.g., triple-shape).
- Create new shape-memory functions of the composite by using non-shape-memory materials.
- Tune the switch temperature, mechanical properties, and biomedical properties of SMP.
- Fabricate shape-memory materials sensitive to a thermal stimuli (e.g., electricity, magnetic, light and moisture).

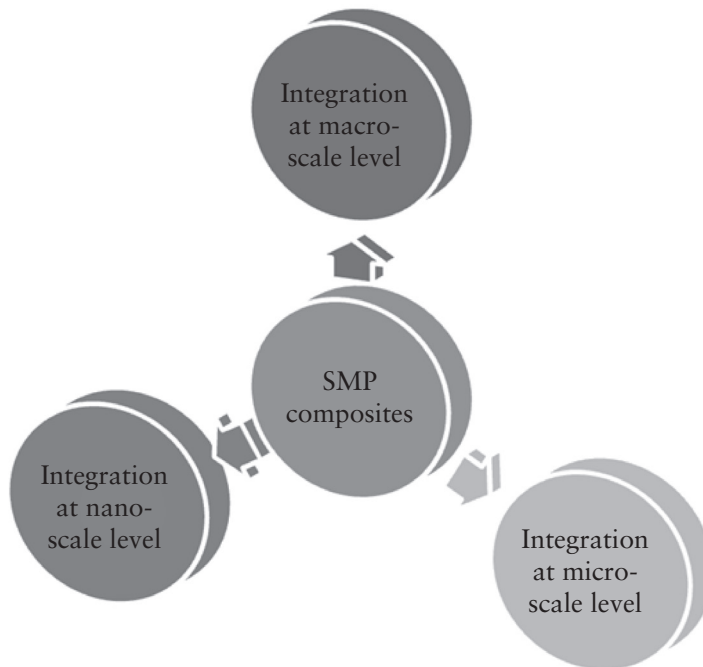
SMP composites can be divided into three categories according to the scale of the integration of the fillers and polymer matrix (**Figure 3.1**):

- Composites at macro-scale integration by reinforcing the SMP matrix with fabrics or other macro-scale structures, such as those studied by Leng and co-workers [3].
- Composites at micro-scale integration in which fillers of micrometer size are embedded in polymers.
- Nanocomposites comprising a SMP matrix and nano-scale fillers.

Enhancement of SMP properties or introduction of new functionalities in the SMP structure is greatly dependent on the nature of fillers used for their production. In general, most of the fillers can improve the stiffness of SMP significantly. Microfibres and fabrics are superior to microparticles or nanoparticles for improvement of the mechanical strength of SMP. Microparticles are not as effective as nanoparticles for improving the mechanical properties and shape recovery stress of SMP. Furthermore, a small amount of microparticles can damage the shape recovery properties of SMP. Nanoparticles can more effectively improve the shape recovery stress of SMP. However, a high loading of nanoparticles (>3 wt%) decreases the shape recovery ratio [4]. Simple physical filling of SMP by various fillers does not elicit a satisfactory effect for improving the shape-memory properties and mechanical properties of SMP simultaneously. Fillers that can bond chemically with SMP chains may be more efficient for improving the shape-memory performance of SMP.

Among the other groups of SMP composites, nanocomposites are more attractive because of their size effects, which bring better performance. Incorporation of various nanofillers into SMP allows tailoring of the properties of the composites. In most cases, nanofillers having a relatively higher modulus exhibit a reinforcing effect as they are introduced into the polymer bulk having a relatively lower modulus in appropriate compositions [5]. Furthermore, some new properties that were previously absent from the polymer matrix may be ‘implanted’ into the composites due to the introduction

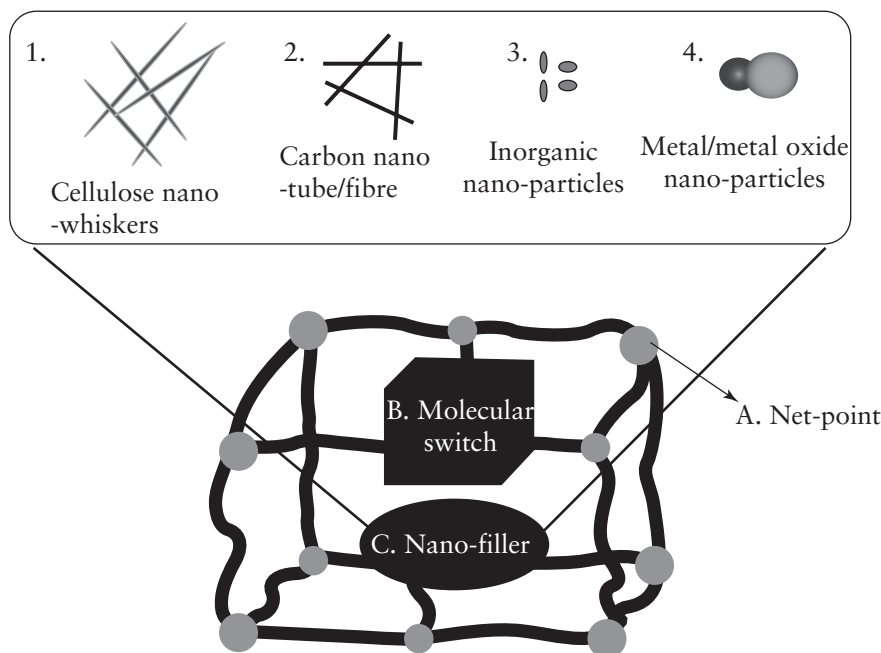
of the nanofillers [6]. According to their structural characteristics, polymeric shape-memory nanocomposites can be summarised as a three-element model, as shown in **Figure 3.2**. In addition to the netpoints and switches originally present in the SMP matrix, introducing nanofillers provides enormous possibilities to improve the properties or obtain new functionalities of the composites.



**Figure 3.1** Categorisation of SMP composites based on the scale of integration of fillers

Four types of nanofillers (cellulose nanowhiskers (CNW), carbon nanotubes (CNT)/carbon nanofibres (CNF), inorganic nanoparticles, and metal/metal oxides nanoparticles) have been researched extensively [7]. It has been observed that CNW primarily have a role of reinforcement as they are introduced into SMP whereas the SME of composites is determined by the polymer matrix [8, 9]. Incorporation of CNT/CNF endows composites with pronounced improved mechanical properties. Furthermore, the addition makes the composites electrosensitive, which is the greatest incentive for exploration of this type of nanocomposite [10, 11]. Inorganic

nanoparticles that are widely introduced into SMP commonly include graphene, silica, and SiC. Metal/metal oxide nanoparticles, including Neo magnet (NdFeB), magnetite ( $\text{Fe}_3\text{O}_4$ ), titanium dioxide, and zinc oxide nanorods, have also attracted intense research interest in terms of combination with SMP [12].



**Figure 3.2** Structure of polymeric shape-memory nanocomposites (schematic)

In summary, SMP nanocomposites are materials that can memorise temporary shapes and revert back to their permanent shape upon exposure to an external stimulus, such as heat, light (ultraviolet (UV), infrared (IR) and visible), moisture/water, electricity and magnetic fields, by mixing different nanofillers with SMP or elastomeric matrices. Such SMP nanocomposites have greatly extended the capacity of polymers from a chemistry approach. They have also enabled novel functions that enhance SME and expand the spectrum of SMP applications, including deployable space structures, smart implants, controlled medical instruments, adaptive optical devices, dry/wet adhesives, and fasteners. Nevertheless, the performance of nanocomposites is dependent upon the ratio, dispersion and type of nanofiller. This chapter will throw light on the characteristics, applications, as well as the recent developments and trends of SMP composites.

## 3.2 Nanowhisker/Shape-memory Polymer Composites

### 3.2.1 Cellulose Nanowhiskers

Cellulose is the most abundant biological polymer available to humans. Besides wide usage in fabrics and yarns, the attributes of low cost, low density, high stiffness, consumable nature and biodegradability of cellulose constitute the major incentives for exploring new uses. Natural cellulose and its polymorphs and has been attracting academic and industrial interest for >100 years. Natural cellulose molecules are unbranched chains of up to 20,000 1,4-linked  $\beta$ -D-glucose residues (Figure 3.3). Because of the extensive van der Waals' attraction forces as well as hydrogen bonds among them, the cellulose chains are always in a compact parallel alignment and a crystalline structure. This results in a straight, stable heterogeneous supramolecular structure as well as low accessibility to chemicals and solvents [7]. Hydrogen bonding between the hydroxyl groups and oxygen of adjacent molecules stabilises the threadlike bundles of cellulose molecules in a lateral direction, leading to the formation of cellulose microfibrils. Dissolution of natural cellulose is of great significance for the development of cellulose-based products.

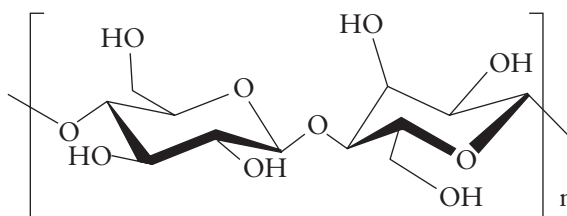


Figure 3.3 Molecular structure of natural cellulose

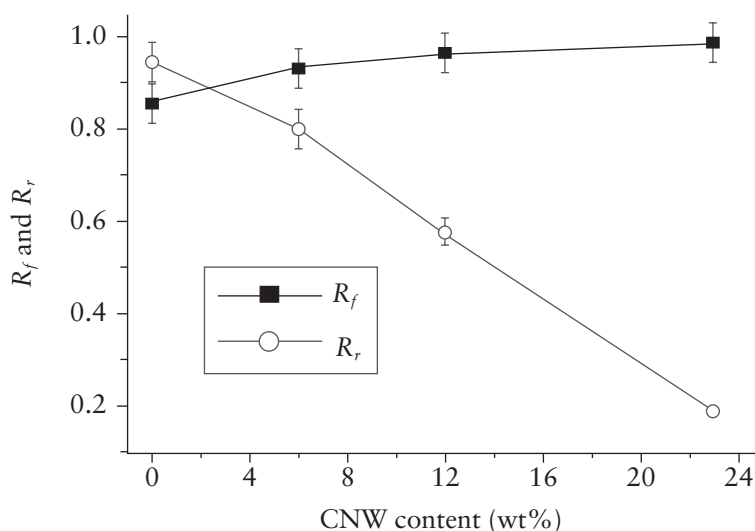
CNW can be prepared from natural cellulose microfibrils. Several 'cellulose whiskers' are assembled into microfibrils by amorphous domains which can be removed by chemical, biological or mechanical treatment. A stable water suspension of cellulose whiskers usually originates from microcrystalline cellulose (MCC) by hydrolysis with sulfuric acid [13]. The whisker size obtained is 200–400 nm in length and <10 nm in width. Processing parameters (concentrations of MCC and sulfuric acid, hydrolysis time, temperature, and duration of ultrasonic treatment) have a pronounced influence on the resultant cellulose whiskers [7].

CNW have been used in polymeric nanocomposites as reinforcements because of their high stiffness, great strength, and unique surface chemistry [8, 9]. CNW prepared from different natural resources have diameters of 2–20 nm with lengths that can be several tens of microns. The modulus of CNW can be close to the perfect crystal of native cellulose ( $\approx 150$  GPa). The most popular applications for CNW are reinforcement of the polymer matrix and improvement of their mechanical and thermal properties [14, 15]. In comparison with other reinforcing components, such as glass fibres and metal/non-metal oxides, the cellulose filler has outstanding advantages: low cost, low density ( $1.5 \text{ g/cm}^3$ ), lack of abrasion to processing equipment, ease of incineration, environmental-friendliness and abundance. In particular, the high aspect ratio, modulus and strength of CNW have urged researchers to study reinforcement effects. In recent years, application of cellulose whiskers has been broadened from simple reinforcement to responsiveness to stimuli [16, 17]. Reversibly regulated hydrogen bonding among the hydroxyl groups of CNW has served as a new mechanism to establish architecture and achieve mechanical adaptability of polymer composites similar to that seen in the sea cucumber.

### **3.2.2 Integration of Cellulose Nanowhiskers**

Incorporating CNW in polymer matrix results in new shape-memory functionalities and enhances the mechanical properties of the resultant SMP composite. CNW exhibit extraordinary reinforcing effects when introduced into various polymer matrices, such as isotactic polypropylene [18], polyvinyl acetate [19] and poly(butyl acrylate–methyl methacrylate) [20]. A switchable effect upon the percolation cellulose network (PCN), rather than only the reinforcing effect, was first reported by Capadona and co-workers in 2008 [16]. The strong hydrogen bonding among nanowhiskers *via* hydroxyl groups on the cellulose surface could be reversibly disrupted by a competitive reagent to the hydrogen bonding, giving rise to the mechanical adaptability of the nanocomposites.

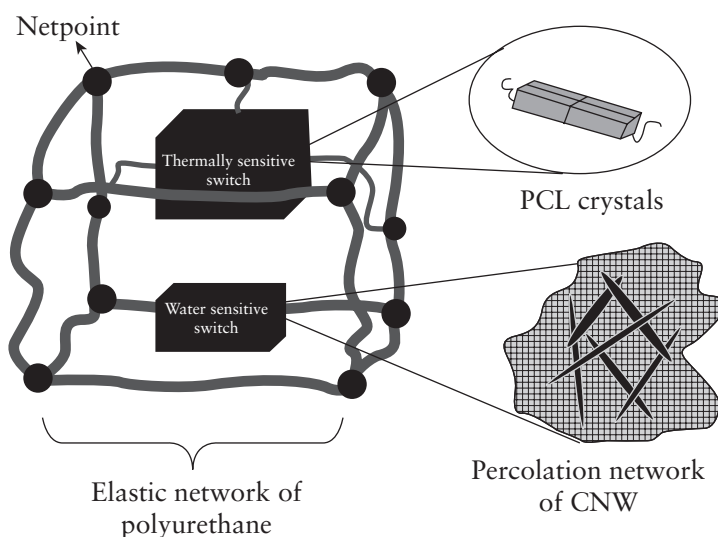
Hu and co-workers [21] reported novel CNW-shape-memory thermoplastic polyurethane (TPU) nanocomposites showing tunable shape-memory properties. In their work, both the poly( $\epsilon$ -caprolactone) (PCL) crystals and dry-state PCN contributed to shape fixing. Thermal stimuli triggered only one part of the recovery due to PCL, whereas the other part due to PCN was maintained. Combination of crystallised PCL and dry-state PCN contributed to shape fixing when the extended composites were cooled down and dried *in vacuo*. The research team led by Hu studied the shape-memory performance of CNW/TPU nanocomposites extensively and identified several factors influencing themomechanical properties. They found that the percentage of thermally induced recovery decreased in proportion with the increase in CNW content (**Figure 3.4**).



**Figure 3.4** Dependence upon compositions of the shape-fixity ratio ( $R_f$ ) and shape-recovery ratio ( $R_r$ ). Reproduced with permission from H.S. Luo, J.L. Hu and Y. Zhu, *Materials Letters*, 2011, 65, 23-24, 3583. ©2011, Elsevier [21]

The Hu research team also proposed a mechanism for the shape-memory process for CNW/TPU nanocomposites (**Figure 3.5**) [22]. This mechanism showed the characteristic microstructure of CNW/TPU and details of switchable water-sensitive SME programming (in which water sensitivity is based on the chemo-mechanical adaptability of CNW/TPU nanocomposites). Combination of a percolation network of cellulose whiskers and an elastomer matrix is the microstructural prerequisite for the rapidly switchable water-sensitive shape-memory effect in these CNW/TPU. Initially (original shape), wetting can soften the CNW/TPU through water molecules attacking the hydrogen bonds between the nanowhiskers. This allows the easy transformation into a temporary shape, and subsequent drying leads to shape fixation through formation of a hydrogen-bonded, three-dimensional network of individualised whiskers after removal of water molecules. In the recovery procedure, the wetting as the external stimulus leads to decoupling of the network of whiskers, and triggers the spontaneous shape recovery of programmed samples.





**Figure 3.6** CNW/TPU nanocomposites with twin-switches. Reproduced with permission from H.S. Luo, J.L. Hu and Y. Zhu, *Macromolecular Chemistry and Physics*, 2011, **212**, 18, 1981. ©2011, John Wiley & Sons [23]

The microstructural characteristics (whisker-network/elastomer) of CNW/TPU and the corresponding shape-memory programming promote rapidly switchable SME. This finding provides possible approaches to tailor the SME of nanocomposites on demand for different applications, and could contribute to the development of new SMP composites. More recently, Zhu and co-workers [22] conducted a more in-depth study into CNW/elastomer nanocomposites that led to totally athermal and rapid water sensitivity. The significance of their work lies in three aspects: (i) water responsiveness happens almost instantly (contrary to other methods that require several days for recovery); (ii) it is the first example of shape-memory function without using a SMP in the composites; and (iii) this water sensitivity is independent of thermal responsiveness.

### 3.3 Carbon/Shape-memory Polymer Composites

Carbon is the 15<sup>th</sup> most abundant element in the Earth's crust. Carbon has a unique diversity of allotropes: diamond, amorphous carbon, fullerenes, graphite, CNT and CNF. Due to their outstanding mechanical, thermal and electrical properties, carbon-based nanostructures are used widely in SMP nanocomposites for electrical



sensitivity and light sensitivity (which are originally absent from the polymer matrix) and improved specific SME (e.g., recovery ratio and recovery stress) of SMP.

### **3.3.1 Carbon Nanotube and Carbon Nanofibre/Shape-memory Polymer Composites**

Due to the exceptional mechanical strength with high elastic modulus and high aspect ratios, CNT and CNF are also effective for improving the mechanical strength and shape recovery stress of SMP [24–29]. Another advantage of CNT/CNF as fillers of SMP is the potential electrical and IR light-active SME of prepared SMP composites. Efforts to improve the CNT/CNF dispersion in the polymer matrix include the use of microscale twin screw extruders, surfactants, oxidation or chemical functionalisation of CNT/CNF surfaces, and *in situ* polymerisation [27, 30–33].

Gunes and co-workers [34] fabricated CNF/SMPU composites by melt mixing after the chain extension of a melting temperature ( $T_m$ )-type SMPU. CNF with a diameter of 60–200 nm and length of 30–100 nm were used. The CNF diminished the shape-memory function of SMPU, which was ascribed to the interference of CNF on the crystallisation of the soft segment. Polyurethanes (PU) filled with surface-oxidised CNF showed better dispersion, crystallinity, tensile properties, and higher shape recovery force than their counterparts with untreated CNF. Koerner and co-workers [35] fabricated CNF/SMPU composites by solution mixing in a polar solvent, and slow evaporation of the solvent. The CNF had an average diameter of 100 nm and length >10 nm. Anisotropic distributed CNF were obtained, which increased the rubber modulus by a factor of 2–5. Shape fixity was improved due to enhanced strain-induced crystallisation. In comparison with pure SMP, shape-memory composites with a uniform dispersion of 1–5 vol% CNF produced ≤50% more recovery stress. Similarly, Ni and co-workers [36] prepared CNF/SMPU composites by a solution mixing process with ultrasonic distribution. The CNF had a diameter of >150 nm and length 10–20 nm. The recovery stress of the composites at 3.3 wt% CNF loading increased almost twofold from pure SMPU. Mondal and Hu [33] prepared functionalised multiwalled carbon nanotube (MWCNT)/SMPU composites by solution blending. The MWCNT (with diameter ≈15 nm and length ≈50 nm) were functionalised in aniline at high temperature. It was found that the hard segment together with MWCNT helped to recover the deformed shape. They also prepared MWCNT/SMPU composites by *in situ* polymerisation after chemical functionalisation of MWCNT [37]. It was also found that CNT improved the shape recovery stress of SMPU. It was found that CNT and CNF with different sizes and contents could have different influences on the structural, shape-memory and thermal properties of SMPU (Table 3.1) [37, 38]. In addition to the SMPU system, CNT have been used to reinforce shape-memory polyvinyl alcohol (PVA). Miaudet and co-workers [39] prepared CNT/PVA shape-

memory fibres by a special coagulation spinning method. Surfactant-stabilised CNT were injected in a co-flowing stream of coagulating PVA solution. The maximal stress generated by the composite fibres was 1–2 orders of magnitude greater than that produced by conventional SMP. The recovery stress was close to that of shape-memory alloys (SMA). In conclusion, most of the studies mentioned above suggest that CNT/CNF can improve the stiffness and recovery stress of SMP.

	Content of MWCNT				
	0 wt%	0.25 wt%	1.0 wt%	2.0 wt%	3.0 wt%
$T_m$ (°C)	45.8	46.4	45.4	44.4	43.5
Heat of fusion ( $\Delta H$ ) (J/g)	22.7	23.9	21.8	19.6	18.3
Crystallinity (%)	16.2	17.1	15.6	14.0	13.1

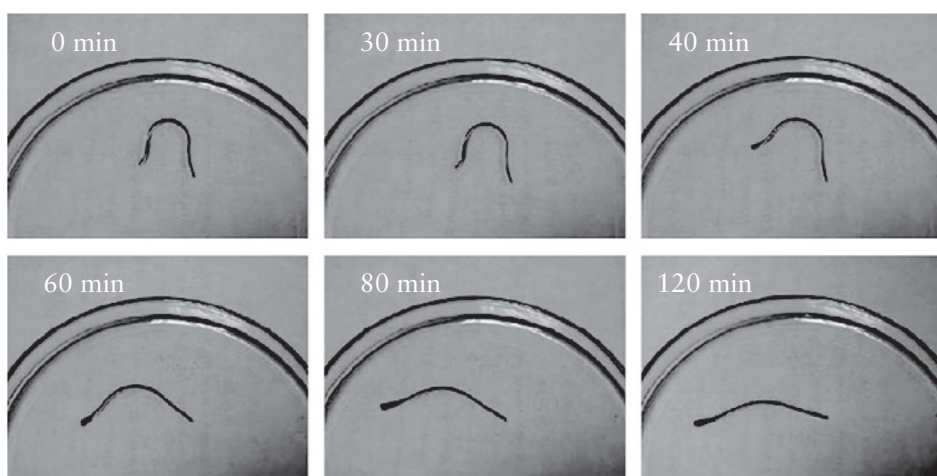
Reproduced with permission from Q.H. Meng, J.L. Hu and S. Mondal, *Journal of Membrane Science*, 2008, 319, 1-2, 102. ©2008, Elsevier [37]

### 3.3.2 Carbon Black/Shape-memory Polymer Composites

Polymer composites filled with conducting carbon black(s) (CB) have broad applications in electric and electronics industries as polymer conductors, semi-conductors and the media for heat transfer. Compared with CNT and CNF, CB are not as effective for improving the mechanical strength and shape recovery stress of SMP. Furthermore, CB deteriorate the shape recovery of SMP severely. Li and co-workers [40] prepared CB/PU composites hoping that the composites possessed SME accompanied by good electrical conductivity. The composites were made by solution mixing and solution precipitation. The CB decreased the shape recovery ratio and shape recovery speed of SMP, especially at high content, which was ascribed to the decreased crystallinity of SMP by CB. Gunes and co-workers [34] prepared CB/SMP composites by melt mixing. They also found that the soft segment crystallinity decreased due to the constraining effect of CB on the mobility of the soft segment during crystallisation.

CB was found to realise water-/solvent-sensitive SME. Glass transition temperature ( $T_g$ )-type SMP (glass transition as the switch) drops if SMP is exposed to a high humidity environment or solution after a certain period of time because water

molecules have a plasticising effect on polymeric materials, and can subsequently increase the flexibility of macromolecule chains. The two functions mentioned above lead to the shape recovery of a deformed SMP [41, 42]. It was found that added carbon powders can lower the  $T_g$  [41, 43]. However, results suggested that high CB content decreases the moisture sensitivity of the composites. The water-driven shape recovery effect of a CB/SMPU composite in water is presented in **Figure 3.7**. A straight CB/SMPU wire is bent into a circular shape and the circular shape fixed in a dry state. After being immersed in water at room temperature for  $\approx 2$  h, the CB/SMPU recovers most of its original shape.

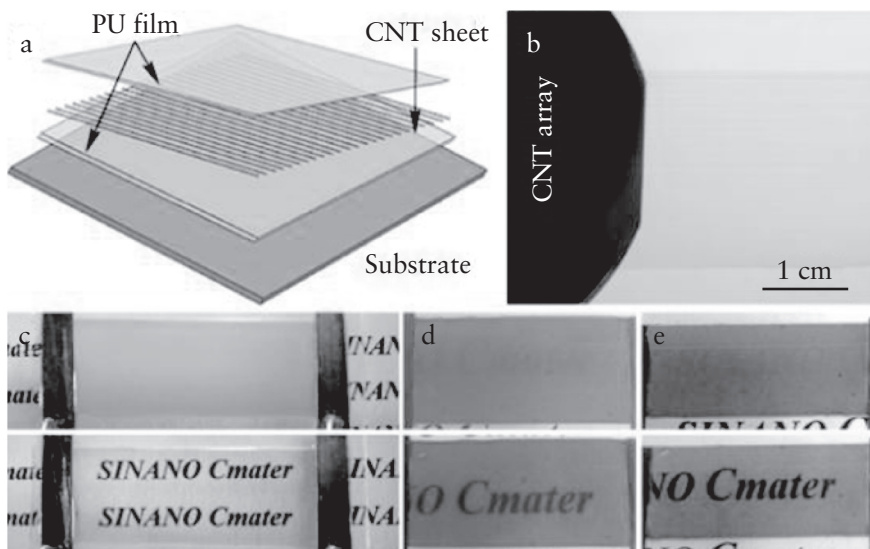


**Figure 3.7** Water-driven shape recovery effect of a CB/SMPU composite. Reproduced with permission from B. Yang, W.M. Huang, C. Li and J.H. Chor, *European Polymer Journal*, 2005, 41, 5, 1123. ©2005, Elsevier [43]

### **3.3.3 Electrically Sensitive Shape-memory Polymer Nanocomposites**

Incorporation of CNT/CNF into various SMP matrices is a facile alternative to make the materials electrically sensitive. Well-dispersed CNT/CNF tend to form a network when the content reaches a certain threshold that enhances the electrical conductivity of the composites considerably. When the nanocomposites are exposed to the appropriate electrical field, electrical current goes through the carbon network, generating heat ('Joule heating'), which triggers the polymer segments to experience

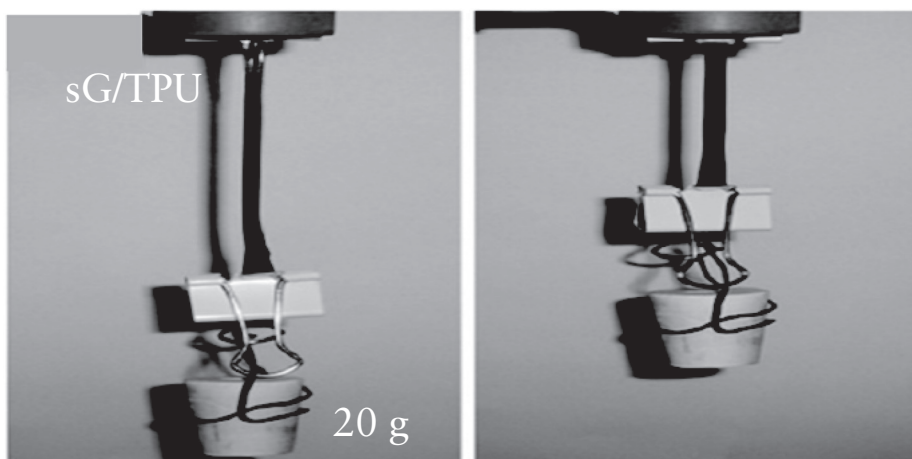
glass transition or melting transition. As a result, the nanocomposites exhibit electrical sensitivity [1, 11]. Zhang and co-workers [44] measured the electrical resistivity of SMP with different weight fractions of CNT. The results showed that even a low weight fraction of CNT could achieve a high level of conductivity that was also dependent upon the temperature of the composites. Lee and Yu achieved excellent conductivity by blending PU with single-walled carbon nanotubes (SWCNT) [45]. The conductivity of the PU-SWCNT hybrids increased dramatically from  $4.86 \times 10^{-7} \text{ S cm}^{-1}$  (1% SWCNT) to  $0.2677 \text{ S cm}^{-1}$  (5% SWCNT). Meng and co-workers [46] fabricated a nanocomposite by sandwiching a CNT sheet between PU films that showed interesting electrical sensitivity. The nanocomposite could be switched from opaque to transparent in seconds after turning on the voltage, and reversed back to opaque after turning off the voltage (Figure 3.8). Jung and co-workers [47] studied PU nanocomposites filled with nanotubes by using conventional blending and crosslinking polymerisation methods. They found that the covalent linkages between the nanotubes and PU prevented re-aggregation of the tubes within the polymer matrix, and provided high-performance, electrically sensitive shape-memory.



**Figure 3.8** (a) Layered structure of a CNT/PU composite film; (b) a transparent and uniform CNT sheet is drawn from an array; (c–e) the opaque (top) and transparent (bottom) composite films induced by electric current. Reproduced with permission from F.C. Meng, X.H. Zhang, G. Xu, Z.Z. Yong, H.Y. Chen, M.H. Chen, Q.W. Li and Y.T. Zhu, *ACS Applied Materials & Interfaces*, 2011, 3, 3, 658. ©2011, American Chemical Society [46]

### 3.3.4 Light-sensitive Shape-memory Polymer Nanocomposites

Remote stimulation of SMP nanocomposites is attractive due to the great number of potential applications. Adding CNT and graphene into the polymer matrix can serve as a practical approach to capture IR photons for the composites and to transfer light energy into heat, thereby triggering thermal transitions of the polymers. Koerner and co-workers [35] uniformly dispersed 1–5 vol% of CNT in a thermoplastic elastomer. Exposure to IR light increased the internal temperature of the composites, which melted the polymer crystallites and remotely triggered the release of stored strain energy. Leng and co-workers [48] found that a thermoset SMP filled with nanocarbon particles exhibited higher shape recovery ability and shape recovery speed as actuated by IR light *in vacuo* compared with those made of pure SMP. Liang and co-workers [49] used graphene as the optical-absorber and a nanoscale energy transfer unit, which imparted additional IR-triggered actuation behaviour to the TPU matrix. In their research, graphene/TPU nanocomposites with 1 wt% sulfonated graphene (sG) exhibited intriguing and repeatable IR-triggered actuation, which could contract and lift a 21.6 g weight a distance of 3.1 cm with 0.21 N of force upon exposure to IR light (Figure 3.9).



**Figure 3.9** Demonstration of SME of a 1 wt% sG/TPU film which contracted and lifted a 21.6-g weight 3.1 cm with 0.211 N of force upon exposure to IR light.

Reproduced with permission from J.J. Liang, Y.F. Xu, Y. Huang, L. Zhang, Y. Wang, Y.F. Ma, F.F. Li, T.Y. Guo and Y.S. Chen, *Journal of Physical Chemistry C*, 2009, 113, 22, 9921. ©2009, American Chemical Society [49]

### **3.3.5 Enhanced General Shape-memory Effect**

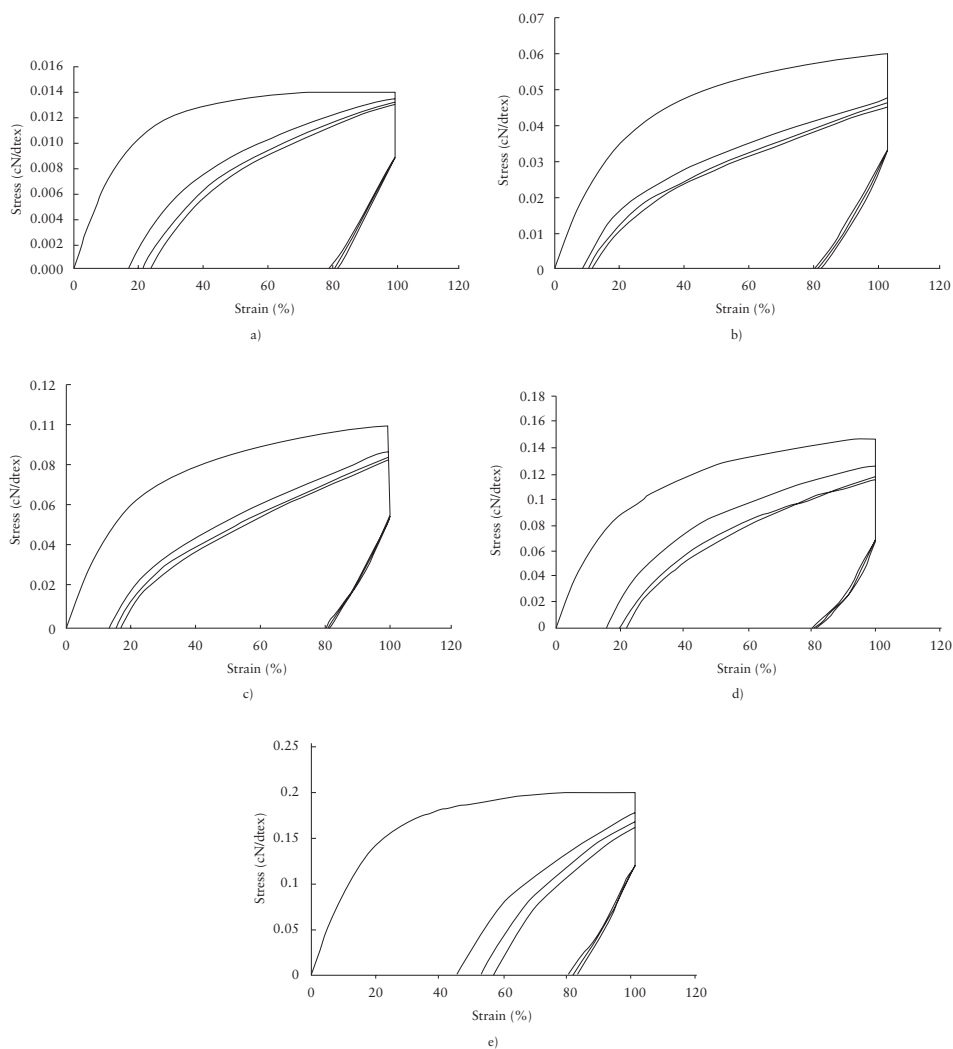
In general, the shape-memory properties of SMP can be enhanced by incorporating CNT or CNF. Meng and co-workers [50, 51] studied the influence of MWCNT content on the properties of SMPU nanocomposite fibres. The shape recovery ratio and recovery force of fibres were improved by incorporating a small amount of MWCNT (**Figure 3.10**). Similar results were found in CNF/SMPU nanocomposites, as reported by the Ni research team [36]. They found that nanocomposites with 3.3 wt% CNF had the largest shape recovery stress. If the fillers exceed a certain amount, the properties of the nanocomposites are reduced, mainly due to the poor interaction between the fillers and SMPU matrix. However, Poulin and co-workers [39, 52, 53] chose PVA as the matrix because it possesses strong interactions with CNT. They utilised a special coagulation spinning method to create CNT/PVA nanocomposite fibres with an extremely high content of nanotubes ( $\approx 20$  wt%). Consequently, the maximal stress of the fibres (nearly 150 MPa) was 1–2 orders of magnitude greater than that produced by conventional SMP (which is closer to that of SMA). They also observed a broadening of the switch temperature and temperature-memory effect in these systems. Additionally, Lu and Gou reported that another type of SMP nanocomposite demonstrated fast electrically responsive behaviour ( $\approx 90$  s) and  $\approx 100\%$  recovery ratio due to the synergistic effect of MWCNT nanopaper and vertically aligned nickel nanostrands in the nanocomposites [54, 55]. Jung and co-workers [56] fabricated electrically conductive, optically transparent and mechanically strong SMPU films by incorporating photo-chemically, surface-modified MWCNT.

## **3.4 Fibre/Fabric-reinforced Shape-memory Polymer Composites**

### **3.4.1 Microfibre or Fabric/Shape-memory Polymer Composites**

Chopped and continuous (especially continuous) microfibrils and fabrics are superior to microparticles and nanoparticles when improving the mechanical strength of SMP. Due to the high elastic modulus of fibres or fabrics, good SME cannot be observed in the fibre direction of the composite. SME are usually determined by bending the composite in the fibre transverse direction but not by tensile testing in the fibre direction. Studies [57] have provided the protocols of bending SME tests. SMP reinforced by microfibrils/fabrics are used mainly for two applications: spacecraft self-deployable devices and vibration-control devices. Fibre-/fabric-reinforced SMP for self-deployable space structure applications are also called elastic memory composites (EMC). EMC can be compacted on earth, stored in a compacted shape, and then self-deployed in space. As vibration-control materials, SMP composites

have the advantages of high energy-absorption efficiency, low density, and high shape deformability.

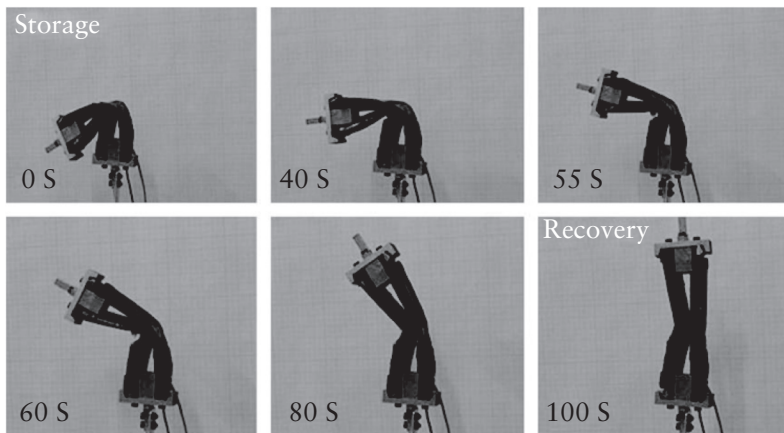


**Figure 3.10** Thermo-mechanical cyclic tensile curves of (a) pure SMF and (b–e) SMP MWCNT fibres with 1.0, 3.0, 5.0 or 7.0 wt % MWCNT, respectively. SMF: Shape-memory fibres. Reproduced with permission from Q.H. Meng, J L. Hu and Y. Zhu, *Journal of Applied Polymer Science*, 2007, 106, 2, 837. ©2007, John Wiley & Sons [50]



Studies of the reinforcement effect of chopped fibre-glass, unidirectional Kevlar fibre, and woven fibre-glass on thermoplastic SMPU suggest that fibres/fabrics can significantly increase the strength and stiffness of SMP [58]. Results on epoxy laminates reinforced by carbon fibre, glass fibre and Kevlar fibre have also demonstrated that microfibrils or fabrics are effective in increasing the stiffness of epoxy SMP resins [59, 60]. The bending strain of the thermoset styrene-based SMP resin reinforced by fabric (plain weave) is mainly because of ‘microbuckling’. Studies on carbon fibre-/fabric-reinforced SMPU laminates have shown that the sequence and position of SMPU films and carbon fibre fabrics in laminates have significant influence on shape-memory properties [57]. The failure mechanisms and deployment accuracy of EMCs have been studied by Campbell and co-workers [61]. Lan and co-workers [3] prepared a self-deployable hinge using a thermoset styrene-based SMP reinforced with carbon fibre plain-weave fabrics. **Figure 3.11** shows the fabricated hinge, which consists of two curved circular SMP composite shells. The voltage applied in the embedded resistor heater in each laminate activates the deployment.

As vibration-control materials, SMP composites can absorb vibration energy efficiently by shape deformation at around the  $T_g$ . Yang and co-workers [62] prepared a sandwich-structure composite sheet of SMPU with an epoxy beam as a vibration-control material. The composite laminate showed up to fourfold-higher impact strength than the epoxy beam alone.



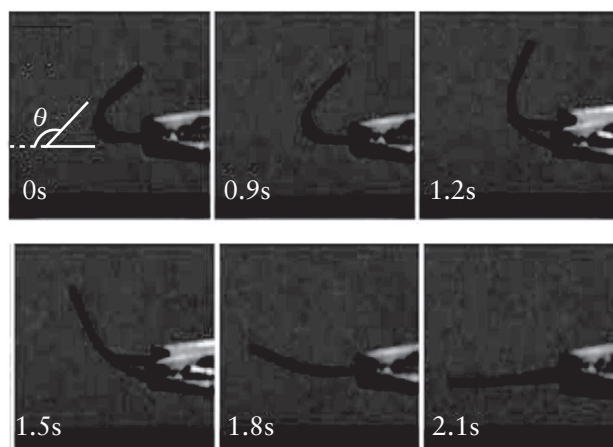
**Figure 3.11** Self-deployment of a SMP hinge made of a thermoset styrene-based SMP reinforced with carbon fibre plain-weave fabrics. Reproduced with permission from X. Lan, Y.J. Liu, H.B. Lv, X.H. Wang, J.S. Leng and S.Y. Du, *Smart Materials & Structures*, 2009, 18, 2. ©2009, IOP Publishing [3]



### **3.4.2 Electrospun Nanofibre Shape-memory Polymer Nanocomposites**

Electrospun nanofibres can be used to construct different shape-memory nanocomposites with high functionality, such as triple SME and rapid electrical sensitivity. These works are mainly done by Mather and Luo. Physically combining a ‘switching’ non-woven nanofibre (average diameter 760 nm) with an elastic-silicon polymer matrix allows the nanocomposite to behave like a two-phase copolymer in appropriate shape–memory cycles [63]. They incorporated a non-woven PCL network into the polymer matrix, the nanocomposites showed thermally sensitive one-way SME that was very similar to that of PCL-based SMPU. Subsequently, triple SME was also achieved in a similar system, using a  $T_g$ -based SMP as the nanocomposite matrix [64]. The resulting nanocomposites displayed two well-separated transitions, one from the glass transition of the matrix and the other from the melting of the PCL nanofibres, which are used for the fixing/recovery of two temporary shapes. Three thermo-mechanical programming stages with different shape fixing protocols are proposed and explored. The intrinsic versatility of this composite approach enables an unprecedentedly large degree of design flexibility for creating functional triple-shape polymers and systems.

By incorporating electrospun continuous non-woven carbon nanofibres (CNF) into an epoxy-based SMP matrix, Luo and Mather [65] developed a SMP nanocomposite with unprecedentedly high-speed electrical actuation capabilities (**Figure 3.12**). The fibre morphology and nanometer size provide a percolating conductive network with a large interfacial area, resulting not only in high electrical conductivity but also in simultaneous enhancement of heat transfer and recovery stress. Similar work has been reported by Lu and co-workers [66]. They studied the synergistic effect of CNF and carbon nano-paper on the shape recovery of the SMP nanocomposites. The actuation of the nanocomposites was achieved by the electrical resistive heating of the carbon nanopaper. The electrical resistivity of the nanocomposites is lowered by a factor of  $10^{16}$  compared to the pure SMP resin by coating it with a nano-paper containing 1.8 g CNF. This improved thermal conductivity allows the SMP composite to respond quickly to electrical resistive heating. However, the shape recovery ratio was reduced due to the interfacial friction among the SMP macromolecular segments, the carbon nano-paper and the blended CNF particles.



**Figure 3.12** Electrically activated shape recovery of epoxy/CNF nanocomposites. Reproduced with permission from X.F. Luo and P.T. Mather, *Soft Matter*, 2010, **6**, 10, 2146. ©2010, Royal Society of Chemistry [65]

### 3.5 Metal and Metal Oxides/Shape-memory Polymer Composites

Thermomagnetically or electromagnetically induced SME in SMP nanocomposites can be achieved by incorporating metal or metal oxides fillers, including iron(III) oxide [12, 67], ferromagnetic particles [68], NdFeB particles [69], Ni-Mn-Ga single-crystal [70] and nickel powder [71]. Among these nanocomposites, most of their magnetically or electromagnetically induced shape recovery ratios have been confirmed to be comparable with thermally induced recovery ratios. However, to attain the desired SME, a homogeneous distribution of metal or metal oxides in the SMP matrix is necessary. Thus, there are different approaches to enhance the compatibility between the two composite components because their interaction force is relatively weak. For example, iron(III) oxide particles were embedded in a matrix of silica before they were incorporated into an SMP network to reduce the formation of micron-sized agglomerates, and to form a homogenous system [72]. Leng and co-workers [71] found that the shape of nanocomposites with treated nickel powder could be recovered in a magnetic field by using a silane coupling agent, whereas those with naked nickel powder could not change. This behaviour provides further evidence that the dispersion of inorganic particles in SMP matrices is a very crucial aspect in creating a magnetically induced SME.

Aside from one-way SME triggered by magnetic fields, relatively complex SME such as triple SME have been realised. Recently, Kumar and co-workers [73] demonstrated the non-contact actuation of triple SME in the aforementioned network composed of PCL segments and polycyclohexyl methacrylate (MACL) network (composed of PCL segments and polycyclohexyl methacrylate) segment nanocomposites with embedded silica coated iron(III) oxide nanoparticles. Two-step recovery was shown when the material was stimulated by stepwise increases in magnetic field strength from  $H = 14.6$  and  $29.4$  kA/m, corresponding to the two switching temperatures in the MACL network (**Figure 3.13**).

Magnetic-sensitive shape-memory materials have potential biomedical applications. Compared with the conventional methods of triggering of shape recovery by direct heating, magnetic-active SME have several advantages, as shown below:

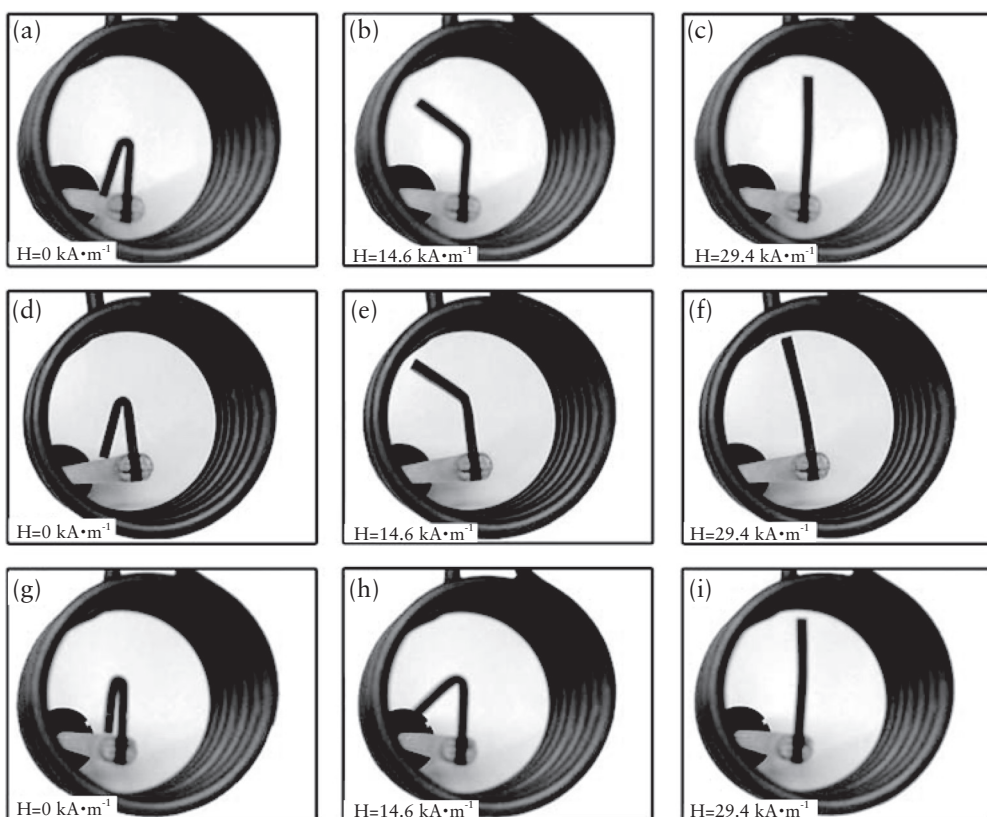
- By selecting a ferromagnetic particle material with a ferromagnetic material's Curie temperature within safe medical limits, Curie thermoregulation eliminates the danger of overheating.
- Power transmission lines leading to a SMP device are eliminated.
- More complex device shapes can be activated because consistent heating is expected for any type of device geometry.
- Selective heating of specific device areas is possible.
- Remote actuation allows for the possibility of embedded devices that can be actuated subsequently by an externally applied magnetic field [74–76].

## **3.6 Other Shape-memory Polymer Composites**

### **3.6.1 Nanoclay/Shape-memory Polymer Composites**

Organic-exfoliated nanoclay is a good material in some circumstances to prepare functional composites with advanced properties. Organic-exfoliated nanoclay is also a good candidate for improving shape recovery stress and the mechanical properties of SMP. Kim and co-workers [77] intercalated macroazoinitiator (MAI), which has a hydrophilic polyethylene glycol (PEG) segment, as shown in **Figure 3.14**, into the gallery of sodium montmorillonite (Na-MMT). The Na-MMT intercalated with MAI was used to prepare polyethyl methacrylate nanocomposites by *in situ* radical polymerisation. The Na-MMT/PEG block linked to polyethyl methacrylate has a role as a hard phase contributing to shape-memory properties, and also as a moiety

to enhance mechanical properties. Cao and Jana [78] synthesised organoclay/SMPU composites in a Brabender Plasticorder. The molar ratio of isocyanine  $-NCO$  and alcoholic  $-OH$  groups was maintained at 1:1 with  $-CH_2CH_2OH$  groups of the quaternary ammonium ions in organoclay contributing a part of the total  $-OH$  functionality. The tethered reactive clay on PU chains offers a new network which adds additional constraints to the chain motion of SMPU (especially of the hard segments). The nanocomposite at 1 wt% organoclay offers 20% higher recovery stress compared with pure SMPU.



**Figure 3.13** Triple SME under different triple-shape creation procedures (TCP) shown by the MACL network (a–c) TCP-2s-I, (d–f) TCP-2s-II and (g–h) TCP-1s (one-step procedure). Reprinted with permission from U.N. Kumar, K. Kratz, W. Wagermaier, M. Behl and A. Lendlein, *Journal of Materials Chemistry*, 2010, 20, 17, 3404. ©2010, Royal Society of Chemistry [73]

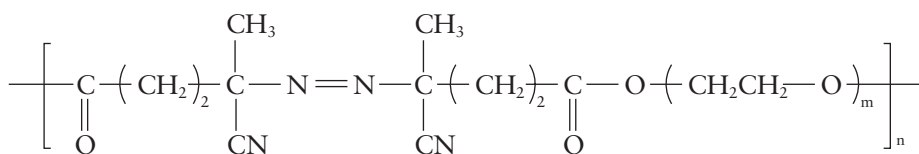


Figure 3.14 Structure of macroazoinitiator

### 3.6.2 Other Inorganic Filler/Shape-memory Polymer Composites

Poly(D,L-lactide) (PDLLA) is a good shape-memory biomaterial with good biodegradability and biocompatibility. Zheng and co-workers [79] reinforced PDLLA with hydroxylapatite ( $\text{Ca}_{10}(\text{PO}_4)_6(\text{OH})_2$ ) for hard-tissue engineering. The composite showed good biodegradation, biocompatibility and shape-memory properties. PDLLA/hydroxylapatite composites at a suitable fraction ratio (2.0:1 to 2.5:1) had much higher shape recovery ratios and recover speed than pure PDLLA.

Celite is a product of the Earth which is composed primarily of silica and alumina. It has surface hydroxyl groups that can be coupled with SMPU chains. Park and co-workers [80] fabricated celite/SMPU composites with celite as a crosslinker, which was added in the middle of the PU polymerisation. The celite improved the shape-memory and mechanical properties of SMPU. The best mechanical properties and good SME were obtained at 0.2 wt% celite content.

### 3.6.3 Organic Filler/Shape-memory Polymer Composites

Silsesquioxanes have a general formula  $(\text{RSiO}_{1.5})_n$ , where R is an organic group or hydrogen. Silsesquioxanes with a cage structure are called polyhedral oligomeric silsesquioxanes (POSS). POSS molecules with covalently bonded reactive functionalities can be suitable for polymerisation or grafting POSS monomers to other polymer chains [81–83]. Jeon and co-workers [84] studied the shape-memory properties of norbornyl-POSS copolymers having cyclohexyl-POSS corner groups or cyclopentyl-POSS corner groups. It was found that the POSS macromers aggregated to form cylindrical domains, the size of which influenced shape-memory properties. A preferred direction of the POSS–POSS correlation appeared and was oriented along the draw axis, whereas orientation of polynorbornene chains along the draw axis was hindered (relative to pure polynorbornene). The POSS composites showed two stages of strain recovery: a fast strain-recovery process related to the polynorbornene relaxation in the norbornyl

matrix, and a second slow strain-recovery process which was assumed to be related to the POSS-rich domains. The POSS comonomers decreased the recovery ratios slightly, but increased thermal stability significantly [84, 85].

Cellulose is the second organic filler used to reinforce SMP. Cellulose (the main material in a wide variety of plant life) is one of the most abundant substances in nature. It has polar groups that can interact with PU. Auad and co-workers [9] reinforced SMPU using nanocellulose crystals by suspension casting. A small amount of well-dispersed nanocellulose markedly improved the stiffness of SMP, whereas no obvious shape-memory properties decreased.

### **3.6.4 Shape-memory Polymer Composites with Special Functions**

Several researchers have studied the novel properties of CNT-reinforced SMP and explored their potential applications. Zhang and co-workers [44] investigated the electromagnetic interference shielding effectiveness (EMISE) of multiwall CNF-reinforced SMPU. The evaluation of EMISE was carried out in three frequency bands, 8–26.5 GHz (K band), 33–50 GHz (Q band) and 50–75 GHz (V band). The EMISE of vapour grown carbon fibre (VGCF)/SMPU nanocomposite was strongly dependent upon VGCF content and specimen thickness. VGCF/SMPU nanocomposites are excellent shielding materials for electromagnetic interference [86].

CNT-reinforced SMP can have good UV protection properties arising from the UV-absorption property of CNT [87, 88]. Hu and co-workers [89] treated cotton fabrics with hydrophilic SMPU solution containing MWCNT hoping to fabricate fabrics with not only smart water-vapour permeability but also good UV-protection (Table 3.2). Hydrophilic PU was synthesised using polytetramethylene oxide glycol and PEG as the soft segment. Scoured and bleached fabrics were coated by a roller machine. The coated fabrics showed excellent protection against UV radiation.

Mass transport through breathable dense PU membranes is strongly dependent upon the microstructure of PU. Jeong, Chen, and Mondal studied the water vapour permeability (WVP) of PU membranes. Jeong and co-workers [90, 91] modified PU structure by employing hydrophilic segments such as dimethylpropionic acid and diol-terminated polyethylene oxide to enhance the sensitivity of thermoresponsive WVP. Chen and co-workers [92] improved WVP by increasing the hydrophilic segment molecular weight and decreasing the density of the chemical cross-bonding. Hu and co-workers [93–96] also found that the mass-transfer properties were influenced not only by the amorphous region, but also by the interaction between the polymer chains. A study on the influence of MWCNT on the WVP of SMPU showed that MWCNT at a high content increase the WVP of the membrane. This is because in one aspect,

MWCNT constrain the formation of an ordered soft segment phase structure. In another aspect, straight MWCNT with large aspect ratios offer a relatively straight ‘free’ pathway for the diffusion of water molecules on the surface of MWCNT or within MWCNT to pass through [37].

**Table 3.2 UV Properties of treated and untreated fabrics**

Samples	Mean transmission (%)		Calculated UPF	UPF rating
	UVA	UVB		
F <sub>o</sub>	18.523	13.112	5.600	Non-rateable
F-PU	2.590	0.940	46.128	Very good (<50+)
F-PU-0.25CNT	1.709	0.709	61.919	Excellent (50+)
F-PU-1.00CNT	0.550	0.196	173.987	Excellent (50+)
F-PU-2.50CNT	0.291	0.105	421.198	Excellent (50+)

F: Fabric  
 F<sub>o</sub>: Uncoated fabric  
 UVA: Ultraviolet A (long-wave) (320 or 315 to 400 nm)  
 UVB: Ultraviolet B (shortwave) (290 to 315 or 320 nm)  
 UPF: Ultraviolet protection factor  
 Reproduced with permission from S. Mondal and J.L. Hu, *Journal of Applied Polymer Science*, 2007, **103**, 5, 3370. ©2007, John Wiley & Sons [89]

Beloshenko and co-workers [97–99] in a series of reports described that, in some polymer composite systems with weak interphase interactions, the shape of the composite changes significantly. This phenomenon is associated with relaxation of micro-stresses at interfaces, which results in material loosening. It was revealed that SME is accompanied by a considerable increase in volume for the smart systems mentioned above. A similar result was found in other systems such as ultra-high-molecular polyethylene, and polypropylene as a matrix and cast graphite or carbon as fillers. This enables preparation of products with unusual behaviour under heating: rods increasing in length with the diameter kept constant; bushes increasing in internal diameter with length and external diameter kept constant; discs increasing in diameter with height kept constant.



### 3.7 Conclusions

The present chapter examined research on SMP. The trends of development of SMP composites were also discussed. SMP composites and blends are prepared mainly for five aims: (i) improving shape recovery stress and mechanical properties; (ii) decreasing shape recovery induction time by increasing thermal conductivity; (iii) tuning switch temperature, mechanical properties, and biomedical properties of available SMP; (iv) preparing SMP sensitive to electricity, magnetic fields, light and moisture/water; and (v) creating new polymer/polymer blends possessing SME.

Even though the aims mentioned above have almost been achieved, more work needs to be conducted. First, specific application situations necessitate specific requirements for all of the properties of SMP composites. Extensive and intensive studies are needed on the relationship between the structure of SMP composites, properties of the material, and requirements of specific applications. Second, the recovery stress of SMP composite is too low, which limits many of their applications. Furthermore, at temperatures above the switch temperature of SMP composites, the materials become too soft. Though shape recovery stress can be improved to a certain degree by compounding or blending with other materials, in most circumstances, this method causes low shape recovery ratios and low deformable strain. Third, most of the present SME are simple shape shrinkage or bending processes. Studies on multiple-step and two-way SME are in their infancy. A complicated SME with controllable recovery speed, recovery level, exact recovery shape, and recovery force at different steps is preferred in most complicated applications. Finally, most shape recovery is triggered by direct or indirect heating of SMP composites and blends. Further study is needed to develop multi-sensitive SMP materials that can respond to different parameters of their applied environments so that real environmentally sensitive composites or blends can be obtained.

In general, SMP composites can exhibit novel properties that are significantly different from their pure counterparts so that they can be suitable for more applications. Due to the versatility of SMP composites, it is anticipated that research on SMP composites will grow as a result of their promising potential applications.

### References

1. J.L. Hu, Y. Zhu, H.H. Huang and J. Lu, *Progress in Polymer Science*, 2012, 37, 12, 1720.
2. Q.H. Meng, J.L. Hu, L.Y. Yeung and Y. Hu, *Journal of Applied Polymer Science*, 2009, 111, 3, 1156.



3. X. Lan, Y.J. Liu, H.B. Lv, X.H. Wang, J.S. Leng and S.Y. Du, *Smart Materials & Structures*, 2009, **18**, 2.
4. I.S. Gunes and S.C. Jana, *Journal of Nanoscience and Nanotechnology*, 2008, **8**, 4, 1616.
5. B. Xu, Y.Q. Fu, M. Ahmad, J.K. Luo, W.M. Huang, A. Kraft, R. Reuben, Y.T. Pei, Z.G. Chen and J.T.M. De Hosson, *Journal of Materials Chemistry*, 2010, **20**, 17, 3442.
6. L. Hsu, C. Weder and S.J. Rowan, *Journal of Materials Chemistry*, 2011, **21**, 9, 2812.
7. H. Luo in *Study on Stimulus-responsive Cellulose-based Polymeric Materials*, The Hong Kong Polytechnic University, Hong Kong, China, 2012. [PhD Thesis]
8. M.L. Auad, M.A. Mosiewicki, T. Richardson, M.I. Aranguren and N.E. Marcovich, *Journal of Applied Polymer Science*, 2010, **115**, 2, 1215.
9. M.L. Auad, V.S. Contos, S. Nutt, M.I. Aranguren and N.E. Marcovich, *Polymer International*, 2008, **57**, 4, 651.
10. I.S. Gunes, G.A. Jimenez and S.C. Jana, *Carbon*, 2009, **47**, 4, 981.
11. J.W. Cho, J.W. Kim, Y.C. Jung and N.S. Goo, *Macromolecular Rapid Communications*, 2005, **26**, 5, 412.
12. X.J. Yu, S.B. Zhou, X.T. Zheng, T. Guo, Y. Xiao and B.T. Song, *Nanotechnology*, 2009, **20**, 23.
13. D. Bondeson, I. Kvien and K. Oksman, *ACS Symposium Series*, 2006, **938**, 10.
14. A. Dufresne, J.Y. Cavaille and W. Helbert, *Polymer Composites*, 1997, **18**, 2, 198.
15. N.E. Marcovich, M.L. Auad, N.E. Bellesi, S.R. Nutt and M.I. Aranguren, *Journal of Materials Research*, 2006, **21**, 4, 870.
16. J.R. Capadona, K. Shanmuganathan, D.J. Tyler, S.J. Rowan and C. Weder, *Science*, 2008, **319**, 5868, 1370.

17. S.J. Eichhorn, A. Dufresne, M. Aranguren, N.E. Marcovich, J.R. Capadona, S.J. Rowan, C. Weder, W. Thielemans, M. Roman, S. Renneckar, W. Gindl, S. Veigel, J. Keckes, H. Yano, K. Abe, M. Nogi, A.N. Nakagaito, A. Mangalam, J. Simonsen, A. S. Benight, A. Bismarck, L.A. Berglund and T. Peijs, *Journal of Materials Science*, 2010, **45**, 1, 1.
18. N. Ljungberg, J.Y. Cavaille and L. Heux, *Polymer*, 2006, **47**, 18, 6285.
19. N.L.G. de Rodriguez, W. Thielemans and A. Dufresne, *Cellulose*, 2006, **13**, 3, 261.
20. E. Trovatti, L. Oliveira, C.S.R. Freire, A.J.D. Silvestre, C.P. Neto, J.J.C.C. Pinto and A. Gandini, *Composites Science and Technology*, 2010, **70**, 7, 1148.
21. H.S. Luo, J.L. Hu and Y. Zhu, *Materials Letters*, 2011, **65**, 23-24, 3583.
22. Y. Zhu, J.L. Hu, H.S. Luo, R.J. Young, L.B. Deng, S. Zhang, Y. Fan and G.D. Ye, *Soft Matter*, 2012, **8**, 8, 2509.
23. H.S. Luo, J.L. Hu and Y. Zhu, *Macromolecular Chemistry and Physics*, 2011, **212**, 18, 1981.
24. B.G. Demczyk, Y.M. Wang, J. Cumings, M. Hetman, W. Han, A. Zettl and R.O. Ritchie, *Materials Science and Engineering: A*, 2002, **334**, 1-2, 173.
25. H.M. Huang, I.C. Liu, C.Y. Chang, H.C. Tsai, C.H. Hsu and R.C.C. Tsiang, *Journal of Polymer Science, Part A: Polymer Chemistry Edition*, 2004, **42**, 22, 5802.
26. W.D. Zhang, L. Shen, I.Y. Phang and T.X. Liu, *Macromolecules*, 2004, **37**, 2, 256.
27. Y.C. Jung, N.G. Sahoo and J.W. Cho, *Macromolecular Rapid Communications*, 2006, **27**, 2, 126.
28. M. Cadek, J.N. Coleman, K.P. Ryan, V. Nicolosi, G. Bister, A. Fonseca, J.B. Nagy, K. Szostak, F. Beguin and W.J. Blau, *ACS Nano Letters*, 2004, **4**, 2, 353.
29. H.H. Gommans, J.W. Alldredge, H. Tashiro, J. Park, J. Magnuson and A.G. Rinzler, *Journal of Applied Physics*, 2000, **88**, 5, 2509.

30. H.Q. Hou, J.J. Ge, J. Zeng, Q. Li, D.H. Reneker, A. Greiner and S.Z.D. Cheng, *Chemistry of Materials*, 2005, **17**, 5, 967.
31. J. Kwon and H. Kim, *Journal of Polymer Science, Part A: Polymer Chemistry Edition*, 2005, **43**, 17, 3973.
32. W. Chen and X.M. Tao, *Macromolecular Rapid Communications*, 2005, **26**, 22, 1763.
33. S. Mondal and J.L. Hu, *Iran Polymer Journal*, 2006, **15**, 2, 135.
34. I.S. Gunes, F. Cao and S.C. Jana, *Polymer*, 2008, **49**, 9, 2223.
35. H. Koerner, G. Price, N.A. Pearce, M. Alexander and R.A. Vaia, *Nature Materials*, 2004, **3**, 2, 115.
36. Q.Q. Ni, C.S. Zhang, Y.Q. Fu, G.Z. Dai and T. Kimura, *Composite Structures*, 2007, **81**, 2, 176.
37. Q.H. Meng, J.L. Hu and S. Mondal, *Journal of Membrane Science*, 2008, **319**, 1-2, 102.
38. N.G. Sahoo, Y.C. Jung, H.J. Yoo and J.W. Cho, *Composites Science and Technology*, 2007, **67**, 9, 1920.
39. P. Miaudet, A. Derre, M. Maugey, C. Zakri, P.M. Piccione, R. Inoubli and P. Poulin, *Science*, 2007, **318**, 5854, 1294.
40. F.K. Li, L.Y. Qi, J.P. Yang, M. Xu, X.L. Luo and D.Z. Ma, *Journal of Applied Polymer Science*, 2000, **75**, 1, 68.
41. B. Yang, W.M. Huang, C. Li, L. Li and J.H. Chor, *Scripta Materialia*, 2005, **53**, 1, 105.
42. H.B. Lv, J.S. Leng, Y.J. Liu and S.Y. Du, *Advanced Engineering Materials*, 2008, **10**, 6, 592.
43. B. Yang, W.M. Huang, C. Li and J.H. Chor, *European Polymer Journal*, 2005, **41**, 5, 1123.
44. C.S. Zhang, Q.Q. Ni, S.Y. Fu and K. Kurashiki, *Composites Science and Technology*, 2007, **67**, 14, 2973.
45. H.F. Lee and H.H. Yu, *Soft Matter*, 2011, **7**, 8, 3801.

46. F.C. Meng, X.H. Zhang, G. Xu, Z.Z. Yong, H.Y. Chen, M.H. Chen, Q.W. Li and Y.T. Zhu, *ACS Applied Materials & Interfaces*, 2011, **3**, 3, 658.
47. Y.C. Jung, H.J. Yoo, Y.A. Kim, J.W. Cho and M. Endo, *Carbon*, 2010, **48**, 5, 1598.
48. J.S. Leng, X.L. Wu and Y.J. Liu, *Journal of Applied Polymer Science*, 2009, **114**, 4, 2455.
49. J.J. Liang, Y.F. Xu, Y. Huang, L. Zhang, Y. Wang, Y.F. Ma, F.F. Li, T.Y. Guo and Y.S. Chen, *Journal of Physical Chemistry C*, 2009, **113**, 22, 9921.
50. Q.H. Meng, J.L. Hu and Y. Zhu, *Journal of Applied Polymer Science*, 2007, **106**, 2, 837.
51. Q.H. Meng and J.L. Hu, *Composites Part A: Applied Science and Manufacturing*, 2008, **39**, 2, 314.
52. C. Bartholome, P. Miaudet, A. Derre, M. Maugey, O. Roubeau, C. Zakri and P. Poulin, *Composites Science and Technology*, 2008, **68**, 12, 2568.
53. L. Viry, C. Mercader, P. Miaudet, C. Zakri, A. Derre, A. Kuhn, M. Maugey and P. Poulin, *Journal of Materials Chemistry*, 2010, **20**, 17, 3487.
54. H.B. Lu and J.H. Gou, *Polymers for Advanced Technologies*, 2012, **23**, 12, 1529.
55. H.B. Lu, F. Liang and J.H. Gou, *Soft Matter*, 2011, **7**, 16, 7416.
56. Y.C. Jung, H.H. Kim, Y.A. Kim, J.H. Kim, J.W. Cho, M. Endo and M.S. Dresselhaus, *Macromolecules*, 2010, **43**, 14, 6106.
57. C.S. Zhang and Q.Q. Ni, *Composite Structures*, 2007, **78**, 2, 153.
58. C. Liang, C.A. Rogers and E. Malafeew, *Journal of Intelligent Material Systems and Structures*, 1997, **8**, 4, 380.
59. Z.G. Wei, R. Sandstrom and S. Miyazaki, *Journal of Materials Science*, 1998, **33**, 15, 3763.
60. K. Gall, M. Mikulas, N.A. Munshi, F. Beavers and M. Tupper, *Journal of Intelligent Material Systems and Structures*, 2000, **11**, 11, 877.
61. D. Campbell and A. Maji, *Journal of Aerospace Engineering*, 2006, **19**, 3, 184.

62. J.H. Yang, B.C. Chun, Y.C. Chung, J.W. Cho and B.G. Cho, *Journal of Applied Polymer Science*, 2004, **94**, 1, 302.
63. X.F. Luo and P.T. Mather, *Macromolecules*, 2009, **42**, 19, 7251.
64. X.F. Luo and P.T. Mather, *Advanced Functional Materials*, 2010, **20**, 16, 2649.
65. X.F. Luo and P.T. Mather, *Soft Matter*, 2010, **6**, 10, 2146.
66. H.B. Lu, Y.J. Liu, J.H. Gou, J.S. Leng and S.Y. Du, *Applied Physics Letters*, 2010, **96**, 8.
67. U.N. Kumar, K. Kratz, M. Behl and A. Lendlein, *eXPRESS Polymer Letters*, 2012, **6**, 1, 26.
68. J. M. Cuevas, J. Alonso, L. German, M. Iturrondobeitia, J.M. Laza, J.L. Vilas and L.M. Leon, *Smart Materials & Structures*, 2009, **18**, 7.
69. A. Golbang and M. Kokabi, *Advanced Materials Research-Switz*, 2010, **123-125**, 999.
70. M. Zeng, S.W. Or and H.L.W. Chan, *Journal of Applied Physics*, 2010, **107**, 9.
71. D.W. Zhang, Y.J. Liu and J.S. Leng, *Advanced Materials Research-Switz*, 2010, **123-125**, 995.
72. R. Mohr, K. Kratz, T. Weigel, M. Lucka-Gabor, M. Moneke and A. Lendlein, *Proceedings of the National Academy of Sciences USA*, 2006, **103**, 10, 3540.
73. U.N. Kumar, K. Kratz, W. Wagermaier, M. Behl and A. Lendlein, *Journal of Materials Chemistry*, 2010, **20**, 17, 3404.
74. Z. Varga, G. Filipcsei and M. Zrinyi, *Polymer*, 2006, **47**, 1, 227.
75. M.Y. Razzaq, M. Anhalt, L. Frommann and B. Weidenfeller, *Materials Science and Engineering: A*, 2007, **444**, 1-2, 227.
76. M.Y. Razzaq, M. Anhalt, L. Frommann and B. Weidenfeller, *Materials Science and Engineering: A*, 2007, **471**, 1-2, 57.
77. M.S. Kim, J.K. Jun and H.M. Jeong, *Composites Science and Technology*, 2008, **68**, 7-8, 1919.

78. F. Cao and S.C. Jana, *Polymer*, 2007, **48**, 13, 3790.
79. X.T. Zheng, S.B. Zhou, X.H. Li and H. Weng, *Biomaterials*, 2006, **27**, 24, 4288.
80. J.S. Park, Y.C. Chung, S. Do Lee, J.W. Cho and B.C. Chun, *Fibers and Polymers*, 2008, **9**, 6, 661.
81. R.H. Baney, M. Itoh, A. Sakakibara and T. Suzuki, *Chemical Reviews*, 1995, **95**, 5, 1409.
82. R.A. Mantz, P.F. Jones, K.P. Chaffee, J.D. Lichtenhan, J.W. Gilman, I.M.K. Ismail and M.J. Burmeister, *Chemistry of Materials*, 1996, **8**, 6, 1250.
83. A. Fina, D. Tabuani, F. Carniato, A. Frache, E. Boccaleri and G. Camino, *Thermochimica Acta*, 2006, **440**, 1, 36.
84. H.G. Jeon, P.T. Mather and T.S. Haddad, *Polymer International*, 2000, **49**, 5, 453.
85. P.T. Mather, H.G. Jeon, A. Romo-Urbe, T.S. Haddad and J.D. Lichtenhan, *Macromolecules*, 1999, **32**, 4, 1194.
86. R.M. Simon, *Polym-Plastics Technology and Engineering*, 1981, **17**, 1, 1.
87. W. Hoenlein, F. Kreupl, G.S. Duesberg, A.P. Graham, M. Liebau, R. Seidel and E. Unger, *Materials and Science Engineering: C*, 2003, **23**, 6-8, 663.
88. M. Freitag, J. Chen, J. Tersoff, J.C. Tsang, Q. Fu, J. Liu and P. Avouris, *Physical Review Letters*, 2004, **93**, 7.
89. S. Mondal and J.L. Hu, *Journal of Applied Polymer Science*, 2007, **103**, 5, 3370.
90. H.M. Jeong, B.K. Ahn, S.M. Cho and B.K. Kim, *Journal of Polymer Science, Part B: Polymer Physics Edition*, 2000, **38**, 23, 3009.
91. H.M. Jeong, B.K. Ahn and B.K. Kim, *Polymer International*, 2000, **49**, 12, 1714.
92. W. Chen, C.Y. Zhu and X.R. Gu, *Journal of Applied Polymer Science*, 2002, **84**, 8, 1504.
93. S. Mondal and J.L. Hu, *Journal of Membrane Science*, 2006, **276**, 1-2, 16.

94. S. Mondal and J.L. Hu, *Journal of Membrane Science*, 2006, **274**, 1-2, 219.
95. S. Mondal and J.L. Hu, *Carbohydrate Polymers*, 2007, **67**, 3, 282.
96. S. Mondal, J.L. Hu and Z. Yong, *Journal of Membrane Science*, 2006, **280**, 1-2, 427.
97. V.A. Beloshenko and Y.V. Voznyak, *Polymer Science Series: A*, 2009, **51**, 4, 416.
98. V.A. Beloshenko, V.N. Varyukhin and Y.V. Voznyak, *Composites Part A: Applied Science and Manufacturing*, 2005, **36**, 1, 65.
99. V.A. Beloshenko, Y.E. Beygelzimer, A.P. Borzenko and V.N. Varyukhin, *Composites Part A: Applied Science and Manufacturing*, 2002, **33**, 7, 1001.

# 4 Shape-memory Polymer Blends

## 4.1 Introduction

Shape-memory polymers (SMP) have received increasing attention in recent years on account of their interesting properties and potential applications. Such applications include medical devices, actuators, sensors, artificial muscles, switches, smart textiles and self-deployable structures [1–4]. Increasing numbers of scientists and engineers are turning to the design of new SMP for more extensive and in-depth applications.

According to the mechanism of action of shape-memory, the features of SMP should include a transition that can be used to fix the secondary shape at low temperatures and trigger shape recovery at high temperatures, elasticity for shape recovery above the transition temperature, and ability of fixing the temporary shapes [1]. Based on the concept, SMP can be divided into four main classes [2], as described below.

1. *Covalently crosslinked glassy thermoset networks* are the simplest type of SMP. The rubbery elasticity derived from covalent crosslinks elicits excellent shape recovery, which is tunable through adjustment of the extent of covalent crosslinking. However, the covalently fixed primary shape makes it difficult to reshape thereafter once processed.
2. *Covalently crosslinked semi-crystalline networks*: The melting transition of semi-crystalline networks can also be employed to trigger shape recovery as well as the glass transition.
3. *Physically crosslinked glassy copolymers*: In this system, crystalline or rigid amorphous domains, in the form of phase-separated block copolymers, act as physical crosslinks providing the super-glass transition temperature ( $T_g$ ) elasticity required for shape-memory effects (SME).
4. *Physically crosslinked semi-crystalline block copolymers*: The soft phase of some block copolymers crystallises and their melting temperature ( $T_m$ ) values function as the transition temperature instead of the  $T_g$ . Thus, the secondary shapes are fixed by crystallisation of the soft phase.

It has been suggested that the shape-memory ability of SMP is dominated by the



thermal and mechanical properties of polymer networks. The precise design of polymer networks seems to be necessary to achieve the desired SME. However, synthesising and characterising new types of SMP is complicated and inconvenient [5–8]. Hence, polymer blending methods (which simplify the technology, lower the cost, and make it possible to reprocess or recycle these materials easily [2, 3]) have been proposed as ideal methods for preparing novel SMP systems and improving the shape-memory properties of conventional SMP.

Based on the miscibility of the blend components, this chapter will throw light on the preparation and characteristics of miscible/immiscible SMP blends. Blending and post-crosslinking polymer components to form polymer networks such as interpenetrating networks (IPN) are also introducing as promising strategies to fabricate novel SMP.

## **4.2 Miscible Polymer Blends**

Blending miscible polymers is an attractive method to prepare new SMP because the fabrication strategy is simple and applicable. Miscible amorphous/crystalline polymers blends can be used to create new shape-memory materials with one polymer forming the fixing phase and the other the reversible phase. Miscible SMP/crystalline polymer blends can be used to ‘tune’ or improve the properties of available SMP.

### **4.2.1 Shape-memory Polymer/Polymer Blends**

Utilising a thermoplastic SMP as one component and a miscible polymer as the other to prepare binary SMP blends is an effective method to lower the costs as well as to adjust switch temperatures and mechanical properties while maintaining a certain level of SME of SMP.

Polyurethane (PU) is one of the most familiar SMP and has received increasing attention due to its excellent shape-memory properties [4]. Jeong and co-workers developed a novel SMP blend by means of thermoplastic polyurethane (TPU) and phenoxy resin [5]. The soft segment of TPU acted as a reversible phase and was miscible with phenoxy resin at any composition in the blends, whereas the hard domain was utilised as the fixed phase. The switching temperature could be tuned between the  $T_g$  of the soft segment of the TPU and phenoxy resin. Jeong and Song reported on the miscibility and shape-memory properties of TPU/polyvinyl chloride (PVC) blends [6]. PVC was miscible with the poly( $\epsilon$ -caprolactone) (PCL) segment in TPU, and the switching temperature of the miscible amorphous domain varied smoothly with composition. They observed that permanent deformation was fixed by the hard segment domain in TPU, and that recoverable deformation of the reversible

phase was formed by the miscible PVC/PCL segment domain.

Ajili and co-workers reported on the SME of PU/PCL blends [7]. A PU copolymer based on a PCL diol was partially miscible with PCL. It was shown that all PU/PCL blends except for PU/PCL (80/20) showed SME and that the recovery temperatures were around the melting temperature of PCL. The shape recovery response of the PU/PCL blends was strongly influenced by the deformation temperature (melting or solution temperature) and shape fixing temperature (transition temperature). When a deformation was made above the  $T_m$ , shape recovery took place over a wide temperature range from the temperature at which secondary crystallites melts ( $T_{m,s}$ ) to the temperature at which primary crystallites melts ( $T_{m,p}$ ). This happened because primary and secondary crystalline entities were formed (Figure 4.1a). However, when the deformation was made between  $T_{m,s}$  and  $T_{m,p}$ , steep recovery curves and almost complete recovery ratios could be obtained in the range of  $T_{m,s}$ . This phenomenon occurred while the temporary shape was fixed by formation of secondary crystals (Figure 4.1b).

The composition and crystallisation conditions of PU/PCL blends clearly influenced the switching temperature. Hence, tuning shape recovery to the range of body temperature for the blends was challenging. PU/PCL blends showed great biocompatibility as evaluated by human bone-marrow mesenchymal stem cells, and might be a potential SMP as a stent implant.

Behl and co-workers examined the shape-memory properties of binary copolymer blends of poly(*p*-dioxanone) (PPDO)/PCL blends [8]. The hard segment PPDO and switching segment PCL were immiscible, but the polyalkylene adipate mediator segment was incorporated in both multiblock copolymers to improve the miscibility of PPDO/PCL blends. The switching temperature was dependent upon the switching domains and the  $T_m$  of PCL. Shape-memory properties were excellent at all weight ratios of the two blend components, and the mechanical properties could be varied systematically. The binary blend system had several advantages (biodegradability, economically efficient, variation of mechanical properties, and a switching temperature around body temperature) making it a suitable candidate for biomedical applications.

Madbouly and co-workers developed a degradable PU/soybean protein (SP) blend which was synthesised using an environmentally friendly aqueous dispersion method [9]. The SP and PCL segment of PU were miscible at the entire range of compositions investigated. The  $T_m$  decreased with increasing SP content in the binary miscible blend due to the decreasing hard domain of PU. Figure 4.2 shows the scanning electron micrographs of PU/SP foams of different blend compositions. Porous structures were fabricated by the scCO<sub>2</sub> foaming method. The degree of porosity reached 85% at the wt% of soybean protein in PU/SP blend ( $w_{sp}$ ) = 0.4 and decreased with increasing

SP content, whereas no porous structure could be obtained at  $w_{SP} = 0.4$  owing to the decreasing stability of the foams. The polymer films and foams obtained from the PU/SP blends which possessed hydrolytic degradability and shape-memory capability could be utilised as potential biomedical materials.

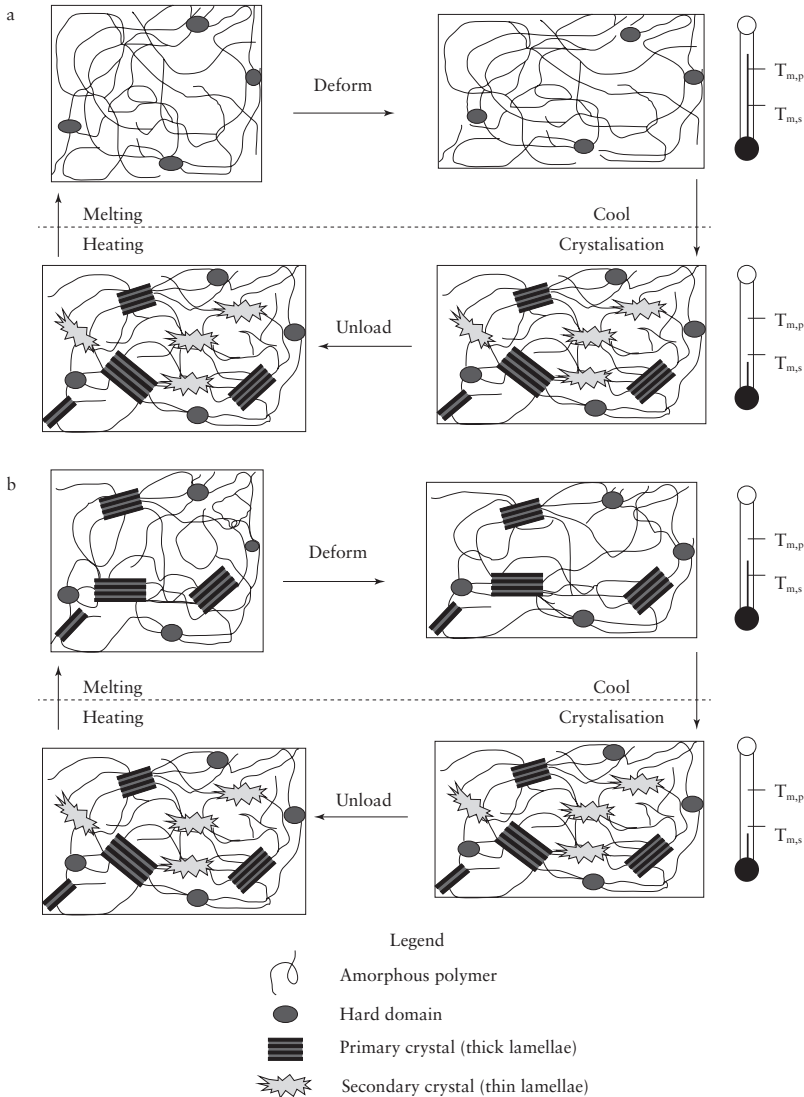
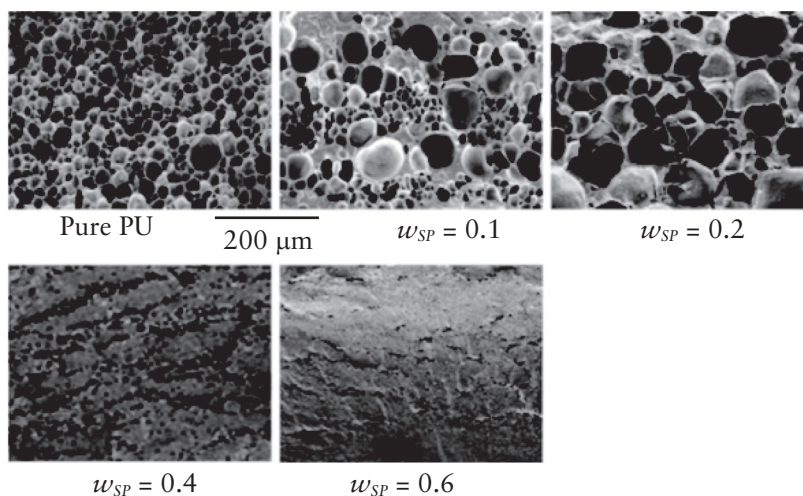


Figure 4.1 Molecular mechanism of SME for PU/PCL blends (schematic): (a) deformation above the  $T_{m,p}$ ; and (b) deformation temperature between  $T_{m,s}$  and  $T_{m,p}$ . Reproduced with permission from S.H. Ajili, N.G. Ebrahimi and M. Soleimani, *Acta Biomaterialia*, 2009, 5, 5, 1519. ©2009, Elsevier [7]

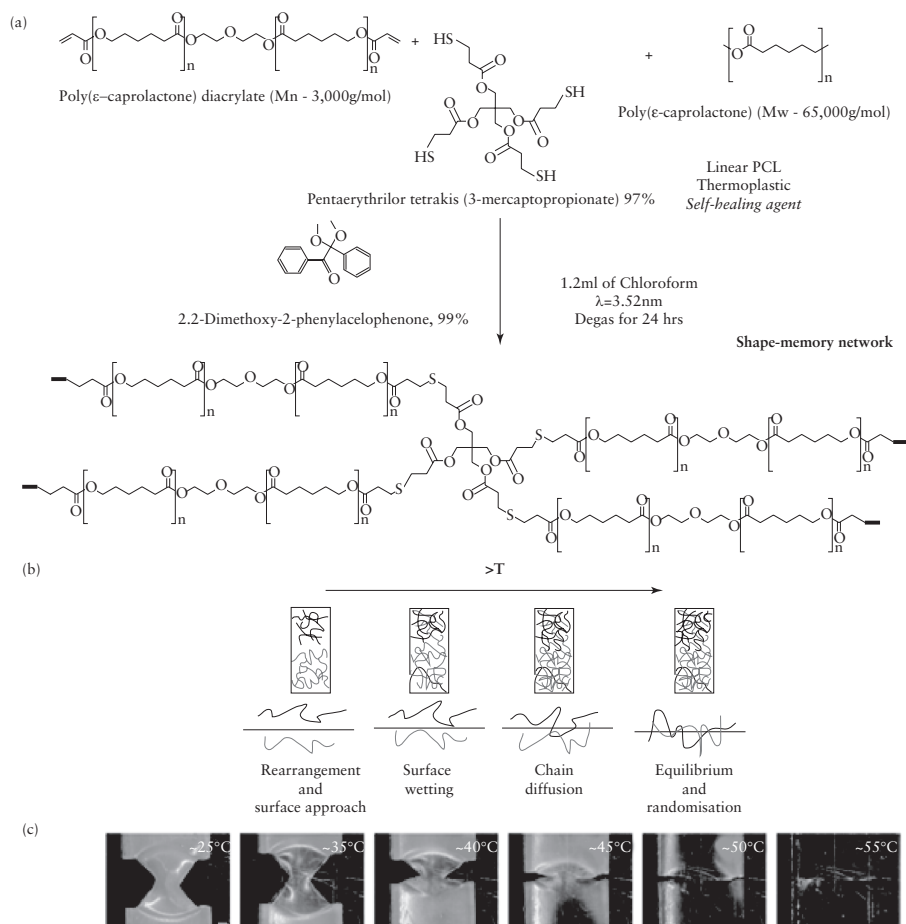


**Figure 4.2** Scanning electron micrographs for the porous structure of PU/SP blends of different concentrations generated using the scCO<sub>2</sub> method at a foaming temperature of 35 °C, 100 bar, and 30-min saturation time. Reproduced with permission from S.A. Madbouly and A. Lendlein, *Macromolecular Materials and Engineering*, 2012, 297, 12, 1213. ©2012, John Wiley & Sons [9]

Erden and co-workers reported on TPU/polybenzoxazine (PB) blends [10]. It was shown that benzoxazine/PU prepolymer formed miscible blends, and that some degree of reaction between the phenolic –OH groups of PB and isocyanate groups of PU took place, during the thermal curing of benzoxazine. The PU/PB blends showed excellent shape-memory properties and higher shape recovery forces, faster shape recovery, and greater shape recovery ratio than shape-memory polyurethanes (SMPU).

A novel miscible blend with shape-memory-assisted self-healing (SMASH) properties was reported by Rodriguez and co-workers [11]. The blend was prepared by blending a crosslinked PCL network (n-PCL) and linear PCL (l-PCL) (Figure 4.3a). l-PCL interpenetrated the crosslinked PCL network. The blend exhibited a combination of shape-memory response from the network component (n-PCL) and SH capacity from the linear component (l-PCL). The blend containing n-PCL exhibited excellent shape-memory responses owing to the recovery of strain by rubber elasticity in the network and fixing of strain by PCL crystallisation [12, 13]. As the l-PCL content increased from 20 to 70 wt% in the blend, the fixity ratio ( $R_f$ ) increased from 74.1% to 80.9% and the recovery ratio ( $R_r$ ) decreased from 92.7 to 69.1%. The l-PCL chains could diffuse through the n-PCL network and could ‘heal’ the cracks by molecular diffusion above the  $T_m$ . The authors envisioned that the healing process could take

place over five stages (Figure 4.3b). Figure 4.3c shows the ‘snapshots’ of the self-healing process. The healing was nearly complete for samples with l-PCL content >25 wt%. Remarkably, the high  $R_r$  could increase the probability of SH because this recovery would assist in the closing of cracks. Such SMASH blends could be utilised for self-healing bladders, inflated membranes, and architectural building envelopes.



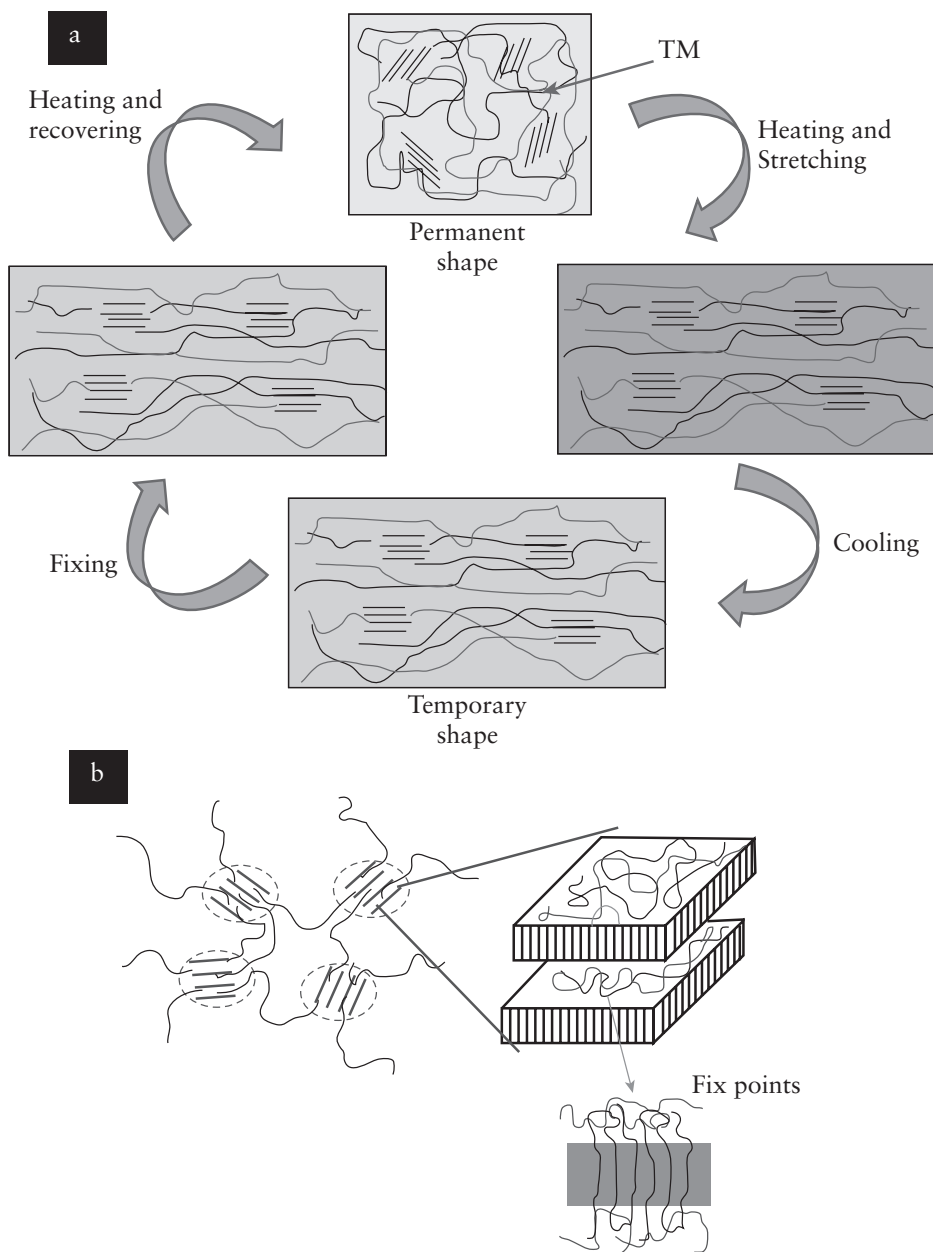
**Figure 4.3** (a) Preparation blends containing n-PCL and l-PCL by UV-initiated thiol-ene polymerisation in the presence of non-reactive l-PCL. (b) Schematic of the five stages of healing. (c) Snapshots of crack closure and crack rebonding when the sample was unclamped from the Linkam tensile stage and heated to the temperatures shown above (stereo micrographs scale bar: 500  $\mu\text{m}$ ). UV: ultraviolet. Reproduced with permission from E.D. Rodriguez, X. Luo and P.T. Mather, *ACS Applied Materials & Interfaces*, 2011, 3, 2, 152. ©2011, American Chemical Society [11]

### **4.2.2 Amorphous Polymer/Crystalline Polymer Blends**

Amorphous/crystalline polymer blends are completely miscible with a single phase and the  $T_g$ , whereas the crystalline phase acts as the fixing phase to keep a permanent shape above the  $T_g$  but below the  $T_m$ . The  $T_g$  and shape-memory properties of the blends can be manipulated by changing compositions.

Mather and co-workers reported on the miscible amorphous/semi-crystalline polymer blend systems of amorphous polyvinyl acetate (PVAc)/semi-crystalline polylactide (PLA) and amorphous polymethyl methacrylate (PMMA)/semicrystalline polyvinylidene fluoride (PVDF) [14]. The polymer blends of both systems were totally melt miscible within the experimental ranges, and formed only one single  $T_g$  for all blend ratios. PVAc and PMMA were totally amorphous, but PLA and PVDF each showed semi-crystalline features and had a degree of crystallinity of  $\approx 50\%$ . According to the blend ratio, the rubbery modulus could be governed by a degree of crystallinity of the blends that varied from 0 to 50%, and the crystals served as physical crosslinks. The  $T_g$  of the amorphous phase worked as the critical temperature for triggering the shape recovery, and could be tailored between the  $T_g$  values of the two homopolymers.

Recently, You and co-workers reported on the shape-memory performance of miscible amorphous/crystalline polymer blends of PVDF/acrylic copolymer (ACP) which could be reused readily many times [15]. They showed that simple melt-mixed PVDF/ACP blends with 40–50 wt% PVDF demonstrated good shape-memory performance. The shape-memory properties are depicted schematically in **Figure 4.4a**. The small PVDF crystals acted as the fixed phase and the amorphous phase between the PVDF crystals acted as the switching phase. Shape recovery properties were affected by tie molecules between the fixing PVDF crystal phases. This was because there was a loose and elastic network of PVDF crystals connected by tie molecules which prevented molecular slip upon deformation (**Figure 4.4b**). Blends containing 50 wt% PVDF in which a small amount of tie molecules formed a deformable elastic network possessed the best shape-memory recovery properties. Conversely, when there were few or many tie molecules in the blends, the blends exhibited relatively low shape-memory performance owing to slipping of the amorphous molecules or the large fibrillar crystal structure during deformation.



**Figure 4.4** Schematic diagrams for (a) the shape-memory properties of PVDF/acrylic copolymer blends; and (b) the molecular mechanism. TM: Tie molecules. Reproduced with permission from J. You, W. Dong, L. Zhao, X. Cao, J. Qiu, W. Sheng and Y. Li, *The Journal of Physical Chemistry B*, 2012, 116, 4, 1256. ©2012, American Chemical Society [15]



Furthermore, You and co-workers also investigated the crystal morphologies and shape-memory properties of PVDF/ACP (50/50) blends at different cold crystallisation temperatures [16]. Blends cold crystallised at high temperature exhibited a low shape recovery ratio value due to large spherulites and high crystallinity, whereas high fixity and high shape recovery ratio could be achieved when tiny crystals (100 nm in length) produced at low cold crystallisation temperature acted as the effective fixed phase in the blends. The switching temperature of the obtained blends could be tuned at  $\approx 5$  °C by cold crystallisation. Such SMP could be utilised for biomedical applications because the switching temperature could be very close to body temperature.

### **4.3 Immiscible Polymer Blends**

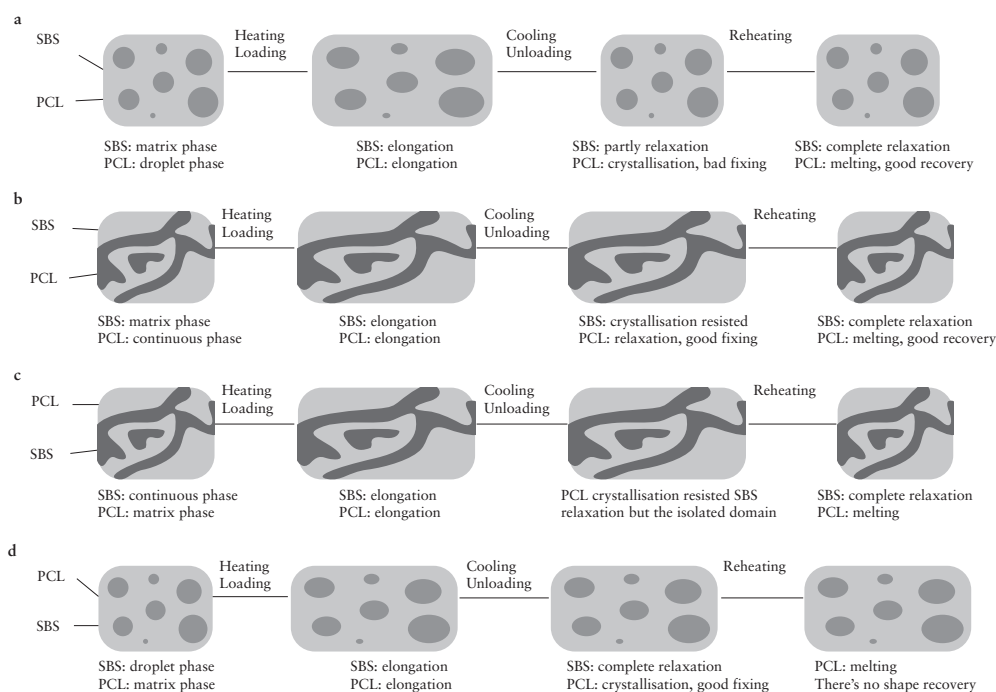
Polymers are immiscible if polymers are not mixed at the molecular level. Immiscible blends show a phase-separated structure. The phase-separated morphology influences the shape-memory properties and other properties of immiscible polymer blends. Alternatively, incorporating the same mediator segment type in both multiblock copolymers is an effective way to promote miscibility.

#### **4.3.1 Elastomer/Polymer Blends**

In elastomer/polymer blends, there are two immiscible components: one is an elastomer and the other is a switch polymer that can demonstrate good shape-memory properties. The elastomer can be any rubber or thermoplastic elastomer. The switch polymer can be any amorphous or crystalline polymer. The shape-memory properties of elastomer/polymer blends can be optimised by controlling the phase morphology of the two components.

Zhang and co-workers prepared novel immiscible styrene-butadiene-styrene tri-block copolymer (SBS)/PCL blends with different compositions [17]. They investigated the shape-memory properties of SBS/PCL blends. The shape-memory mechanism was classified into four series with different phase morphologies (**Figure 4.5**). In the immiscible blends, the SBS elastomer provided the stretching and recovery performances, and the switch polymer provided the fixing and unfixing performances. Shape-memory properties were largely influenced by the phase morphology. When the SBS elastomer formed a major continuous phase and the PCL segment formed a minor continuous phase, the best SME could be attained through careful design of the morphology of the immiscible phase.



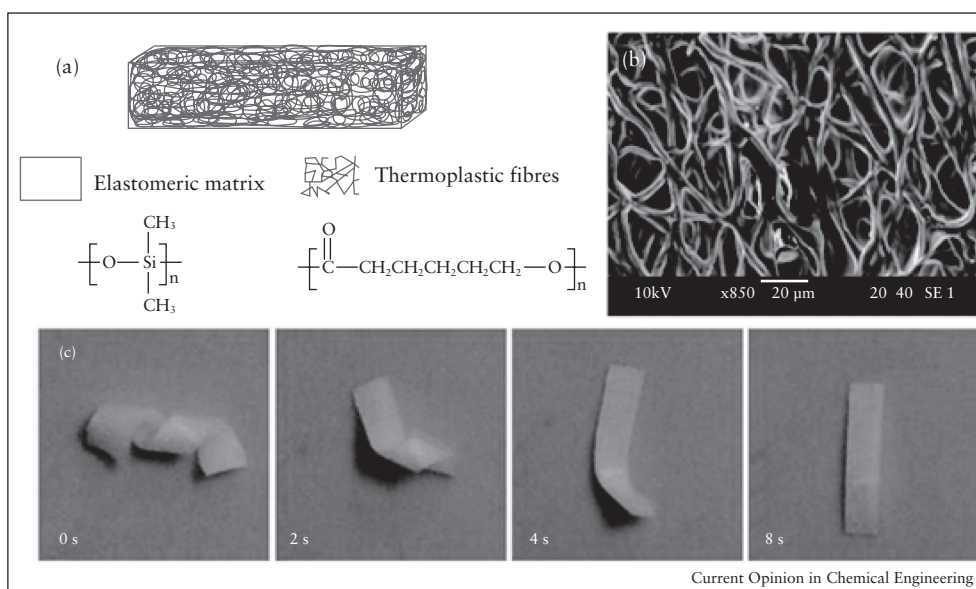


**Figure 4.5** Shape-memory mechanisms of elastomer/switch polymer blends concluded from SBS/PCL blends (schematic). Reproduced with permission from H. Zhang, H. Wang, W. Zhong and Q. Du, *Polymer*, 2009, 50, 6, 1596. ©2009, Elsevier [17]

Zhang and co-workers reported another immiscible blend SMP by blending SBS and poly(D,L-lactic acid) (dl-PLA) [18]. The shape-memory effect was dominated by the formation of bicontinuous structures. These bicontinuous structures showed much higher shape recovery and fixing ratios than the blends beyond the bicontinuous range. Compared with SBS/PCL blends, the shape recovery was notable even if the elastic SBS became an isolated domain in the SBS/dl-PLA blends. The SBS/PLA blend system proved to be an example of a dual-domain shape-memory system.

Weiss and co-workers designed a type of SMP by blending an elastomeric ionomer with low molar mass fatty acids and their salts [19]. Nanophase separation of the ionomer was used to develop a crosslinking network and fatty acids (salts) were used to produce a  $T_m$  as the switch. However, the interactions between FA crystals and polymers were not strong enough to provide a robust crosslink without the ionomer. The switch temperature of this type of SMP was varied readily by choosing fatty acids with different melting points.

Luo and Mather prepared a shape-memory elastomeric composite (SMEC) by means of infiltrating an electrospun PCL mat with liquid Sylgard and curing below the  $T_m$  of PCL [20]. Although the two components in SMEC were not blended in a melted or solution state, the new design strategy of SMEC by infiltrating two components could be regarded as a specific blending method to prepare SMP. Figures 4.6a and b show that the SMEC exhibited a two-phase morphology in which semi-crystalline PCL was present as a non-woven fabric distributed evenly in a continuous Sylgard matrix. The SMEC exhibited excellent shape-memory performance, with Sylgard providing a stationary phase and PCL serving as a  $T_m$ -based switching segment (Figure 4.6c). This new design strategy for SMEC is versatile and has broad applicability due to no specific chemical or physical interactions. Furthermore, it is possible to tune the shape-memory behaviour and material properties by controlling the properties of the individual components.



**Figure 4.6** SMEC: (a) Composite structure (schematic); (b) scanning electron micrograph image showing bulk composite morphology; and (c) a series of photographs showing the recovery form affixed, in the temporary shape and permanent shape on a hot-plate at 80 °C. Reproduced with permission from X. Luo and P.T. Mather, *Macromolecules*, 2009, **42**, 19, 7251. ©2009, American Chemical Society [20]

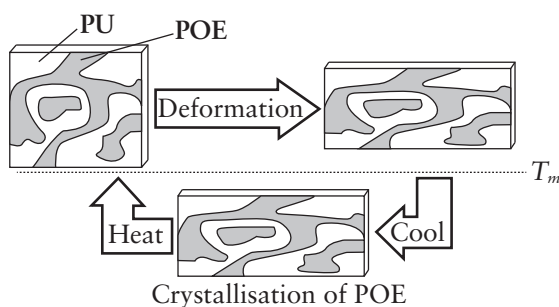
By following the same design strategy, Luo and Mather also developed a series of triple-shape polymeric composites (TSPC) based on the fibre/elastomeric matrix composite approach [21]. During fabrication of TSPC, an epoxy-based copolymer chemically composed of an aromatic diepoxide (diglycidyl ether of bisphenol-A), an aliphatic diepoxide (neopentyl glycol diglycidyl ether), and a diamine curing agent (polypropylene glycol (*bis*(2-aminopropyl))) was prepared. Then, a piece of PCL fibre mat was immersed into the liquid resin mixture, which could wet the mat readily due to its low starting viscosity. The TSPC also exhibited excellent shape-memory performance, with an epoxy-based copolymer providing a stationary phase and PCL serving as switching phase. The TSPC could fix two independent temporary shapes and recover sequentially from the first to the second temporary shape and eventually to the permanent shape upon continuous heating. One can control the transition temperatures by simply selecting different polymers for the fibres and matrix, or functionalising them separately to achieve other novel functions (in addition to triple-shape), such as controlled drug delivery or reversible adhesion.

#### **4.3.2 Other Types of Immiscible Blends**

Immiscible SMP/polymer blends, immiscible crystalline/amorphous polymer blends, and immiscible crystalline polymer blends can also demonstrate shape-memory behaviour.

Kurahashi and co-workers reported an immiscible polymer blend based on TPU and crystalline polyoxyethylene (POE) [22]. The soft segment in PU acted as the reversible phase, and the crystallisation and solidification phases of POE were used to fix the temporary shape. The PU/POE blend showed good shape-memory properties, and the shape-memory mechanism is represented in **Figure 4.7**. The molecular weight of POE did not have a remarkable influence on the SME of the blend. The  $R_f$  below the crystallisation temperature had a sharp rise of nearly 100% and the  $R_r$  above the  $T_m$  grew much slower with increased POE content in the blend.

To improve the SME of PLA, Lai and co-workers prepared a bio-based PLA/TPU blend through melt-blending and investigated its shape-memory properties [23]. The  $R_f$  of the PLA/TPU (50/50) blend showed a significant increase (up to  $93.5 \pm 0.4\%$ ) with the introduction of TPU compared with that of PLA at the pre-deformation temperature of 25 °C. The blend had enhanced shape-fixing ability with increase in pre-deformation temperature, which was contrary to the trend of shape-recovery ability. Furthermore, upon heating under full-strain constraint, the recovery stress for all samples pre-deformed at different temperatures showed a maximum peak with increasing temperature.



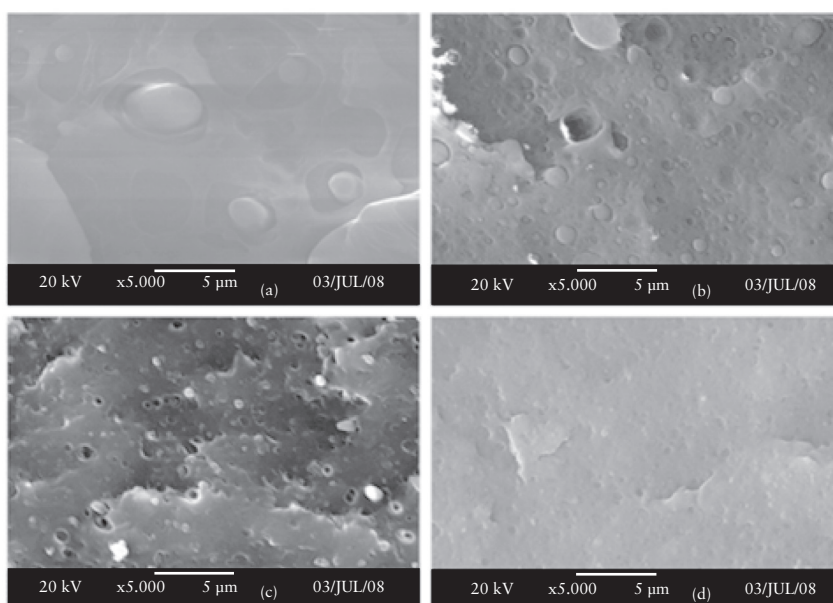
**Figure 4.7** Shape-memory mechanism of a PU/POE polymer blend (schematic). Reproduced with permission from E. Kurahashi, H. Sugimoto, E. Nakanishi, K. Nagata and K. Inomata, *Soft Matter*, 2012, 8, 2, 496. ©2012, Royal Society of Chemistry [22]

Immiscible high-density polyethylene (HDPE) and nylon 6 (PA6) were blended by Li and co-workers to prepare a shape-memory blend through melt extrusion [24]. To improve the poor SME of the blend caused by the incompatibility of both components, ethylene-octane copolymer graft maleic anhydride (POE-*g*-MAH), which could increase the melt viscosity of the blend at low shear rate range and decrease that at high shear rate range, was introduced into the system as a reactive compatibiliser. When POE-*g*-MAH content increased, phase separation could be improved and the average particle size of PA6 decreased gradually in PA6/HDPE/PA6/POE-*g*-MAH blends (Figure 4.8). With the increase in POE-*g*-MAH content, the HDPE/PA6 blend increased the shape recovery rate and speed. The optimal shape response temperature of HDPE/PA6/POE-*g*-MAH blend was slightly higher than the  $T_m$  of HDPE.

Li and co-workers also blended HDPE with polyethylene terephthalate (PET) to prepare SMP using ethylene-butyl acrylate-glycidyl methacrylate terpolymer (EBAGMA) as a reactive compatibiliser [25]. PET was designed as the fixed phase and melted HDPE crystals above the  $T_m$  acted as the reversible phase. In the same way as the HDPE/PA6/POE-*g*-MAH blend, addition of a compatibiliser clearly improved shape-memory properties. The blend with 5 phr EBAGMA had the best SME when the ratio of HDPE/PET was 90/10.

A novel polymer blend of polyamide (PA) and linear low-density polyethylene (LLDPE) was prepared in a modular inter-meshing co-rotating twin-screw extruder with maleated polyethylene (PE-G) as a compatibiliser by Lin and co-workers [26]. According to the shape-memory investigation, LLDPE contributed to the fixing and PA contributed to the recovery with the help of PE-G. The SME of the blend was

investigated, and the results showed that incorporation of PE-G strongly affected the tensile properties and morphology of the blend. PA content in the blend had a significant effect on the SME of the blend, which performed best with 60 wt% LLDPE, 20 wt% PA, and 20% PE-G. The optimised phase morphology of the blend could be designed to contain the major continuous-phase LLDPE and dispersion-phase PA.



**Figure 4.8** Scanning electron micrographs of HDPE/PA6/POE-g-MAH blends HDPE/PA6/POE-g-MAH: (a) 80/20/0; (b) 80/20/3; (c) 80/20/5; and (d) 80/20/10.

Reproduced with permission from S-C. Li and L. Tao, *Polymer-Plastics Technology and Engineering*, 2010, 49, 2, 218. ©2010, Taylor & Francis [24]

LLDPE was also used by Liu and co-workers and blended with polypropylene (PP) to prepare a shape-memory blend by melt-blending with moderate crosslinked LLDPE/PP blend as a compatibiliser [27]. The compatibiliser enhanced the melt strengths of the blend as well as improving compatibility. In the LLDPE/PP blend, dispersed PP particles acted as the fixed phase and continuous LLDPE acted as the switch phase. The shape-memory mechanism of LLDPE/PP/LLDPE-PP blend is presented in **Figure 4.9**. Bad shape fixity and recovery performances for the LLDPE/PP blend are shown in **Figure 4.9A** and occurred because the fixed-phase PP could not provide sufficient

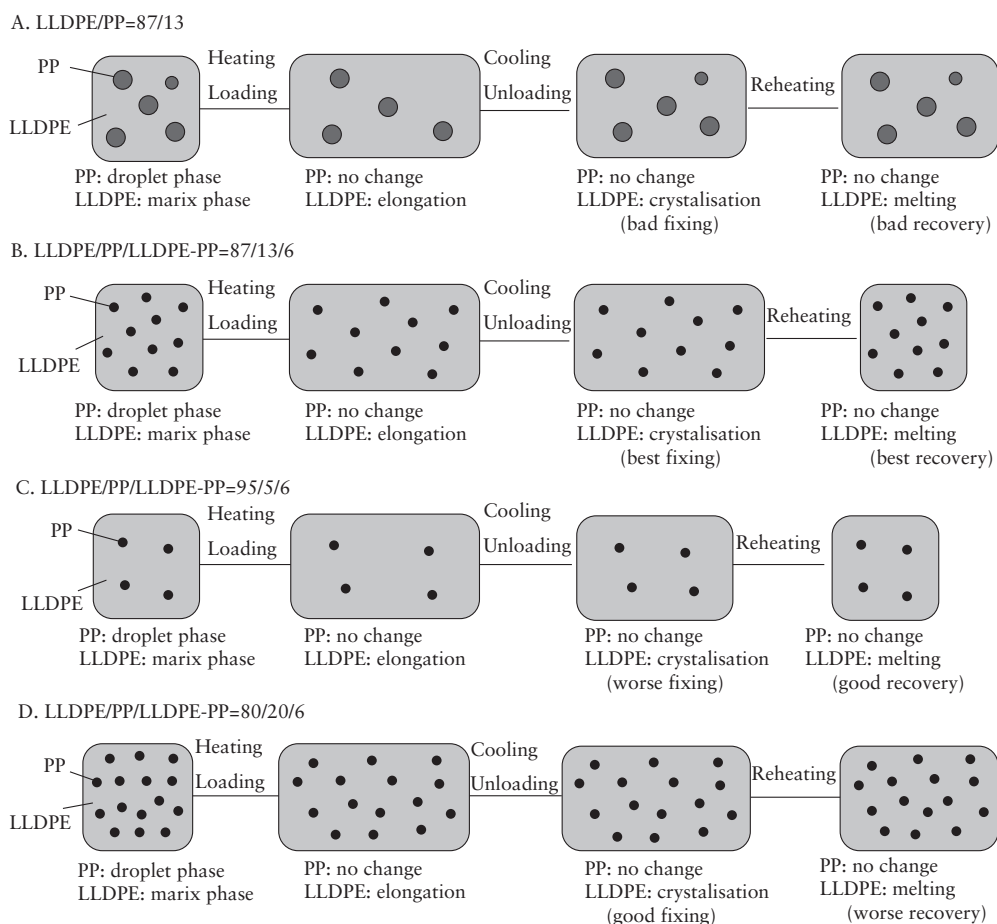
restraining force to reversible LLDPE phase. With addition of the compatibiliser, there were more small PP particles which dispersed more uniformly in the matrix of LLDPE (**Figure 4.9B**). The blend showed the best shape fixity and recovery performances because of the enhanced interaction between the fixed phase and switch phase. However, the blend exhibited good shape recovery performance but bad shape fixity performance if the PP content was too low (**Figure 4.9C**). This was due to the insufficient constraining effect of the fixed phase on the switch phase. Conversely, if the PP content was too high, the switch phase was relatively low, which made the irreversible plastic deformation more likely to occur under identical conditions, leading to the bad shape recovery effect of the blend. Liu and co-workers also made a systematic investigation on the melt rheological properties of the LLDPE/PP/LLDPE-PP blend. They found that PP particles could be dispersed better and wrapped in the LLDPE matrix at a high shear rate [28]. The higher the shear rate, the smaller the temperature sensitivity of the melt viscosity of the blends would be. The die swell ratio of the blends increased with increase in shear rate.

Cui and co-workers developed a similar blend system based on PP and PET through melting extrusion using POE-*g*-MAH as the compatibiliser [29]. Melted PP crystals above the  $T_m$  acted as the switch phase and the dispersed PET domains contributed to the fixation as the physical crosslinks. Incorporation of the compatibiliser affected the blend in various aspects. First, it improved the compatibility of the PP/PET blend, enhancing the interfacial adhesion between PP and PET phases. Second, PP particle sizes became smaller and their crystallisation properties in the blend were reduced. Third, the recovery rate and speed of the blend increased with higher recovery temperature whereas the  $R_f$  value remained almost unchanged. Except for the abovementioned effects, addition of POE-*g*-MAH also affected mechanical and rheological properties to a certain extent.

Meng and co-workers reported on the shape-memory behaviour of chitosan/poly(L-lactide) (PLLA) blends [30]. Chitosan does not significantly affect the  $T_g$  and  $T_m$  of the PLLA. Pure PLLA and chitosan/PLLA composites showed SME arising from the viscoelastic properties of PLLA comprising semi-crystalline structures. The shape recovery ratio of the chitosan/PLLA blends decreased significantly with increasing chitosan content due to the incompatibility between PLLA and chitosan. Phase separation structures of the composites were observed using atomic force microscopy. To obtain good SME, the chitosan content should be <15 wt%. The blends may have biodegradability and biocompatibility, and be suitable for biomedical applications.

Sahoo and co-workers developed a novel electro-active SMP blend consisting of polypyrrole (PPy) formed by chemical oxidative polymerisation and SMPU [31]. It was found that the conductivity of the blend increased in the presence of PPy, and high conductivity ( $10^{-2}$  S/cm) was obtained at 6–20 wt% PPy. However, the elongation at

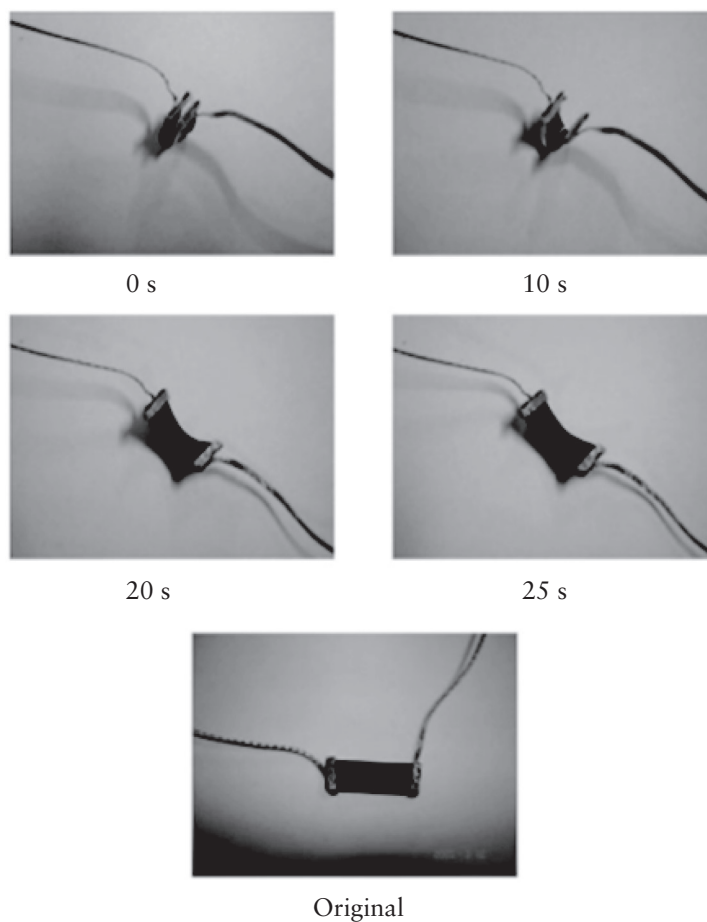
break and tensile strength of the PU/PPy blend decreased with increase in PPy content in the blends owing to the brittle network of PPy. PU has a transition temperature near 46 °C, so the PU/PPy blends could show electro-active shape recovery by heating above the transition temperature due to melting of the PCL soft segment domain. If constant voltage (40 V) was applied, the PU/PPy blend changed spontaneously to its original shape, and a good shape recovery of 85–90% could be obtained (Figure 4.10).



**Figure 4.9** Shape-memory mechanisms of LLDPE/PP/LLDPE-PP blends (schematic). Reproduced with permission from S.C. Li, H. Liu and W. Zeng, *Journal of Applied Polymer Science*, 2011, 121, 5, 2614. ©2011, John Wiley & Sons [27]



Sahoo and co-workers also reported on electro-active shape-memory blends based on SMPU block copolymers, multiwalled carbon nanotubes (MWCNT) and PPy [32]. These blends also showed good conductivity and electro-active shape recovery. The shape  $R_r$  of the PU/PPy/MWCNT (95/2.5/2.5) could reach 90–96% in 20 s with a bending mode if an electric field of 25 V was applied.



**Figure 4.10** Electroactive shape recovery behaviour of PU/PPy = 80/20 blends. Reproduced with permission from N.G. Sahoo, Y.C. Jung, N.S. Goo and J.W. Cho, *Macromolecular Materials and Engineering*, 2005, **290**, 11, 1049. ©2005, John Wiley & Sons [31]



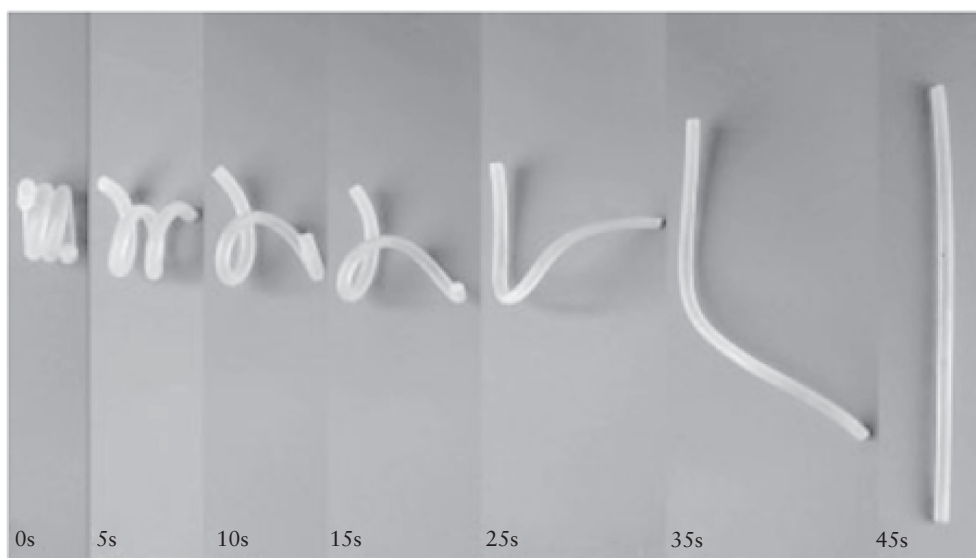
## 4.4 Blending and Post-crosslinking Polymers Networks

### 4.4.1 Interpenetrating Polymer Networks

Interpenetrating polymer networks (IPN) can be prepared by simultaneous polymerisation and polycondensation of low-molecular-weight monomers or macromonomers that are capable of netpoint formation. The generated netpoints of both polymer networks determine the permanent shape, whereas polymer networks contribute to the switching domains. The characteristics of IPN are dependent upon the weight ratio of the IPN components and the resulting morphology of the polymer network.

Liu and co-workers designed a PMMA-polyethylene glycol (PEG) semi-IPN which exhibited two independent shape-memory behaviours at the  $T_m$  of the PEG crystals and the  $T_g$  of the semi-IPN [33]. The PMMA-PEG semi-IPN were synthesised by radical homopolymerisation and crosslinking PMMA in the presence of linear PEG. For the shape-memory behaviour at the  $T_m$  of PEG crystals, the fixing phase was the PMMA network and the reversible phase was the PEG crystal. For the shape-memory behaviour at the  $T_g$  of the semi-IPN, the fixing phase was the chemical crosslinked point, whereas the reversible phase was the PMMA-PEG complex phase. **Figure 4.11** demonstrates the shape-memory behaviour of PMMA-PEG2000 semi-IPN below and above the  $T_g$  of the semi-IPN. Because of the large gap between the storage modulus below and above the  $T_g$  of the semi-IPN, and a reversible order–disorder transition of the crystals around the  $T_m$  of PEG, the polymer had a recovery ratio of 99 and 91%.

In accordance with the concept of PMMA-PEG semi-IPN, Liu and co-workers also prepared a novel polymer PMMA-*co*-(vinyl-2-pyrrolidone) (PMMA-*co*-VP)/PEG semi-IPN based on hydrogen bonding, which showed excellent shape-memory behaviour [34]. PMMA-*co*-VP/PEG semi-IPN were prepared by radical copolymerisation of 37.5–59.5 wt% methyl methacrylate and 26 wt% *N*-vinyl pyrrolidone in the presence of 0.5 wt% 2,2-Azo-bisisobutyronitrile as an initiator, 1 wt% ethylene-glycol-dimethylacrylate as a crosslinker, and 15–40 wt% linear PEG. Addition of PEG to PMMA-*co*-VP networks not only decreased the  $T_g$  and stiffness of PMMA-*co*-VP networks, it also altered the dynamic mechanical behaviour of PMMA-*co*-VP networks. Hydrogen bonding interactions between the hydroxyl group (hydrogen donor) of PEG and carbonyl group (hydrogen acceptor) of polyvinyl pyrrolidone (PVP) promoted the formation of physical networks between PVP and PEG, which partially restricted the side-chain movements of PVP and slightly increased the stiffness of PMMA-*co*-VP/PEG semi-IPN. For the PMMA-*co*-VP/PEG semi-IPN, the fixing phase was the chemical crosslinked point, whereas the reversible phase was the PEG-PVP complex phase. The recovery ratio of these polymers could reach 99%.



**Figure 4.11** Shape-memory phenomena of PMMA-PEG2000 semi-IPN. The initial rod was heated to 100 °C and deformed into a spiral shape, then cooled to room temperature under constrained conditions. After withdrawing the external force, the spiral-shaped sample was put into a glass container and kept at constant temperature at 100 °C for a short time. A snapshot of the sample was captured by a digital camera. Reproduced with permission from G. Liu, X. Ding, Y. Cao, Z. Zheng and Y. Peng, *Macromolecular Rapid Communications*, 2005, 26, 8, 649. ©2005, John Wiley & Sons [33]

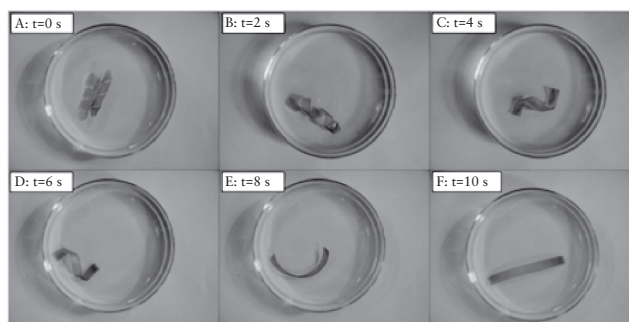
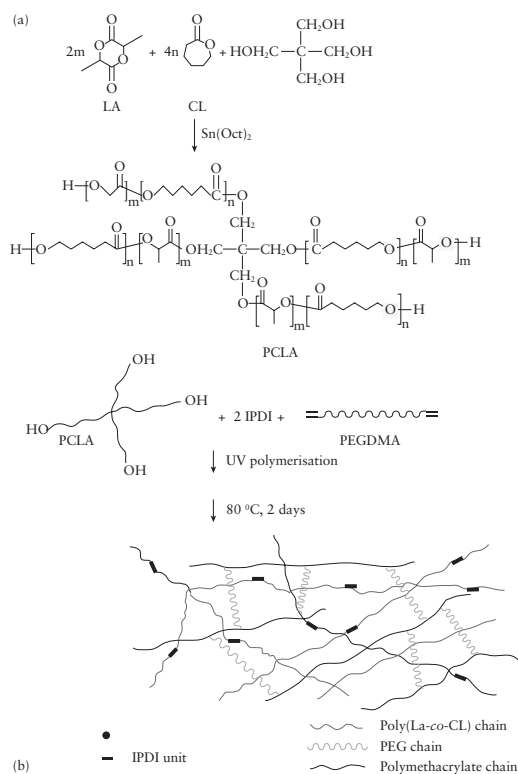
Zhang and co-workers incorporated polyethylene glycol dimethacrylate (PEGDMA) into poly(lactide-*co*-glycolide) (PLGA)/isophorone diisocyanate (IPDI) systems and achieved IPNs with good shape-memory and hydrophilic properties for biomedical applications [35]. First, a hydrophilic network was formed by irradiation crosslinking of dimethacrylate groups in PEGDMA. Second, a PU network was generated by the reaction of hydroxyl telechelic PLGA and IPDI. The chemical crosslinking points acted as the fixed phase to memorise the original shape, whereas the amorphous domains of miscible PLGA and PEG acted as the reversible phase. The crosslinking densities of PU networks could be controlled by varying the arm lengths of oligomeric PLGA. The hydrophilicity, mechanical properties and  $T_{trans}$  of IPN were tuned conveniently by variation of compositions. The switch temperature of the IPN could be adjusted at around body temperature for potential clinical applications.

Feng and co-workers synthesised an elastic amorphous IPN of polyester urethane/PEGDMA by UV-photopolymerisation of PEGDMA and thermal polymerisation of poly( $\epsilon$ -caprolactone-*co*-lactide) (PCLA) with IPDI [36]. Synthesis of four-armed oligomer PCLA and IPN is represented in **Figure 4.12a**. Polyester urethane-PEG IPN showed good shape-memory properties with good strain fixity and strain recovery ability. In the IPN, the chemical crosslinking points of PCL acted as the fixed phase to memorise the original shape whereas the amorphous domains of PCLA and PEG acted as a reversible phase. The strain recovery rate and strain fixity rate were found to be >90%. The IPN could quickly recover to their original shape in 10 s above the  $T_g$  (**Figure 4.12b**). The wettability, mechanical properties and  $T_g$  of the polymer networks could be adjusted readily by variation of the compositions of hydrophobic PCLA and hydrophilic PEGDMA. Polyester urethane-PEG IPN had a high potential for biomedical applications such as smart implants, medical devices, site-specific controlled drug delivery systems, and stents in the treatment of cardiovascular disease.

Ratna and Kager-Kocsis synthesised a series of crystalline polyethylene oxide (PEO)/crosslinked polymethyl methacrylate (x-PMMA) semi-IPN SMP, which were prepared at various PMMA/PEO ratios using different amounts of crosslinker [37]. They observed that the recovery time increased with increasing crosslinker concentration, whereas the shape fixity tended to decrease with decreasing crosslink density for all the recovery temperatures. The shape-memory properties (shape recovery and shape fixity) of the semi-IPN could be tailored upon the x-PMMA/PEO ratio and crosslinking degree of x-PMMA. A semi-IPN having a composition of PMMA/PEO=68/32 and crosslinker concentration of 4 wt% offered the best shape-memory properties. The creep compliance of the semi-IPN was influenced primarily by the degree of crosslinking of x-PMMA without an obvious change over the compositional change in the range studied.

#### **4.4.2 Crosslinked Polymer Blends**

SMP with polymer network structures can be prepared through blending and radiation crosslinking. The polymer components and the density of netpoints affect blend properties. The blends could be applied to commodity devices with specific thermomechanical needs, of which the shape-memory properties can be controlled by enhancing the crosslinks with blending sensitisers in polymer networks.



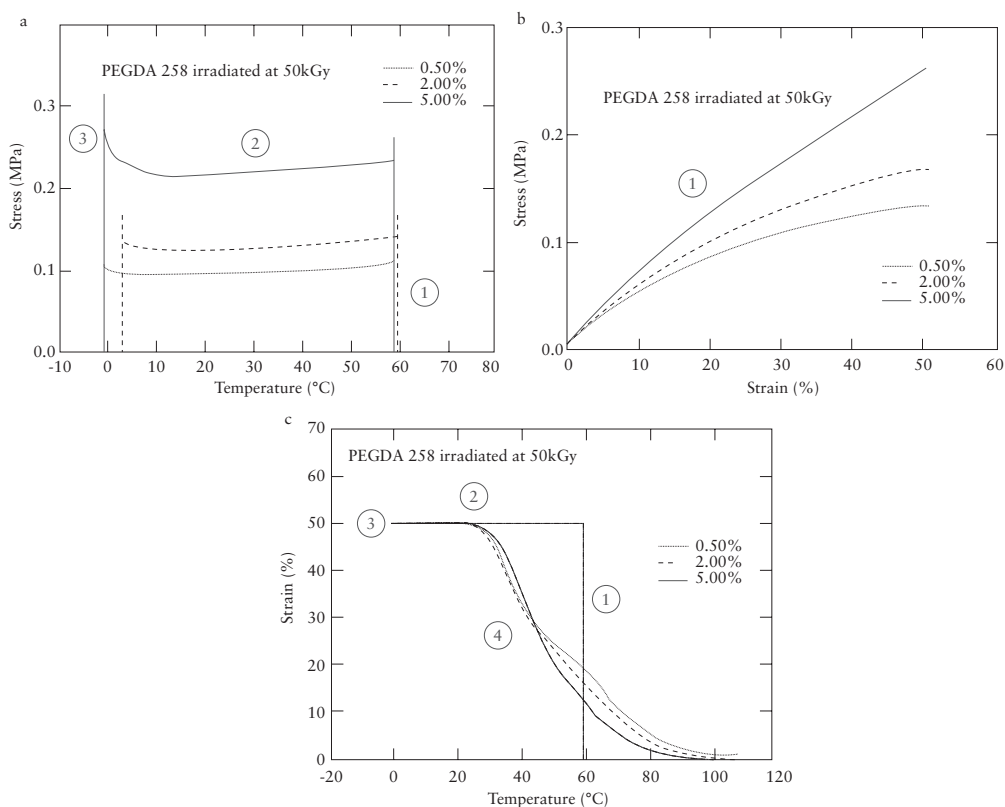
**Figure 4.12** (a) Synthesis of four-armed oligomeric PCLA and IPN. (b) Shape-memory photographs (A–F, 2-s interval) of polyester urethane–PEG IPN showed the transition from a temporary to permanent shape. The initial rod strip-shaped film (F) was deformed into a spiral shape in an oven at 5 °C (A), cooled to 0 °C, and the external force withdrawn. Then the deformed sample was placed in water at 50 °C and recovered its permanent shape. Poly(LA-co-CL): Polylactide-co- $\epsilon$ -caprolactone. Reproduced with permission from Y. Feng, H. Zhao, L. Jiao, J. Lu, H. Wang and J. Guo, *Polymers for Advanced Technologies*, 2012, **23**, 3, 382.

©2012, John Wiley & Sons [36]

Zhu and co-workers reported on the SME of sensitising radiation-crosslinked PCL with polyfunctional polyester acrylate (PEA) [38]. PCL is a novel biocompatible and biodegradable material. Although radiation-crosslinked PCL exhibited SME at low temperatures, the radiation-crosslinking efficiency of pure PCL was very low [39]. By blending polyfunctional PEA with PCL, the efficiency of the radiation crosslinking of PCL was improved distinctly because the double bonds of the polyfunctional PEA were readily ‘unlocked’ by rays and participated in the crosslinking chemical reactions. The radiation crosslinking of PCL in the presence polyfunctional PEA followed the Chen–Liu–Tang relationship. It was shown that enhanced radiation crosslinking increased the heat deformation temperature of PCL and presented a higher and wider rubbery-state *plateau*. The shape-memory results revealed that enhanced crosslinking PCL elicited 100% recoverable deformation and a quicker recovery rate than pure PCL.

Using an analogous approach, Zhu and co-workers improved the radiation efficiency of PCL by blending it with polymethyl vinyl siloxane (PMVS) before radiation crosslinking [40]. PMVS is a highly flexible material with a breaking elongation ratio as high as 1500%. Like PCL, PMVS is biocompatible and nontoxic. The double bond of PMVS is sensitive to irradiation crosslinking. Owing to the addition of PMVS (which decreased the gelation dose and ratio of degradation to crosslinking), the radiation crosslinking efficiency of PCL/PMVS blends was significantly higher than that of pure PCL. The crosslinked PCL/PMVS blends exhibited better SME such as narrower switch temperature, higher heat sensitivity, and higher recovery speed in comparison with pure PCL.

Ware and co-workers prepared a radiation crosslinked SMP based on blending and irradiating a system of polymethyl acrylate (PMA) and polyethylene glycol diacrylate (PEGDA) in various ratios. PEGDA is miscible in PMA and sensitises the radiation crosslinking of PMA [41]. The extent of crosslinking increased with an increase in the molar concentration of PEGDA of a constant number average molecular weight. Although longer PEGDA molecules were more effective for sensitising crosslinking at a given molar ratio of sensitiser to PMA, shorter PEGDA molecules were more effective at sensitising crosslinking at a given weight ratio. **Figure 4.13** demonstrates the shape-memory properties of PMA/PEGDA blends at 50 kGy. There was a greater increase in stress with increased molar ratio of PEGDA and lower residual strains after a full shape-memory cycle in *steps 1* and *2*. PMA/PEGDA showed a more rapid and uniform recovery with an increased molar ratio of PEGDA in *step 4*. The shape fixity was >99% for the PMA/PEGDA blend. Shape recovery over one cycle was between 97% and 99%, and increased with increasing molar ratio of PEGDA (**Figure 4.13**).



**Figure 4.13** Shape-memory cycle of blends of PMA and PEGDA 258 irradiated at 50 kGy as a (a) stress–temperature relationship; (b) stress–strain relationship; and (c) strain–temperature relationship. Step 1 is isothermal loading; step 2 is cooling at constant load; step 3 is isothermal unloading; and step 4 is shape recovery upon heating. Reproduced with permission from T. Ware, W. Voit and K. Gall, *Radiation Physics and Chemistry*, 2010, 79, 4, 446. ©2010, Elsevier [41]

A SMP network composed of carboxylated telechelic PCL and epoxidised natural rubber (ENR) was prepared by Chang and co-workers. This network was formed by the reaction between the reactive groups of PCL and ENR during thermal moulding. In the ENR/PCL blends, the degree of crosslinking and crystalline melting transition temperatures were influenced by the blend compositions and molecular weight of the PCL segment [42]. If there was an adequately high degree of crosslinking for the crystalline melting transition, the recovery temperatures were well matched with the crystalline melting temperature of each sample, and the ENR/PCL blends showed good shape fixation and shape recovery.

Kolesov and Radusch synthesised peroxidic crosslinked binary and ternary blends based on linear HDPE and two ethylene-1-octene copolymers (EOC) through medium and high degrees of branching [43]. HDPE/EOC blends were prepared by mixing HDPE and EOC with 2 wt% of liquid peroxide 2,5-dimethyl-2,5-di-(*tert*-butylperoxy)-hexane at 190 °C through melt blending. The average crosslink density of HDPE/EOC blends was dependent upon the component ratios and temperature. HDPE/EOC blends showed multiple shape-memory behaviours which appeared only at consequent stepwise application of convenient programming strains and temperatures. All binary and tertiary HDPE/EOC blends except the HDPE/EOC (50/50) blend exhibited triple and quadruple SME because of the large amount of poorly separated peaks formed during multiple melting of these blends. HDPE/EOC blends could be used as functional materials that gradually changed the sample geometry with low thermally induced recovery strain rate.

## 4.5 Conclusions

In this chapter, a comprehensive overview of recent progress in SMP blends was presented. The design strategy of blending polymers can not only improve shape-memory properties and mechanical properties while maintaining the SME of SMP, they can also create new polymer/polymer blends possessing SME. Constructing binary SMP/polymer blends using a thermoplastic SMP as one component and a commodity polymer as the other component was an effective method to lower costs as well as to adjust shape-memory properties and mechanical properties. SMP can be obtained by blending polymers which have no shape-memory properties on their own. The shape-memory properties of SMP can be tuned *via* changing the ratio of components, adding a compatibiliser, or selecting a blending method. It is also possible to synthesise novel SMP with IPN or crosslink networks by means of blending and post-crosslinking commodity polymers. This type of SMP could be used as functional materials that gradually change sample geometry with low thermally induced recovery strain rate because shape-memory properties such as shape recovery ratio can be tuned *via* changing crosslinking methods and the density of netpoints. The strategies presented here are an effective avenue for SMP with remarkable characteristics. SMP prepared by blending appropriate polymers could have shape stability, excellent recovery stress and strain, biocompatibility, and biodegradability.

## References

1. X. Luo and P.T. Mather, *Current Opinion in Chemical Engineering*, 2012, 2, 1, 103.

2. C. Liu, H. Qin and P. Mather, *Journal of Materials Chemistry*, 2007, **17**, 16, 1543.
3. P.T. Mather, X. Luo and I.A. Rousseau, *Annual Review of Materials Research*, 2009, **39**, 445.
4. J. Hu, H. Meng, G. Li and S.I. Ibekwe, *Smart Materials & Structures*, 2012, **21**, 5, 053001.
5. H.M. Jeong, B.K. Ahn and B.K. Kim, *European Polymer Journal*, 2001, **37**, 11, 2245.
6. H.M. Jeong, J.H. Song, S.Y. Lee and B.K. Kim, *Journal of Materials Science*, 2001, **36**, 22, 5457.
7. S.H. Ajili, N.G. Ebrahimi and M. Soleimani, *Acta Biomaterialia*, 2009, **5**, 5, 1519.
8. M. Behl, U. Ridder, Y. Feng, S. Kelch and A. Lendlein, *Soft Matter*, 2009, **5**, 3, 676.
9. S.A. Madbouly and A. Lendlein, *Macromolecular Materials and Engineering*, 2012, **297**, 12, 1213.
10. N. Erden and S.C. Jana, *Macromolecular Chemistry and Physics*, 2012.
11. E.D. Rodriguez, X. Luo and P.T. Mather, *ACS Applied Materials & Interfaces*, 2011, **3**, 2, 152.
12. A. Lendlein and S. Kelch, *Angewandte Chemie International Edition*, 2002, **41**, 12, 2034.
13. K.M. Lee, P.T. Knight, T. Chung and P.T. Mather, *Macromolecules*, 2008, **41**, 13, 4730.
14. C.J. Campo and P.T. Mather, *Polymeric Materials: Science & Engineering*, 2005, **93**, 933.
15. J. You, W. Dong, L. Zhao, X. Cao, J. Qiu, W. Sheng and Y. Li, *The Journal of Physical Chemistry B*, 2012, **116**, 4, 1256.
16. J. You, H. Fu, W. Dong, L. Zhao, X. Cao and Y. Li, *ACS Applied Materials & Interfaces*, 2012, **4**, 9, 4825.
17. H. Zhang, H. Wang, W. Zhong and Q. Du, *Polymer*, 2009, **50**, 6, 1596.



18. H. Zhang, Z. Chen, Z. Zheng, X. Zhu and H. Wang, *Materials Chemistry and Physics*, 2012.
19. R. Weiss, E. Izzo and S. Mandelbaum, *Macromolecules*, 2008, **41**, 9, 2978.
20. X. Luo and P.T. Mather, *Macromolecules*, 2009, **42**, 19, 7251.
21. X. Luo and P.T. Mather, *Advanced Functional Materials*, 2010, **20**, 16, 2649.
22. E. Kurahashi, H. Sugimoto, E. Nakanishi, K. Nagata and K. Inomata, *Soft Matter*, 2012, **8**, 2, 496.
23. S-M. Lai and Y-C. Lan, *Journal of Polymer Research*, 2013, **20**, 5, 1.
24. S-C. Li and L. Tao, *Polymer-Plastics Technology and Engineering*, 2010, **49**, 2, 218.
25. S.C. Li, L.N. Lu and W. Zeng, *Journal of Applied Polymer Science*, 2009, **112**, 6, 3341.
26. G.M. Lin, G.X. Sui and R. Yang, *Journal of Applied Polymer Science*, 2012, **126**, 1, 350.
27. S.C. Li, H. Liu and W. Zeng, *Journal of Applied Polymer Science*, 2011, **121**, 5, 2614.
28. Y. Liu, S-C. Li and H. Liu, *Polymer-Plastics Technology and Engineering*, 2013, **52**, 8, 841.
29. Y-Y. Cui, B-J. Dong, B-L. Li and S-C. Li, *International Journal of Polymeric Materials and Polymeric Biomaterials*, 2013, **62**, 13, 671.
30. Q. Meng, J. Hu, K. Ho, F. Ji and S. Chen, *Journal of Polymers and the Environment*, 2009, **17**, 3, 212.
31. N.G. Sahoo, Y.C. Jung, N.S. Goo and J.W. Cho, *Macromolecular Materials and Engineering*, 2005, **290**, 11, 1049.
32. N.G. Sahoo, Y.C. Jung and J.W. Cho, *Materials and Manufacturing Processes*, 2007, **22**, 4, 419.
33. G. Liu, X. Ding, Y. Cao, Z. Zheng and Y. Peng, *Macromolecular Rapid Communications*, 2005, **26**, 8, 649.

34. G. Liu, C. Guan, H. Xia, F. Guo, X. Ding and Y. Peng, *Macromolecular Rapid Communications*, 2006, **27**, 14, 1100.
35. S. Zhang, Y. Feng, L. Zhang, J. Sun, X. Xu and Y. Xu, *Journal of Polymer Science, Part A: Polymer Chemistry Edition*, 2007, **45**, 5, 768.
36. Y. Feng, H. Zhao, L. Jiao, J. Lu, H. Wang and J. Guo, *Polymers for Advanced Technologies*, 2012, **23**, 3, 382.
37. D. Ratna and J. Karger-Kocsis, *Polymer*, 2011, **52**, 4, 1063.
38. G. Zhu, Q. Xu, G. Liang and H. Zhou, *Journal of Applied Polymer Science*, 2005, **95**, 3, 634.
39. G. Zhu, G. Liang, Q. Xu and Q. Yu, *Journal of Applied Polymer Science*, 2003, **90**, 6, 1589.
40. G. Zhu, S. Xu, J. Wang and L. Zhang, *Radiation Physics and Chemistry*, 2006, **75**, 3, 443.
41. T. Ware, W. Voit and K. Gall, *Radiation Physics and Chemistry*, 2010, **79**, 4, 446.
42. Y-W. Chang, J-P. Eom, J-G. Kim, H-T. Kim and D-K. Kim, *Journal of Industrial and Engineering Chemistry*, 2010, **16**, 2, 256.
43. I. Kolesov and H. Radusch, *eXPRESS Polymer Letters*, 2008, **2**, 461.



# 5 Shape-memory Polymers Sensitive to Different Stimuli

## 5.1 Introduction

Shape-memory polymers (SMP) can change their shapes rapidly with respect to configuration or dimension under the influence of suitable stimuli such as heat [1], electricity [2], light [3], magnetic field [4], moisture/water [5], and pH [6]. They offer flexibility to modify their structure, which can be stimulated under different triggering conditions that depend on the application of SMP products. They can be applied in: smart textiles and apparels [7]; intelligent medical instruments and auxiliaries [8]; artificial muscles [9]; electrochemical devices; robotics; biomimetic devices [10]; heat-shrinkable materials [11]; micro-electro-mechanical systems [12]; self-deployable sun sails in spacecrafts [13]; miniature manipulators [14], actuators and sensors [15]; active sound-absorbing materials.

Undeniably, among all of stimulus-sensitive SMP, thermally sensitive ones have been the most widely studied and employed in academic studies and industrial applications [16]. Compared with other SMP, the major advantage of thermally sensitive SMP is that the transition temperature can be adjusted readily by appropriate choice of the hard-segment content and molecular weight of soft segments. Thermally sensitive SMP can realise excellent shape-memory effects (SME). However, they require heating devices and such heating cannot be localised most of the time. Such a requirement can hinder the application of SMP, especially if heat causes damage to surrounding tissue or if precise control of heating is required. To solve such problems, several breakthroughs have been made in developing SMP with novel stimulus-active mechanisms [17]. This chapter reviews the mechanisms and fabrication strategies of stimulus-active polymers which are sensitive to heat, light, electrical fields, magnetic fields, and moisture/water.

## 5.2 Thermally sensitive Shape-memory Polymers

Thermally sensitive polymers based on SMP have been applied in many fields. Several review articles on SMP have detailed the vast potential of thermally sensitive SMP [17–26]. These SMP can ‘memorise’ their original (or permanent) shape and change

their shape rapidly from a temporary shape to their original (or permanent) shape under the influence of heat. Different forms of SMP, such as solution [27], emulsion [28], film [29], fibre, foam [30], and bulk [8], have been developed for specific conditions. According to the shape-memory switch mechanisms, thermally sensitive SMP can be divided into the categories described below.

### **5.2.1 Shape-memory Effect based on Conventional Glass or Melting Transition**

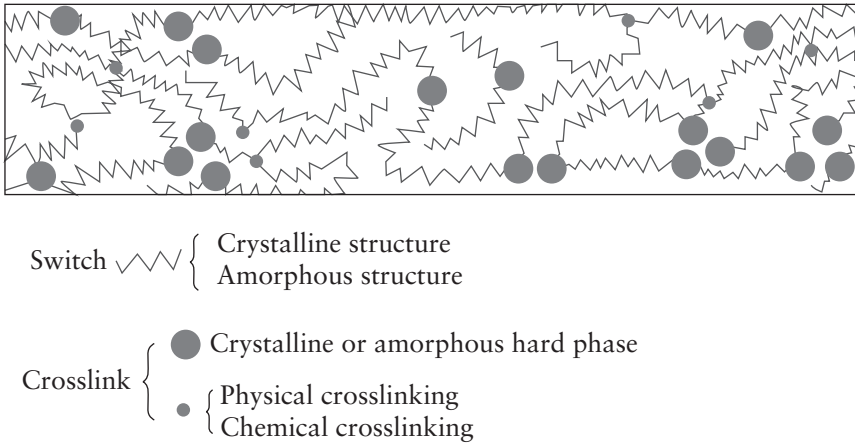
With glass or melting transition acting as the switch, several polymer systems have been reported to possess SME. Liu and co-workers [25] have detailed hundreds of SMP based on glass or melting transitions as the shape-memory switch, of which shape-memory polyurethanes (SMPU) have been studied widely and applied commercially [31, 32]. SMPU are synthesised from isocyanates, chain extenders and polyol components using step growth polymerisation. The basic requirement for making thermally sensitive SMPU is a two-phase heterogeneous structure, i.e., hard and soft segments. The hard segments contain urethane rich segments formed by the reaction of diisocyanate with diols or diamines. The long-chain polyester or polyether glycols behave like soft segments. Both segments differ significantly with regard to molecular polarity, and show incompatibility to finally form a two-phase heterogeneous structure and morphology. This microphase separation is the essential requirement for shape-memory properties. One can control the microphase separation (and hence the SME of SMPU) by using different raw materials, choosing different molecular weights of monomers, and changing reaction procedures. Table 5.1 lists the melting temperature ( $T_m$ ) or glass transition temperature ( $T_g$ ) for some conventional SMPU having different hard and soft segments.

Figure 5.1 shows the molecular mechanism of SME based on glass or melting transition acting as the switch. These SMP usually have a physical crosslinking structure, crystalline/amorphous hard phase, or chemical crosslinking structure to 'store' internal stress and a low temperature glass or melting transition acting as the shape-memory switch [30, 43]. SMP can be processed or thermally set to obtain an original shape. In general, in the original shape, internal stress is zero or negligible. If the SMP is subject to deformation, the deformation stress is stored in the crosslinking structure after cooling the polymer to below its switch transition temperature. If the SMP is heated to a temperature above the switch transition temperature, it recovers its original shape with the release of internal stress stored in the crosslinking structure.

With respect to application, the prerequisite for thermally active polymers as shape-memory materials is that their switch transition temperature must be greater than the temperature of the environment in which they are applied. Most SME of SMP based

on glass or melting transition are one-way SME. Hence, the SME is irreversible by the reverse stimulation (i.e., cooling). The temporary shape can be obtained only by deformation using external forces such as direct stretching and bending.

Table 5.1 Overview of SMPU with varying segments and different switching temperatures [33–42]			
Hard domain	Soft domain	Transition temperature (°C)	Reference
MDI/1,4-BD	PTMG	$T_g = -13$ to $54$	[33]
MDI/ethylene diamine	PTMG	$T_g = 15$ to $25$	[34]
MDI/1,4-BD	Polyester acrylate	$T_g = 50$ to $60$	[35]
MDI/1,4-BD	Polybutyleneadipate	$T_g = 29$ to $64$	[36]
2,4-Toluene diisocyanate /1,4-BD	Poly(L-lactide-co- $\epsilon$ -caprolactone)	$T_g = 28$ to $53$	[37]
Poly(L-lactic acid)	Poly(glycolide-co-caprolactone)	$T_g = 40$ to $47$	[38]
MDI/1,4-BD	PCL	$T_m = 43$ to $49$	[39]
MDI/1,4-BD/ <i>N,N</i> -bis(2-hydroxyethyl) <i>iso</i> -nicotinamide	PCL	$T_m = 45$ to $50$	[40]
Poly( <i>p</i> -dioxanone)	PCL	$T_m = 40$	[41]
HDI/ 4,4'-dihydroxy biphenyl	PCL	$T_m = 38$ to $59$	[42]
1,4-BD: 1,4-Butanediol HDI: 1,6-Hexamethylene diisocyanate MDI: 4,4-Diphenylmethane diisocyanate PCL: Poly( $\epsilon$ -caprolactone) PTMEG: Polytertramethylene ether glycol			



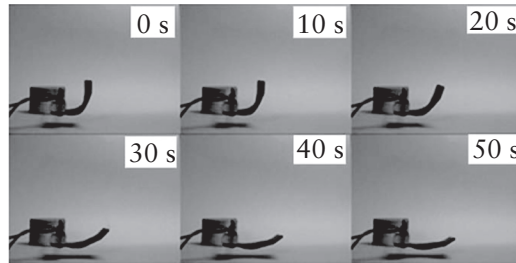
**Figure 5.1** Molecular mechanism of thermally active SME. Reproduced with permission from Q.H. Meng and J.L. Hu, *Composites Part A: Applied Science and Manufacturing*, 2009, 40, 11, 1661. ©2009, Elsevier [23]

### 5.2.2 Shape-memory Effect by Indirect Heating

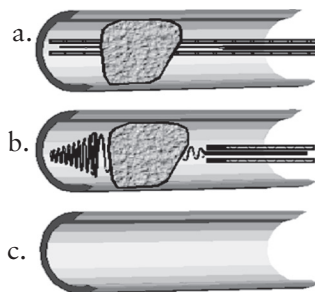
If electrical conductive materials are incorporated into thermally active SMP, certain levels of electric conductivity of the SMP can be achieved. If a current passes through the network of conductive materials within the SMP, the induced Joule heating can raise the internal temperature to above the switch transition temperature of the polymer to trigger shape recovery (**Figure 5.2**) [8, 17, 44, 45]. The conductive materials which have been used as conductive fillers include carbon nanotubes (CNT), polypyrrole, carbon black (CB), and short carbon fibres (SCF). To obtain an effective electroactive SME, high conductivity is necessary. Many research efforts have been made to improve the electrical conductivity of composites [46, 47]. More examples and elaborative discussion are provided in **Section 5.6**.

Light absorbed by a deformed SMP can also increase the SMP temperature to the switch transition temperature to trigger shape recovery [48]. To improve light-absorbing efficiency, dyes such as indocyanine green and Epolight 4121 [49], CB, and CNT can be incorporated in SMP [50]. **Figure 5.3** shows a schematic of a light-activated SMP microactuator as an intravascular, laser-activated therapeutic device [51]. In the straight-rod form, the microactuator is pushed through or around the blockage. Later, the SMP device is pushed out of the guide catheter and actuated. Thereafter, the catheter, expanded device (in coil shape), and clot are pulled in unison

proximally to relieve the ischemia delivered through a catheter distal to the thrombotic vascular occlusion by minimally invasive surgery.



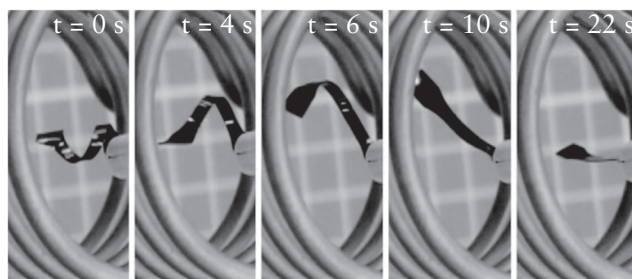
**Figure 5.2** Electro-activate SMP filled with CB/SCF induced by the application of 25 V. Reproduced with permission from Y.J. Liu, H.B. Lv, X. Lan, J.S. Leng and S.Y. Du, *Composites Science and Technology*, 2009, **69**, 13, 2064. ©2009, Elsevier [44]



**Figure 5.3** A SMP microactuator used in the treatment of ischemic stroke (schematic). a) The guide catheter is pushed through or around the blockage. b) The SMP device is pushed out of the guide catheter and actuated. The SMP device must have a small enough diameter to pass through an appropriate neurovascular guide catheter. Current design goals have set this diameter to be 0.012" (300  $\mu$ m) or less. Two appropriate devices, nominally named a coil and an umbrella, are described in this paper. c) The catheter, expanded device (coil depicted in this schematic), and clot are pulled in unison proximally to relieve the ischemia. Reproduced with permission from D.J. Maitland, M.F. Metzger, D. Schumann, A. Lee and T.S. Wilson, *Lasers in Surgery and Medicine*, 2002, **30**, 1, 1. ©2002, John Wiley & Sons [51]



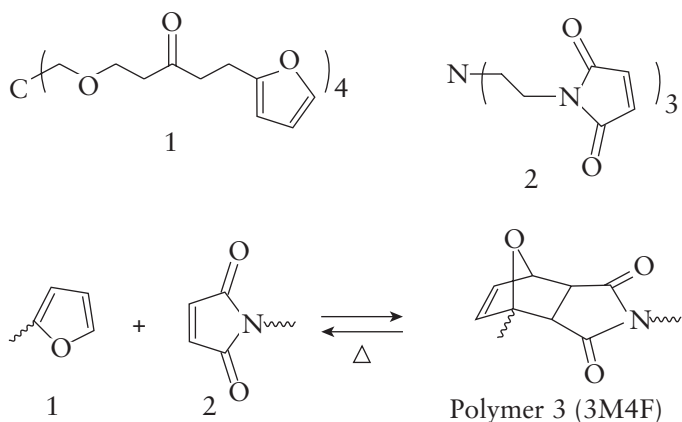
If ferromagnetic fillers are employed in SMP, magnetic-active SME can also be achieved by induced heating as a result of a magnetic field. By incorporation of nano iron (II, III) oxide nanoparticles or Ni-Zn ferrite particles into SMP, remote actuation of SMP has been achieved (Figure 5.4) [52–54]. SMP with magnetic-active SME are intended to be used in biomedical applications [18, 26, 55].



**Figure 5.4** Magnetically induced SME of an SMPU filled with magnetic nanoparticles inside a magnetic field. Reproduced with permission from R. Mohr, K. Kratz, T. Weigel, M. Lucka-Gabor, M. Moneke and A. Lendlein, *Proceedings of the National Academy of Sciences USA*, 2006, 103, 10, 3540. ©2006, United States National Academy of Sciences [52]

### **5.2.3 Shape-memory Effect based on a Thermally Reversible Reaction**

Another thermally reversible structure that can be used as the switch of SME in SMP is a thermally reversible reaction. The thermally reversible reaction shown in Figure 5.5 is a thermally reversible Diels–Alder cycloaddition of a multi-diene (multi-furan) and a multidienophile (multi-maleimide) [56, 57]. Monomer 1 contains four furan moieties on each molecule, and monomer 2 includes three maleimide moieties on each molecule. Thermal reversibility can be accomplished by the retro-Diels–Alder (DA) reaction. Ishida and Yoshie [58] prepared a reversible polymer network consisting of furan-terminated telechelic polyesters of poly(1,4-butylene succinate-co-1,3-propylene succinate) reacted by DA addition with a trifunctional maleimide. The mechanical properties of the polymer can be adjusted by changing temperature as a result of depolymerisation–repolymerisation and melt–recrystallisation processes. These materials might have good SME under suitable thermomechanical deformation processes, but the SME of these materials has not been studied extensively.

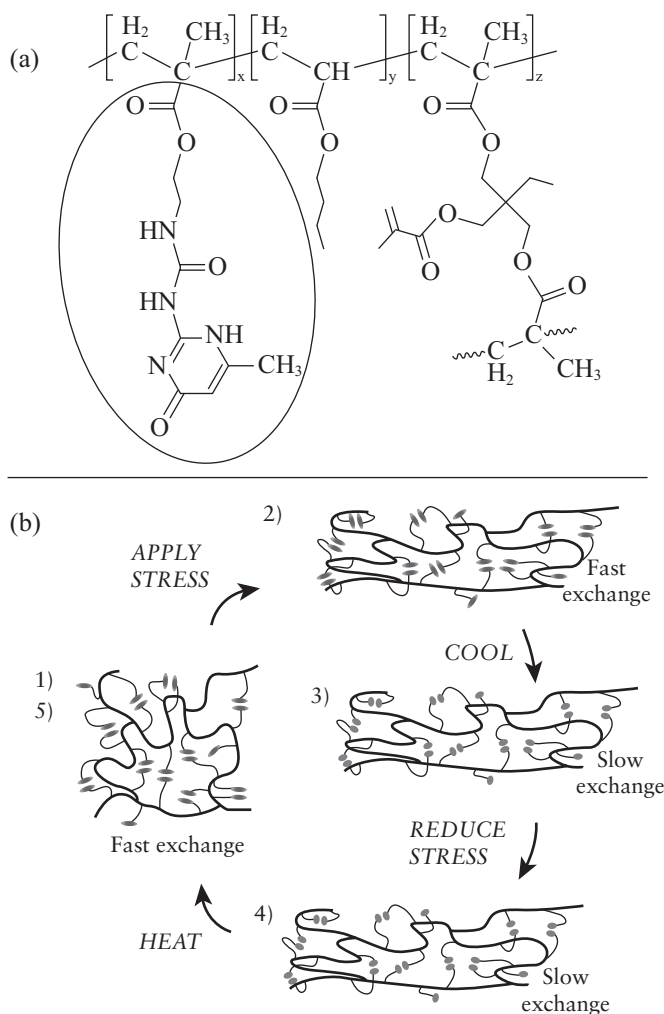


**Figure 5.5** A thermally reversible crosslinked structure. 3M4F: 3 Multi-maleimide 4 multi-furan. Reproduced with permission from X.X. Chen, M.A. Dam, K. Ono, A. Mal, H.B. Shen, S.R. Nutt, K. Sheran and F. Wudl, *Science*, 2002, **295**, 5560, 1698. ©2002, The American Association for the Advancement of Science [56]

#### 5.2.4 Shape-memory Effect based on Supramolecular Structure

Supramolecular structures containing donors and acceptors can act as switches in SMP. Li and co-workers [59] employed a thermally reversible associating quadruple hydrogen-bonding structure as the switch of SMP. The SMP consists of a lightly crosslinked network which is bonded to a reversibly associating ureidopyridinone (UPy) moiety. The UPy moiety forms a quadruple hydrogen bonding interaction. The molecular structure of the SMP network is presented in **Figure 5.6a**. The shape-memory mechanism with thermally reversible hydrogen bonding presented by Li and co-workers [59] as the switch is shown in **Figure 5.6b**. During the fixity process, the thermally reversible hydrogen bonding forms new netpoints, which ‘pin’ the elastic recovery of the elastomer. As a result, the deformed shape is fixed. Upon heating to a high temperature, the netpoints formed by the hydrogen bonding collapse. The polymer recovers its original shape as a result of entropy elasticity. Hu and co-workers [60, 61] incorporated self-complementary quadruple hydrogen bonding units into SMPU and studied the SME of polyurethane. The self-complementary quadruple hydrogen bonding had significant influences on the shape-memory properties of the polyurethanes. Hu and co-workers [62] also prepared SMPU by using *N,N*-bis(2-hydroxyethyl) isonicotinamine, diisocyanate, and 1,4-BD. The supramolecular structure of hydrogen bonding was incorporated into the polyurethane by *N,N*-bis(2-hydroxyethyl) isonicotinamine. In addition to a thermally reversible hydrogen bonding

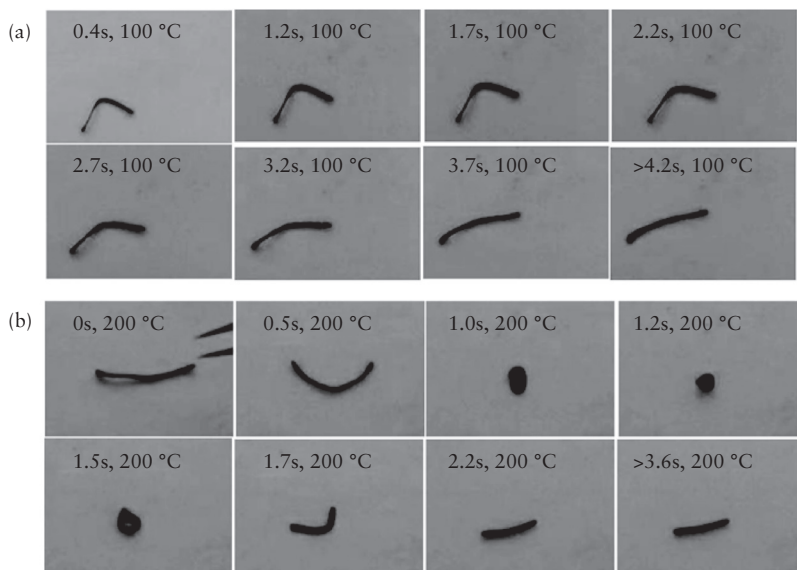
structure acting as a switch, other thermally reversible supermolecular interactions which may be used as the switches of SMP are ion–ion and ion–dipole interactions [17]. More information on supramolecular SMP are provided in Chapter 7.



**Figure 5.6** (a) Lightly crosslinked SMP containing pendent UPy side groups; and (b) shape-memory mechanism of a SMP with thermally reversible hydrogen bonding. Reproduced with permission from J.H. Li, J.A. Viveros, M.H. Wrue and M. Anthamatten, *Advanced Materials*, 2007, **19**, 19, 2851. ©2007, John Wiley & Sons [59]

### 5.2.5 Two-way Shape-memory Effect based on Change in the Conformation of Anisotropic Chains

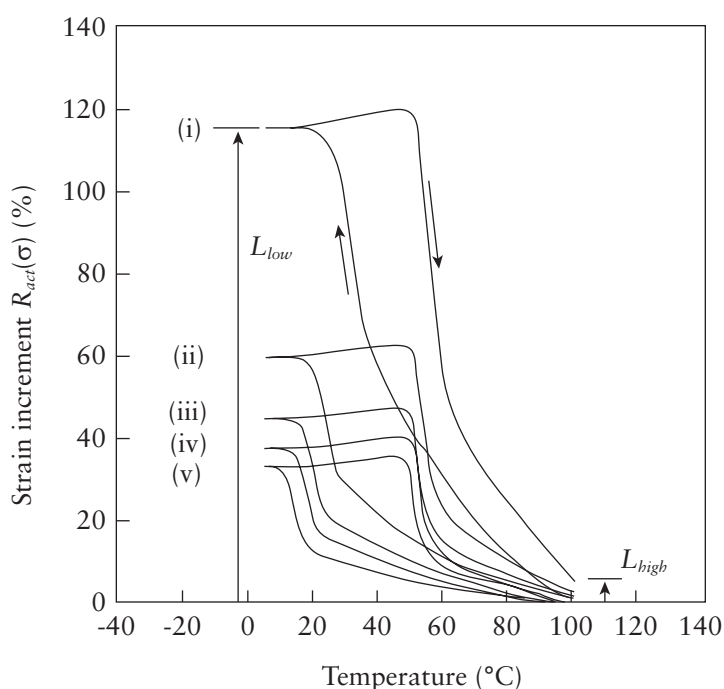
Many applications of SMP, such as continuously moving devices, require reversible two-way SME otherwise the device can undergo only one-step movement under stimulation. Ahir and co-workers [63] as well as Qin and Mather [64] studied the two-way SME of liquid-crystalline polymers. Ahir and co-workers [63] synthesised thermoplastic liquid-crystalline elastomers using the telechelic principle of microphase separation in triblock copolymers. In the polymer, the large central block consisted of a main-chain nematic polymer renowned for its large spontaneous elongation along the nematic director. Crosslinking was established by small terminal blocks formed of terphenyl moieties. Fibres were made from the liquid-crystalline elastomers. In the spinning process, the nematic ordering and telechelic crosslinking formed simultaneously. Reversible nematic–isotropic transition caused contraction upon heating and elongation upon cooling of the polymer. Qin and Mather [64] prepared a glass-forming, polydomain nematic network by crosslinking a thermotropic unsaturated polyester, and observed two-way SME in it (Figure 5.7).



**Figure 5.7** Two-way SME observed in SMP developed by crosslinking a thermotropic unsaturated polyester. (a) Initial unbending recovery; and (b) second shrinking recovery. Reproduced with permission from H.H. Qin and P.T. Mather, *Macromolecules*, 2009, 42, 1, 273. ©2009, American Chemical Society [64]

### 5.2.6 Two-way Shape-memory Effect based on Cooling-induced Crystallisation Elongation

Chung and co-workers [65] studied the SME of a semi-crystalline network polycyclooctene (PCO). The cooling-induced crystallisation of crosslinked PCO films under tension (not deformation to obtain a temporary shape) led to significant elongation, and subsequent heating to melt the network resulted in contraction of the polymer film. They found that the two-way SME was affected by the crosslinking density of the PCO network (Figure 5.8) and the stress applied to stretch the PCO chains at high temperature. Finite external stress was required for the two-way SME.

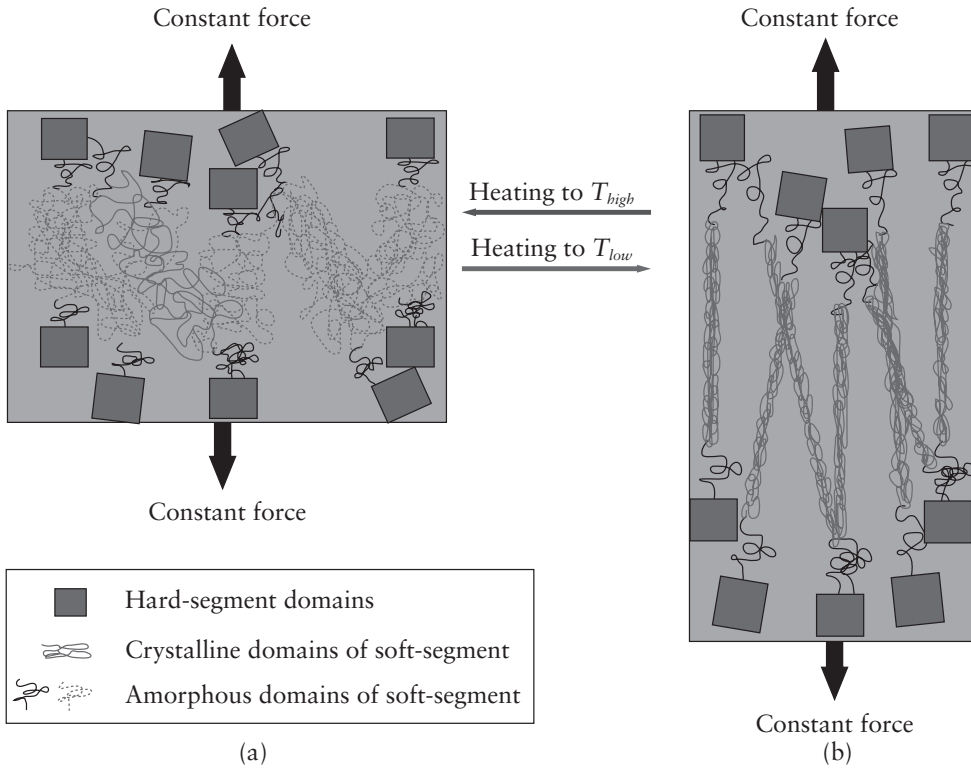


**Figure 5.8** Two-way shape-memory behaviour of PCO cured with different concentrations of crosslinking agent, i.e., dicumyl peroxide: (i) 1.0; (ii) 1.25; (iii) 1.5; (iv) 1.75; and (v) 2.0 wt%.  $L_{high}$ : Length at high-temperature;  $L_{low}$ : length of the sample at low temperature; and  $R_{act}$ : actuation magnitude. Reproduced with permission from T. Chung, A. Rorno-Urabe and P.T. Mather, *Macromolecules*, 2008, 41, 1, 184. ©2008, American Chemical Society [65]

Based on a similar principle, Hong and co-workers [66] also showed two-way SME in a SMPU network under constant stress. They reported on the reversible and repeatable extension and contraction behaviour of a SMPU network during cooling and heating cycles under a bias load condition. The shape-memory mechanism for two-way SME is shown in **Figure 6.9**. Under a constant length condition, the SMPU experiences stress because a constant length condition prevents the SMPU from recovering its permanent shape (i.e., the stretched molecules in the soft segments are prevented from contracting). The constant length condition is then released and instead a constant stress condition is provided. Upon cooling under constant stress, amorphous molecules in the soft segment transform into crystallites to generate an ordered structure because of stress-induced crystallisation. This results in macroscopic extension in the direction of stress (**Figure 5.9b**). However, if the SMPU is reheated, the ordered structure is lost and the same molecules transform into an amorphous phase. This promotes the shape-recovery process to return to its undeformed conformation. The SMPU contracts (i.e., recovers its shape) because the contraction force is larger than the applied stress (**Figure 5.9a**). If cooled again, the SMP will exhibit similar behaviour (i.e., extension upon cooling and contraction upon heating). As a result, the SMPU repeats its contraction and extension behaviour according to alternating cooling and heating cycles, thereby showing two-way SME.

### ***5.2.7 Two-way Shape-memory Effect based on Shape-memory Polymer/Carbon Nanotube Composites***

Two-way SME have also been observed in a multiwalled carbon nanotube (MWCNT)/elastomer composite by Ahir and Vaia [67] (**Figure 5.10**). Infrared light was used as the heat source to heat the CNT/elastomer composite. They found that the expansion or contraction of the composite is dependent upon the extent to which the composite is strained. If the material is pulled slightly, it expands if it is exposed to infrared light. Conversely, if the material is subject to a strain >10%, it contracts under identical exposure to infrared light. This process is completely reversible and persists after numerous cycles. The origin of the bimodal response has not been identified completely.

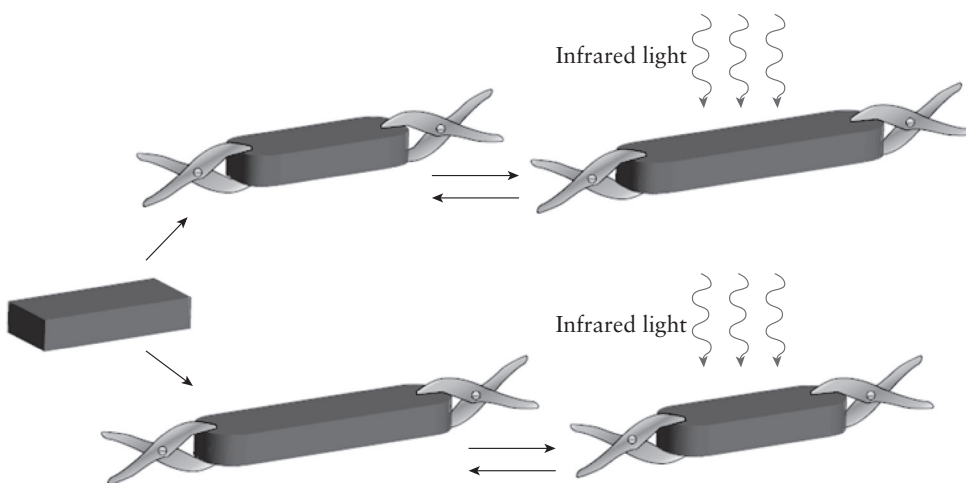


**Figure 5.9** Two-way shape-memory mechanism of SMPU under constant stress (schematic).  $T_{high}$ : Higher order transition temperature and  $T_{low}$ : lower order transition temperature. Reproduced with permission from S.J. Hong, W.R. Yu and J.H. Youk, *Smart Materials & Structures*, 2010, 19, 3. ©2010, IOP Publishing [66]

### 5.2.8 Multiple Shape-memory Effect based on Combined Switches

If several switches are combined in a single SMP, an SMP with ‘multiple SME’ can be developed [17, 64]. **Figure 5.11** shows the triple SME of a polycaprolactone- and polyethylene glycol (PEG)-based polymer network. The permanent shape is determined by the chemical crosslinking of the network. The two thermal transitions of two different crystallisable phases of polycaprolactone and PEG are used as the two switches to fix and release the two temporary shapes [68]. Another immediately available method of preparing SMP with multiple SME is by blending different SMP

to obtain well-separated transition temperatures of the polymer blend. Kolesov and Radusch [69] blended linear high-density polyethylene, ethylene-1-octene copolymers, and short-chain branched polyethylenes. They observed triple- and quadruple- SME after two- and three-step programming of the blends. The switch transition of multiple SME can be any of the switch structures mentioned above, besides conventional glass and melting transitions. Qin and Mather [64] prepared a glass-forming, polydomain nematic network. The material exhibited a first step recovery (one-way SME) related to the glass transition and a second recovery (two-way SME) related to the polydomain soft elasticity intrinsic to the nematic phase.

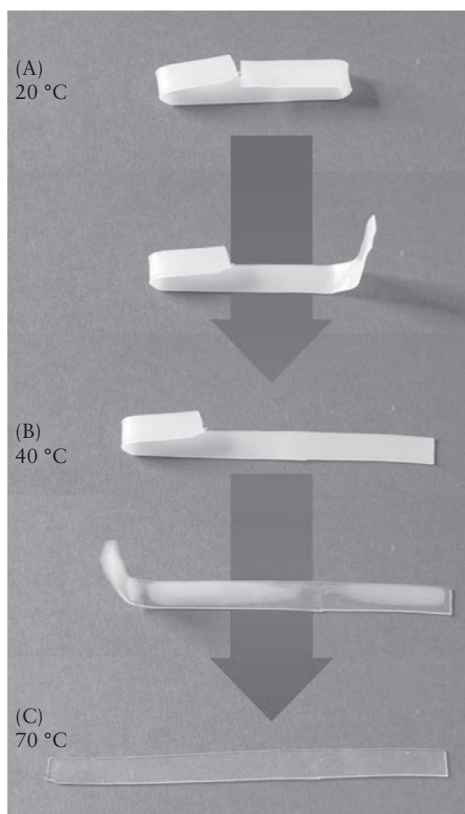


**Figure 5.10** New light on nanocomposites. Bimodal and reversible actuation of a CNT/elastomer nanocomposite induced by infrared irradiation. Reversible expansion occurs at small pre-strains (top) and reversible contraction at large pre-strains (bottom). Reproduced with permission from S.V. Ahir and E.M. Terentjev, *Nature Materials*, 2005, 4, 6, 491. ©2005, Nature Publishing Group [67]

Thermally active SMP have been used in a wide range of applications. These applications include: intelligent medical devices; smart textiles and apparels; heat-shrinkable packages for electronics, sensor and actuators; smart water vapour-permeable materials; self-deployable structures in spacecraft; micro-systems; damping materials; self-peeling reversible adhesives; vehicle components; toys; hair treatments; chemical feeding in chemical reactions [17]. Among these applications, the medical



applications of SMP have been studied the most extensively and intensively [8]. The medical applications of SMP include: laser- or magnetic-activated devices for cardiovascular stents; aneurysm coils for the treatment of intracranial injuries; biodegradable intelligent-surgery sutures; orthodontic appliances; self-deployable neuronal materials; dialysis-needle adapters; drug-release devices.



**Figure 5.11** Triple-SME of a polymer network with two melting transition temperatures as two shape-memory switches. The series of photographs demonstrates the recovery of shapes (b) and (c) by subsequent heating to 40 °C and 70 °C (from top to bottom). Shape (a) had been created before by heating the sample (flat film) to 70 °C, deforming the left end of the sample and cooling to 40 °C (resulting in shape (b)), and finally cooling to 20 °C while keeping the right side of the polymer film deformed. Reproduced with permission from I. Bellin, S. Kelch and A. Lendlein, *Journal of Materials Chemistry*, 2007, 17, 28, 2885. ©2007, Royal Society of Chemistry [68]

### **5.2.9 Thermally active and pH-active Polymeric Hydrogels**

Stimulus-active gels increase or decrease their degree of swelling in response to temperature, pH, solvents, light intensity/wavelength, ionic strength, magnetic field, electrical field, or pressure [17]. Among stimulus-active polymeric gels, thermally and pH-active hydrogels have been studied the most extensively because of their important applications in physiological, biological, and biomedical areas for human use.

Thermally active hydrogels are three-dimensional chemically or physically crosslinked polymeric networks containing a large fraction of water within their structure. The common feature of thermally active hydrogels is that hydrophobic (e.g., methyl, ethyl, propyl) and hydrophilic (e.g., amide, carboxyl) groups coexist in a single macromolecular network. Thermally active hydrogels transform from a hydrophilic to hydrophobic structure at a critical temperature: the lower critical solution temperature. At a lower temperature, hydrogen bonding between hydrophilic segments of the polymer chain and water molecules dominate, which leads to enhanced dissolution in water. At a higher temperature, hydrophobic interactions among hydrophobic segments become strengthened, whereas the hydrogen bonding becomes weaker, which results in the shrinkage of the hydrogel due to inter-polymer chain association through hydrophobic interactions [70]. Poly(*N*-isopropyl acrylamide) (PNIPAAm) and its copolymers are a well-studied class of hydrogels [71]. The phase transition of PNIPAAm can be controlled by kinetic and thermodynamic means by adjusting the copolymer composition and topology [72]. Researchers have developed copolymer P(MEO<sub>2</sub>MA-*co*-OEGMA) composed of 2-(2-methoxyethoxy)ethyl methacrylate (MEO<sub>2</sub>MA) and oligo(ethylene glycol) methacrylate (OEGMA) as an ideal substitute to PNIPAAm [73].

Hydrogels with weak acid or alkaline groups, such as carboxyl or amino, can have pH sensitivity [74, 75]. A typical example of a pH-active hydrogel is a polyacrylic acid system [76]. If a thermally active monomer is copolymerised with a pH-active monomer such as acrylic acid or methacrylic acid, a dual action of thermally active and pH-active effects may be achieved [74].

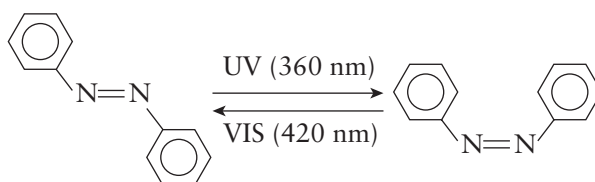
Thermally active hydrogels and pH-active hydrogels have been used in: smart textiles [77]; tissue scaffolds [78]; burn- and wound-dressing materials [79]; molecular recognition [80], biosensor and bio-microelectromechanical system devices [81]; gene-delivery vectors [82]; drug-carrier and drug-delivery media [83]; artificial muscles [84]; chemical valves [81]; immobilisation of enzymes [85] and cells [86]; bioseparation [87].

### 5.3 Light-sensitive Shape-memory Polymers

Photodeformable polymers are based primarily on: (a) photoisomerisable molecules such as azobenzenes; (b) photoreactive molecules such as cinnamates [88]; (c) addition–fragmentation chain transfer reactions using allyl sulfides [89]; and (d) reversible photoinduced ionic dissociation such as triphenylmethane leuco. Complicated movements such as oscillating, twisting, swimming [90], rotation [91], and ‘inchworm walking’ have been obtained in photoactive polymer films and laminated films [92].

#### 5.3.1 Photodeformability Induced by Photoisomerisation

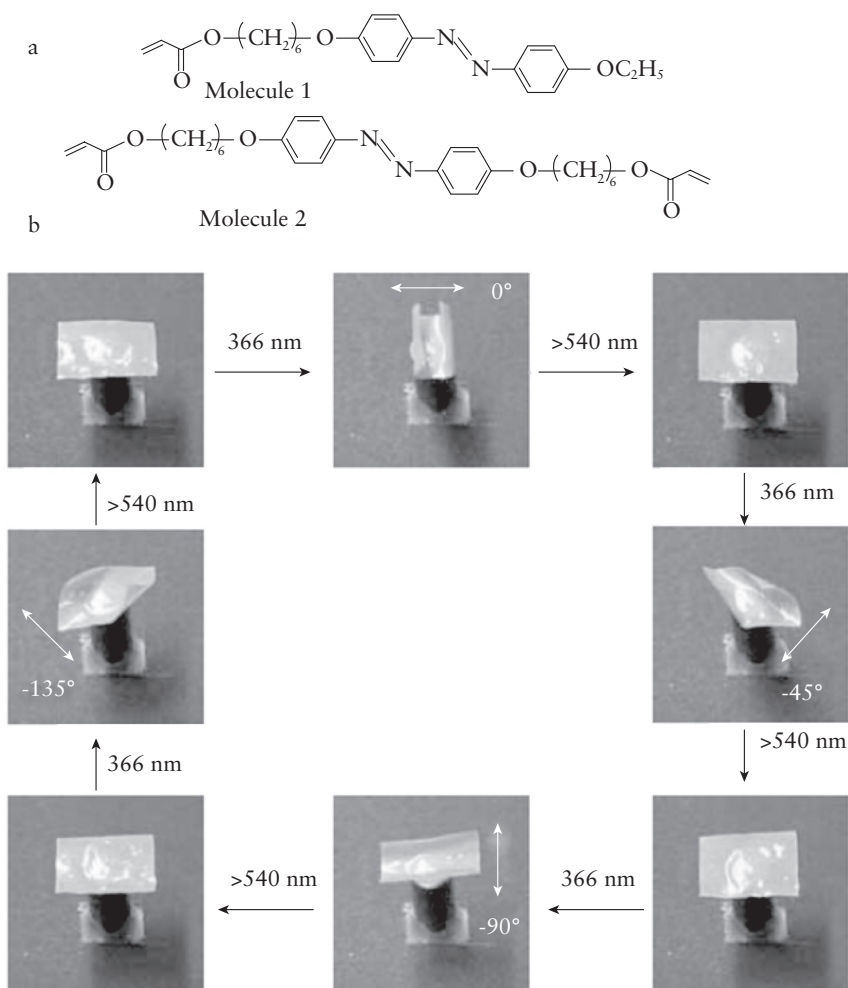
Upon exposure to light of appropriate wavelength, azobenzenes show reversible *trans*–*cis* isomerisation (Figure 5.12). This *trans*–*cis* isomerisation leads to a change in the angle between the two aromatic rings, with the distance between the 4- and 4'-carbons decreasing from 9.0 Å (*trans*) to 5.5 Å (*cis*). If azobenzene groups are linked to macromolecules, the interconversion between the two photoisomers can induce macroscopic changes in the polymeric material.



**Figure 5.12** Photoisomerisation of azobenzene. UV: Ultraviolet; and VIS: visible. Reproduced with permission from H. Meng and J.L. Hu, *Journal of Intelligent Material Systems and Structures*, 2010, **21**, 9, 859. ©2010, SAGE Publications [17]

The research teams of Ikeda [93, 94], Finkelmann [95], and Terentjev [96] prepared several light-active liquid-crystal elastomers containing azobenzene. These liquid-crystal elastomers experience a reduction in alignment order and even liquid-crystal-to-isotropic transition due to the *trans*–*cis* photoisomerisation of azobenzene moieties upon light irradiation [95]. Ikeda and co-workers [93, 94] prepared a photodeformable polymer film by thermal polymerisation of a liquid-crystal monomer and a diacrylate

crosslinker. **Figure 5.13a** presents the chemical structures of the liquid-crystal monomer and crosslinker used in preparation of the film, both of which contain azobenzene groups. **Figure 5.13b** shows the controlled photo-induced bending in precise directions achieved in the polymer in response to light of different angles of polarisation (white arrows).



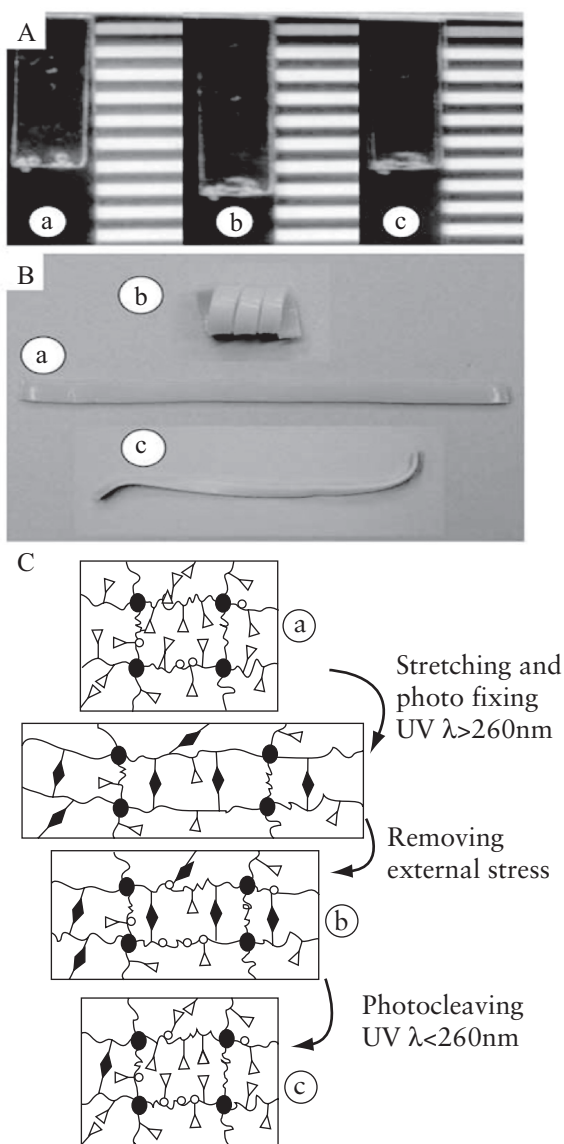
**Figure 5.13** Precisely controlled light-active effect of a liquid-crystal film containing azobenzene by linearly polarised light. Reproduced with permission from Y.L. Yu, M. Nakano and T. Ikeda, *Nature*, 2003, 425, 6954, 145. ©2003, Nature Publishing Group [93]

### **5.3.2 Photodeformability induced by Photoreactive Molecules**

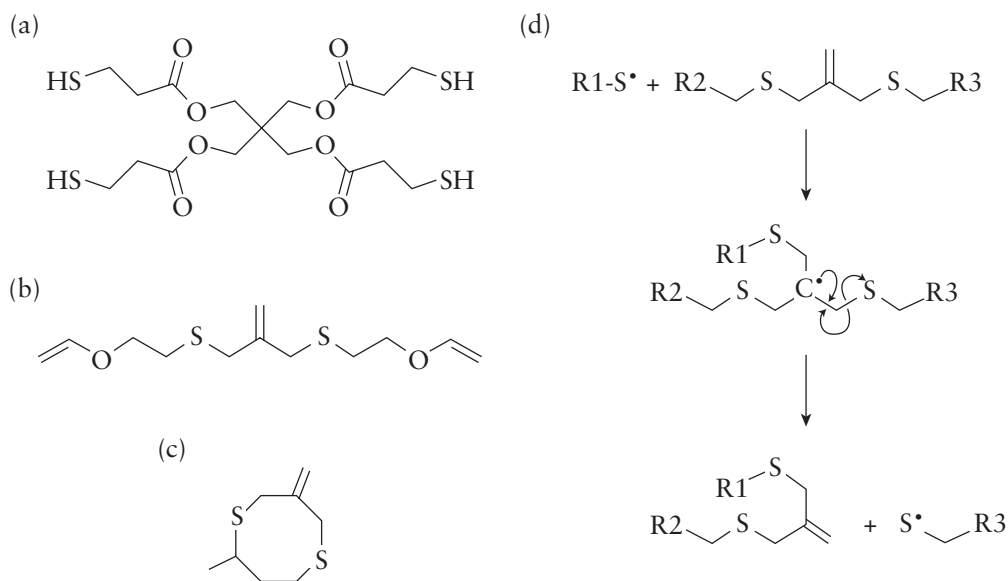
Photochemically reactive molecules can form photoreversible covalent crosslinks in polymers. By using a reversible photo-crosslinking reaction, Lendlein and co-workers [97] prepared light-active grafted polymers with cinnamic acid (CA) as the terminal groups (Figure 5.14(A)). Figure 5.14(B) shows the light-active effect of the grafted polymer. Figure 5.14(C) shows the molecular mechanism of light-active SME of the grafted polymer network (filled circles) with crosslinking (filled diamonds) and cleaving (open triangles) of CA in the molecule chains. The film is first stretched and irritated by UV light longer than 260 nm. The photo-induced cycloaddition reaction of the CA groups increases the elastic modulus of the polymer, which induces the fixity of the polymer film. Then, the film is released and recovers partially as a result of instant elasticity. Finally, irradiation with UV light shorter than 260 nm on the deformed sample causes the photocleaving of CA groups and a decrease in the elastic modulus, which leads to the shape recovery of the polymer. The shape recovery force is supplied by the permanent polymer network (filled circles). Beblo and Weiland [98] presented a chemical kinetic model that could predict the through-thickness evolution of the elastic modulus of light-active polymer samples when the light-active polymer was irradiated.

### **5.3.3 Photoactive Effect from the Addition–fragmentation Chain Transfer Reaction**

Scott and co-workers [99] developed a light-active covalently crosslinked network which underwent reversible photo cleavage in its backbone chain to allow chain rearrangement. The switch mechanism of the reversible backbone cleavage was addition–fragmentation chain transfer. Reaction diffusion of radicals through the crosslinked matrix occurs initially by the reaction of a radical with in-chain functionality to form an intermediate, which in turn fragments, reforming the initial functionality and radical. The monomers used to produce the crosslinking network are shown in Figure 5.15. The light-active polymer is formed from pentaerythritol tetra (3-mercaptopropionate) (PETMP), 2-methylenepropane-1,3-di(thioethyl vinyl ether) (MDTVE) and 25 wt% of 2-methyl-7-methylene-1,5-dithiacyclooctane (MDTO). The network from a stoichiometric PETMP/MDTVE possesses one allyl sulfide group per crosslink, whereas addition of MDTO to the mixture produces a network with approximately two allyl sulfide groups per crosslink. Figure 5.15d shows the addition–fragmentation process through the polymer backbone of the photoactive network. Long and co-workers [100] proposed a photomechanic model of the above-prepared light-activated polymer by integrating four coupled phenomena: photophysics, photochemistry, chemomechanical coupling, and mechanical deformation. The simulation results compared nicely with the experimental results.



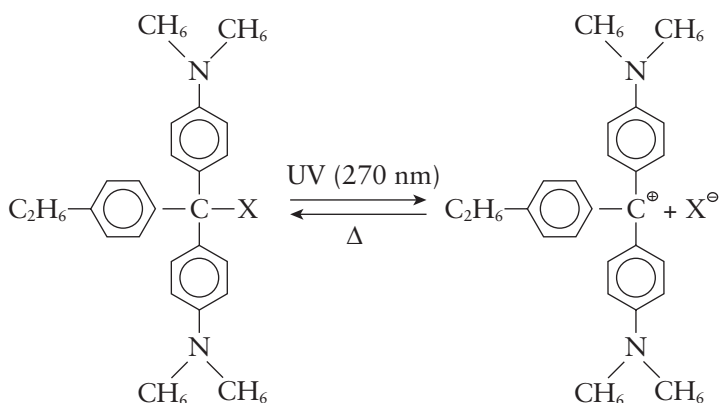
**Figure 5.14** (A) The light-active cinnamic acid group, (B) the shape recovery of the grafted polymer ((a) permanent shape, (b) temporary shape, (c) recovered shape) and (C) the molecular mechanism of the light-active SME. Reproduced with permission from A. Lendlein, H.Y. Jiang, O. Junger and R. Langer, *Nature*, 2005, 434, 7035, 879. ©2005, Nature Publishing Group [97]



**Figure 5.15** Monomers used for the synthesis of a photoactive polymer network: (a) PETMP; (b) MDTVE; (c) MDTO, and (d) addition–fragmentation mechanism through the polymer backbone of the photoactive network illustrated by the addition–fragmentation of allyl sulfides. Reproduced with permission from T.F. Scott, A.D. Schneider, W.D. Cook and C.N. Bowman, *Science*, 2005, 308, 5728, 1615. ©2005, The American Association for the Advancement of Science [99]

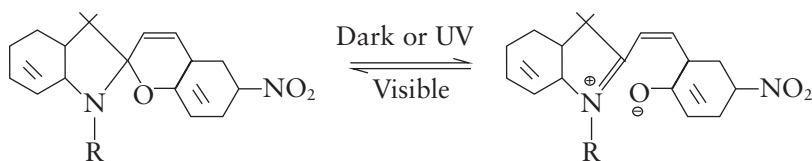
### 5.3.4 Light-active Polymeric Hydrogels

Leuco derivatives of triphenylmethane dissociate into ion pairs upon exposure to UV light. The back reaction by recombining the ion pair occurs thermally in the dark. The reversible photo-induced ionic dissociation of a triphenylmethane leuco derivative is shown in **Figure 5.16**. If triphenylmethane leuco derivatives are incorporated in hydrogels, the reversible variation of electrostatic repulsion between photogenerated charges gives rise to photo-induced expansion and shrinkage of the hydrogels [17]. Light-active azobenzene moieties can also be incorporated into hydrogels to prepare light-active hydrogels [101]. Kamenjicki and co-workers [102, 103] prepared light-active gels containing azobenzene with an embedded crystalline colloidal array.



**Figure 5.16** Photo-induced ionic dissociation of a triphenylphosphine leuco derivative. Reproduced with permission from H. Meng and J.L. Hu, *Journal of Intelligent Material Systems and Structures*, 2010, 21, 9, 859. ©2010, SAGE Publications [17]

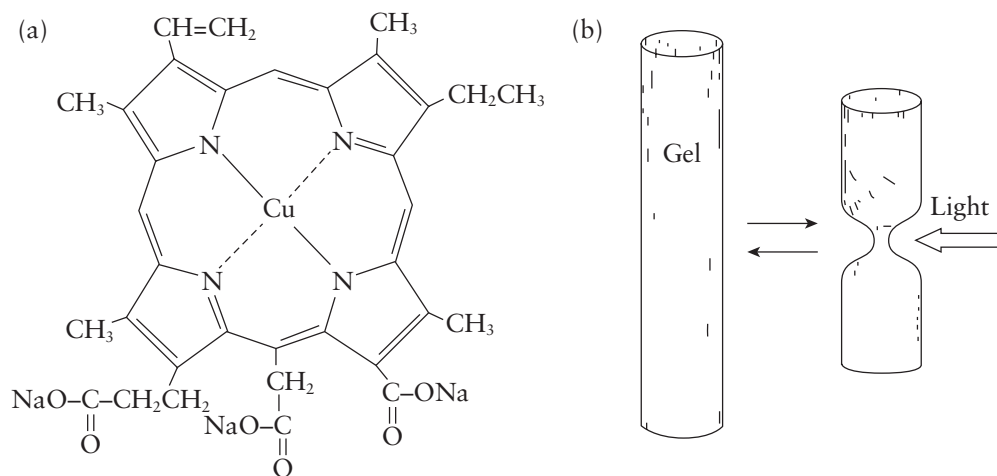
Another strategy for preparing light-active hydrogels is by incorporation of spirocyan (or its derivatives) into hydrogel networks [104, 105]. The molecular structural change of the spirocyan structure between closed and open forms upon a light trigger is shown in **Figure 5.17**. Sumaru and co-workers [105] prepared PNIPAAm and acrylamide-functionalised spirobenzopyran copolymer hydrogel which could respond to light irradiation. Similarly, Garcia and co-workers [106] coupled spirocyan bearing a carboxylic acid group to the amide bond of PNIPAAm-allylamine copolymer microgels to prepare light-active hydrogels.



**Figure 5.17** Change in the structure of spirocyan between closed and open forms. Reproduced with permission from H. Meng and J.L. Hu, *Journal of Intelligent Material Systems and Structures*, 2010, 21, 9, 859. ©2010, SAGE Publications [17]



Light absorbed by molecules of thermally active hydrogels can increase the temperature of the hydrogel and, as a result, the swelling capability of the hydrogels is changed [107]. Suzuki and Tanaka [108] combined the trisodium salt of a copper chlorophyllin chromophore to PNIPAAm hydrogels and observed the light-active effect of PNIPAAm hydrogels (Figure 5.18).



**Figure 5.18** (a) Chemical structure of the trisodium salt of copper chlorophyllin. (b) Light activity of the gel incorporated with the trisodium salt of copper chlorophyllin. Reproduced with permission from A. Suzuki and T. Tanaka, *Nature*, 1990, 346, 6282, 345. ©1990, Nature Publishing Group [108]

Light as a stimulus is exclusively efficient because it is readily available in the environment and does not include the use of secondary sources of energy such as heat, electricity, or magnetic field. Hence, it is environmentally friendly. Light-active polymers have been proposed to be used in: bioseparation; spring-lock truss elements for large boom structures; solar sails; morphing skins of aircrafts; remotely triggered drug-delivery systems; cardiovascular therapeutic devices; surgical stents; recordable and erasable memories; micro-robots in medicine or optical micro-tweezers; optical storage, valves and switches in micro-devices; light-modulators; display devices [8, 17].

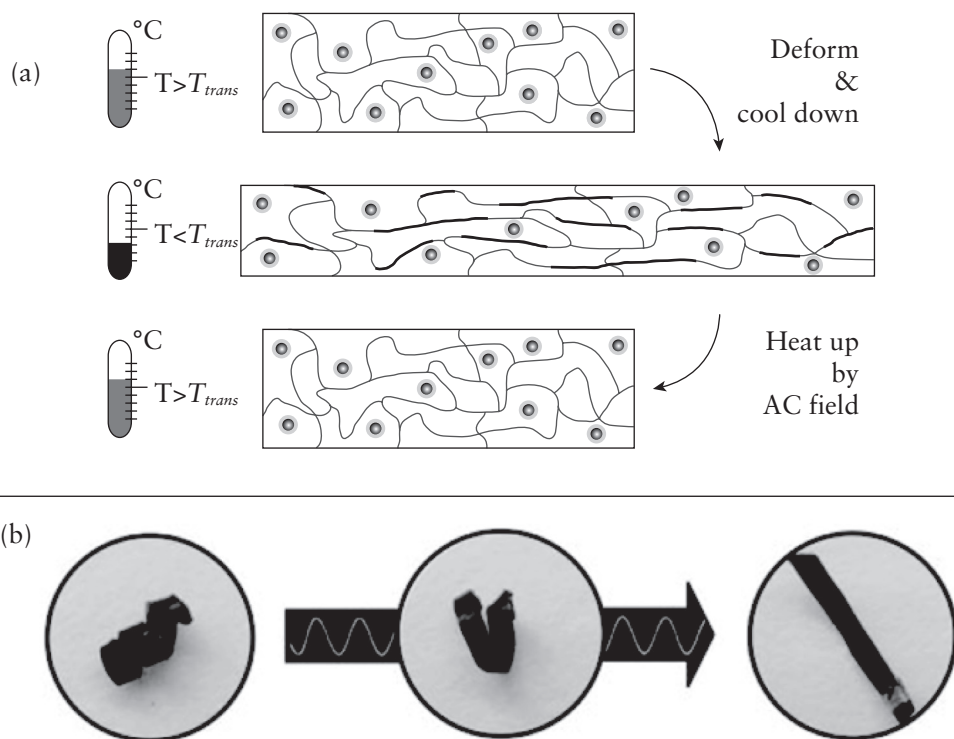
## **5.4 Magnetic-sensitive Shape-memory Polymers**

Magnetic-active SMP show magnetic-active effects with changes in magnetic fields. They are composites of a polymer matrix filled with small magnetic particles. Magnetic-active SMP systems can be used for bearings and vibration absorbance, drug targeting, automotive bushings, magnetic tapes, magnetic gums, soft actuators, micro-manipulators, artificial muscles, and suspension devices [17]. Some of magnetic-sensitive SMP systems are mentioned below.

### ***5.4.1 Shape-memory Polymer Matrices filled with Magnetic Particles***

Surface-modified super-paramagnetic nanoparticles can be incorporated into SMP matrices. This aids the remote actuation of complex shape transitions by electromagnetic fields. Magnetic-active SMP can be developed as composites consisting of a polymer matrix filled with nanoparticles or microparticles. The filler particles can be from ferrimagnetic and ferromagnetic materials. Ferromagnetic shape-memory materials exhibit comparatively large strains in response to an applied magnetic field [17]. Embedded in a SMP matrix, they offer the opportunity to induce a thermal shape transition ‘contactless’ by a specific ‘remote control’. If a magnetic field is applied to the SMP composite, all forces acting on the magnetic particles are transmitted to the polymer matrix, resulting in a shape change in the SMP composite [109]. Magnetic nanoparticles not only possess good magnetic sensitivity for SME they are non-toxic and show harmless biodegradability with a half-life of  $\approx 45$  days [109].

Schmidt [110] showed the SME for SMP composite consisting of  $\text{Fe}_3\text{O}_4$  nanoparticles as fillers in the polymer matrix (**Figure 5.19**). They demonstrated that, by incorporation of magnetic nanoparticles in a SMP matrix, it is possible to initiate an originally thermally activated SME by a contactless and highly selective electromagnetic stimulus, whereas the basic thermal and mechanical behaviour are maintained. This provides a wide scope for medical applications as well as for sensor and actuator systems [18, 26, 55].

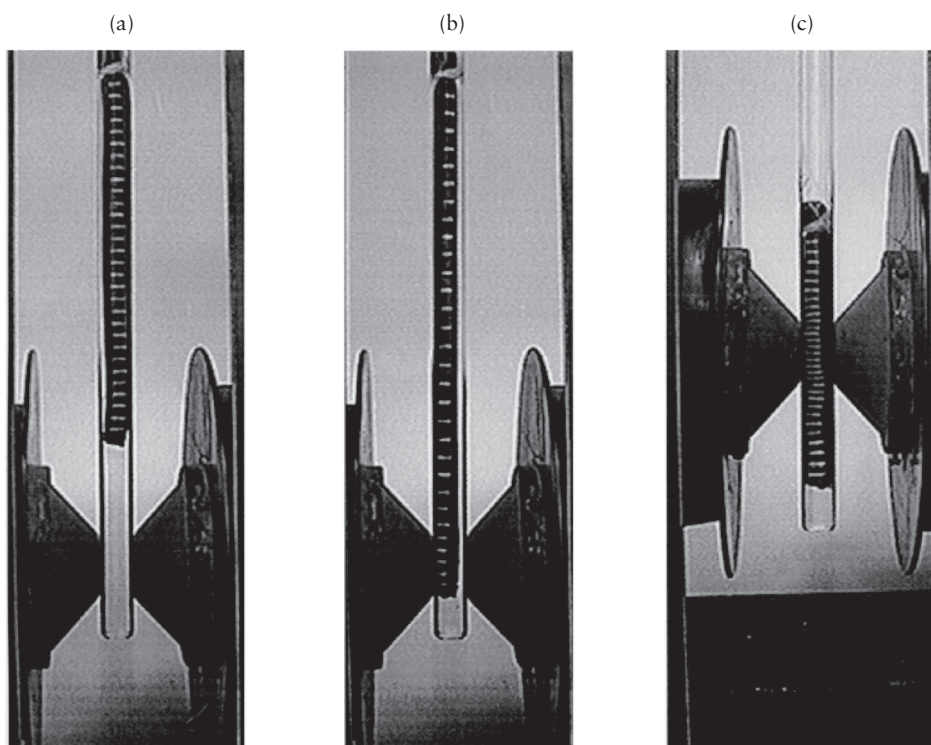


**Figure 5.19** (a) Electromagnetically induced SME in SMP composites and (b) shape recovery of SMP composites in an electromagnetic field (schematic). Reproduced with permission from A.M. Schmidt, *Macromolecular Rapid Communications*, 2006, 27, 14, 1168. ©2006, John Wiley & Sons [110]

### 5.4.2 Magnetic-active polymeric gels

Magnetic-active polymeric gels (also called ‘ferrogels’) are super-paramagnetic particle-filled swollen networks [17]. They can also be regarded as chemically crosslinked polymers swollen by a ferrofluid. Ferrofluids are colloidal dispersions of monodomain magnetic particles with a typical size of  $\approx 10$  nm [111]. In a magnetic-active polymeric gel, the finely distributed ferromagnetic particles are attached to a flexible network by adhesive forces, resulting in direct coupling between the magnetic and mechanical properties of the magnetic-active polymeric gel. If a magnetic-active polymeric gel is subject to a non-uniform magnetic field, wherein the average field gradient is perpendicular to the axis of the gel, the gel will bend toward higher field

strengths. Significant elongation, contraction, and curvature can be induced in <1 s in magnetic-active polymeric gels (Figure 5.20) [112].



**Figure 5.20** Elongation and contraction of magnetic field-sensitive polymer gels: (a) no magnetic field is applied; (b) elongation induced by a magnetic field; and (c) contraction induced by a magnetic field. Reproduced with permission from M. Zrinyi, D. Szabo and H.G. Kilian, *Polymer Gels and Networks*, 1998, 6, 6, 441. ©1998, Elsevier [112]

## **5.5 Water/solvent-sensitive Shape-memory Polymers**

Water-active SME can be obtained in deformed thermally active SMP because water molecules have a plasticising effect upon polymeric materials, and can then increase the flexibility of the macromolecular chains of thermally active SMP [113, 114]. If a

thermally active SMP has a hydrophilic or water-soluble ingredient in its structure, the shape recovery can be accelerated [18]. The research team of Yang [113] undertook a detailed analysis of the effects of moisture on the  $T_g$  of an ether-based polyurethane SMP and its thermomechanical properties (Figure 5.21). They found that the  $T_g$  of the SMP decreased with increasing immersion time in room-temperature water (Figure 5.21a). They proposed that the hydrogen bonding between N–H and C=O groups weakens in the presence of water (Figure 5.21b), which causes a significant decrease in the  $T_g$ .

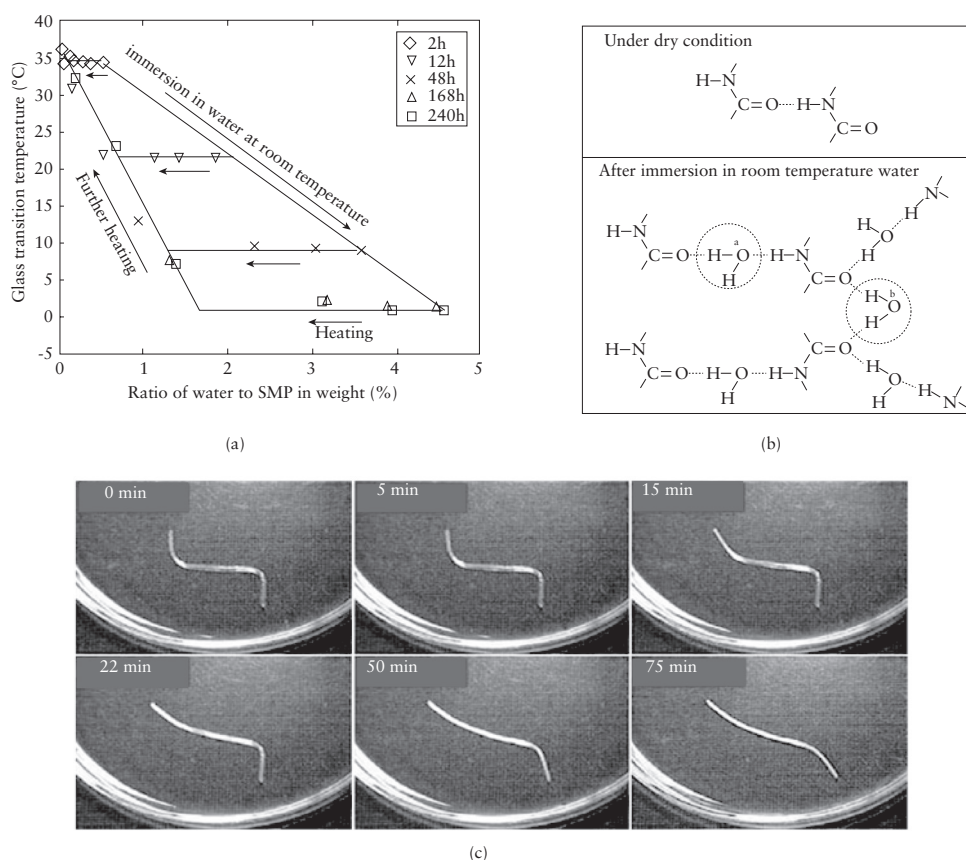


Figure 5.21 (a) Glass transition temperature *vs* ratio of water to SMP in weight percent, (b) effects of water on the hydrogen bonding in polyurethane SMP, and (c) recovery of the functional gradient of SMP actuated by water in a sequence.

Reproduced with permission from B. Yang, W.M. Huang, C. Li and L. Li, *Polymer*, 2006, 47, 4, 1348. ©2006, Elsevier [113]

Pyridine is responsive to moisture and can be used to improve the moisture absorption of polyurethane [5, 115–117]. Chen and co-workers [60, 62] introduced a pyridine unit into SMPU using *N,N*-bis(2-hydroxyethyl) isonicotinamine (BINA) and prepared moisture-active SMPU (PUPy). The synthesis route of PUPy is presented in Figure 5.22. First, HDI reacts with BINA to form a pre-polymer. Then, the pre-polymer is extended with 1,4-BD. High-strain recovery with fast recovery speed is obtained by putting the polymer into water. It can be deduced that SMP sensitive to suitable solvents can be obtained (which is similar to hydrophilic SMP that are sensitive to water/moisture). Lv and co-workers [114] and Lu and co-workers [118] observed that *N,N'*-Dimethylformamide (a good solvent of SMPU) active SME of SMPU.

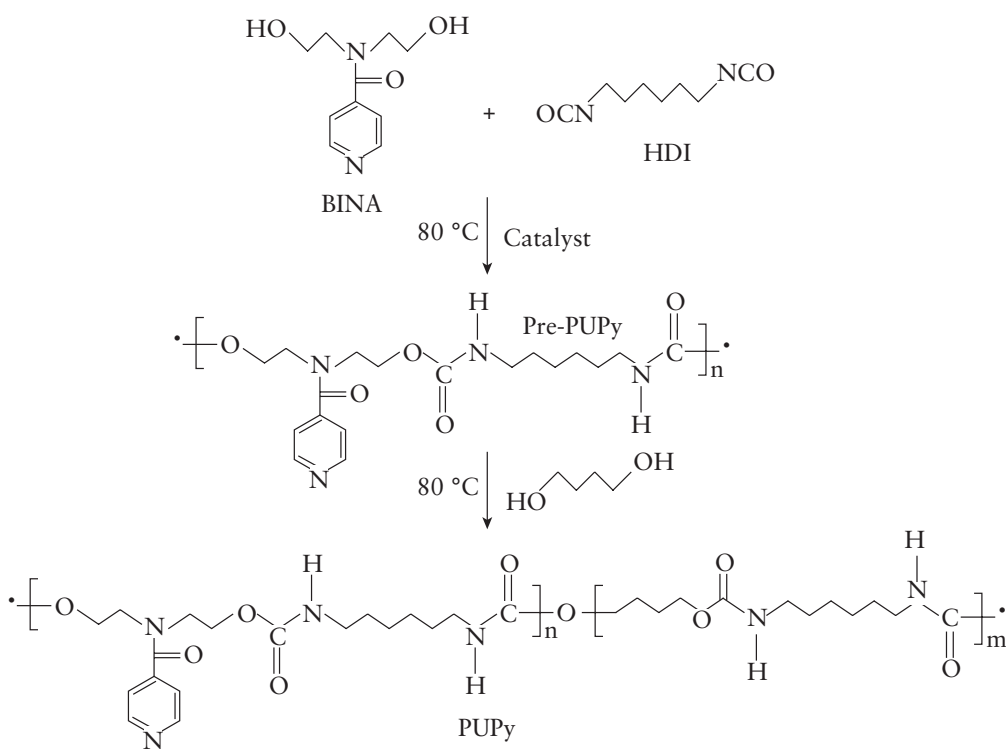


Figure 5.22 Synthetic routine of PUPy. Reproduced with permission from H. Meng and J.L. Hu, *Journal of Intelligent Material Systems and Structures*, 2010, 21, 9, 859. ©2010, SAGE Publications [17]

Chen and co-workers [119] prepared a water-active biodegradable stent made of chitosan (CS) films crosslinked with an epoxy compound. The raw materials (CS and PEG-400) used in the stent were relatively hydrophilic. They found that the developed stent could expand rapidly from a ‘crimped’ state to an expanded state if stimulated by hydration in an aqueous environment (Figure 5.23). Jung and co-workers [120] prepared water-active SMPU using polyhedral oligomeric silsesquioxane (POSS) molecules and PEG acting as the hydrophobic and hydrophilic groups, respectively (Figure 5.24).

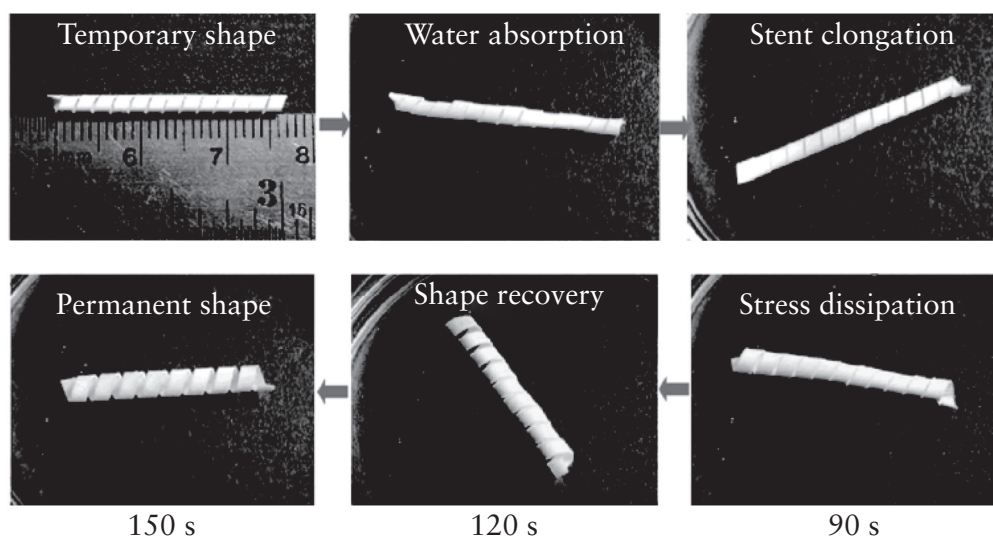
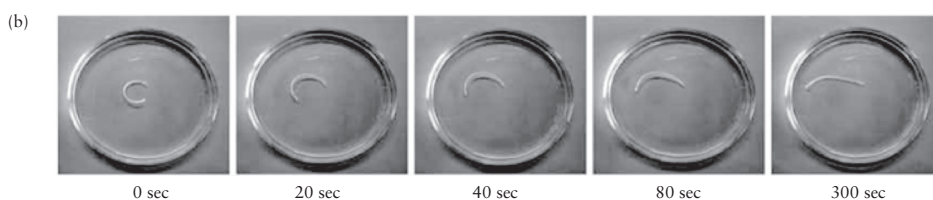
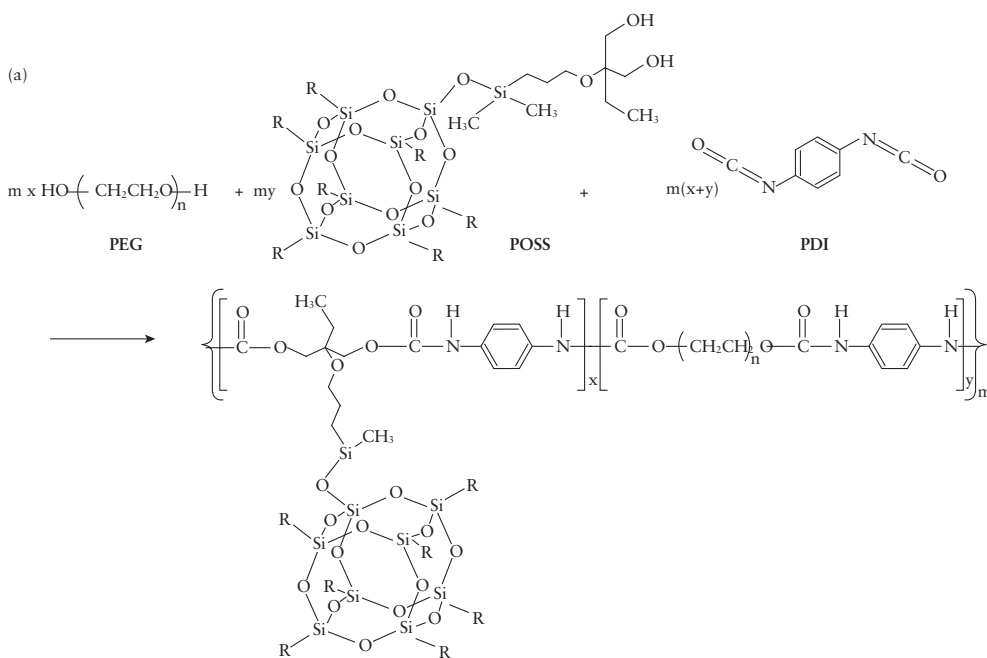


Figure 5.23 Photographs of the time courses of self-expansion of the polymeric (CS/glycerol/PEO400) stent, immersed in PBS solution, and stimulated by hydration. PBS: Phosphate-buffered saline and PEO: Polyethylene oxide. Reproduced with permission from M.C. Chen, H.W. Tsai, Y. Chang, W.Y. Lai, F.L. Mi, C.T. Liu, H.S. Wong and H.W. Sung, *Biomacromolecules*, 2007, 8, 9, 2774. ©2007, American Chemical Society [119]

## 5.6 Electric-sensitive Shape-memory Polymers

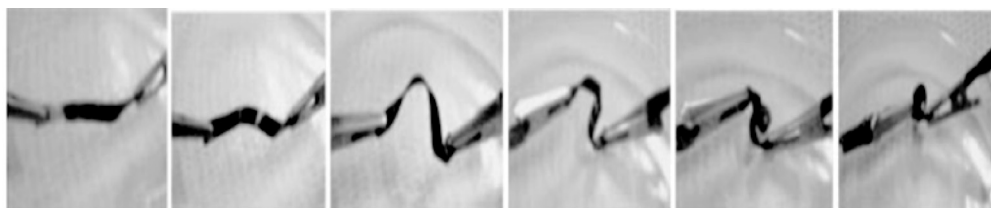
SMP matrices filled with electric-active filler particles can allow actuation by indirect heating. Because of the conducting nature of these electric-active particles, they can

convert the electrical energy to thermal energy required to trigger SME above the transition temperature for a thermally induced SMP. Cho and co-workers [121] developed electric-active SMPU by incorporating MWCNT (Figure 5.25). They found that MWCNT in the polymer matrix not only resulted in faster actuation (shape recovery) but also improved the mechanical properties of the SMP composites. They proposed that these SMPU-MCWNT composites could be used as smart actuators.



**Figure 5.24** (a) Polymerisation procedure of the POSS-PU block copolymer. (b) Water-sensitive shape recovery behaviour of the POSS-PU sample at 35 °C. PU: polyurethane. Reproduced with permission from Y.C. Jung, H.H. So and J.W. Cho, *Journal of Macromolecular Science, Part B: Physics*, 2006, 45, 4, 453. ©2006, Taylor & Francis [120]



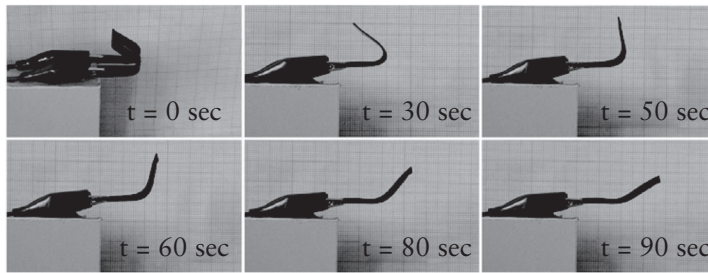


**Figure 5.25** Electric-active shape-recovery behaviour of SMPU-MCWNT composites (MCWNT content = 5 wt%). The sample undergoes transition from a temporary shape (linear, left) to a permanent shape (helix, right) within 10 s if a constant voltage of 40 V is applied. Reproduced with permission from J.W. Cho, J.W. Kim, Y.C. Jung and N. Goo, *Macromolecular Rapid Communications*, 2005, 26, 5, 412. ©2005, John Wiley & Sons [121]

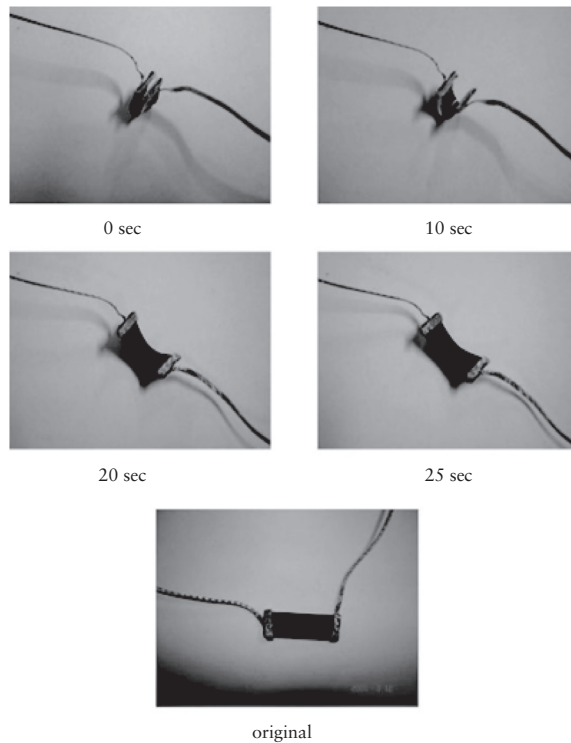
The research team of Leng have done important work in developing electric-active SMP composites and used different nanofillers to analyse the shape-memory performance of SMP composites. They used nanocarbon powders as filler materials to develop electric-sensitive SMP composites (**Figure 5.26**). They found that the  $T_g$  of the SMP composite shifts slightly toward a low temperature range and its storage modulus increases with increasing content of nanocarbon powders [122]. They also observed a uniform dispersion of conductive nanoparticles and fibre fillers in the polymer matrix, and obtained enhanced mechanical performances of SMP composites [123].

The research team of Leng also tried to find simple methods to further reduce the electrical resistivity of thermo-responsive SMP to obtain easy triggering conditions for shape recovery by Joule heating at a low electrical voltage [46, 47, 124]. They tried to incorporate Ni microparticles into a PU SMP matrix filled with CB. They showed that, by forming conductive Ni chains under a weak static magnetic field (0.03 T), the electrical conductivity of the SMP composite in the chain direction could be improved significantly, thereby making it more suitable for Joule heating-induced shape recovery. If the Ni particles were aligned into chains, the drop in electrical resistivity was significant [46]. In addition, Ni chains reinforce the SMP significantly but their influence on the  $T_g$  is about the same as that of randomly distributed Ni powders.

Sahoo and co-workers [125, 126] developed electric-active SMP composites using PU block copolymers and conducting polypyrrole (PPy) by chemical oxidative polymerisation. **Figure 5.27** shows the shape-memory effect of the PU/PPy composite. They suggested that a high degree of crystallinity of soft segments may be required. However, good electrical conductivity and a minimum extent of elongation at break are also important to show the electric-active shape-memory behaviour of this system [126].



**Figure 5.26** Sequences of the shape recovery of a SMP composite containing nanocarbon powders. Reproduced with permission from J.S. Leng, X. Lan, Y.J. Liu and S.Y. Du, *Smart Materials and Structures*, 2009, 18, 7. ©2009, IOP Science [122]



**Figure 5.27** Electric-active shape recovery behaviour of PU/PPy = 80/20 composite. Reproduced with permission from N.G. Sahoo, Y.C. Jung, N.S. Goo and J.W. Cho, *Macromolecular Materials and Engineering*, 2005, 290, 11, 1049. ©2005, John Wiley & Sons [126]

## 5.7 Conclusions

This chapter presented a brief overview of the different mechanisms and fabrication strategies of different SMP that can change their shapes (configuration or dimension) or produce mechanical power in response to heat, light, electricity, magnetic field, and water/solvent.

Even though many SMP have been developed and many new applications of SMP have been studied in the past several decades, research in this area is far from mature. First, most of the movements of present SMP are simple shrinkage, bending, or rotation. Complicated movements with controllable strains, deformation speed, and exact deformation stress with multiple steps are preferred. Second, most of the SMP are sensitive to only one specific stimulus signal acting within a specific stimulus range. Multiple stimuli-active SMP could be obtained by combining the different stimulus-active structures into one single polymer so that the stimulus-active products can be active to different signals. Third, continued molecular simulations and mechanical modelling are needed to optimise molecular structures and obtain the optimal stimulus-active properties. Fourth, the primary property of SMP may be stimulus-active properties but environmental stabilities (e.g., thermal stability and chemical stability) of stimulus-active polymers need to be taken into consideration for better application. The environmental stabilities of SMP may affect the repeatability and lifetime of SMP significantly. Finally, size, configuration, and form have significant influences on the properties of stimulus-active polymers, and need to be considered for some applications. Several prototype devices of SMP have been reported but many problems have been encountered during practical applications. Material scientists, engineers, and technicians from different disciplines need to work in collaboration to build competitive SMP with excellent properties.

## References

1. F.L. Ji, J.L. Hu and J.P. Han, *High Performance Polymers*, 2011, **23**, 3, 177.
2. X.F. Luo and P.T. Mather, *Soft Matter*, 2010, **6**, 10, 2146.
3. J. S. Leng, D.W. Zhang, Y. Liu, K. Yu and X. Lan, *Applied Physics Letters*, 2010, **96**, 11.
4. U.N. Kumar, K. Kratz, M. Behl and A. Lendlein, *eXPRESS Polymer Letters*, 2012, **6**, 1, 26.
5. S.J. Chen, J.L. Hu and S.G. Chen, *Polymer International*, 2012, **61**, 2, 314.

6. H. Feil, Y. H. Bae, J. Feijen and S.W. Kim, *Macromolecules*, 1992, **25**, 20, 5528.
7. J.L. Hu, H.P. Meng, G.Q. Li and S.I. Ibekwe, *Smart Materials and Structures*, 2012, **21**, 5.
8. J.L. Hu, Y. Zhu, H.H. Huang and J. Lu, *Progress in Polymer Science*, 2012, **37**, 12, 1720.
9. K. Takashima, J. Rossiter and T. Mukai, *Sensors and Actuators A: Physical*, 2010, **164**, 1-2, 116.
10. T. Xie and X.C. Xiao, *Chemical Materials*, 2008, **20**, 9, 2866.
11. T. Saito, inventor; Yazaki Corporation, assignee; US 6531659, 2003.
12. K. Gall, M.L. Dunn, Y.P. Liu, D. Finch, M. Lake and N.A. Munshi, *Acta Materialia*, 2002, **50**, 20, 5115.
13. W.M. Sokolowski and S.C. Tan, *Journal of Spacecraft and Rockets*, 2007, **44**, 4, 750.
14. E. Smela, O. Inganas and I. Lundstrom, *Science*, 1995, **268**, 5218, 1735.
15. Y. Bar-Cohen and Q.M. Zhang, *MRS Bulletin*, 2008, **33**, 3, 173.
16. W.M. Huang, B. Yang, Y. Zhao and Z. Ding, *Journal of Materials Chemistry*, 2010, **20**, 17, 3367.
17. H. Meng and J.L. Hu, *Journal of Intelligent Material Systems and Structures*, 2010, **21**, 9, 859.
18. M. Behl and A. Lendlein, *Materials Today*, 2007, **10**, 4, 20.
19. B. Dietsch and T. Tong, *Journal of Advanced Materials-Covina*, 2007, **39**, 2, 3.
20. H. Tobushi, K. Hoshio, S. Hayashi and N. Miwa, *Key Engineering Materials*, 2007, **340-341**, 1187.
21. I.S. Gunes and S.C. Jana, *Journal of Nanoscience and Nanotechnology*, 2008, **8**, 4, 1616.
22. P.T. Mather, X.F. Luo and I.A. Rousseau, *Annual Review of Materials Research*, 2009, **39**, 445.

23. Q.H. Meng and J.L. Hu, *Composites Part A: Applied Science and Manufacturing*, 2009, **40**, 11, 1661.
24. D. Ratna and J. Karger-Kocsis, *Journal of Materials Science*, 2008, **43**, 1, 254.
25. C. Liu, H. Qin and P.T. Mather, *Journal of Materials Chemistry*, 2007, **17**, 16, 1543.
26. A. Lendlein and M. Behl, *Advances in Science and Technology*, 2009, **54**, 96.
27. J.L. Hu and J. Lu, *Smart and Interactive Textiles*, 2013, **80**, 30.
28. J.L. Hu and S.J. Chen, *Journal of Materials Chemistry*, 2010, **20**, 17, 3346.
29. F.C. Meng, X.H. Zhang, G. Xu, Z.Z. Yong, H.Y. Chen, M.H. Chen, Q.W. Li and Y.T. Zhu, *ACS Applied Materials & Interfaces*, 2011, **3**, 3, 658.
30. Q. Meng, J. Hu, Y. Zhu, J. Lu and Y. Liu, *Journal of Applied Polymer Science*, 2007, **106**, 2515.
31. Q.H. Meng, J.L. Hu and L. Yeung, *Smart Materials and Structures*, 2007, **16**, 3, 830.
32. Q.H. Meng, J.L. Hu and Y. Zhu, *Journal of Applied Polymer Science*, 2007, **106**, 2, 837.
33. J.R. Lin and L.W. Chen, *Journal of Applied Polymer Science*, 1998, **69**, 8, 1563.
34. B.C. Chun, T.K. Cho and Y.C. Chung, *European Polymer Journal*, 2006, **42**, 12, 3367.
35. F.L. Ji, Y. Zhu, J.L. Hu, Y. Liu, L.Y. Yeung and G.D. Ye, *Smart Materials and Structures*, 2006, **15**, 6, 1547.
36. Y. Zhu, J.L. Hu, L.Y. Yeung, Y. Liu, F.L. Ji and K.W. Yeung, *Smart Materials and Structures*, 2006, **15**, 5, 1385.
37. W.S. Wang, P. Ping, X.S. Chen and X.B. Jing, *Journal of Applied Polymer Science*, 2007, **104**, 6, 4182.
38. C.C. Min, W.J. Cui, J.Z. Bei and S.G. Wang, *Polymers for Advanced Technologies*, 2005, **16**, 8, 608.

39. F.K. Li, X. Zhang, J.N. Hou, M. Xu, X.L. Lu, D.Z. Ma and B.K. Kim, *Journal of Applied Polymer Science*, 1997, **64**, 8, 1511.
40. Y. Zhu, J. Hu, K.W. Yeung, K.F. Choi, Y.Q. Liu and H.M. Liem, *Journal of Applied Polymer Science*, 2007, **103**, 1, 545.
41. A. Lendlein and R. Langer, *Science*, 2002, **296**, 5573, 1673.
42. H.M. Jeong, B.K. Kim and Y.J. Choi, *Polymer*, 2000, **41**, 5, 1849.
43. J. L. Hu and S. Mondal, *Polymer International*, 2005, **54**, 5, 764.
44. Y.J. Liu, H.B. Lv, X. Lan, J.S. Leng and S.Y. Du, *Composites Science and Technology*, 2009, **69**, 13, 2064.
45. N.S. Goo, I.H. Paik and K.J. Yoon, *Smart Materials and Structures*, 2007, **16**, 4, N23.
46. J.S. Leng, W.M. Huang, X. Lan, Y.J. Liu and S.Y. Du, *Applied Physics Letters*, 2008, **92**, 20.
47. J.S. Leng, X. Lan, Y.J. Liu, S.Y. Du, W.M. Huang, N. Liu, S.J. Phee and Q. Yuan, *Applied Physics Letters*, 2008, **92**, 1.
48. W. Small, T.S. Wilson, W.J. Bennett, J.M. Loge and D.J. Maitland, *Optics Express*, 2005, **13**, 20, 8204.
49. W. Small, M.F. Metzger, T.S. Wilson and D.J. Maitland, *IEEE Journal of Selected Topics in Quantum Electronics*, 2005, **11**, 4, 892.
50. R. Langer and D.A. Tirrell, *Nature*, 2004, **428**, 6982, 487.
51. D.J. Maitland, M.F. Metzger, D. Schumann, A. Lee and T.S. Wilson, *Lasers in Surgery and Medicine*, 2002, **30**, 1, 1.
52. R. Mohr, K. Kratz, T. Weigel, M. Lucka-Gabor, M. Moneke and A. Lendlein, *Proceedings of the National Academy of Sciences USA*, 2006, **103**, 10, 3540.
53. T. Weigel, R. Mohr and A. Lendlein, *Smart Materials and Structures*, 2009, **18**, 2.
54. C.M. Yakacki, N.S. Satarkar, K. Gall, R. Likos and J.Z. Hilt, *Journal of Applied Polymer Science*, 2009, **112**, 5, 3166.

55. M.Y. Razzaq, M. Anhalt, L. Frommann and B. Weidenfeller, *Materials Science and Engineering: A*, 2007, **471**, 1-2, 57.
56. X.X. Chen, M.A. Dam, K. Ono, A. Mal, H.B. Shen, S.R. Nutt, K. Sheran and F. Wudl, *Science*, 2002, **295**, 5560, 1698.
57. X.X. Chen, F. Wudl, A.K. Mal, H.B. Shen and S.R. Nutt, *Macromolecules*, 2003, **36**, 6, 1802.
58. K. Ishida and N. Yoshie, *Macromolecules*, 2008, **41**, 13, 4753.
59. J.H. Li, J.A. Viveros, M.H. Wrue and M. Anthamatten, *Advanced Materials*, 2007, **19**, 19, 2851.
60. S.J. Chen, J.L. Hu, C.W.M. Yuen and L.K. Chan, *Materials Letters*, 2009, **63**, 17, 1462.
61. Y. Zhu, J.L. Hu and Y.J. Liu, *The European Physical Journal E*, 2009, **28**, 1, 3.
62. S.J. Chen, J.L. Hu, C.W.M. Yuen and L.K. Chan, *Polymer*, 2009, **50**, 19, 4424.
63. S.V. Ahir, A.R. Tajbakhsh and E.M. Terentjev, *Advanced Functional Materials*, 2006, **16**, 4, 556.
64. H.H. Qin and P.T. Mather, *Macromolecules*, 2009, **42**, 1, 273.
65. T. Chung, A. Rorno-Urbe and P.T. Mather, *Macromolecules*, 2008, **41**, 1, 184.
66. S.J. Hong, W.R. Yu and J.H. Youk, *Smart Materials and Structures*, 2010, **19**, 3.
67. S.V. Ahir and E.M. Terentjev, *Nature Materials*, 2005, **4**, 6, 491.
68. I. Bellin, S. Kelch and A. Lendlein, *Journal of Materials Chemistry*, 2007, **17**, 28, 2885.
69. I.S. Kolesov and H.J. Radusch, *eXPRESS Polymer Letters*, 2008, **2**, 7, 461.
70. J. Kopecek, *The European Journal of Pharmaceutical Sciences*, 2003, **20**, 1, 1.
71. Y. Qiu and K. Park, *Advanced Drug Delivery Reviews*, 2001, **53**, 3, 321.

72. Y. Suzuki, K. Tomonaga, M. Kumazaki and I. Nishio, *Polymer Gels and Networks*, 1996, **4**, 2, 129.
73. A.M. Jonas, K. Glinel, R. Oren, B. Nysten and W.T.S. Huck, *Macromolecules*, 2007, **40**, 13, 4403.
74. A.S. Hoffman, P.S. Stayton, V. Bulmus, G.H. Chen, J.P. Chen, C. Cheung, A. Chilkoti, Z.L. Ding, L.C. Dong, R. Fong, C.A. Lackey, C.J. Long, M. Miura, J.E. Morris, N. Murthy, Y. Nabeshima, T.G. Park, O.W. Press, T. Shimoboji, S. Shoemaker, H.J. Yang, N. Monji, R.C. Nowinski, C.A. Cole, J.H. Priest, J.M. Harris, K. Nakamae, T. Nishino and T. Miyata, *Journal of Biomedical Materials Research*, 2000, **52**, 4, 577.
75. M.J. McGann, C.L. Higginbotham, L.M. Geever and M.J.D. Nugent, *International Journal of Pharmaceutics*, 2009, **372**, 1-2, 154.
76. G.R. Mahdavinia, A. Pourjavadi, H. Hosseinzadeh and M.J. Zohuriaan, *European Polymer Journal*, 2004, **40**, 7, 1399.
77. B.H. Liu, J.L. Hu and Q.H. Meng, *Journal of Biomedical Materials Research: B*, 2009, **89B**, 1, 1.
78. F. Khan, R.S. Tare, R.O.C. Oreffo and M. Bradley, *Angewandte Chemie International Edition*, 2009, **48**, 5, 978.
79. C.R. Arciola, L. Radin, P. Alvergnà, E. Cenni and A. Pizzoferrato, *Biomaterials*, 1993, **14**, 15, 1161.
80. X.J. Ju, L.Y. Chu, L. Liu, P. Mi and Y.M. Lee, *The Journal of Physical Chemistry: B*, 2008, **112**, 4, 1112.
81. D.T. Eddington and D.J. Beebe, *Advanced Drug Delivery Reviews*, 2004, **56**, 2, 199.
82. C.C. Lin and A.T. Metters, *Advanced Drug Delivery Reviews*, 2006, **58**, 12-13, 1379.
83. D.C. Coughlan, F.P. Quilty and O.I. Corrigan, *Journal of Controlled Release*, 2004, **98**, 1, 97.
84. Y. Ueoka, J. Gong and Y. Osada, *Journal of Intelligent Material Systems and Structures*, 1997, **8**, 5, 465.



85. I.M. Helander, K. Latva-Kala and K. Lounatmaa, *Microbiology*, 1998, **144**, 385.
86. A.C. Jen, M.C. Wake and A.G. Mikos, *Biotechnology and Bioengineering*, 1996, **50**, 4, 357.
87. M.Y. Arica, G. Bayramoglu, B. Arica, E. Yalcin, K. Ito and Y. Yagci, *Macromolecular Bioscience*, 2005, **5**, 10, 983.
88. H.Y. Jiang, S. Kelch and A. Lendlein, *Advanced Materials*, 2006, **18**, 11, 1471.
89. W.D. Cook, S. Chausson, F. Chen, L. Le Pluart, C.N. Bowman and T.F. Scott, *Polymer International*, 2008, **57**, 3, 469.
90. T.J. White, N.V. Tabiryan, S.V. Serak, U.A. Hrozhyk, V.P. Tondiglia, H. Koerner, R.A. Vaia and T.J. Bunning, *Soft Matter*, 2008, **4**, 9, 1796.
91. M. Yamada, M. Kondo, J.I. Mamiya, Y.L. Yu, M. Kinoshita, C.J. Barrett and T. Ikeda, *Angewandte Chemie International Edition*, 2008, **47**, 27, 4986.
92. M. Yamada, M. Kondo, R. Miyasato, Y. Naka, J. Mamiya, M. Kinoshita, A. Shishido, Y.L. Yu, C.J. Barrett and T. Ikeda, *Journal of Materials Chemistry*, 2009, **19**, 1, 60.
93. Y.L. Yu, M. Nakano and T. Ikeda, *Nature*, 2003, **425**, 6954, 145.
94. M. Nakano, Y.L. Yu, A. Shishido, O. Tsutsumi, A. Kanazawa, T. Shiono and T. Ikeda, *Molecular Crystals and Liquid Crystals Science and Technology*, 2003, **398**, 1.
95. H. Finkelmann, E. Nishikawa, G.G. Pereira and M. Warner, *Physical Review Letters*, 2001, **87**, 1.
96. J. Cviklinski, A.R. Tajbakhsh and E.M. Terentjev, *The European Physical Journal E*, 2002, **9**, 5, 427.
97. A. Lendlein, H.Y. Jiang, O. Junger and R. Langer, *Nature*, 2005, **434**, 7035, 879.
98. R.V. Beblo and L.M. Weiland, *Journal of Applied Mechanics: Transactions of the A SME*, 2009, **76**, 1.

99. T.F. Scott, A.D. Schneider, W.D. Cook and C.N. Bowman, *Science*, 2005, **308**, 5728, 1615.
100. K.N. Long, T.F. Scott, H.J. Qi, C.N. Bowman and M.L. Dunn, *Journal of the Mechanics and Physics of Solids*, 2009, **57**, 7, 1103.
101. F.D. Jochum and P. Theato, *Polymer*, 2009, **50**, 14, 3079.
102. M. Kamenjicki, I.K. Lednev and S.A. Asher, *The Journal of Physical Chemistry B*, 2004, **108**, 34, 12637.
103. M. Kamenjicki and S.A. Asher, *Macromolecules*, 2004, **37**, 22, 8293.
104. J.F. Mano, *Advanced Engineering Materials*, 2008, **10**, 6, 515.
105. K. Sumaru, M. Kameda, T. Kanamori and T. Shinbo, *Macromolecules*, 2004, **37**, 21, 7854.
106. A. Garcia, M. Marquez, T. Cai, R. Rosario, Z.B. Hu, D. Gust, M. Hayes, S.A. Vail and C.D. Park, *Langmuir*, 2007, **23**, 1, 224.
107. R. Akashi, H. Tsutsui and A. Komura, *Advanced Materials*, 2002, **14**, 24, 1808.
108. A. Suzuki and T. Tanaka, *Nature*, 1990, **346**, 6282, 345.
109. S. Conti, M. Lenz and M. Rumpf, *Journal of the Mechanics and Physics of Solids*, 2007, **55**, 7, 1462.
110. A.M. Schmidt, *Macromolecular Rapid Communications*, 2006, **27**, 14, 1168.
111. G. Filipcsei, I. Csetneki, A. Szilagyí and M. Zrinyi, *Advanced Polymer Science*, 2007, **206**, 137.
112. M. Zrinyi, D. Szabo and H.G. Kilian, *Polymer Gels and Networks*, 1998, **6**, 6, 441.
113. B. Yang, W.M. Huang, C. Li and L. Li, *Polymer*, 2006, **47**, 4, 1348.
114. H.B. Lv, J.S. Leng, Y.J. Liu and S.Y. Du, *Advanced Engineering Materials*, 2008, **10**, 6, 592.
115. S.J. Chen, J.L. Hu, S.G. Chen and C.L. Zhang, *Smart Materials and Structures*, 2011, **20**, 6.

116. S.J. Chen, J.L. Hu and H.T. Zhuo, *Journal of Materials Science*, 2011, **46**, 20, 6581.
117. S.J. Chen, J.L. Hu, H.T. Zhuo and S.G. Chen, *Journal of Materials Science*, 2011, **46**, 15, 5294.
118. H.B. Lu, Y.J. Liu, J.S. Leng and S.Y. Du, *Smart Materials and Structures*, 2009, **18**, 8.
119. M.C. Chen, H.W. Tsai, Y. Chang, W.Y. Lai, F.L. Mi, C.T. Liu, H.S. Wong and H.W. Sung, *Biomacromolecules*, 2007, **8**, 9, 2774.
120. Y.C. Jung, H.H. So and J.W. Cho, *Journal of Macromolecular Science, Part B: Physics*, 2006, **45**, 4, 453.
121. J.W. Cho, J.W. Kim, Y.C. Jung and N. Goo, *Macromolecular Rapid Communications*, 2005, **26**, 5, 412.
122. J.S. Leng, X. Lan, Y.J. Liu and S.Y. Du, *Smart Materials and Structures*, 2009, **18**, 7.
123. J.S. Leng, H.B. Lv, Y.J. Liu and S.Y. Du, *Applied Physics Letters*, 2007, **91**, 14.
124. X. Lan, W.M. Huang, N. Liu, S.Y. Phee, J.S. Leng and S.Y. Du, *Electroactive Polymer Actuators and Devices (EAPAD) 2008*, 2008, **6927**.
125. N.G. Sahoo, Y.C. Jung, H.J. Yoo and J.W. Cho, *Composites Science and Technology*, 2007, **67**, 9, 1920.
126. N.G. Sahoo, Y.C. Jung, N.S. Goo and J.W. Cho, *Macromolecular Materials and Engineering*, 2005, **290**, 11, 1049.

# 6 Modelling of Shape-memory Polymers

## 6.1 Introduction

Specifically, modelling can be used for the molecular design, shape-memory programming, and prediction of shape-memory responses of shape-memory polymers (SMP) under different application conditions. Modelling can also be used to analyse the device structure and improve the practicality of engineering of the SMP. Significant progress has been made in the past decade from simple predictions of deformation, stress–strain relationships, shape-memory processes and stress relaxation under different constrained conditions to structural analyses at different levels using various methods [1].

With regard to theoretical modelling, thermally sensitive SMP have dominated most of the research efforts over the past decade. Up to now, modelling of thermally sensitive SMP has covered: structural analyses; macroscale, mesoscale and microscale models; molecular dynamic simulations; quantum-chemical calculations in 1–3 dimensions and in small-to-large deformation. Through modelling, several shape-memory phenomena can be predicted and verified, such as stress–strain responses under isothermal and non-isothermal conditions and shape-memory effects with or without constraints, as well as their dependence upon temperature, time, and applied strain rates. More importantly, modelling can help us to understand the mechanisms and principles that cause various changes.

Modelling fields have great variety, e.g., from modelling reactions, physical properties, and microstructure to modelling hydrogen-bonding interactions, and mechanical properties. Modelling methods also show great diversity: mathematical models, molecular simulations, quantum chemistry modelling, and mechanical models. There are many simulation methods, such as molecular dynamics (MD) [1–5] and Monte Carlo (MC) methods [6–9] at the atomistic level, dissipative particle dynamics (DPD) [10] at the mesoscopic scale, and the finite element method (FEM) [11] at the macroscopic scale. Simultaneously, some programme scripts have been developed for special modelling requirements, such as mathematical modelling [12–15]. Using atomistic simulation tools (i.e., MD and MC) we can analyse the molecular structure and dynamic behaviour of molecules. DPD can predict more realistic structures on

a mesoscopic scale and reflect the mixture process between  $\geq 2$  polymers. The FEM can capture the material properties and deformation process without having detailed information of the chemical structure. In the FEM, the entire structural domain can be divided in many small subdomains represented by a set of element equations. These equations are combined systematically into a global system of equations and subsequently solved by suitable numerical methods. This chapter focuses on the several efficient and advanced modelling approaches used for the predictions of different properties of SMP and understanding shape-memory mechanisms.

## 6.2 Macroscale Constitutive Modelling

Based on the thermodynamic concepts of entropy and internal energy, it is possible to interpret the thermo-mechanical behaviour of SMP from a macroscopic viewpoint without explicitly incorporating details of their molecular interactions. Thus, constitutive modelling is a simplified phenomenological approach to model the temperature-dependent shape-memory behaviour of a viscoelastic polymer. Models based on linear viscoelasticity are usually employed to describe the rate-dependent behaviour of a polymer at the macroscopic level.

Polymer materials exhibit viscoelastic properties of a viscoelastic material, with the elastic properties of a solid. They adhere to Hooke's law and as a viscous liquid as specified by Newton's law [16]. The behaviour of stress relaxation in such materials can be described using mechanical models, such as the basic model of a spring and dashpot. The spring should be visualised as an element representing the elastic properties of the polymer according to Hooke's law. The dashpot is the viscous component of the deformation, which is not completely recoverable and is time-dependent (Figure 6.1). A 'Hookean' spring is described as:

$$\sigma_s = E\varepsilon_s \tag{6.1}$$

where  $\sigma_s$  and  $\varepsilon_s$  are the stress and strain (which are analogous to the force and displacement of the spring) and the spring constant  $\kappa$  is analogous to the elastic modulus  $E$ ;  $E$  has the unit of  $\text{N/m}^2$ . The spring model represents the instantaneous elastic response of the material, which is completely recoverable.

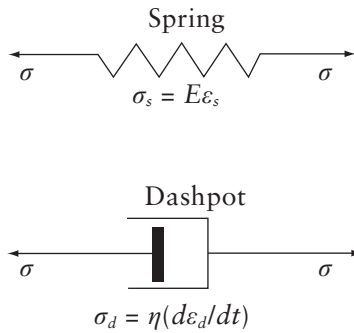


Figure 6.1 Spring and dashpot model to describe stress relaxation in polymers (schematic)

The behaviour of the viscous component (i.e., dashpot) is described by Newton's law as:

$$\sigma_d = \eta \bar{\epsilon}_d \quad (6.2)$$

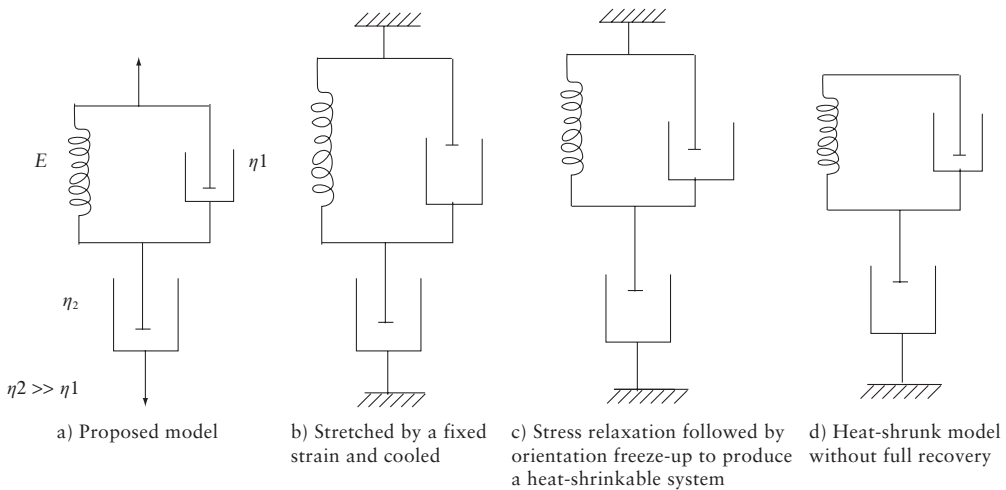
where  $\sigma_d$  and  $\bar{\epsilon}_d = \frac{d\epsilon_d}{dt}$ , are the stress and strain rate in the dashpot respectively, and  $\eta$  is the coefficient of viscosity with units of N-s/m<sup>2</sup>. The ratio of the coefficient of viscosity to stiffness is a useful measure of the response time of the viscoelastic response of the material; this is denoted as:

$$\tau = \frac{\eta}{E} \quad (6.3)$$

The unit of  $\tau$  is seconds, and this ratio is also called as the 'relaxation time'. This ratio helps to determine the viscoelastic response of the material, indicating the time needed to move from the old (unrelaxed) to the new equilibrium (relaxed) state of the material. One can make several variations of the basic models (e.g., Maxwell, Kelvin, standard linear solid) using different combinations of these basic elements to predict the characteristics of the complex deformation of SMP [16, 17].

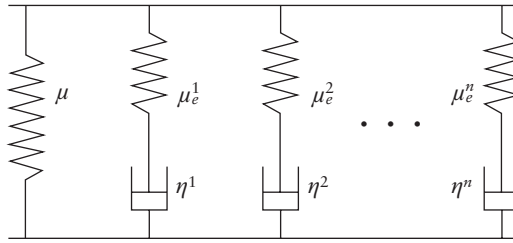
**6.2.1 Stress–strain Characteristics**

A thermo-viscoelastic model for melting temperature ( $T_m$ )-type SMP was first developed by Morshedian and co-workers [17]. They proposed a mechanical model to describe the stress–strain–time behaviour of a shape-memory crosslinked polyethylene (PE) under isothermal conditions. The stress–strain, stress relaxation and irrecoverable strain behaviours of the model were established by deriving the constitutive equation. Their mechanical model was based on a combination of a Voigt unit (the spring,  $E$ , and the dashpot,  $\eta_1$ , in parallel) and a dashpot unit,  $\eta_2$ , in series  $\eta_2 \gg \eta_1$  (Figure 6.2a). They predicted the time-dependent recovery behaviour of heat-shrinkable products in gaining their original shape under constant temperature conditions. Subsequently, they developed a new method to describe the shape-memory effect (SME) by considering non-isothermal conditions separately from previous parameters [18].



**Figure 6.2** Proposed mechanical model for shape-memory induction and heat recovery. Reproduced with permission from J. Morshedian, H.A. Khonakdar and S. Rasouli, *Macromolecular Theory and Simulations*, 2005, **14**, 7, 428. ©2005, John Wiley & Sons [17]

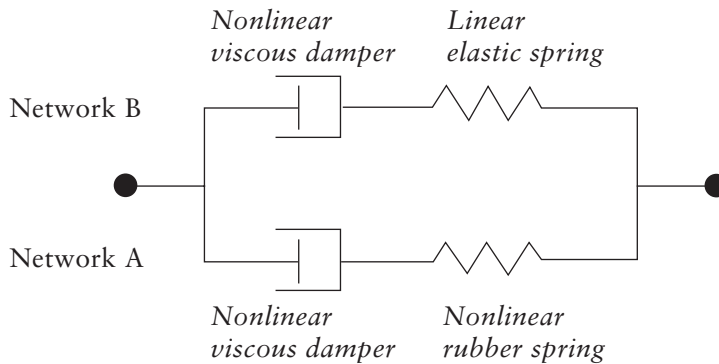
Johlitz and co-workers [19, 20] developed an extended phenomenological continuum mechanics-based model (Figure 6.3) which was thermo-mechanically consistent and could represent the phenomena observed during the experiments.



**Figure 6.3** Rheological model of viscoelasticity with  $j = 1, \dots, n$  Maxwell elements.

Each spring element is of non-linear Neo-Hooke-type. Reproduced with permission from M. Johlitz, H. Steeb, S. Diebels, A. Chatzouridou, J. Batal and W. Possart, *Journal of Materials Science*, 2007, **42**, 23, 9894. ©2007, Springer [19]

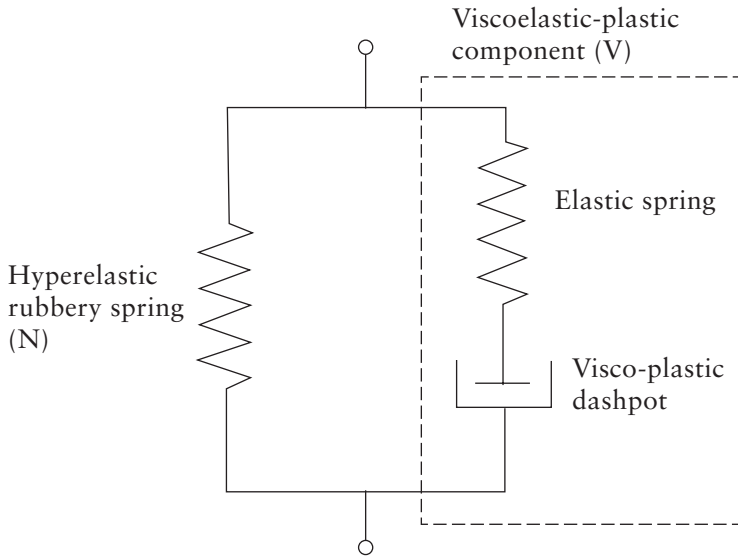
Shim [21] developed a new nonlinear viscoelastic finite strain constitutive model (**Figure 6.4**) based on a rheological model composed of two parallel Maxwell elements. The soft rubbery response is represented by a Gent spring whereas nonlinear viscous evolution equations are proposed to describe the time-dependent material response. The model provides a good prediction of the response under monotonic loading over a wide range of strain rates, but it overestimates stiffness during unloading.



**Figure 6.4** Proposed rheological model composed of two Maxwell elements in parallel to predict stress–strain behaviour. Reproduced with permission from J. Shim and D. Mohr, *International Journal of Plasticity*, 2011, **27**, 6, 868. ©2011, Elsevier [21]



Qi and co-workers [22] presented a constitutive model that captured the major features of stress–strain behaviour, including nonlinear hyperelastic behaviour, time dependence, hysteresis, and softening (Figure 6.5). The constitutive model splits material behaviour into a rate-independent equilibrium part and rate-dependent viscoelastic-plastic part. Amirkhizi and co-workers [23] produced a complete temperature-, pressure- and strain-rate-dependent nonlinearly viscoelastic constitutive model for the viscoelastic response under various conditions.



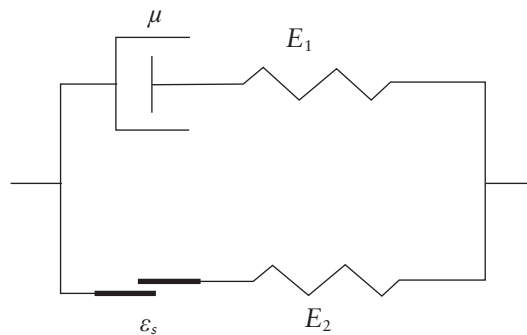
**Figure 6.5** One-dimensional schematic of the constitutive model. Reproduced with permission from H.J. Qi and M.C. Boyce, *Mechanics of Materials*, 2005, 37, 8, 817. ©2005, Elsevier [22]

Ask and co-workers 2010 [24] developed a finite deformation electro-viscoelastic material model for electrostrictive polyurethane (PU) elastomers that fits into nonlinear finite element formulations. The model captures electro-viscoelastic effects and also fits into iterative finite element formulations to simulate general boundary-value problems.

### 6.2.2 Shape-memory Properties

Early thermo-viscoelastic treatments of glass transition temperature ( $T_g$ )-type SMP

applied small, one-dimensional deformations ( $\leq \pm 10\%$  nominal strain) and rheological models with temperature-dependent parameters of viscosity and modulus. The initial method was a parallel combination of the Prandl (thixotropic) and Maxwell (rheopectic) models (Figure 6.6) used by Tobushi and co-workers [25]. The model involved a slip element due to internal friction, and took account of thermal expansion. A nonlinear thermo-mechanical constitutive model was developed in their later work [26] by extending the linear model described above in which nonlinear terms of stress were considered for an elastic term and a viscous term in the linear model. These models could capture the characteristic shape-memory behaviour of SMP but had limited prediction capability due to the loss of strain storage and release mechanisms. Buckley and co-workers [27] used the Kohlrausch–Williams–Watts equation for rubbery materials to describe the temperature dependence of the retardation time.



**Figure 6.6** Four-element model.  $E_1$  and  $E_2$  denote linear springs,  $\mu$  is a dashpot, and  $\epsilon_s$  is the creep irrecovery strain. Reproduced with permission from H. Tobushi, T. Hashimoto, S. Hayashi and E. Yamada, *Journal of Intelligent Material Systems and Structures*, 1997, 8, 8, 711. ©1997, SAGE Publications [25]

Based on thermodynamic considerations and motivated by a mechanical understanding of the stress–strain–temperature behaviours of SMP, Diani and co-workers [28] proposed a three-dimensional (3D) thermo-viscoelastic model in the context of finite strain to represent the thermo-mechanical behaviour of SMP (Figure 6.7). The model accurately estimated the remaining strain during stress release, and provided a reasonable prediction of the stress–temperature curves during the constrained thermo-mechanical recovery of SMP.

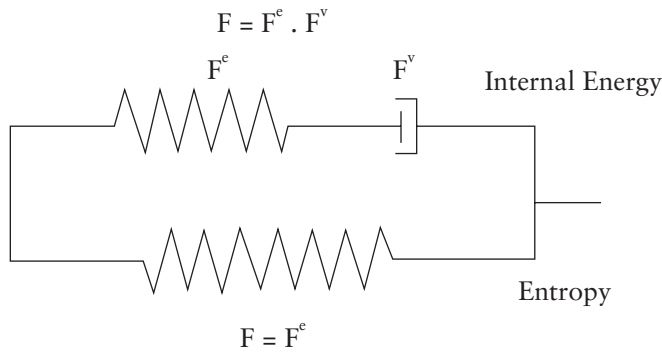


Figure 6.7 Model rheological scheme. Reproduced with permission from J. Diani, Y P. Liu and K. Gall, *Polymer Engineering & Science*, 2006, 46, 4, 486. ©2006, John Wiley & Sons [28]

Wong and co-workers [29] derived a one-dimensional constitutive model that comprises an elastic spring element in series with a rubber network and viscoplastic dashpot elements arranged in parallel to describe shape-memory behaviour. Stress-strain behaviours during deformation, isothermal recovery and recovery at a constant heating rate were investigated using a set of model constants. In addition, Heuchel and co-workers [30] explored relaxation curves with a modified Maxwell–Weichert model of two Maxwell units and a spring (Figure 6.8), in which stress relaxation produced a combination of a slow and fast decaying process. Westbrook and co-workers [31] developed a constitutive model to describe semi-crystalline polymers that exhibit stretch-induced crystallisation, which describes one-way and two-way SME.

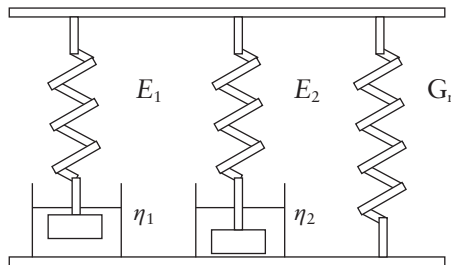
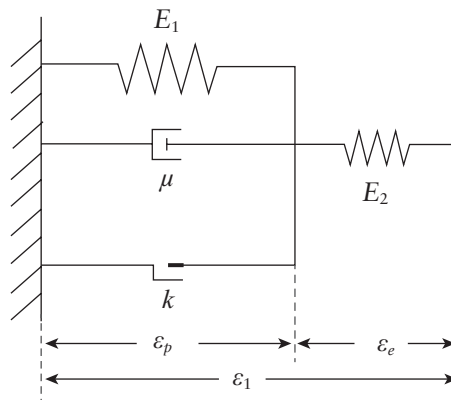


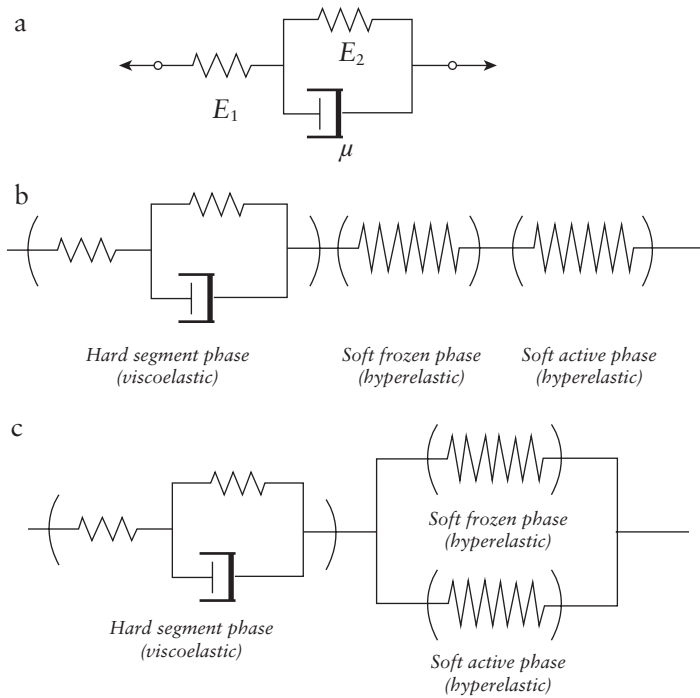
Figure 6.8 Modified Maxwell–Weichert model comprising two Maxwell units and a third spring in parallel. Reproduced with permission from M. Heuchel, J. Cui, K. Kratz, H. Kosmella and A. Lendlein, *Polymer*, 2010, 51, 26, 6212. ©2010, Elsevier [30]

Ghosh and co-workers [32] developed a two-network thermo-mechanical model (Figure 6.9) demonstrating a Helmholtz potential-based approach for the development of constitutive equations. The model can simulate the response of the material during heating and cooling cycles as well as the sensitive dependence of the response on thermal expansion. Li [33] developed a micromechanical multi-scale-viscoplastic theory involving cyclic hardening and stress recovery responses. The proposed theory takes into account the stress-induced crystallisation process and evolution of the morphological texture based on the applied stresses.



**Figure 6.9** Proposed mechanical model for shape-memory polyurethanes (SMPU). The spring  $E_1$  together with the viscous dashpot  $\mu$  represents the rubbery response of the material. The spring  $E_2$  represents that glassy response and the frictional element  $k$  represents the locking behaviour. Reproduced with permission from P. Ghosh and A.R. Srinivasa, *International Journal of Engineering Science*, 2011, 49, 9, 823. ©2011, Elsevier [32]

Kim [34] developed three-phase phenomenological models (Figure 6.10) featuring two phases in the soft segment (active and frozen) and one in the hard segment. The stress and strain relationships of each phase are described mathematically using one three-element viscoelastic and two Mooney–Rivlin hyperelastic equations, respectively. The total stress is calculated by combining the equations *via* certain internal variables.

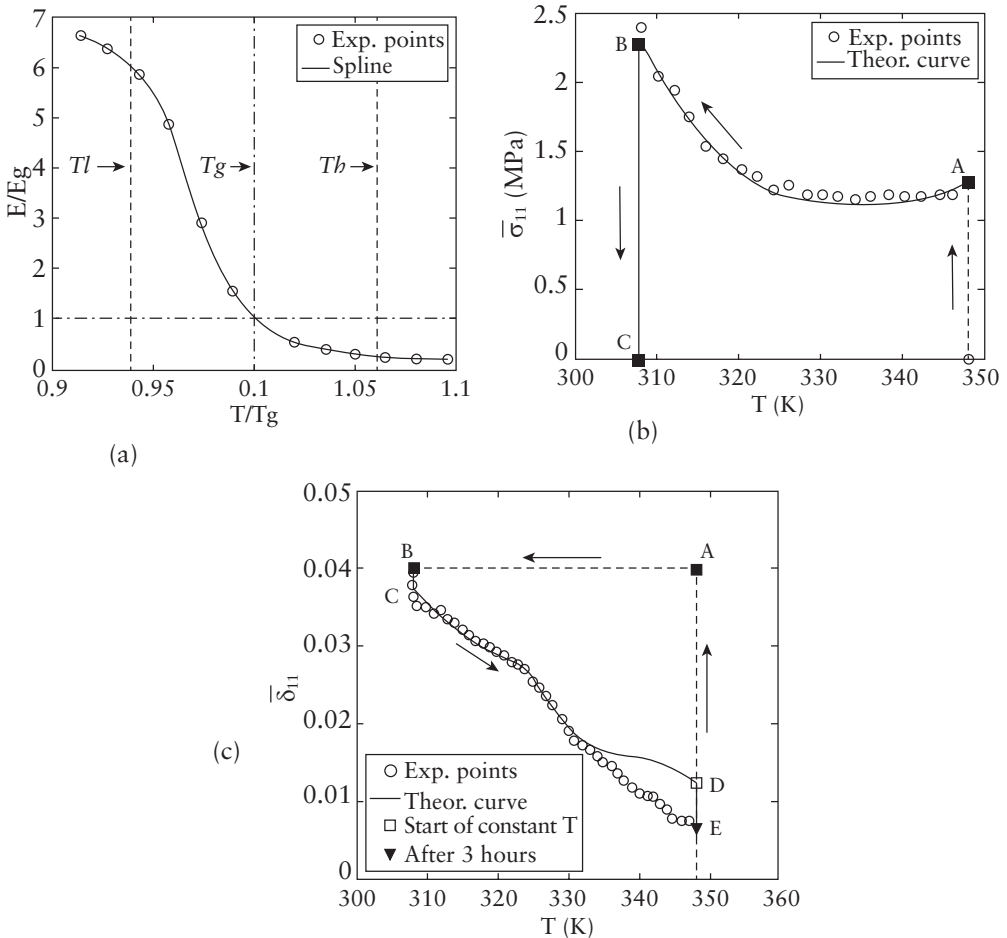


**Figure 6.10** Phenomenological models of the soft and hard segments of SMPU: (a) three-element viscoelastic, (b) series and (c) parallel models. Reproduced with permission from J.H. Kim, T.J. Kang and W-R. Yu, *International Journal of Plasticity*, 2010, 26, 2, 204. ©2010, Elsevier [34]

### 6.3 Mesoscale Modelling

Kafka [35] took a different approach from the researchers discussed above. He applied a ‘meso-mechanical’ approach to study SMP. His model considered an SMP composed of two different continuous sub-structural components: a resistant component that maintains elasticity with a constant Young’s modulus, and a compliant component that deforms in a time/temperature-dependent elastic-plastic-viscous manner. The internal variables (which describe the mechanical properties as well as the volume fractions of the two substructures) are estimated on the basis of experimental data and an approximation scheme. He predicted the complete response of a SMP in a thermo-mechanical test cycle using the model and found a good fit between experimental and theoretical results (Figure 6.11). The model was demonstrated in a small-strain shape-memory system, but the concept appeared promising for future applications to

large-strain systems. The mesoscale model can help us to understand the mechanisms at a detailed level.



**Figure 6.11** (a) Change in the macroscopic Young's modulus with temperature: continuous representation with the use of a 'spline' function; (b) experimental and theoretical representation of the changes of macroscopic stress with decreasing temperature at fixed strain; and (c) experimental and theoretical representation of the decrease in macroscopic strain due to unloading and temperature increase. Reproduced with permission from V. Kafka, *International Journal of Plasticity*, 2008, 24, 9, 1533. ©2008, Elsevier [35]

Another mesoscale model that accounts for a nonlinear material response and contains a phenomenological 3D formulation for  $T_g$ -activated SMP (Figure 6.12) was developed by Liu and co-workers [36]. It is suitable for small deformations under uniaxial loading conditions. This model additively decomposes the strain into its thermal, elastic and stored components, and utilises two internal variables (frozen volume fraction and stored strain) to describe the evolution of the microstructure. The model assumes that the deformation in the material is ‘frozen’ and thus contributes to the term accounting for the stored strain. This work develops a constitutive theory at the continuum level, which includes internal variables to describe the evolution of the microstructures of SMP. It can be argued that the model treats SMP as a special elastic problem without consideration of time dependence, but it captures the essential shape-memory responses to temperature events.

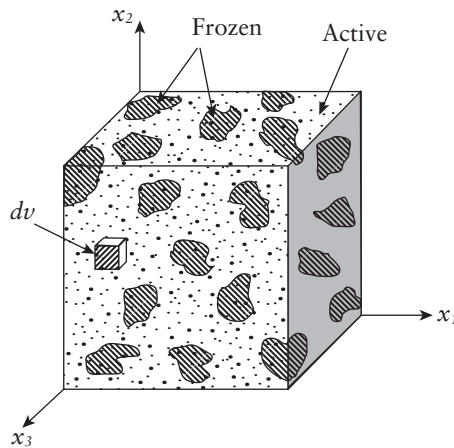
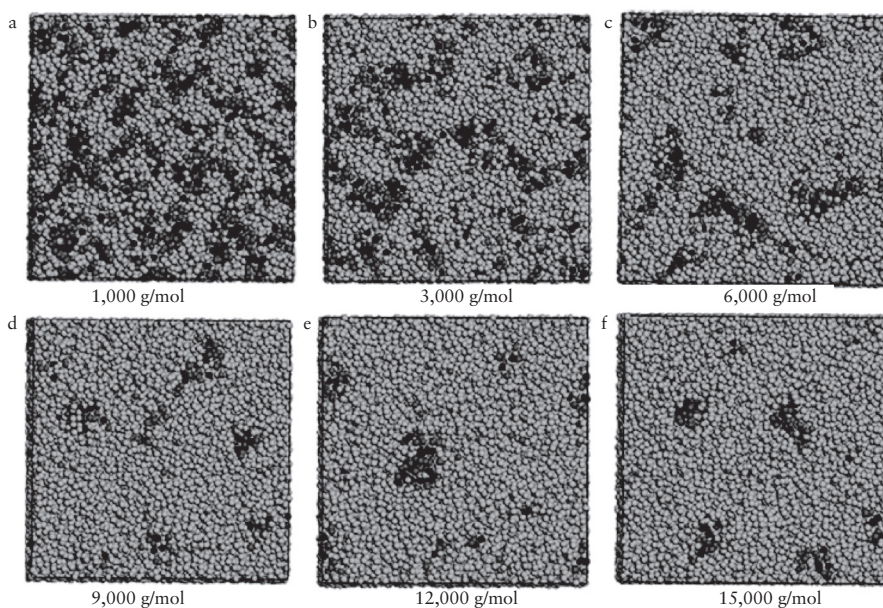


Figure 6.12 Micromechanical foundation of 3D SMP (schematic). Reproduced with permission from Y.P. Liu, K. Gall, M.L. Dunn, A.R. Greenberg and J. Diani, *International Journal of Plasticity*, 2006, 22, 2, 279. ©2006, Elsevier [36]

Following the approach of Liu and co-workers [36], Chen and Lagoudas [37] developed a relationship for the time-dependent averaged deformation gradient as a function of the stress state. The constitutive equation proposed by this model includes terms that account for the deformation in each of the active and frozen phases of the material. The volume of the material in each phase is defined by a frozen volume fraction. Deformation of the material in the frozen phase is presented through a multiplicative

decomposition of the deformation gradient, which describes the deformation stored during cooling and the deformation gradient of the material when deformed in a low-temperature reference configuration. The deformation gradients are assumed to be functions of the first Piola–Kirchhoff stress and the absolute temperature. This model was linearised further, and small deformation data from an epoxy SMP used to calibrate the model and analyse its validity [38]. Recently, Volk and co-workers [39] focused on the calibration and validation of a finite deformation constitutive model.

Yildirim and co-workers [10] used DPD simulation to investigate the microphase separation and morphology of segmented silicone-urea copolymers. The phase-separated morphology was observed with decreasing urea phase (dark grey) and *bis*(4-methylcyclohexyl) methane (black) as the molecular weight of the polydimethyl siloxane (PDMS) segments (grey) increased (Figure 6.13).



**Figure 6.13** Microphase morphologies of silicone-urea copolymers as a function of urea hard segment content obtained by bead representation using dissipative particle dynamic calculations. PDMS segments are shown in grey, urea segments in dark-grey and *bis*(4-methylcyclohexyl) methane groups are in black. Reproduced with permission from E. Yildirim, M. Yurtsever, E. Yurtsever, I. Yilgor and E. Yilgor, *Journal of Inorganic and Organometallic Polymers and Materials*, 2012, 22, 3, 604. ©2012, Springer [10]



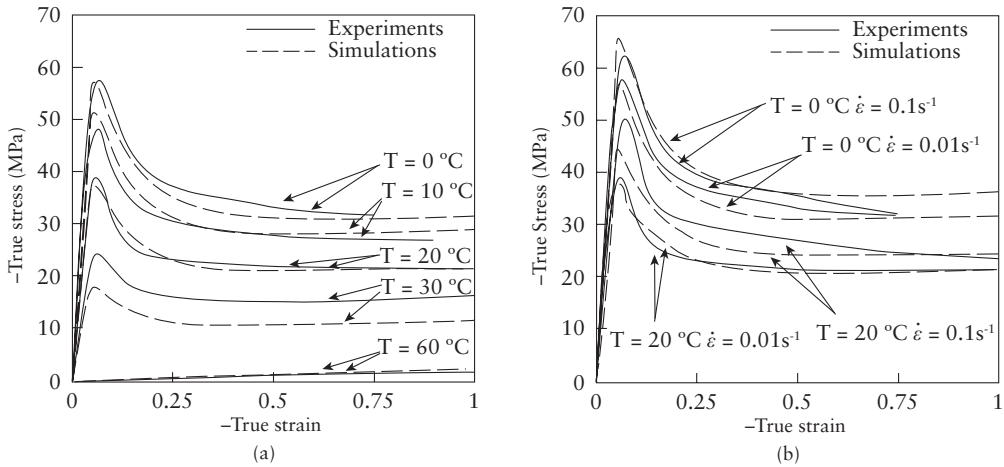
## 6.4 Microscale Modelling

Macroscopic and mesoscopic modelling cannot provide sufficient information about the parameters directly linked to the microstructure of a material. The micromechanical concept presented in the following section is motivated by the need to work with parameters that are physically interpretable and can provide a deeper understanding of the mechanisms operating in SME.

Based on their work on the modelling of polymer crystallisation, Rao [40] developed a 3D constitutive model for  $T_m$ -type SMP. This modelling consisted of four components to describe the rubbery phase, semi-crystalline phase, crystallisation process, and melting process. A multiple natural framework was employed to model the shape-memory response in  $T_m$ -activated SMP. Within this framework, the amorphous and crystalline components of the SMP have their own natural configurations (stress-free states). For the amorphous phase (which is regarded as an entropic rubber), the stress-free state would be the under-formed state that corresponds to maximum entropy. For the crystalline phase, it is assumed that all crystals are formed in a stress-free state. The tendency of each phase to return to its natural configuration represents the basis of the shape-memory behaviour in this approach. The model was applied to qualitatively represent typical shape-memory cycles under uniaxial deformation and circular shear, and could capture most of the features exhibited by  $T_m$ -type SMP. This model predicted a strain increase during cooling under constant tensile stress (cooling-induced elongation), which is a counter-intuitive phenomenon. This predicted behaviour was observed experimentally by others and utilised for two-way SME [41]. In their later work, Barot and co-workers [42] extended the model to fit a full thermodynamic framework and derived constitutive equations that are invariant in their description of mechanical stress and strain (e.g., multiaxial and uniaxial). These models are fully 3D and fulfil general physical requirements such as frame invariance and the second law of thermodynamics. However, their application requires the solution of advanced numerical problems.

In addition, Qi and co-workers [43] developed a 3D finite deformation constitutive model for the thermo-mechanical behaviours of SMP using a phase-transition approach. They considered three distinct phases: the rubbery phase; the initial glassy phase presented in the undeformed configuration at the beginning of the analysis; and the frozen glassy phase that is newly formed during cooling. These phases were assumed to deform in parallel, and the rule of mixtures was used to calculate the stress response of SMP from those of the individual phases. A phenomenological relationship was developed for the rate-independent temperature evolution of the volume fraction of each phase. For the case with thermal cooling/heating, the model captured the SME and shape recovery. **Figure 6.14** shows a comparison of the results from numerical simulations and experiments of isothermal uniaxial compressions

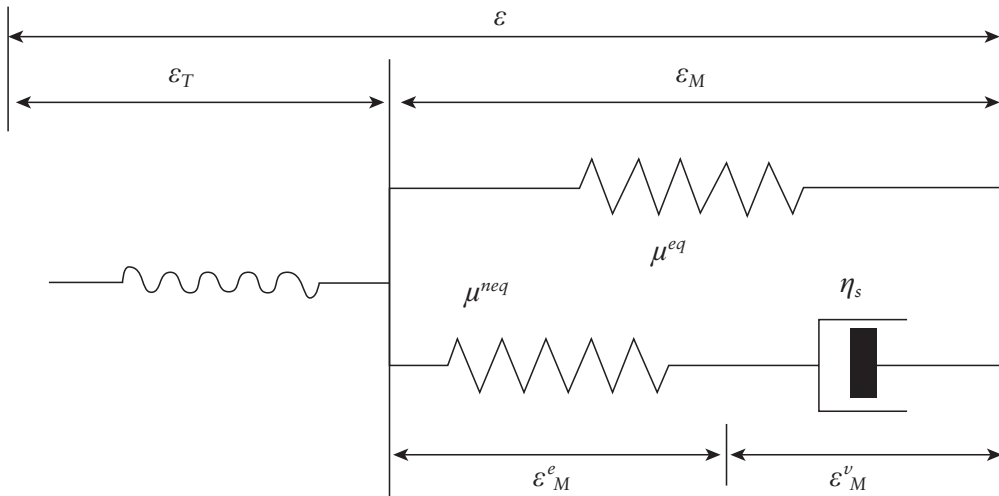
at different temperatures and strain rates. However, the model could not capture the hysteresis in the stress–temperature response observed in constrained recovery experiments.



**Figure 6.14** Numerical simulations of stress–strain behaviour of SMP from isothermal uniaxial compressions: (a) at different temperatures, and (b) at different strain rates. Reproduced with permission from H.J. Qi, T.D. Nguyen, F. Castroa, C.M. Yakacki and R. ShandaSa, *Journal of the Mechanics and Physics of Solids*, 2008, 56, 5, 1730. ©2008, Elsevier [43]

A different concept that attributed SME to structural and stress relaxation was presented by Nguyen and co-workers [44] (**Figure 6.15**). They investigated shape-memory behaviour through a structural and stress relaxation mechanism. They proposed that the shape-memory phenomena of SMP were motivated primarily by a dramatic change in molecular-chain mobility induced by the glass transition. Chain mobility underpins the ability of the chain segments to rearrange locally and equilibrate the macromolecular structure and stress response. The model could predict the key features of the stress hysteresis of a constrained recovery response, including the peak stress and associated temperature. The important feature of this approach is that it reasonably and physically interprets the underlying mechanism for SME, and the time-dependence behaviour of the shape-memory can be reproduced. However, utilisation of the model requires incorporation of several other sophisticated models, which not only complicates the entire constitutive model but also requires

additional fundamental assumptions. Some of these hypotheses, such as the parameter of activation of free energy in Adams–Gibbs modelling (which was considered to be invariant with temperature and pressure) are controversial [45, 46].



**Figure 6.15** Rheological representation of the constitutive model for covalently crosslinked amorphous networks. Reproduced with permission from T.D. Nguyen, H.J. Qi, F. Castro and K.N. Long, *Journal of the Mechanics and Physics of Solids*, 2008, 56, 9, 2792. ©2008, Elsevier [44]

Recently, Li and Xu [47] adopted Nguyen’s concept [44] and developed a finite deformation theory and a mechanism based thermo-viscoelastic constitutive model to predict the nonlinear shape-memory behaviour of an SMP trained below its  $T_g$ . This study validated programming by cold-compression as a viable alternative for thermally responsive thermoset SMP. Chen and Nguyen [48] investigated the influence of material properties and loading conditions on the recovery performance of  $T_g$ -type SMP using the above-developed thermo-viscoelastic model [44]. A parameter study was developed to investigate the relationship between the thermo-mechanical material properties and loading conditions during programming, recovery of the unconstrained strain recovery response, and the constrained recovery stress response of  $T_g$ -based SMP.

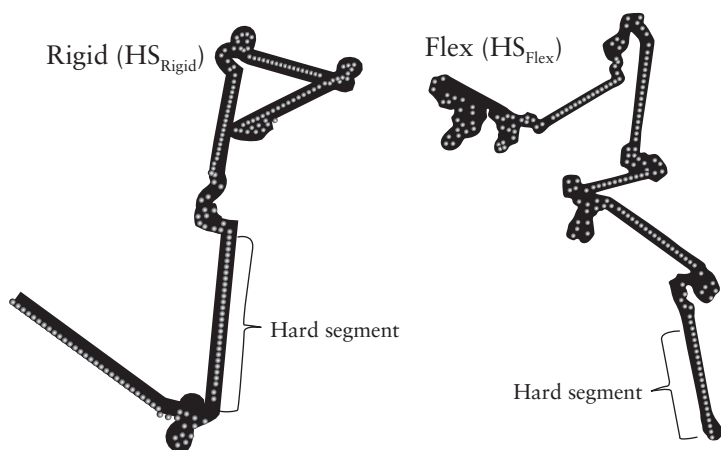
## **6.5 Molecular Dynamics and Monte Carlo Simulations**

### **6.5.1 Reaction Characteristics**

In reaction modelling, MC simulations are used to obtain the velocity, concentration, temperature, viscosity, and pressure profiles, as well as reaction mechanisms, reactive processes, and rate constants. Such simulations are dependent largely upon random sampling to obtain numerical results using computational methods. Speckhard and co-workers [6, 49] developed a MC simulation utilising several simplifying assumptions proposed by Peebles [7] to describe the effects of various reaction parameters on the composition and molecular-weight distributions of PU block copolymers. Commonly used assumptions in the literature were proposed by Peebles [7]: an irreversible reaction between hydroxyl-isocyanate, independent reactivity of different isocyanate groups, identical reactivity for each hydroxyl group, and no side reaction or other reaction. Later, Speckhard and co-workers [8] developed three models to predict the molecular weight, composition and hard-segment length distributions of PU block copolymers. Dubois and co-workers [9] obtained the evolutive rheological behaviour of a PU reactive mixture and molecular-weight distribution from stochastic simulations.

### **6.5.2 Physical Properties**

The method used by Sun [50], i.e., condensed-phase optimised molecular potentials for atomistic simulation studies (COMPASS), have received much attention for the prediction of: diffusion; mass transfer; structure and structure–physical properties; separation properties; morphology and rate-dependent stress-strain behaviour; cohesive energy density; adsorption; filtration; bending electrostriction. COMPASS is a high-quality force-field method suitable for condensed-phase application, and can be used even if the details at the electron level are not available. Here, the structure is divided into different groups of atoms or molecules in similar chemical environments. Repáková and co-workers 2004 [2] carried out MD simulations to study the structure and structure–physical property relationships. Rahmati and co-workers [51] investigated structural, physical and separation properties by configuration bias grand canonical MC and MD methods. All interactions were modelled using the COMPASS force field [50]. Chantawansri [52] utilised coarse-grained molecular dynamic simulations to elucidate the effects of hard segment content (**Figure 6.16**), intermolecular interaction, and rigidity of the interface between hard and soft segments on local morphology and rate-dependent stress–strain behaviour in the ballistic regime.



**Figure 6.16** Representative CG chains of PUU for flexed and rigid models. CG: Coarse-grained molecular; HS: hard segment; and PUU: polyurethane urea.

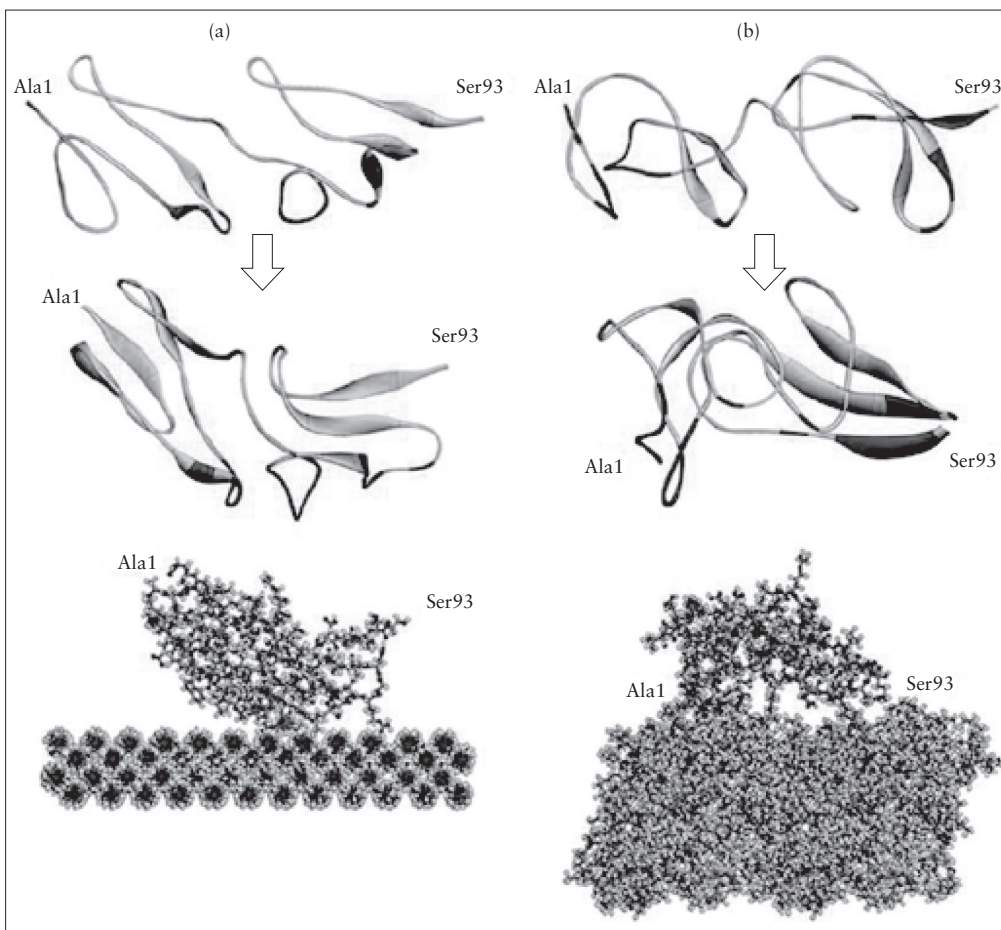
Reproduced with permission from T.L. Chantawansri, Y.R. Sliozberg, J.W. Andzelm and A.J. Hsieh, *Polymer*, 2012, 53, 20, 4512. ©2012, Elsevier [52]

Zhou and co-workers [1] used MD simulations to study the diffusivity of water at low concentrations. The canonical (i.e., composition, volume and temperature remain constant) and isothermal-isobaric (i.e., pressure and temperature remain constant) ensembles were used to mimic non-swollen and swollen behaviour, respectively. Raghu and co-workers [3] undertook MD simulations to estimate the cohesive energy density and solubility parameter values using the COMPASS [50] force field. Panos and co-workers [4] studied the mechanisms for fibronectin adsorption (Figure 6.17) using molecular mechanics and molecular dynamic simulations with the COMPASS force field [50].

### 6.5.3 Microstructure

For the modelling of microstructure, molecular simulation methods (MD and MC) were used to predict the localised rotations and phase information of SMP. McKiernan [5] investigated lamellar crystals using MD simulations with the consistent-valence force field, and the localised rotations at the termini of the ester-amide coupled units were predicted. Periodic boundary conditions, with bonds across the boundaries in the chain direction, were used in these dynamic simulations. Tao and co-workers [53] utilised a combination of a molecular simulation method and MC to calculate the phase diagrams of model PU. In their model, the entropic contribution of the Flory–

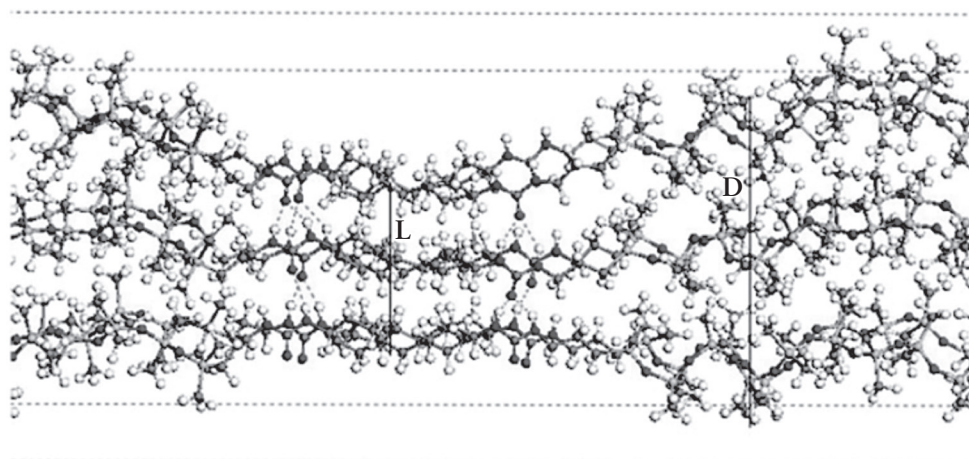
Huggins expression was modified to incorporate the contribution arising from the orientation of hard segments. Miller and co-workers [54] developed a MC simulation to explore the potential effects of premature phase separation on the composition, molecular weight, and hard segment-length distributions of PU block copolymers.



**Figure 6.17** Conformational changes in fibronectin upon adsorption on (a) polyethylene glycol-1,6-hexamethylene diisocyanate (HDI) and (b) castor oil-HDI surfaces: From top to bottom: secondary structure before adsorption, secondary structure after adsorption, atomistic detail on the polymer surface (explicit water molecules are not shown for clarity). Reproduced with permission from M. Panos, T.Z. Sen and M.G. Ahunbay, *Langmuir*, 2012, 28, 34, 12619. ©2012, American Chemical Society [4]

### 6.5.4 Hydrogen bonding Interactions

Yildirim and co-workers [10] used MD simulation methods to investigate the effect of hydrogen bonding on the microphase separation, morphology and various physicochemical properties of segmented silicone-urea copolymers using the COMPASS force field [50] (Figure 6.18). Yang and co-workers [55] investigated the crystallisation mechanism which contains hydrogen-bond units using the MD simulation with the Dreiding force field concept [56]. Zhang and co-workers [57] investigated hydrogen bonding among hard-hard segments and hard-soft segments in a shape-memory PU using the density functional theory. This method gave good structures, reasonable Mulliken charges, binding energies, dipole moments, and good infrared-spectra trends for the prediction of hydrogen bonding. Most of the carbonyl oxygen atoms in PU exist in a hydrogen-bonded form, which enhances the phase separation of the shape-memory PU. Recently, Zhang and co-workers [58] examined hydrogen-bonding interactions by comparing radical distribution functions [59] between carbonyl oxygen atoms or ester oxygen atoms or nitrogen atoms and hydrogen atoms on N-H using fully atomistic MD simulations.



**Figure 6.18** Aggregation of the hard segments in the model as a result of hydrogen bonding. Reproduced with permission from E. Yildirim, M. Yurtsever, E. Yurtsever, I. Yilgor and E. Yilgor, *Journal of Inorganic and Organometallic Polymers and Materials*, 2012, **22**, 3, 604. ©2012, Springer [10]



### 6.5.5 Mechanical Properties

Madkour and co-workers [60] used MD simulations with the COMPASS force field [50] and assigned charges and the Ewald summation method to examine the influence of chain self-assembly on the stress–strain behaviour of thermoplastic polyurethane (TPU) systems (Figure 6.19). MD simulations of SMP were undertaken by Diani and Gall. They investigated the shape-memory behaviour and mechanical properties above and below the  $T_g$  of polyisoprene. A virtual polyisoprene was constructed and subjected to thermo-mechanical cycles of uniaxial stretching and hydrostatic compression. Large strains and pure hydrostatic loadings at high temperatures produced changes in internal energy, leading to an energy state that required mechanical constraints and which could not be retained by applying thermal treatment alone. Those studies shed light on the fundamental mechanisms that drive shape memory and recovery in amorphous polymers, which can help us to understand the mechanisms at the microcosmic level.

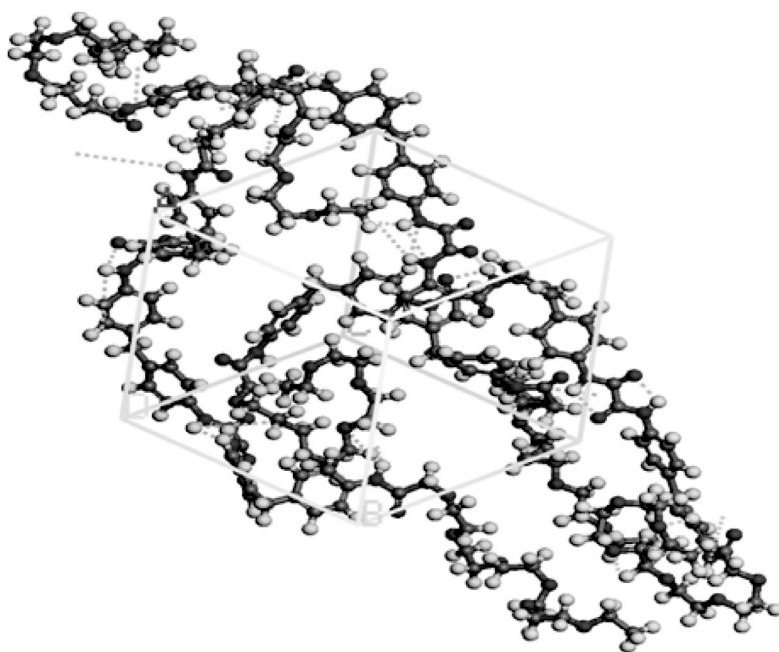


Figure 6.19 Simulated molecular cell of a TPU elastomer having a hard block sequence length of six repeat units (schematic). Reproduced with permission from T.M. Madkour and R.A. Azzam, *European Polymer Journal*, 2013, 49, 2, 439. ©2013, Elsevier [60]



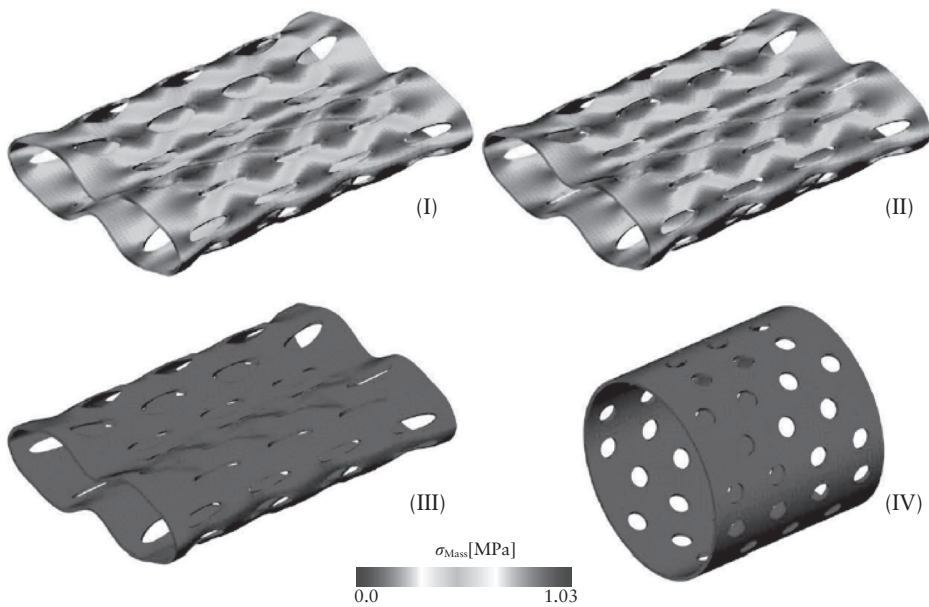
## 6.6 Mathematical Modelling

For prediction of reaction characteristics, Hyun and co-workers [12] used a mathematical model that included the conservation equations of mass, momentum, energy, and chemical species to obtain the velocity, concentration, temperature, viscosity, and pressure profiles of the reactive extrusion process. Duguay and co-workers [13] proposed a mathematical model for elucidating, simulating and distinguishing between various mechanisms of degradation. In 1998, Krol and co-workers [14] developed a mathematical model for a gradual poly addition which followed Flory's assumption and made the reactivities of the oligomers dependent solely on the chemical environment of their functional groups. Eduardo and co-workers [15] developed a mathematical model of the intermediate degree of complexity for kinetics and molecular-weight development in PU production by considering crosslinking and gelation due to allophanate formation. Puaux and co-workers [61] presented a mathematical model based on the linear step growth polymerisation theory to study PU synthesis by reactive extrusion.

For the simulation of physical properties, Arunkumar and co-workers [62] developed a mathematical model to correlate adsorption variables to responses. The response surface methodology was used to optimise the process inputs. Zhou and co-workers [63] studied the mechanism of bending electrostriction through a numerical calculation. Simulations were carried out on a model in which charge carriers were assumed to be electrons injected from the cathode by the Schottky effect, and the positive charges were immobile.

## 6.7 Modelling of Device Structures

Reese and co-workers [64] developed 3D finite element-based simulations that considered a full thermo-mechanical coupling. To establish a close link between the microstructure of the rubber-like material and the theoretical model, they formulated the model in a macromechanical format as well as a micromechanical format. The concept was implemented in the finite element method to investigate complex two- and three-dimensional thermo-mechanical systems (**Figure 6.20**). Finally, they investigated two types of stent structures. Aiming to model the response of thermoset  $T_g$ -type SMP, Srivastava and co-workers [65] adopted a constitutive framework of their former work [66] and developed a thermo-mechanically coupled large-deformation constitutive theory and numerical simulation capability to model the response of thermally actuated SMP. They simulated the shape-recovery response of a stent made from the polymer when it was inserted into an artery (which was modelled to be a compliant elastomeric tube).



**Figure 6.20** Finite element modelling of a stent during a typical thermo-mechanical cycle. Stent I after mechanical loading, II after thermal loading, III after mechanical unloading, and IV after thermal unloading. Reproduced with permission from S. Reese, M. Bol and D. Christ, *Computer Methods in Applied Mechanics and Engineering*, 2010, 199, 21-22, 1276. ©2010, Elsevier [64]

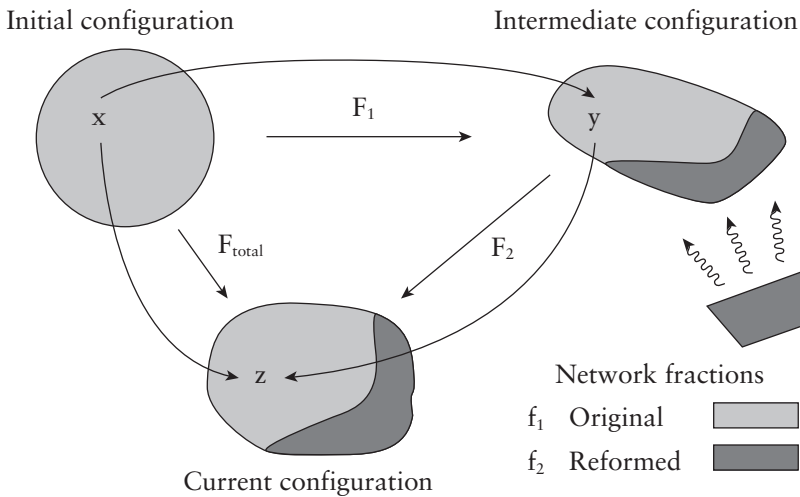
In work by Kim and co-workers [67], the feasibility of developing a temperature-responsive braided stent using an SMPU was studied through finite element analyses. The mechanical behaviour of SMPU fibres was modelled using a constitutive equation describing their one-dimensional, thermally induced shape-memory behaviour. Deployment of the braided stents inside narrowed vessels was simulated to show that the SMPU stents could be implanted comfortably while minimising overpressure on the vessel walls because of their thermo-responsive shape-memory behaviour.

## 6.8 Modelling for Light-sensitive Shape-memory Polymers

### 6.8.1 Three-dimensional Finite Deformation Modelling

The shape-memory process of light-sensitive shape-memory polymers (LSMP) is similar to that of thermally sensitive SMP, but the external stimulus is quite different.

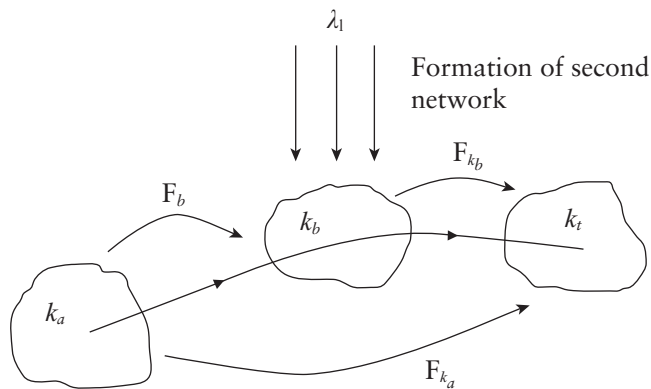
Therefore, most of the models for thermally induced SME are not suitable for light-sensitive SME. In 2009, a 3D finite deformation modelling framework was developed by Long and co-workers [68] to describe the photomechanical response of light-activated polymer systems (Figure 6.21). This framework integrated four coupled phenomena that contribute to the macroscopic photomechanical behaviour: photophysics, photochemistry, chemomechanical coupling, and mechanical deformation. They described this behaviour through decomposition of a crosslinked network into two components: an original network and a photochemically altered network. The modelling framework presented was sufficiently general because it was applicable to light-activated polymer systems that have various operative mechanisms in each of the four areas. By using this approach, they proposed constitutive models for two recently developed light-activated polymer systems [69]. In addition, by using the material developed by Scott and co-workers [69], they validated their model by measuring and numerically simulating photo-induced stress relaxation and bending deformation, and obtained good agreement between measurements and predictions. The model was also used to study the effects of photomechanical parameters and the behaviour of the network evolution rule on material response.



**Figure 6.21** Kinematics of initial, intermediate, and current configurations. The sample, originally at x, is deformed to and held at an intermediate configuration, y. In this intermediate configuration, it is irradiated. After mechanical constraints are released, the sample deforms to the current configuration. Reproduced with permission from K.N. Long, T.F. Scott, H.J. Qi, C.N. Bowman and M.L. Dunn, *Journal of the Mechanics and Physics of Solids*, 2009, 57, 7, 1103. ©2009, Elsevier [68]

### 6.8.2 Multiple Natural Configurations Modelling

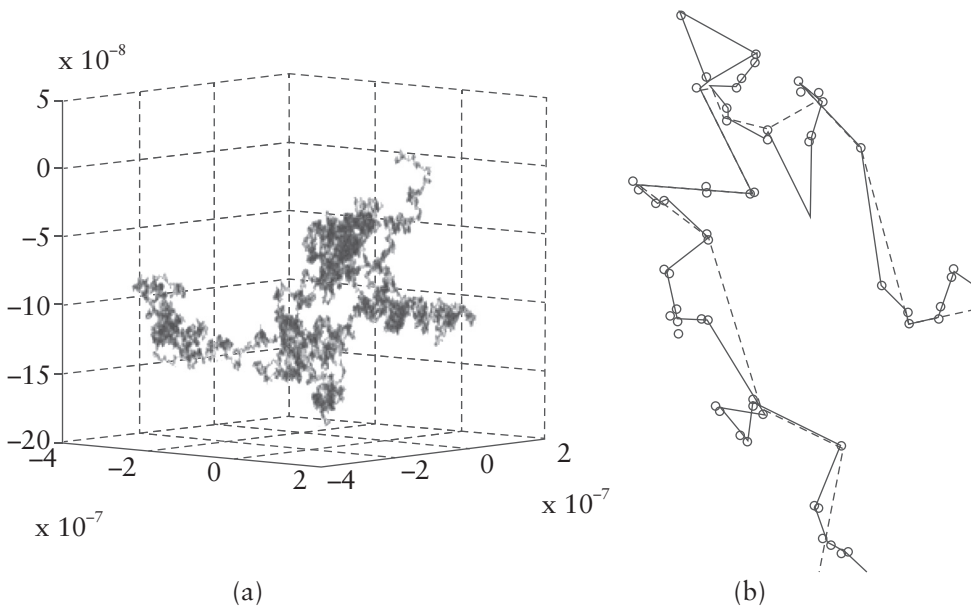
Another model focused on the mechanics associated with light-activated SMP that undergo complex deformations was provided by Sodhi and Rao [70]. The modelling was done using a framework based on the theory of multiple natural configurations taking into consideration the different aspects of modelling LSMP, which include developing a model for the original virgin network and for the other networks with different stress-free states formed due to exposure to light (Figure 6.22). Additionally, by using a framework based on the theory of multiple natural configurations [71], they considered the different aspects of modelling, which include development of a model for the original virgin network and other networks with different stress-free states. The theory was also adopted in  $T_m$ -type SMP modelling in their previous work [40]. Additionally, they modelled the initiation and formation of light-activated networks and the reverse transition that caused dissolution of these networks. Anisotropy in the mechanical response was also incorporated into the model. The model was used to simulate the results for specific boundary value problems, such as uniaxial extension and inflation of a cylinder.



**Figure 6.22** Configurations and deformation gradients involved in a two-network LSMP (schematic). Reproduced with permission from J.S. Sodhi and I.J. Rao, *International Journal of Engineering Science*, 2010, 48, 11, 1576. ©2010, Elsevier [70]

### 6.8.3 Multi-scale Modelling

Beblo and Weiland [72] presented a multi-scale modelling method for LSMP employed to anticipate soft and hard state moduli solely on the basis of a proposed molecular formulation. This approach employed the rotational isomeric state theory to build a molecular-scale model of a polymer chain (Figure 6.23) that yielded distances between the predicted crosslink locations ( $r$ -values). The  $r$ -values were then fitted with Johnson probability density functions and used with Boltzmann statistical mechanics to predict stress as a function of the strain of a phantom polymer network. Empirical adaptation for design added the junction constraint theory, including the effects of neighbouring chain interactions in the modelling process. Empirical fitting led to numerically accurate predictions of Young's modulus. The system was modular in nature and thus lent itself to adaptation to other polymer systems and development applications.



**Figure 6.23** (a) Simulated polymer chain conformation, and (b) enlarged view of simulated polymer chain. Reproduced with permission from R.V. Beblo and L.M. Weiland, *Smart Materials and Structures*, 2010, 19, 9. ©2010, IOP Science [72]

## 6.9 Conclusions

This chapter concentrated on the different approaches used for SMP modelling. Modelling has greatly promoted development of fundamental studies of SMP, reinforcing the theoretical frameworks of SMP. Full atomistic molecular models, mechanical models, and thermo-mechanical, viscoplastic and viscoelastic relaxation models have been used for  $T_m$ - and  $T_g$ -type SMP with small and large deformations. Several other methods have been employed for the modelling of light-sensitive SMP. For SMP, these numerical simulation tools can provide an inexpensive and efficient test platform to explore different combinations of material and design options. In the future, it is desired to develop new programming approaches and constitutive models to govern the corresponding thermo-mechanical behaviour, which depends on understanding the underlying shape-memory mechanisms of different SMP.

## References

1. D. Zhou and P. Choi, *Polymer*, 2012, **53**, 15, 3253.
2. J. Repáková, P. Čapková, M. Studenovský and M. Ilavský, *Journal of Molecular Modeling*, 2004, **10**, 4, 240.
3. A.V. Raghu, G.S. Gadaginamath, S.S. Jawalkar, S.B. Halligudi and T.M. Aminabhavi, *Journal of Polymer Science, Part A: Polymer Chemistry Edition*, 2006, **44**, 20, 6032.
4. M. Panos, T.Z. Sen and M.G. Ahunbay, *Langmuir*, 2012, **28**, 34, 12619.
5. R.L. McKiernan, P. Sikorski, E.D.T. Atkins, S.P. Gido and J. Penelle, *Macromolecules*, 2002, **35**, 22, 8433.
6. T.A. Speckhard, J.A. Miller and S.L. Cooper, *Macromolecules*, 1986, **19**, 6, 1558.
7. L.H. Peebles, *Macromolecules*, 1974, **7**, 6, 872.
8. T.A. Speckhard, J.G. Homan, J.A. Miller and S.L. Cooper, *Polymer*, 1987, **28**, 5, 768.
9. C. Dubois, A. Ait-Kadi and P.A. Tanguy, *Journal of Rheology*, 1998, **42**, 3, 435.

10. E. Yildirim, M. Yurtsever, E. Yurtsever, I. Yilgor and E. Yilgor, *Journal of Inorganic and Organometallic Polymers and Materials*, 2012, **22**, 3, 604.
11. J.H. Kim, T.J. Kang and W-R. Yu, *Journal of Biomechanics*, 2010, **43**, 4, 632.
12. M.E. Hyun and S.C. Kim, *Polymer Engineering & Science*, 1988, **28**, 11, 743.
13. D.G. Duguay, R.S. Labow, J.P. Santerre and D.D. McLean, *Polymer Degradation and Stability*, 1995, **47**, 2, 229.
14. P. Król, *Journal of Applied Polymer Science*, 1998, **69**, 1, 169.
15. E. Vivaldo-Lima, G. Luna-Bárceñas, A. Flores-Tlacuahuac, M.A. Cruz and O. Manero, *Industrial & Engineering Chemistry Research*, 2002, **41**, 21, 5207.
16. B. Kumar, A. Das and R. Alagirusamy, *Biorheology*, 2012, **49**, 1, 1.
17. J. Morshedjian, H.A. Khonakdar and S. Rasouli, *Macromolecular Theory and Simulations*, 2005, **14**, 7, 428.
18. H.A. Khonakdar, S.H. Jafari, S. Rasouli, J. Morshedjian and H. Abedini, *Macromolecular Theory and Simulations*, 2007, **16**, 1, 43.
19. M. Johlitz, H. Steeb, S. Diebels, A. Chatzouridou, J. Batal and W. Possart, *Journal of Materials Science*, 2007, **42**, 23, 9894.
20. M. Johlitz, S. Diebels, J. Batal, H. Steeb and W. Possart, *Journal of Materials Science*, 2008, **43**, 14, 4768.
21. J. Shim and D. Mohr, *International Journal of Plasticity*, 2011, **27**, 6, 868.
22. H.J. Qi and M.C. Boyce, *Mechanics of Materials*, 2005, **37**, 8, 817.
23. A.V. Amirkhizi, J. Isaacs, J. McGee and S. Nemat-Nasser, *Philosophical Magazine*, 2006, **86**, 36, 5847.
24. A. Ask, A. Menzel and M. Ristinmaa, *IOP Conference Series: Materials Science and Engineering*, 2010, **10**, 1, 012101.
25. H. Tobushi, T. Hashimoto, S. Hayashi and E. Yamada, *Journal of Intelligent Material Systems and Structures*, 1997, **8**, 8, 711.

26. H. Tobushi, K. Okumura, S. Hayashi and N. Ito, *Mechanics of Materials*, 2001, **33**, 10, 545.
27. C.P. Buckley, C. Prisacariu and A. Caraculacu, *Polymer*, 2007, **48**, 5, 1388.
28. J. Diani, Y.P. Liu and K. Gall, *Polymer Engineering & Science*, 2006, **46**, 4, 486.
29. Y.S. Wong, Z.H. Stachurski and S.S. Venkatraman, *Polymer*, 2011, **52**, 3, 874.
30. M. Heuchel, J. Cui, K. Kratz, H. Kosmella and A. Lendlein, *Polymer*, 2010, **51**, 26, 6212.
31. K.K. Westbrook, V. Parakh, T. Chung, P.T. Mather, L.C. Wan, M.L. Dunn and H.J. Qi, *Journal of Engineering Materials and Technology - Asme*, 2010, **132**, 4.
32. P. Ghosh and A.R. Srinivasa, *International Journal of Engineering Science*, 2011, **49**, 9, 823.
33. G. Li and A. Shojaei, *Proceedings of the Royal Society A: Mathematical, Physical and Engineering Science*, 2012, **468**, 2144, 2319.
34. J.H. Kim, T.J. Kang and W-R. Yu, *International Journal of Plasticity*, 2010, **26**, 2, 204.
35. V. Kafka, *International Journal of Plasticity*, 2008, **24**, 9, 1533.
36. Y.P. Liu, K. Gall, M.L. Dunn, A.R. Greenberg and J. Diani, *International Journal of Plasticity*, 2006, **22**, 2, 279.
37. Y.C. Chen and D.C. Lagoudas, *Journal of the Mechanics and Physics of Solids*, 2008, **56**, 5, 1752.
38. Y.C. Chen and D.C. Lagoudas, *Journal of the Mechanics and Physics of Solids*, 2008, **56**, 5, 1766.
39. B.L. Volk, D.C. Lagoudas and Y.C. Chen, *Smart Materials and Structures*, 2010, **19**, 7.
40. I. Rao in *Proceedings of SPE-ANTEC Conference*, San Francisco, CA, USA, 2002.



41. T. Chung, A. Rorno-Urbe and P.T. Mather, *Macromolecules*, 2008, **41**, 1, 184.
42. G. Barot, I.J. Rao and K.R. Rajagopal, *International Journal of Engineering Science*, 2008, **46**, 4, 325.
43. H.J. Qi, T.D. Nguyen, F. Castroa, C.M. Yakacki and R. ShandaSa, *Journal of the Mechanics and Physics of Solids*, 2008, **56**, 5, 1730.
44. T.D. Nguyen, H.J. Qi, F. Castro and K.N. Long, *Journal of the Mechanics and Physics of Solids*, 2008, **56**, 9, 2792.
45. F. Tudos and P.K. David, *Journal of Thermal Analysis and Calorimetry*, 1996, **47**, 2, 589.
46. L. Andreozzi, M. Faetti, F. Zulli and M. Giordano, *European Physical Journal B*, 2004, **41**, 3, 383.
47. G.Q. Li and W. Xu, *Journal of the Mechanics and Physics of Solids*, 2011, **59**, 6, 1231.
48. X. Chen and T.D. Nguyen, *Mechanics of Materials*, 2011, **43**, 3, 127.
49. J.A. Miller, T.A. Speckhard, J.G. Homan and S.L. Cooper, *Polymer*, 1987, **28**, 5, 758.
50. H. Sun, *The Journal of Physical Chemistry B*, 1998, **102**, 38, 7338.
51. M. Rahmati, H. Modarress and R. Gooya, *Polymer*, 2012, **53**, 9, 1939.
52. T.L. Chantawansri, Y.R. Sliozberg, J.W. Andzelm and A.J. Hsieh, *Polymer*, 2012, **53**, 20, 4512.
53. H-J. Tao, W.J. MacKnight, S.L. Hsu and C.F. Fan, *Macromolecules*, 1994, **27**, 7, 1720.
54. J.A. Miller, T.A. Speckhard and S.L. Cooper, *Macromolecules*, 1986, **19**, 6, 1568.
55. H. Yang, Z-S. Li, Z-Y. Lu and C-C. Sun, *Polymer*, 2004, **45**, 19, 6753.
56. S.L. Mayo, B.D. Olafson and W.A. Goddard, *The Journal of Physical Chemistry*, 1990, **94**, 26, 8897.

57. C.L. Zhang, J.L. Hu, S.J. Chen and F.L. Ji, *Journal of Molecular Modeling*, 2010, **16**, 8, 1391.
58. C. Zhang, J. Hu, F. Ji, Y. Fan and Y. Liu, *Journal of Molecular Modeling*, 2012, **18**, 4, 1263.
59. A.R. Leach in *Molecular Modelling Principles and Applications*, Addison Wesley Longman, London, UK, 1996.
60. T.M. Madkour and R.A. Azzam, *European Polymer Journal*, 2013, **49**, 2, 439.
61. J-P. Puaux, P. Cassagnau, G. Bozga and I. Nagy, *Chemical Engineering and Processing: Process Intensification*, 2006, **45**, 6, 481.
62. N. Arunkumar, P. Venkatesh, K.S. Srinivas and S. Kaushik, *The International Journal of Advanced Manufacturing Technology*, 2012, **63**, 9-12, 1065.
63. Y. Zhou, Y.W. Wong and F.G. Shin, *Journal of Applied Physics*, 2004, **96**, 1, 294.
64. S. Reese, M. Bol and D. Christ, *Computer Methods in Applied Mechanics and Engineering*, 2010, **199**, 21-22, 1276.
65. V. Srivastava, S.A. Chester and L. Anand, *Journal of the Mechanics and Physics of Solids*, 2010, **58**, 8, 1100.
66. V. Srivastava, S.A. Chester, N.M. Ames and L. Anand, *International Journal of Plasticity*, 2010, **26**, 8, 1138.
67. J.H. Kim, T.J. Kang and W.R. Yu, *Journal of Biomechanics*, 2010, **43**, 4, 632.
68. K.N. Long, T.F. Scott, H.J. Qi, C.N. Bowman and M.L. Dunn, *Journal of the Mechanics and Physics of Solids*, 2009, **57**, 7, 1103.
69. T.F. Scott, A.D. Schneider, W.D. Cook and C.N. Bowman, *Science*, 2005, **308**, 5728, 1615.
70. J.S. Sodhi and I.J. Rao, *International Journal of Engineering Science*, 2010, **48**, 11, 1576.
71. K.R. Rajagopal and A.R. Srinivasa, *International Journal of Plasticity*, 1995, **11**, 6, 653.
72. R.V. Beblo and L.M. Weiland, *Smart Materials and Structures*, 2010, **19**, 9.

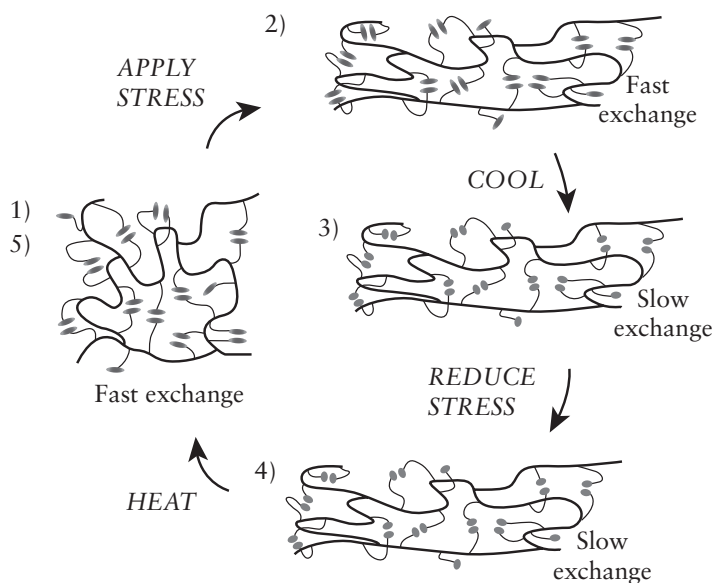


# 7 Supramolecular Shape-memory Polymers

## 7.1 Introduction

In conventional shape-memory polymers (SMP), shape-memory effects (SME) result from the increasing movement of molecular chains at above the glass transition temperature ( $T_g$ ) or melting temperature ( $T_m$ ). However, recently, thermo-reversible non-covalent interactions have been proposed in SMP. In these types of SMP there are many non-covalent bonds (e.g., hydrogen bonds) that can influence the interaction of polymer chains. Dissociation of strong hydrogen bonds results in appreciable movement of a polymer chain whereas the association of non-covalent bonds results in ‘fixing’ of a polymer chain. For example, supramolecular shape-memory elastomers have been produced in polymer networks containing reversibly associating side-groups such as ureidopyridinone (UPy). In this system, the self-complementary hydrogen-bonding interaction was used to mechanically stabilise the strained states in polymer elastomers. Shape recovery was achieved upon heating due to the dissociation of hydrogen bonds (**Figure 7.1**) [1]. In addition to the excellent strain recovery, one unique feature of this new SMP is the dynamics of its shape-memory response. Hence, fabricating SMP with supramolecular switches has been an attractive research direction for SMP [2].

Several studies have demonstrated SMP based on supramolecular networks. These networks include: polyethylene glycol (PEG)-based semi-interpenetrating networks such as PEG–polymethyl acrylate [3], PEG–polymethyl methacrylate (PMMA)-*co*-acrylic acid [4] and PEG–PMMA-*co*-(*N*-vinyl-2-pyrrolidone) [5];  $\alpha$ -cyclodextrin (CD)-based supramolecular SMP such as PEG- $\alpha$ -CD supramolecular polymer networks [6]; and UPy-functionalised supramolecular SMP such as polyacrylate copolymers containing UPy [1] and polyurethane (PU) elastomers containing UPy [7]. The research team of Hu has done extensive research on pyridine-containing shape-memory polyurethanes (PUPy) [8–15]. To give a deeper insight of SMP based on supramolecular chemistry, their structure–property relationships, and potential applications, this chapter is a systematic review of supramolecular SMP. However, for description of the structure–property relationships, SMP networks based on pyridine moieties are selected because our research team are more familiar with them.



**Figure 7.1** Molecular mechanism of supramolecular SMP. Reproduced with permission from J.H. Li, J.A. Viveros, M.H. Wrue and M. Anthamatten, *Advanced Materials*, 2007, **19**, 19, 2851. ©2007, John Wiley & Sons [1]

## 7.2 Supramolecular Chemistry

Supramolecular chemistry aimed at the construction of highly complex chemical systems and advanced materials by the design of arrays of components held together through inter-molecular force was first proposed by Lehn [16–20]. Non-covalent bonding is the dominant type of inter-molecular force in supramolecular chemistry [21, 22]. These non-covalent interactions include ionic bonds [23], hydrophobic interactions, hydrogen bonds, van der Waals forces [24] and dipole–dipole bonds [25]. Non-covalent interactions in smart materials or stimuli-responsive polymers permit a rapid response to a change in environment [26]. A perfect example is the assembly and disassembly of structural motifs such as deoxyribonucleic acid (DNA) [27, 28]. **Figure 7.2** shows that polynucleotide chains form the double-helix structure of DNA through the hydrogen bonding among the four types of nucleotides. For example, A (adenine) forms two hydrogen bonds with T (thymine) on the opposite strand, and G (guanine) forms three hydrogen bonds with C (cytosine) on the opposite strand. Therefore, it is an attractive approach to construct stimuli-responsive soft materials by linking monomers *via* non-covalent interactions, or using non-covalent interactions of functionalised side-chains (**Figure 7.3**) [29, 30].

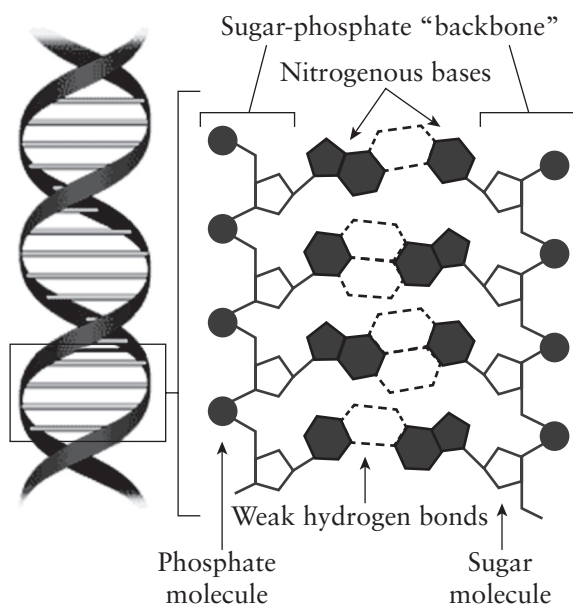


Figure 7.2 Supramolecular chemistry in the DNA structure

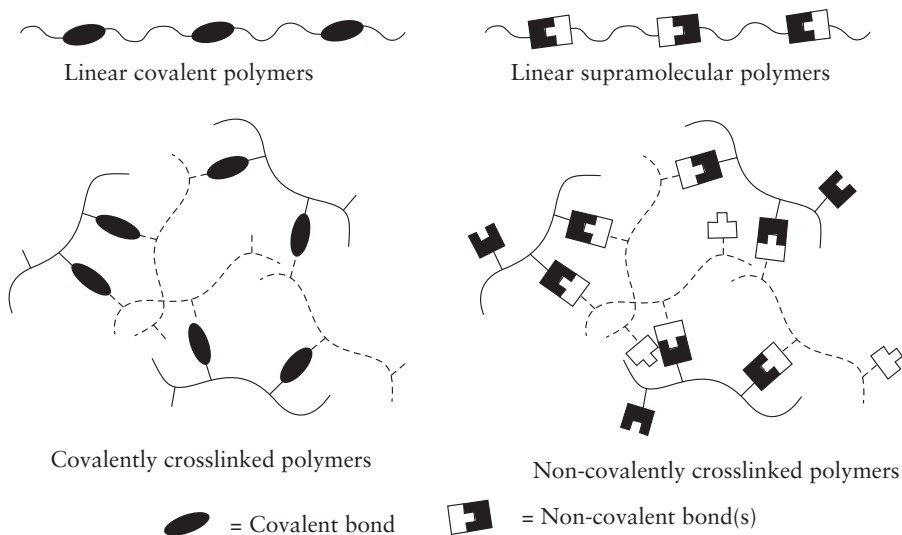


Figure 7.3 Polymer architectures made using covalent and non-covalent links between building blocks. Reproduced with permission from A.J. Wilson, *Soft Matter*, 2007, 3, 4, 409. ©2007, RSC Publishing [26]

### **7.2.1 Hydrogen Bonding**

The non-covalent interactions that hold this molecular assembly together must be specific and directional so that the molecular assembly forms could be intended and could show reversible characteristics. The finished assembly can be annealed or undergo self-healing of defects. The individual non-covalent interactions in question have low bond energies compared with those of covalent bonds. Covalent bonds typically have energies of 250–800 kJ·mol<sup>-1</sup>, whereas the strongest hydrogen bonds have energies of 210 kJ·mol<sup>-1</sup>, with 12–25 kJ·mol<sup>-1</sup> being more usual for OH···O and NH···N hydrogen bonds [30]. During the building of stimuli-responsive soft materials, hydrogen bonds are attractive because they are highly directional. If several hydrogen bonds are used in concert, strong binding is observed. If built into an array, placement of donor and acceptor functionalities creates selectivity [26]. Hence, there has been much interest in the study of hydrogen-bonded polymers because the strength and selectivity of interactions are important for determining the properties of the resulting polymers.

Hydrogen bonds occur between hydrogen atoms and more electronegative atoms such as oxygen, nitrogen and fluorine. They do not involve the exchange or sharing of electrons as in covalent and ionic bonds. Hydrogen bonds occur over short distances and can be formed and broken readily. They can also stabilise a molecule and vary in strength from very weak (1–2 kJ·mol<sup>-1</sup>) to extremely strong (>155 kJ·mol<sup>-1</sup>). The bond strength itself is dependent upon temperature, pressure, bond angle and environment, and usually characterised by the local dielectric constant. For example, the typical length of a hydrogen bond in water is 1.97 Å [31].

### **7.2.2 Relationship between Shape-memory Polymers and Supramolecular Polymer Networks**

In general, polymers exhibit shape-memory functionality if the material can be stabilised in the deformed state within the particular temperature range applied. This can be reached by using polymer network chains equipped with one type of ‘molecular switch’. Chain flexibility should be a function of the temperature in thermally induced SMP. One possibility for a switch function is a thermal transition of network chains. At a temperature above the transition temperature ( $T_{trans}$ ), the chains are flexible; whereas chain flexibility is partly limited below this  $T_{trans}$ . These functions can be achieved due to the glass transition between the rubber-elastic or viscous state to the glassy state in  $T_g$ -type-SMP, or strain-induced crystallisation by cooling the material in  $T_m$ -type-SMP. The permanent shape of SMP networks is stabilised by covalent or non-covalent netpoints at a higher  $T_{trans}$ .

In fact, glass transition and strain-induced crystallisation are related to inter-molecular force. The inter-molecular force plays a key part in the phase transition of the reversible phase and the formation of hard domains. In particular, inter-molecular hydrogen bonding greatly influences the thermo-mechanical properties of SMP. For example, in shape-memory polyurethanes (SMPU) composed of hard and soft segments, hydrogen bonding between the C=O group and N-H influences phase separation and the formation of hard domains (Figure 7.4).

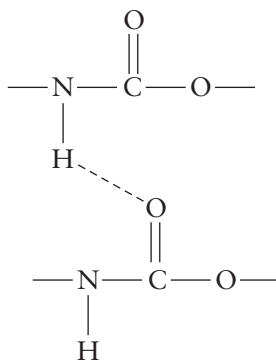


Figure 7.4 Hydrogen bonding between urethane–urethane groups

Furthermore, formation of hydrogen bonding is highly sensitive to a change in temperature, ion concentration and other parameters. For example, polycarboxylic acid(s) form inter-molecular complexes with PEG due to the hydrogen bonding formed between the carboxyl groups of polycarboxylic acid and ether oxygen atoms of PEG [32]. This hydrogen-bonded complex is highly sensitive to a change in the concentration or molecular weight of PEG, temperature and other parameters. In this way, shape-memory properties with a shape recovery of 99% are observed in poly(acrylic acid-*co*-methyl methacrylate)/PEG complexes due to their large differences in storage modulus below and above the  $T_g$ .

In addition, it has been proposed that thermo-reversible, non-covalent interactions could be utilised in SMP because many types of supramolecular polymers have been developed from small molecules or oligomers [32]. Recently, this proposal was confirmed in crosslinked polymer networks containing only a small fraction of reversibly associating side-groups such as UPy. In this system, hydrogen-bonding interactions can mechanically stabilise the strained states in polymer elastomers.



Excellent SME, strain fixity of 90%, and strain recovery of 100%, accompanied by the dynamics of its shape-memory response, can be achieved in this new type of SMP. Zhu and co-workers [7] also synthesised supramolecular PU for utilisation as SMP by grafting the UPy unit to the elastic PU. In addition, supramolecular physical netpoints were achieved through inclusion between CD and guest molecules or long polymer chains by Zhang and co-workers [6, 33–35].

These various investigations imply that a close relationship between shape-memory functionality and supramolecular chemistry. The molecular design of SMP should consider non-covalent interactions (particularly hydrogen bonding). In this condition, introduction of a large fraction of hydrogen-acceptors and hydrogen-donors in the polymer chain greatly influences the properties of SMP networks (including shape-memory properties).

## **7.3 Polymers Containing Pyridine Moieties: a Pathway to Achieve Supramolecular Networks**

### **7.3.1 Function of Pyridine Moieties in Supramolecular Chemistry**

The first use of arrays of hydrogen bonds was reported in chain polymers and crosslinked polymers by Lehn and co-workers [26]. Hitherto, several methods used for forming functional polymers were developed. For example, in hydrogen-bonded liquid crystalline polymers (LCP), several hydrogen-bonded systems are observed: acid-pyridine, acid-aminopyridine, acid-imidazole, and pyridyl-phenol [36]. In particular, carboxyl-pyridyl hydrogen-bonded systems have drawn wide attention because the carboxyl group can form stable hydrogen bonding with a pyridyl group with a stoichiometry of 1:1. They show higher hydrogen bond energy (>45 KJ/mol) and a higher association constant than that of carboxyl dimerisation. These systems suggest that the pyridyl ring plays a key part in the formation of strong hydrogen bonds [37].

The pyridine ring is a rigid heteroaromatic molecule (Figure 7.5). Usually, polymers containing a pyridine ring (particularly in the backbone of the polymer) show good heat tolerance and chemical stability. The dissolvability of a polymer in polar solvent can be improved greatly through the protonisation of the nitrogen in the pyridine ring. Complexation of nitrogen makes the polymer containing a pyridine ring useful as a catalyst carrier. Therefore, polymers containing pyridine moieties have drawn wide attention in recent years. Polymers such as polyacrylate acid, PU and polyester are synthesised to contain pyridine moieties [8–15, 32, 36, 37]. Not only are mechanical

properties, heat tolerance and chemical stability improved due to their strong hydrogen bonding, dissolvability is also enhanced. Even special functions such as liquid crystalline properties or optical–electrical properties can be achieved in some systems. Hence, polymers containing pyridine moieties are expected to find many applications in mechanical, electrical, aeronautic and astronautic fields.

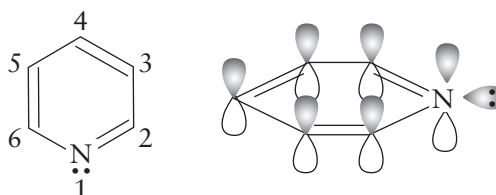


Figure 7.5 Structure of pyridine

### 7.3.2 Supramolecular Pyridine-Containing Polymers

Several studies focusing on molecular recognition in the construction of supramolecular polymer architecture through non-covalent bonds have been reported. For example, telechelic macromonomers end-capped with nucleobase (adenine, thymine) derivatives or a tridentate ligand (e.g., 2,6-*bis*(benzimidazole)pyridine) have shown polymer-like properties in the solid state (nucleobase derivatives) or in the presence of metal ion solutions (tridentate ligands). The synthesis of thermally reversible polymers built by non-covalent crosslinking has been reported [37]. Hence, a soluble polymer containing diacyl-diamidopyridine moieties can be precipitated by non-covalent crosslinking at room temperature using bivalent molecules such as bisthymine. The obtained micron-scale spherical aggregates can be dissolved completely by heating at 50 °C. A cyclobarbitol-imprinted polymer has been prepared from a fluorescent functional monomer such as 2,6-*bis*(acrylamino) pyridine. It indicated not only selective binding based on multiple hydrogen bonds but also enhancement of fluorescence intensity, suggesting that the polymer could be used as a selective fluorescence probe [38]. Finally, hydrogen-bonded polymer complexes have also been reported to comprise macrocycles (crown-ether type) containing a pyridyl moiety and carboxyl-functionalised polystyrenes [39].

### **7.3.3 Supramolecular Liquid Crystalline Polymer-Containing Pyridine Moieties**

Specific intermolecular interactions have major roles in the supramolecular assembly of liquid crystals. For synthetic liquid crystals, hydrogen-bonded materials such as benzoic acids have been known since the early 20<sup>th</sup> century [39, 40]. However, hydrogen-bonded materials had not been recognised to be useful for advanced technologies until supramolecular approaches involving hydrogen bonding were introduced into the design of liquid crystals in 1989 [41]. Kato [41] and Gulikkrzywicki and co-workers [42] reported that complementary inter-molecular hydrogen bonding between different molecules leads to the formation of the well-defined structures of mesogenic complexes. The first examples of supramolecular liquid crystals were more complex: one hydrogen bond exhibited smectic and nematic phases, and was in complex with three hydrogen bonds. Mesogens with rigid rod structures were obtained by the self-assembly of complementary molecular components based on pyridyl moieties. Another example was the liquid-crystalline phase induced by 2:1 complexation of the non-mesomorphic components 4-methoxybenzoic acid and 4,4'-bipyridine [43, 44]. In this case, nematic mesogen was obtained by simple assembly of two independent components. A nematic phase was seen from 153 °C to 163 °C in the monomer. When the methoxybenzoic acid was replaced by a trialkyl-substituted molecule, the resulting complex showed a columnar phase up to 98 °C [45]. These materials could also be functionalised by incorporation of a dye as a hydrogen bond-proton acceptor. Fluorescence was also observed in the supramolecular LCP complex [46] and their properties could be tuned by changing hydrogen-donor components. Mesogenic complexes such as cones and bananas have been obtained by connecting two different components through carboxyl-pyridyl hydrogen bonding [47].

Pyridyl-based hydrogen bonding has also been developed for side-chain LCP in which polymers with mesogenic side chains were prepared by association of functionalised polymers and small molecules through acid-pyridyl interactions. For example, benzoic acid/pyridine mesogenic complexes were obtained through formation of single hydrogen bonds in side chains [48, 49]. This type of structure exhibited thermally stable smectic phases. Another structure with doubly hydrogen-bonded side-chain mesogens showed columnar liquid-crystalline phases [50, 51]. Additionally, polymeric complexes have been obtained by complexation of end-functionalised mesogenic molecules and backbone-functionalised polymers such as polyvinyl pyridine and polyacrylic acid [52, 53]. Moreover, simple alkylphenols which are not mesogenic also form supramolecular LCP complexes [39].

Recently, alternative supramolecular LCP complexes in which the pyridyl unit was introduced on the backbone of the polymer chain have been prepared *via* pyridyl-acid hydrogen bonds [54]. For example, Kato and co-workers described the first examples

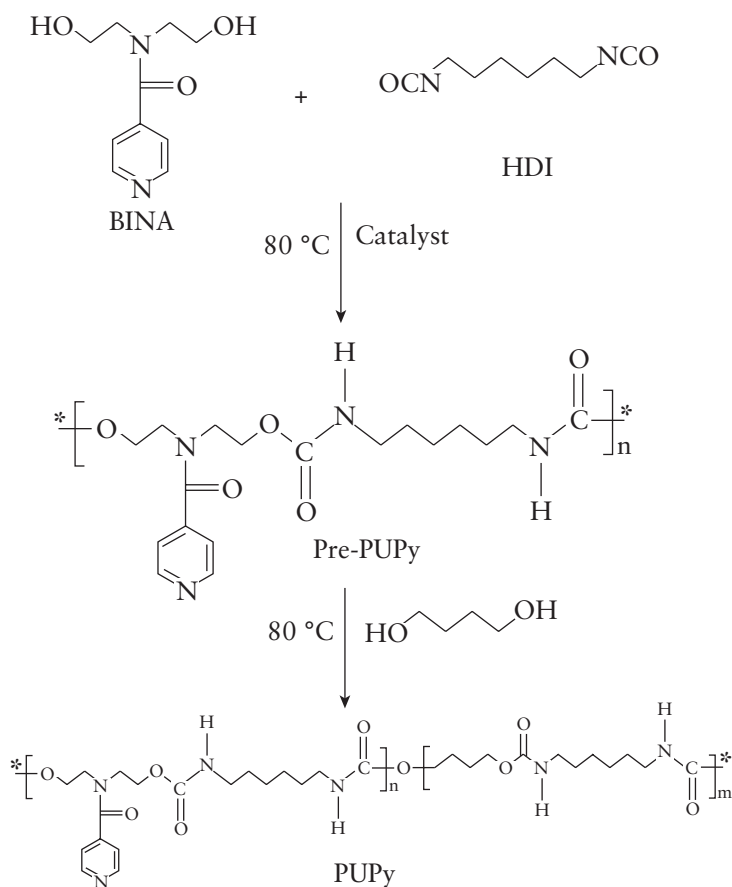
of such supramolecular LCP with complexation of 4-alkoxybenzoic acid derivatives and polyamides containing a 2,6-diaminopyridine moiety in the main chain [55, 56]. Hydrogen-bonded liquid crystalline PU complexes with 4-alkoxybenzoic acid have also been prepared with 2,6-*bis*(hydroxymethyl)pyridine or isonicotinamide [57, 58]. In these systems, complex formation resulted primarily from the hydrogen bonding between pyridine as the hydrogen-acceptor and the carboxylic acid group as the hydrogen-donor.

## **7.4 Supramolecular Shape-memory Polymers based on Pyridine Moieties**

The research team of Hu carried out a series of studies to investigate the supramolecular structure, morphology and shape-memory properties of PUPy [8–15, 32]. The next section focuses mainly on PUPy synthesised from *N,N*-*bis*(2-hydroxyethyl) isonicotinamide (BINA), hexamethylene diisocyanate (HDI), 4,4-diphenylmethane diisocyanate (MDI) and 1,4-butanediol (BDO), i.e., BINA-SMPU.

### **7.4.1 Synthesis**

Extra-pure-grade HDI, BDO and BINA (all from Sigma–Aldrich Chemical Co., St. Louis, MO, USA) were used directly. Dimethylformamide (DMF) from Ajax Finechem Ltd. (Auckland, New Zealand) was dehydrated with 4-Å molecular sieves for several days before use as a solvent. The synthesis routine of PUPy (i.e., BINA-SMPU) is presented in **Figure 7.6**. The composition in each sample was designed with a NCO/OH molar ratio of 1.02. The reaction was carried out in a 500-ml flask filled with nitrogen and equipped with a mechanical stirrer, thermal meter, and condenser. A constant temperature of 80 °C was maintained throughout the entire reaction process. Firstly, BINA powder and 10-ml DMF was added to the flask. After BINA was dissolved completely under mechanical stirring, HDI and 0.02 wt% catalyst (dibutyltin dilaurate) was added to the flask. The reaction was started immediately, and the viscosity observed to increase significantly. After 2 h, BDO was added to the reaction. The reaction was maintained for another 4 h. To control the viscosity of the solution, 10 ml DMF was added to the reaction occasionally during the reaction process. Finally, 10 wt% PUPy/DMF solution was obtained. After casting on a polytetrafluoroethylene mould and placement in a 100 °C oven for 12 h, a film of PUPy with various BINA content was prepared. A series of PUPy with various BINA contents were synthesised by adding BDO to the BINA-HDI pre-polymer. It was found that BINA content as well as pyridine-ring content decreased with increasing BDO content. HDI content (the molar fraction of which reflects the content of urethane groups) increased with decreasing BINA content [13].



**Figure 7.6** Synthetic routine of PUPy. Reproduced with permission from S.J. Chen, J.L. Hu, C.W.M. Yuen and L.K. Chan, *Polymer*, 2009, 50, 19, 4424. ©2009, Elsevier [15]

#### 7.4.2 Structure and Morphology

**Figure 7.7** presents the possible intermolecular hydrogen bonding present in BINA-SMPU. According to the molecular structure of BINA-SMPU, the pyridine ring acts as a pendant and is attached to the PU backbone. The urethane groups ( $-\text{NH}-\text{COO}-$ ), which have a partially negative charge on the oxygen atom, can interact with the hydrogen-donor or hydrogen-acceptor. Hence, it is predicted that there are hydrogen-bonding associations between the  $\text{C}=\text{O}$  and  $\text{NH}$  of the urethane groups. The hydrogen

bonds are beneficial to the formation of hard segment domains (**Figure 7.7a**). Similarly, the C=O group beside the pyridine ring can also form hydrogen bonds with the NH of the urethane groups (**Figure 7.7b**). In general, movement of the polymer chains of SMPU is determined primarily by the ratio of the flexible soft segment and rigid hard segment, or the flexibility of the soft segment. However, in this system, the hydrogen bonding present in the pyridine ring and urethane group plays an important part in movement of the polymer chain. One reason is that the hydrogen bonding present in the urethane group and pyridine ring is much stronger. Another reason is that the fraction of the urethane group and pyridine ring is high.

The hydrogen-bonded supramolecular structure of BINA-SMPU is significantly dependent upon BINA content as confirmed from Fourier transform-infrared (FT-IR) spectra. **Figure 7.8** shows the FT-IR spectra of PUPy with various BINA content. **Figure 7.8a** shows that the band density at 3313–3320  $\text{cm}^{-1}$  representing the N-H stretching vibration of the urethane group increases as BINA content drops. With regard to the band density at  $\approx 3059 \text{ cm}^{-1}$  for the C-H stretching vibration of the pyridine ring and at  $\approx 2935 \text{ cm}^{-1}$  and  $\approx 2868 \text{ cm}^{-1}$  for the  $\text{CH}_2$  vibration, both decrease with decreasing BINA content. **Figure 7.8b** reveals that the C=O stretching vibration of the urethane group shifts to a low frequency as BINA content decreases, and a relatively high density is obtained if BINA content is  $< 30 \text{ wt}\%$  due to their much higher fraction of urethane groups. However, the density of the C=O stretching vibration at  $\approx 1635 \text{ cm}^{-1}$  as well as the density of the C-N-C stretching vibration at  $\approx 1600 \text{ cm}^{-1}$  drops significantly as BINA content decreases. Finally, the stretching vibration of C-N-C tends to be overlapped by the stretching vibration of the C=O of the urethane group in the sample of PUPyBDO10 due to its very low fraction of BINA. Hence, it is confirmed again that the frequency at  $1600 \text{ cm}^{-1}$  is assigned to the C-N-C stretching vibration of the BINA unit. In addition, it is also found that the density at  $\approx 1530 \text{ cm}^{-1}$  increases with respect to increasing HDI content. This finding implies that the frequency at  $1530 \text{ cm}^{-1}$  is assigned to the stretching vibration of the C-N of amide II in the urethane group. Simultaneously, the frequencies at  $1434 \text{ cm}^{-1}$  and  $1411 \text{ cm}^{-1}$  can be assigned to the stretching vibrations of the pyridine ring because their density is found to drop with respect to decreasing BINA content. However, the frequencies at  $1474$ ,  $1337$ ,  $1258$ ,  $1241$  and  $1220 \text{ cm}^{-1}$  may result from urethane groups because they get clearer as HDI content increases, particularly in the spectra of samples PUPyBDO30, PUPyBDO20 and PUPyBDO10. Moreover, the density of frequencies at  $1094 \text{ cm}^{-1}$  and  $1054 \text{ cm}^{-1}$  drops with decreasing BINA content. Finally, it can be concluded that the strength of the hydrogen bonds present in the urethane group becomes stronger, whereas the strength of the hydrogen bonds present in the pyridine ring becomes weaker, as BINA content decreases.

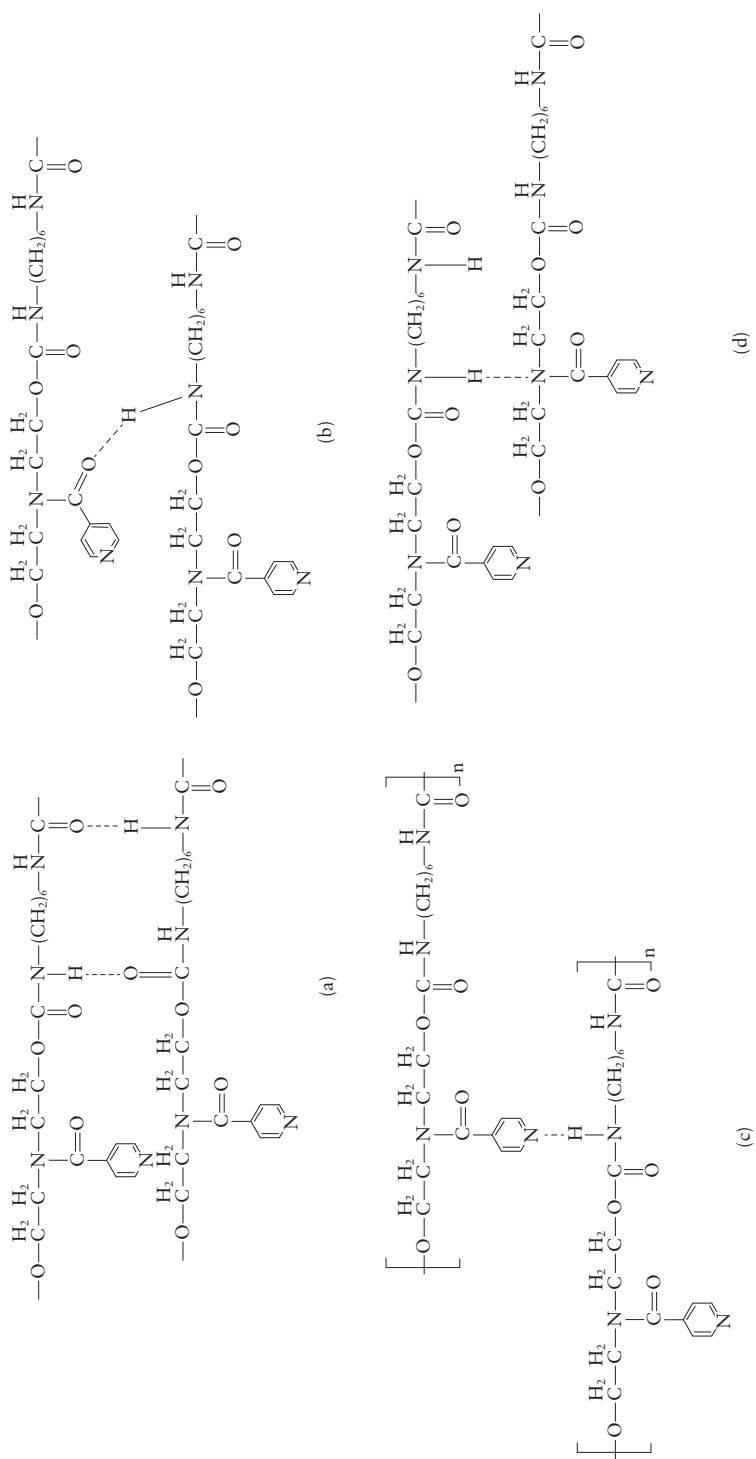
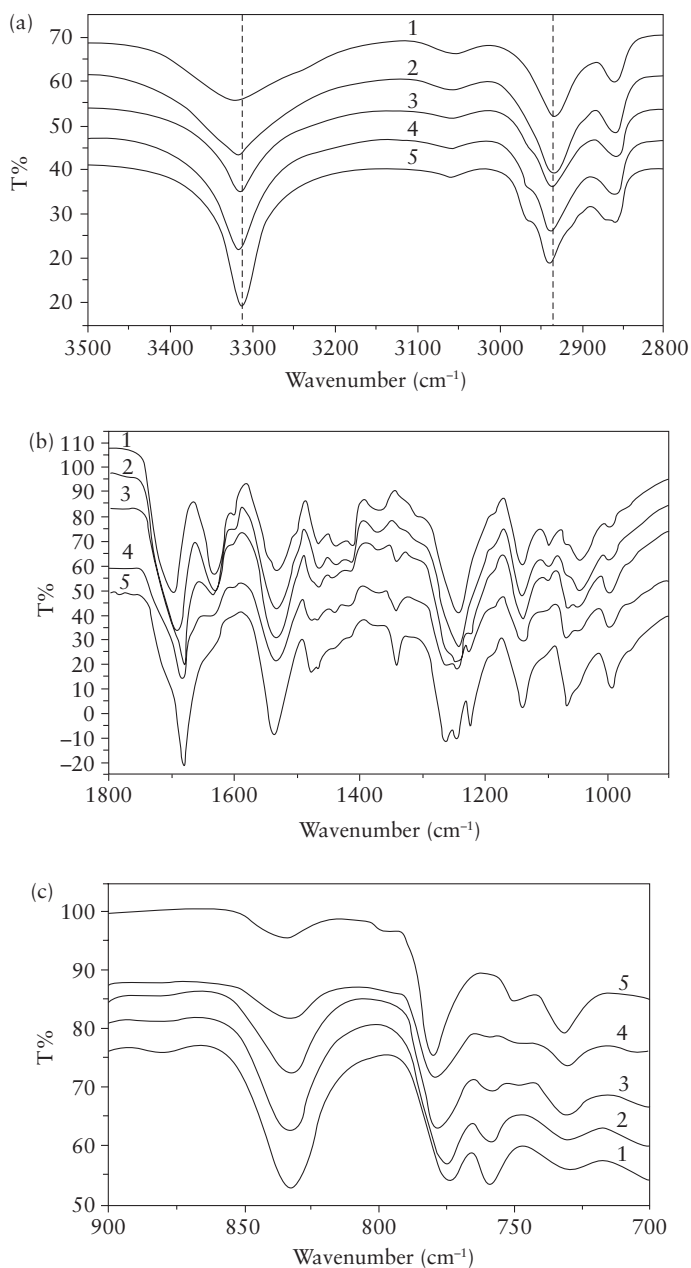


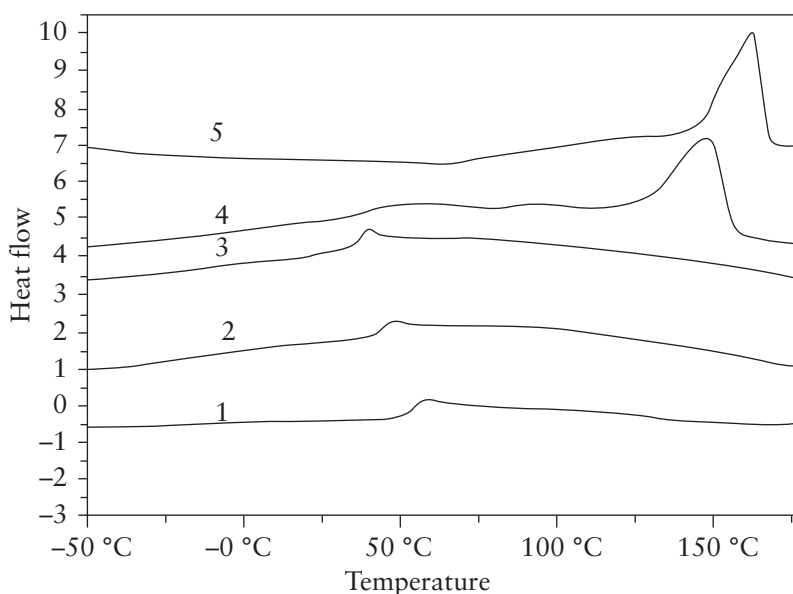
Figure 7.7 Inter-molecular hydrogen bonding in BINA-SMPU



**Figure 7.8** Fourier Transform-infrared (FT-IR) spectra of PUPy with various BINA content. 1: PUPyBDO53; 2: PUPyBDO40; 3: PUPyBDO30; 4: PUPyBDO20; and 5: PUPyBDO10 at the frequency range of (a) 3,500–2,800 cm<sup>-1</sup>; (b) 1,800–900 cm<sup>-1</sup>; and (c) 900–700 cm<sup>-1</sup>. FTIR: Fourier-Transform infrared



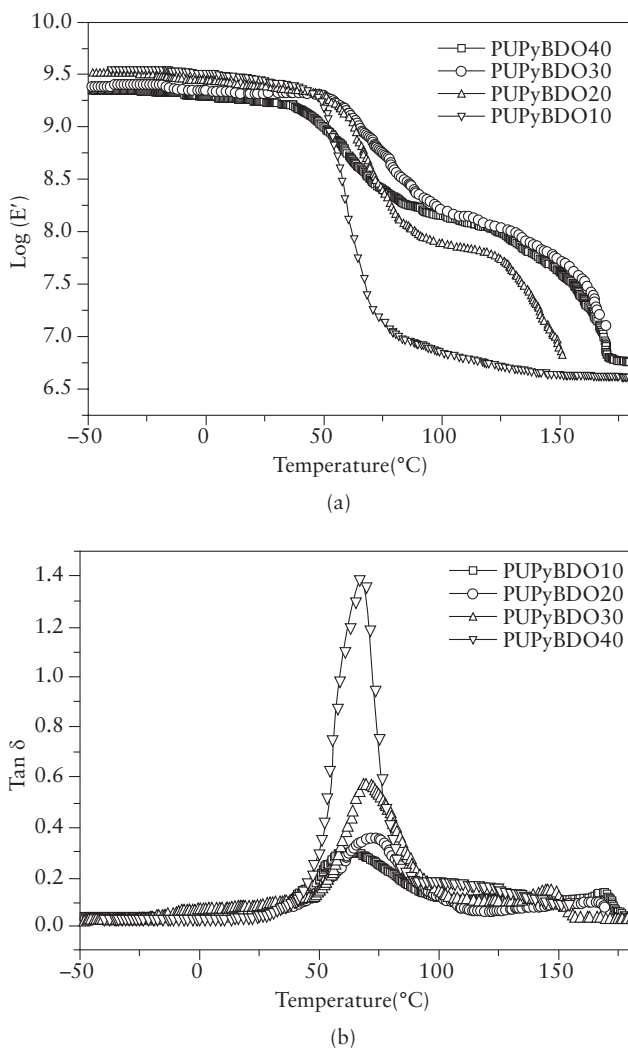
Differential scanning calorimetry (DSC) results also show PUPy to have an amorphous soft phase, and that the  $T_g$  of the soft phase is controlled by the pyridine ring *via* hydrogen bonding. In the PUPy-BDO series of PUPy, the  $T_g$  of the soft phase tends to drop with decreasing BINA content (Figure 7.9), particularly if the BINA content is >30 wt%. In addition, PUPy tends to form a semi-crystalline hard phase if the BINA content drops to <40 wt% whereas PUPy with >40 wt% BINA content mainly forms the amorphous hard phase.



**Figure 7.9** Differential scanning calorimetry (DSC) heating curves of PUPy with various BINA content: 1: PUPyBDO53; 2: PUPyBDO40; 3: PUPyBDO30; 4: PUPyBDO20; and 5: PUPyBDO10.

Dynamic mechanical analysis (DMA) testing confirms that the morphology of micro-phase separation occurs in PUPy. PUPy not only exhibits a much higher glassy modulus, it also shows a significant decrease in modulus and much higher maximum  $\tan \delta$  during glass transition. The rubber modulus enhances with respect to decreasing BINA content. Hence, the modulus ratio ( $E_g/E_r$ ) drops with respect to decreasing BINA content (Figure 7.10a). In addition,  $\tan \delta$  decreases with respect to decreasing pyridine content (Figure 7.10b). Finally, it is also proposed that the micro-phase separation morphology of PUPy changes with respect to the change in BINA content.

That is, as the BINA content drops from 53 to 10 wt% in the PUPy-BDO series of PUPy, the soft phase tends to change gradually from a continuous amorphous phase to a droplet-like dispersion phase. Conversely, the hard phase grows from a droplet-like dispersion amorphous phase to a continuous semi-crystalline phase if there is no irregular MDI unit.



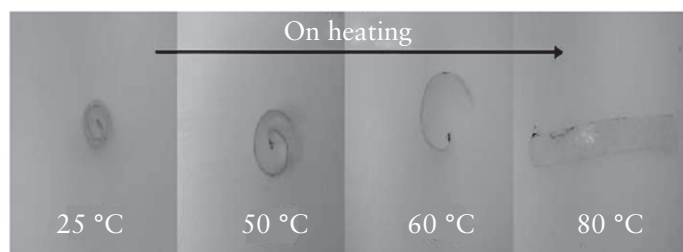
**Figure 7.10** (DMA) curves of (a) modulus (b)  $\text{tan } \delta$  of PUPy samples with various BINA content

### 7.4.3 Thermally induced Shape-memory Effect

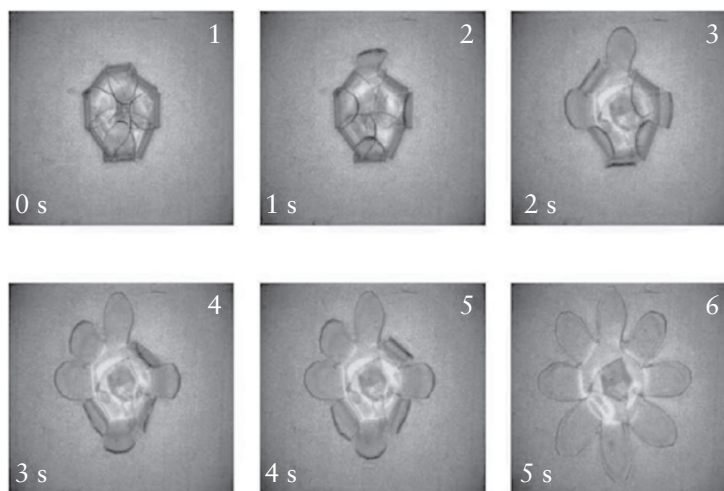
Hu and co-workers [12] used a rectangular film of BINA-SMPU to fabricate a temporary coil shape (Figure 7.11a). This coil shape was kept for a long time after fixing at low temperature (e.g., 20 °C). As temperature was increased from 25 to 80 °C, the coil shape relaxed below 50 °C, and the coil deployed quickly to a flat rectangular film if the temperature was increased to >50 °C. Finally, the original shape was recovered perfectly. Another shape-memory polymeric product is a shape-memory 'flower' having eight 'petals' which is cut from a flat square film made of BINA-SMPU (Figure 7.11b). The original shape is like that of an opening flower. By increasing the temperature to above room temperature (e.g., 80 °C), the petals of the flower are coiled by hand to make a closed flower (Figure 7.11b) (1). After it is cooled to room temperature, the closed flower is fixed. However, if the closed flower is put in an oven at 80 °C, the flower opens its petals one-by-one. Figure 7.11b shows that the petals are opened completely to a beautiful opening flower in <5 s.

To explain thermally induced shape-memory behaviour, a molecular model of the thermally induced SME mechanism of BINA-SMPU is presented in Figure 7.12. It shows that a large fraction of hydrogen bonds with a temperature at melting or solution state of BINA-SMPU ( $T_{ah}$ ) acting as the physical netpoint determines the permanent shape of the polymer network, whereas the large fraction of hydrogen bonds with a lower temperature when all hydrogen bonds are present in BINA-SMPU ( $T_{al}$ ) acting as the reversible 'switch' fixes the deformed strain upon cooling and releases the stored strain upon heating, resulting in shape recovery. When BINA-SMPU is in solution or melting ( $T > T_{ah}$ ), i.e., state 1 in Figure 7.12, the polymer chain is random and free. BINA-SMPU solutions or the melting polymer (i.e., shape *a*) can then be fabricated to any initial shape using a conventional process (e.g., shape *b*). If the temperature cools to below  $T_{al}$  at state 2, two types of hydrogen bonds are associated, and the resultant shape *b* can be remembered. Thereafter, if the temperature is raised to a high temperature ( $T_h$ ) of  $T_{al} < T_h < T_{ah}$  at state 3, the hydrogen bonds with  $T_{al}$  are dissociated or become weaker, whereas the hydrogen bonds with  $T_{ah}$  are strong enough to maintain microscopic shapes. The polymer can then be deformed to a temporary shape (i.e., shape *c*) by applying an external force to the rubber state. A cooling process of low temperature ( $T_l$ ) ( $T_l < T_{al}$ ) at state 4 under a load fixes the deformed shapes (i.e., shape *d*) because the hydrogen bonds with  $T_{al}$  are associated. Moreover, if the temperature is raised to above  $T_h$  again at state 5, the deformed strain will release immediately because the hydrogen bonds with  $T_{al}$  are dissociated. This results in macroscopic shape recovery such as shape *e* and shape fixation again at room temperature (i.e., shape *f*). Basically, shape *f* is very close to shape *b*. Hence, shape fixation and shape recovery can be achieved in BINA-SMPU. Temperature-dependent FT-IR spectra support the notion that the hydrogen bonding in the pyridine ring serves as a molecular switch, whereas the

hydrogen bonding in urethane groups acts as a physical netpoint for utilisation of PUPy as shape-memory material [12].



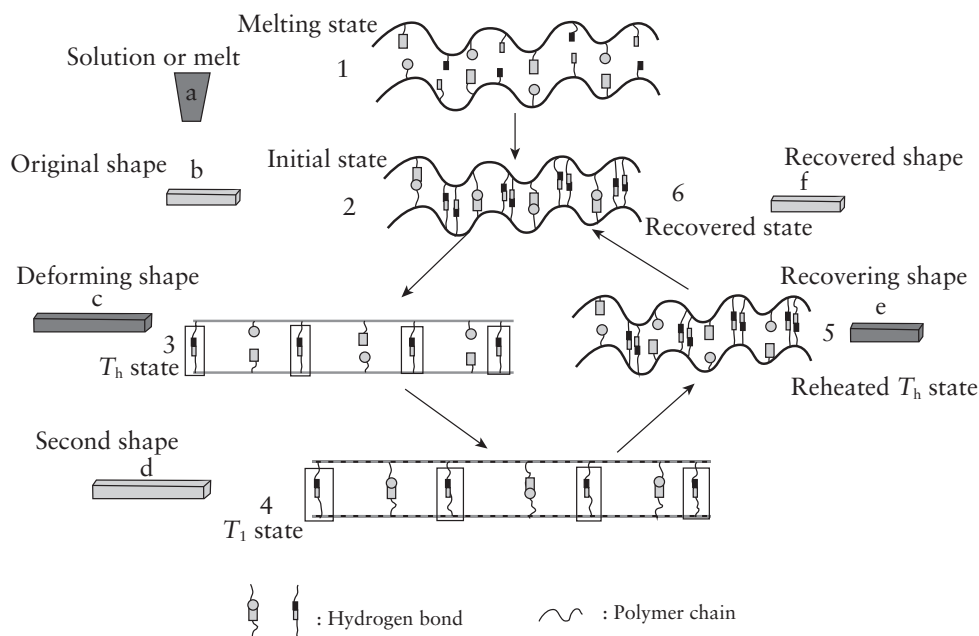
(a)



(b)

**Figure 7.11** Thermally induced SME in BINA-SMPU

Furthermore, Hu and co-workers studied a series of PUPy with different BINA content for the thermally induced SME. Thermo-mechanical testing and temperature-dependent strain recovery showed that the lower limit of BINA content for PUPy exhibiting good SME is 30 wt%. As BINA content decreases, shape fixity decreases slightly, whereas shape recovery decreases significantly. In addition, strain stability is better in higher-BINA content PUPy with lower elongation; and shape recovery force increases with decreasing BINA content.



**Figure 7.12** Shape-memory mechanism of the thermally induced SME of BINA-SMPU

#### 7.4.4 Moisture-sensitive Shape-memory Effect

BINA-SMPU shows high moisture absorption. In the initial stage, the process of moisture absorption is in accordance with Fick's Second Law [32]. Moisture absorption increases with increasing temperature (particularly  $<28\text{ }^{\circ}\text{C}$ ) and moisture absorption increases with increasing relative humidity (RH) (particularly  $>70\%$  RH). In BINA-SMPU, as BINA content increases, moisture absorption at any time, maximum moisture absorption, and the speed of moisture absorption at the initial stage all increase. The response of BINA-SMPU towards moisture allows one to consider a new transition method for SME using moisture or water in BINA-SMPU.

Hu and co-workers obtained moisture-sensitive SME in PUPy (Figure 7.13) [8, 10, 15]. They proposed a shape-memory mechanism for PUPy. Under the stimulus of moisture, the pre-formed hydrogen bonding, N-H...N-Py, at the dry state is replaced by more adaptive hydrogen bonding (Figure 7.14). The pyridine ring tends to be free due to the protonisation of the pyridine ring by water (O-H...N-Py), or is linked *via* water molecules in the form of bridged hydrogen bonding (Py-N-H...O-H-O...H-N-Py), which shows a long bond distance. As a result, the interaction becomes weaker, and the stiffness or modulus of the polymer becomes softer as moisture absorption

increases. Similar to the dissociation of hydrogen bonds induced by temperature, the replacement of hydrogen bonds present in the pyridine ring also results in shape recovery. Therefore, the hydrogen bonds between the pyridine ring and N-H of the urethane group are used as the moisture-sensitive ‘switch’, whereas the hard phase formed *via* hydrogen bonds among the urethane groups are the physical netpoints in moisture-sensitive SMPU.

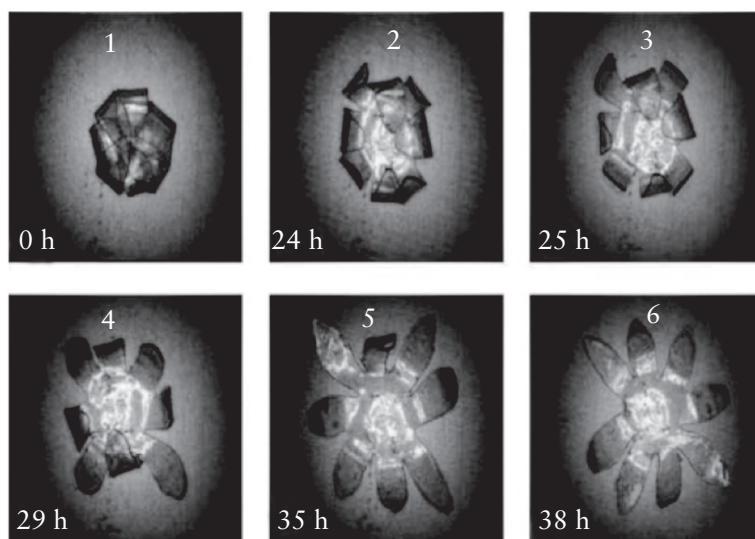


Figure 7.13 Moisture-sensitive SME in BINA-SMPU (RH = 65% and T = 20 °C)

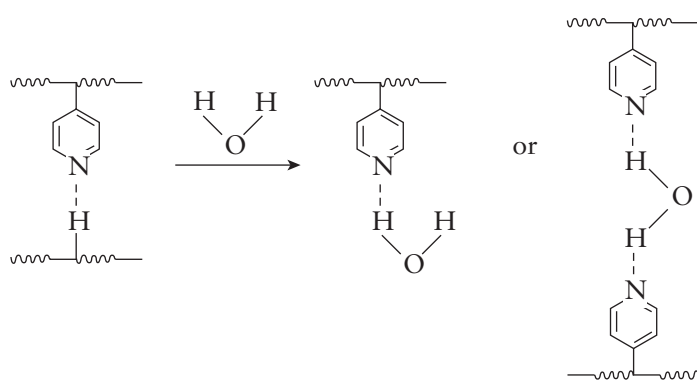
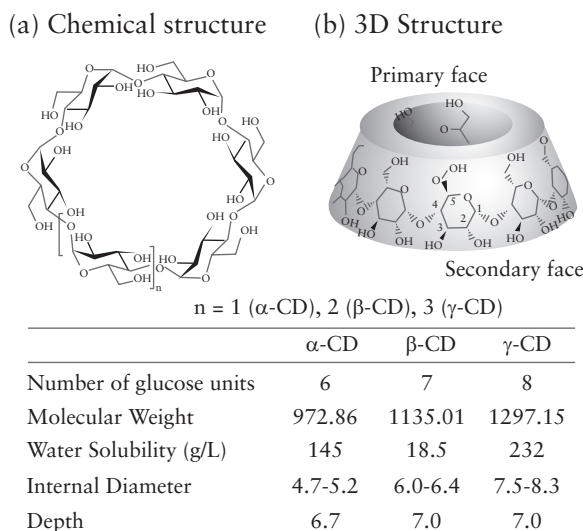


Figure 7.14 Mechanism of moisture absorption at the hydrogen-bonded pyridine ring

## 7.5 Supramolecular Shape-memory Polymers based on Cyclodextrins

### 7.5.1 Cyclodextrins

CD are cyclic oligosaccharides consisting of  $\geq 6$  glucopyranose units attached by  $\alpha$ -1,4-linkages (Figure 7.15). The most common CD comprise 6, 7 or 8 glucopyranose units and are named  $\alpha$ -,  $\beta$ - or  $\gamma$ -CD, respectively. CD have become the most important macrocyclic hosts. This is because they are water-soluble natural products, inexpensive, commercially available, nontoxic, and readily functionalised [59–61].



**Figure 7.15** Structures of CD. Reproduced with permission from A. Harada, Y. Takashima and H. Yamaguchi, *Chemical Society Reviews*, 2009, 38, 4, 875. ©2009, RSC Publishing [59]

Guest molecules can form reversible inclusion complexes with CD, but the long polymer chains can also penetrate CD cavities to form supramolecular inclusion complexes if their shapes match with each other. As the hydroxyl groups of CD on both faces arrange on the outside of the cavity and because the inside of the CD cavity is a hydrophobic microenvironment, CD can capture suitable hydrophobic guests into this hydrophobic cavity in aqueous media [62, 63].

Various supramolecular polymeric materials, such as self-healing supramolecular materials [64], shape-memory supramolecular materials [65] and responsive supramolecular polymer gels [66], have been created using CD and their derivatives.

### 7.5.2 Thermally induced Shape-memory Effect

Zhang and co-workers reported a supramolecular shape-memory material based on partial  $\alpha$ -CD-PEG inclusion complexes (IC) which contained  $\alpha$ -CD/PEG inclusion crystallites as a fixing phase and naked PEG crystallites as a reversible phase [6]. Crystalline complete  $\alpha$ -CD/PEG IC are usually formed by the addition of PEG to a saturated aqueous solution of  $\alpha$ -CD [67, 68]. Hence, a partial PEG/ $\alpha$ -CD IC film can be obtained by casting the solution at room temperature, which contains PEG/ $\alpha$ -CD inclusions and naked PEG segments. If the sample is heated above the  $T_m$  of PEG, the sample can deform under external force because of fusion of the naked PEG crystallites (Figure 7.16 (1)). As the temperature decreases, the sample can be fixed at a temporary shape due to re-crystallisation of the naked PEG segments (Figure 7.16 (2)). Upon heating the sample above the  $T_m$  of PEG again, the naked PEG crystallites fuse and the sample recovers to its original shape owing to its entropy elasticity (Figure 7.16 (3)). The recovery ratio of these materials can reach 97%.

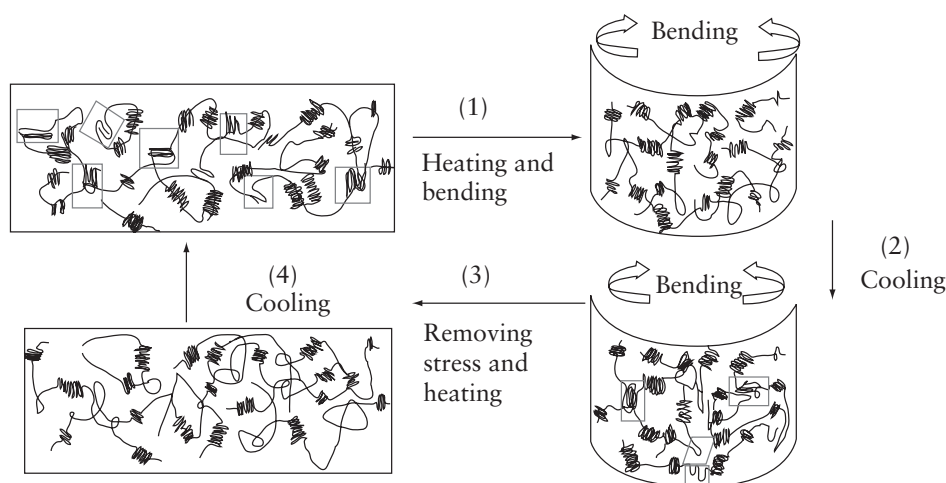
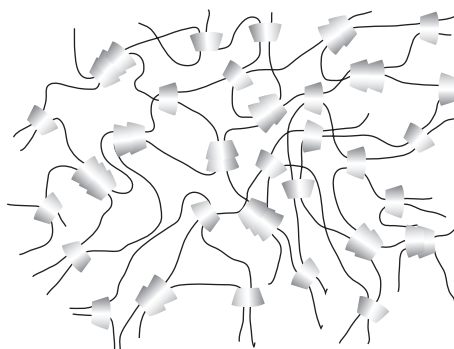


Figure 7.16 Molecular mechanism of SME of partial an  $\alpha$ -CD-PEG inclusion complex:  $\alpha$ -CD/PEG inclusion crystallites (filled oval) as the fix phase and PEG crystallites (ordered lines in rectangles) as the reversible phase. Reproduced with permission from S. Zhang, Z.J. Yu, T. Govender, H.Y. Luo and B.J. Li, *Polymer*, 2008, 49, 15, 3205. ©2008, Elsevier [6]

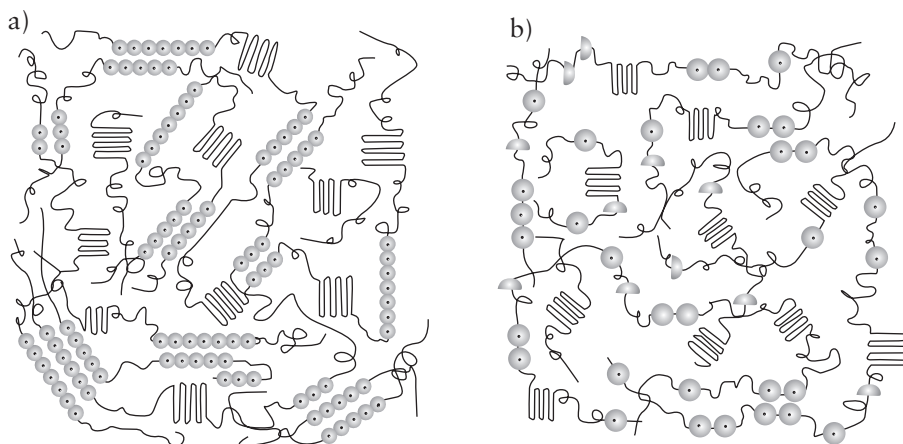


In accordance with the concept derived from shape-memory  $\alpha$ -CD/PEG IC, Zhang and co-workers also prepared a supramolecular material based on the self-assembly of  $\gamma$ -CD with PEG [35]. It was found that  $\gamma$ -CD could include double strands of PEG chains when PEG/ $\gamma$ -CD IC was formed. Partial PEG/ $\gamma$ -CD IC could be formed using the preparation method of  $\alpha$ -CD/PEG IC. **Figure 7.17** shows the proposed chain structures of a partial PEG/ $\gamma$ -CD inclusion complex. In PEG/ $\gamma$ -CD IC, the thermally reversible PEG crystallite phase serves as a switching segment, and the interlock crosslink phase acts as a fixing segment.



**Figure 7.17** Proposed chain structures of a partial PEG/ $\gamma$ -CD inclusion complex (schematic). Solid shapes represent the interlock crosslinking between  $\gamma$ -CD with PEG. Reproduced with permission from M.M. Fan, Z.J. Yu, H.Y. Luo, Z. Sheng and B.J. Li, *Macromolecular Rapid Communications*, 2009, 30, 11, 897. ©2009, John Wiley & Sons [35]

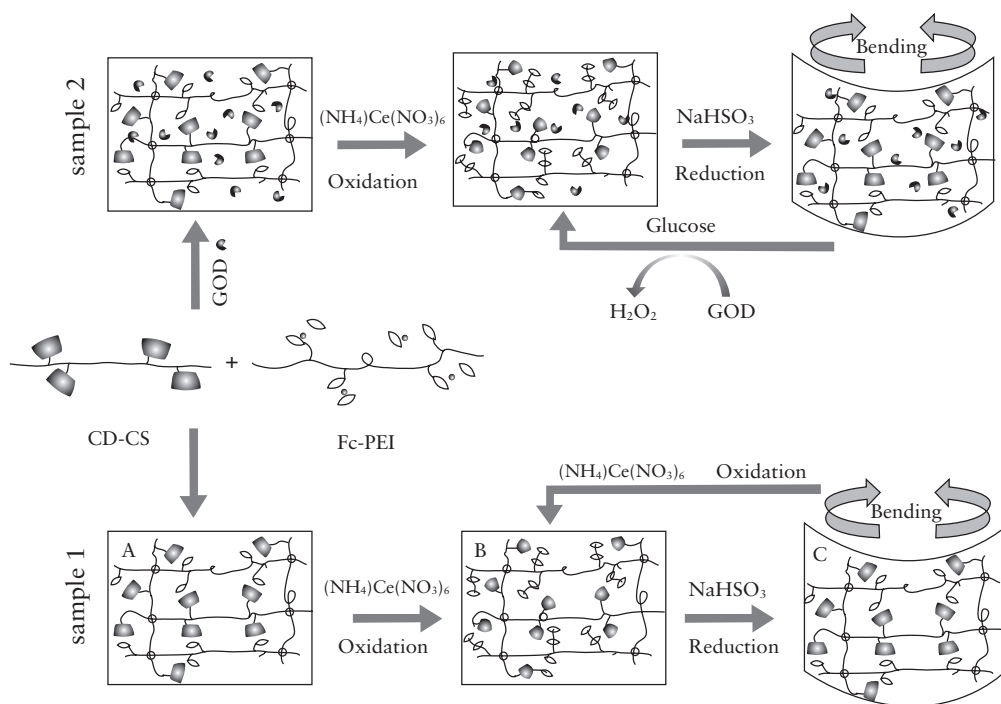
Poly( $\epsilon$ -caprolactone (PCL) ( $M_n = 530\text{--}40,000$ ) was found to form complete IC with  $\alpha$ -CD as PEG/ $\alpha$ -CD IC [69, 70]. Zhang and co-workers reported a shape-memory material based on the inclusion complexes between  $\alpha$ -CD and PCL [33, 34]. In  $\alpha$ -CD/PCL IC, the  $\alpha$ -CD/PCL inclusion crystallites served as a fixing phase, whereas naked PCL crystallites served as a reversible phase. They also found that the shape recovery ratio increased and shape fixation ratio decreased with increasing casting temperature. If the solvent was changed, the chain structures of the  $\alpha$ -CD/PCL IC might be different. **Figure 7.18** shows the possible chain structures for  $\alpha$ -CD/PCL IC using DMF or Pyridina solvent. It is possible to ‘tune’ shape-memory properties by changing the casting temperature or solvent.



**Figure 7.18** Proposed chain structures of (a) 80-30DMF70, and (b) 80-30Pyridine70 (schematic). Reproduced with permission from H.Y. Luo, M.M. Fan, Z.J. Yu, X.W. Meng, B.J. Li and S. Zhang, *Macromolecular Chemistry and Physics*, 2009, **210**, 8, 669. ©2009, John Wiley & Sons [34]

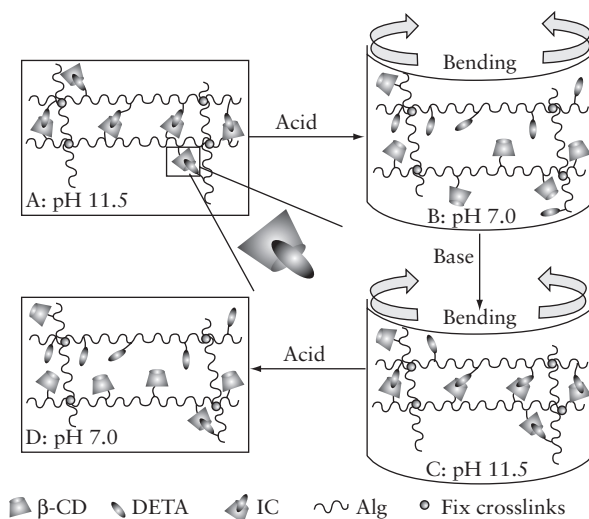
### 7.5.3 Non-thermally Induced Shape-memory Effects

Zhang and co-workers synthesised a novel redox-induced SMP. It was prepared by crosslinking  $\beta$ -CD modified chitosan (CS) and ferrocene-modified branched ethyleneimine polymer (Fc-PEI) [71].  $\beta$ -CD could interact with Fc groups to form inclusion complexes and these complexes could dissociate *via* oxidation. Hence, when mixing  $\beta$ -CD-CS and Fc-PEI solution together, a network was formed due to the interaction between Fc groups and  $\beta$ -CD [72]. In the final  $\beta$ -CD-CS/Fc-PEI supramolecular materials, reversible redox-sensitive  $\beta$ -CD/Fc IC acted as reversible phases and covalent crosslinks served as fixing phases. When the material was immersed in oxidant solution, oxidation of Fc caused the dissociation of  $\beta$ -CD/Fc IC. Then the material became soft and readily deformable by external stress (**Figure 7.19 A–B**). Deformation of the specimen was ‘frozen’ due to reformation of  $\beta$ -CD-Fc IC by immersing the deformed specimen in a reducing agent solution under external stress (**Figure 7.19 B–C**). When immersing in oxidant solution, the material could recover its original shape because of the dissociation of  $\beta$ -CD/Fc IC (**Figure 7.19C–B**). After entrapping glucose oxidase (GOD) molecules into the  $\beta$ -CD-CS/Fc-PEI complex, shape-memory behaviour in response to glucose could be caused by hydrolysis of glucose catalysed by GOD (**Figure 7.19-sample 2**). Such SMP had potential for medical applications because of eliminating the temperature constraints of thermally induced SMP.



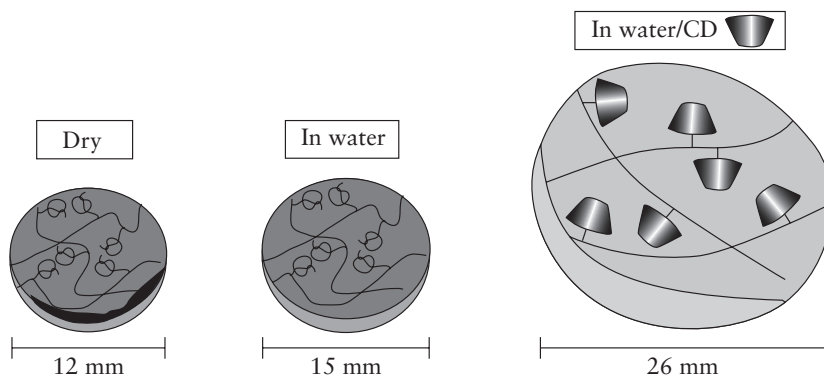
**Figure 7.19** Molecular mechanism of the oxidation–reduction and glucose-induced SME effect. A: Original shape in the reduction state; B: original shape in the oxidation state; and C: temporary shape in the reduction state. Reproduced with permission from Z.Q. Dong, Y. Cao, Q.J. Yuan, Y.F. Wang, J.H. Li, B. J. Li and S. Zhang, *Macromolecular Rapid Communications*, 2013, 34, 10, 867. ©2013, John Wiley & Sons [71]

A novel pH-sensitive SMP based on crosslinking  $\beta$ -CD-modified alginate (Alg) and diethylenetriamine (DETA)-modified Alg was reported by Zhang and co-workers [65]. They found that formation of inclusion complexes between  $\beta$ -CD and DETA showed pH dependence.  $\beta$ -CD and DETA formed 1:1 inclusion complexes in a solution of pH 11.5 but could not form inclusion complexes in neutral conditions. In the resulting  $\beta$ -CD-Alg/DETA-Alg supramolecular material, pH-reversible  $\beta$ -CD/DETA IC served as a reversible phase and the crosslinked Alg chains acted as a fixing phase. Utilising reversible pH-sensitive  $\beta$ -CD/DETA IC, the material could be fixed at a temporary shape in a solution of pH 11.5 and recover to its original shape in a solution of pH 7 (Figure 7.20). The recovery ratio and fixity ratio could reach 96 and 95%, respectively. The material also showed good degradability and biocompatibility. This merit allowed these supramolecular materials to be employed in medical applications.

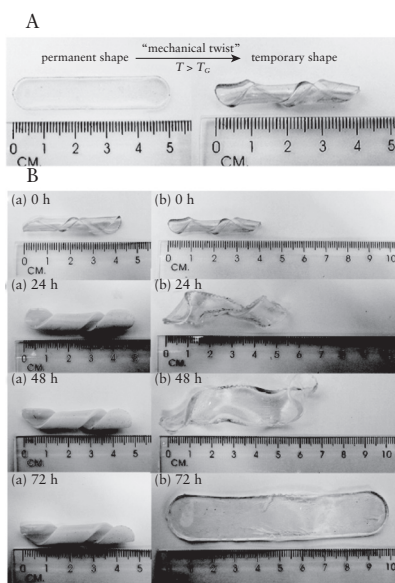


**Figure 7.20** Molecular mechanism of a pH-induced shape-memory effect. Reproduced with permission from X.J. Han, Z.Q. Dong, M.M. Fan, Y. Liu, Y.F. Wang, Q.J. Yuan, B.J. Li and S. Zhang, *Macromolecular Rapid Communications*, 2012, 33, 12, 1055. ©2012, John Wiley & Sons [65]

Peters and Ritter reported a novel method to create smart gels triggered by CD-based host-guest effects [73]. The smart gel showed swelling behaviour and a SME of a switchable hydrophilic material of unlimited dimensions. They prepared the material comprising adamantyl-modified water-swelling polymer networks. The original hydrophobic domains disappeared due to the formation of hydrophilic adamantyl/CD complexes. Accordingly, the material could absorb water and expand drastically. **Figure 7.21** shows that the hydrophobic effect of incorporated 2-(*N'*-(adamantan-1-yl)ureido)ethyl methacrylate (AdMA) was suppressed using an aqueous CD solution with a molar fraction of the hydrophobic co-monomer AdMA of  $\approx 10$  mol%. However, at higher molar fractions of the hydrophobic co-monomer AdMA, the hydrophobic-to-hydrophilic transition could not be observed in  $\alpha$ -CD solution. The material showed an inclusion complex-driven one-way SME. After heating above the  $T_g$ , the material was cooled to room temperature to maintain the temporary shape (**Figure 7.22A**). The twisted gel recovered to its original shape in aqueous CD solution because of the formation of inclusion complexes, which allowed water to move into the network and the network to relax (**Figure 7.22B**).



**Figure 7.21** Photographs and scheme of the swelling in water and aqueous CD solution of disc-shaped polymer samples. Reproduced with permission from O. Peters and H. Ritter, *Angewandte Chemie International Edition*, 2013, 52, 34, 8961. ©2013, John Wiley & Sons [73]



**Figure 7.22** (A) Five-centimetre samples of 1 in the permanent shape and in temporary shape after heating above the  $T_g$  and subsequent mechanical deformation. (B) Relaxation of the programmed SMP samples in water (a) and aqueous CD solution (b) over 72 h. Reproduced with permission from O. Peters and H. Ritter, *Angewandte Chemie International Edition*, 2013, 52, 34, 8961. ©2013, John Wiley & Sons [73]

## 7.6 Potential Applications

### 7.6.1 Reshape Applications

Chen proposed several potential applications of BINA-SMPU [32]. BINA-SMPU shows excellent moisture absorption and moisture-sensitive SME. The higher moisture absorption results in a decrease in the modulus. Hence, the original shape (e.g., shape A) can be deformed easily to a second shape (e.g., shape B) if the polymer becomes soft by conditioning in water at room temperature. The second shape can also be fixed after it is dried. If the polymer is dried under the second shape, the newly associated hydrogen bonds present in the hard phase form new physical netpoints to provide a new polymer network. However, the newly formed hydrogen bonds present in the soft phase serve as the molecular switch again. Finally, the second shape can be remembered as a permanent shape. If the second shape is deformed to any other shape (including shape A) at a temperature above the  $T_{trans}$  of the soft phase but below the  $T_{trans}$  of the hard phase, a new temporary shape can be obtained and fixed by cooling down below the  $T_{trans}$ . Thereafter, the second shape (e.g., shape B) can be recovered in the thermal recovery process. This technology provides an easy method to prepare shape-memory products with any shapes.

### 7.6.2 Shape-memory Effect for Hairstyles in Beauty Care

In addition to hair health, people wish to have different hairstyles for different occasions, or wish to maintain it for a long time. That is, hairstyles are expected to change shapes upon an external stimulus. PUPy are attractive for this SME on hair because they show shape change upon the stimulus of temperature. PUPy can form a large fraction of hydrogen bonds to show good thermally induced SME. Moreover, BINA-SMPU can be dissolved by acetic acid/ethanol mixing solvent to show very fast evaporation. Therefore, PUPy can be coated on hair *via* hydrogen bonds between PUPy and hair in a short time after PUPy solution is sprayed on hair.

### 7.6.3 Two-way Shape-memory Polymer Laminates

Chen and co-workers introduced two-way SMP [74] (i.e., polymer-laminated composites) by a layer method with one-way SMP. In the resultant polymer laminates, not only could two-way SME be achieved, but also reversible deformation could be controlled. Moreover, a wide range of response temperatures could be achieved. With regard to two-way SMP laminated composites, two independent layers are required.

One is an active layer made with SMP, and the other is a substrate layer made with a polymer having a high glassy modulus and slightly higher  $T_g$  than the  $T_{trans}$  of SMP. Hence, the produced bending force of the substrate layer can complement the recovery force of the active layer in the SMP laminate during the recovery (particularly in the cooling) process. **Figure 7.23** shows a typical two-way SME of SMP laminated composites. Based on investigation of the morphology of BINA-SMPU, it is known that BINA-SMPU has a very high glassy modulus ( $>1.0$  GPa) [32]. Also, the glassy modulus of BINA-SMPU does not decrease up to 60 °C. Therefore, BINA-SMPU is used not only as an active layer after deformation, but also serves as a good candidate for the substrate layer because it can provide high contrary recovery force during cooling.

#### **7.6.4 Medical Application: Antibacterial**

It is expected that after quaternisation with alkyl halides such as 1-iodooctadecane and 1-iodooctane, BINA-SMPU is expected to show excellent antibacterial properties due to its pyridinium moieties and high hydrophilicity [32]. In particular, if it is electrospun to nanofibres, antibacterial properties will be better. Hence, BINA-SMPU can be developed further to show excellent antibacterial properties for medical applications.

#### **7.6.5 Intelligent Windows for Smart Textile Applications**

BINA-SMPU not only shows thermally induced SME but also demonstrates good moisture-sensitive SME. By combining thermally induced SME and moisture-sensitive SME into a textile with two soft layers, an intelligent textile system is expected to be achieved. **Figure 7.24** illustrates an intelligent textile system for self-opening and self-closing. It is proposed that the textile is composed of two layers. One is the thermally induced SMP layer whereas the other one is a deformed moisture-sensitive SMP layer. As the moisture content and temperature of inner clothing increases, the moisture-sensitive SMP layer recovers to its original length. The window is then coiled, and the channel used for moisture permeation is opened. Hence, the body feels dry and cool. If the intelligent textile is dried at a temperature above the  $T_{trans}$  for the thermally induced SMP, the pre-stored strain presented by moisture-sensitive recovery will be recovered if the temperature is raised beyond the  $T_{trans}$ . Thermally induced shape recovery will result in self-closing of the window. Simultaneously, the moisture-sensitive layer is dried, and the  $T_g$  increased to above ambient temperature. Hence, the moisture-sensitive layer can show strain recovery with respect to high RH again. This process can be repeated many times.

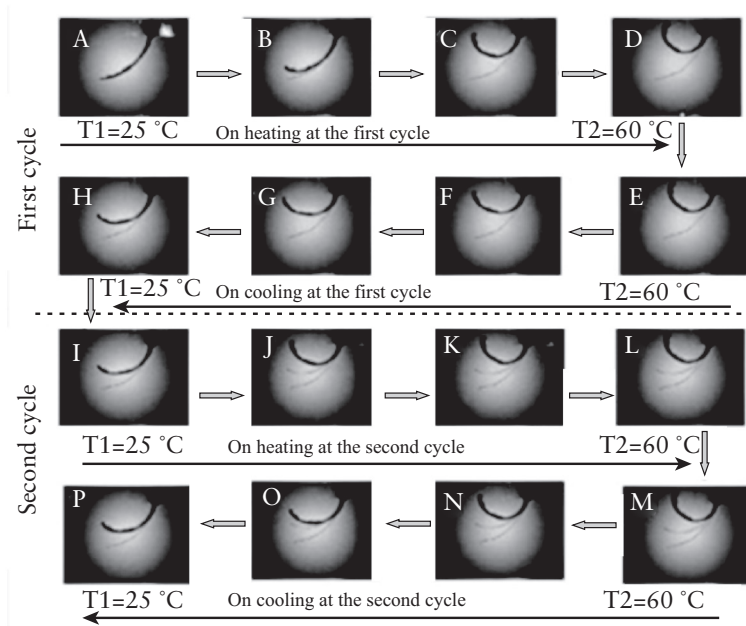


Figure 7.23 Typical two-way SME of SMP laminated composites

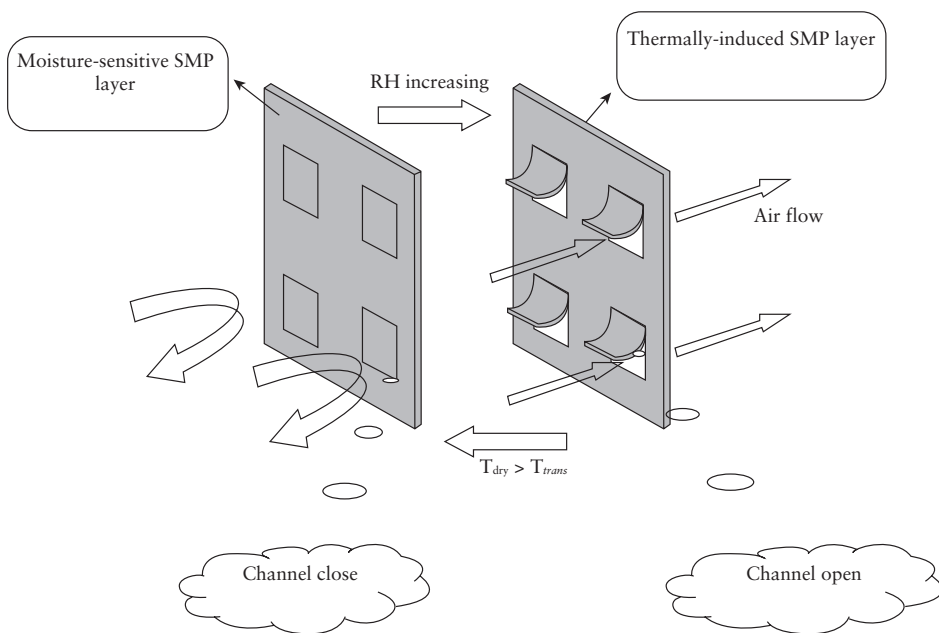


Figure 7.24 Intelligent textiles for self-opening and self-closing



## 7.7 Conclusions

Fabricating SMP with supramolecular switches has been an attractive research topic in recent years. In these SMP, the thermally reversible switching of supramolecular networks based on non-covalent interactions is used to control shape fixing and shape recovery in SMP. This chapter introduced the basic concepts of supramolecular chemistry, characterisation of SMP containing pyridine moieties, structure–property relationships, and potential applications of PUPy. The mechanisms for thermally as well as moisture-sensitive SME in PUPy were also described for deeper understanding of supramolecular SMP. Finally, the potential applications of PUPy, such as smart windows, medical applications, and reshape applications were suggested at the end of the chapter. We hope that our review will increase the number of research directions of SMP to promote the application of supramolecular SMP.

## References

1. J.H. Li, J.A. Viveros, M.H. Wrue and M. Anthamatten, *Advanced Materials*, 2007, **19**, 19, 2851.
2. J.L. Hu, Y. Zhu, H.H. Huang and J. Lu, *Progress in Polymer Science*, 2012, **37**, 12, 1720.
3. G.Q. Liu, X.B. Ding, Y.P. Cao, Z.H. Zheng and Y.X. Peng, *Macromolecular Rapid Communications*, 2005, **26**, 8, 649.
4. G.Q. Liu, X.B. Ding, Y.P. Cao, Z.H. Zheng and Y.X. Peng, *Macromolecules*, 2004, **37**, 6, 2228.
5. G.Q. Liu, C.L. Guan, H.S. Xia, F.Q. Guo, X.B. Ding and Y.X. Peng, *Macromolecular Rapid Communications*, 2006, **27**, 14, 1100.
6. S. Zhang, Z.J. Yu, T. Govender, H.Y. Luo and B.J. Li, *Polymer*, 2008, **49**, 15, 3205.
7. Y. Zhu, J.L. Hu and Y.J. Liu, *The European Physical Journal E*, 2009, **28**, 1, 3.
8. S.J. Chen, J.L. Hu and S.G. Chen, *Polymer International*, 2012, **61**, 2, 314.
9. S.J. Chen, J.L. Hu, H.T. Zhuo and S.G. Chen, *Journal of Materials Science*, 2011, **46**, 15, 5294.

10. S.J. Chen, J.L. Hu and H.T. Zhuo, *Journal of Materials Science*, 2011, **46**, 20, 6581.
11. S.J. Chen, J.L. Hu, S.G. Chen and C.L. Zhang, *Smart Materials and Structures*, 2011, **20**, 6.
12. S.J. Chen, J.L. Hu, H.T. Zhuo, C.W.M. Yuen and L.K. Chan, *Polymer*, 2010, **51**, 1, 240.
13. S.J. Chen, J.L. Hu, C.W.M. Yuen and L.K. Chan, *Polymer International*, 2010, **59**, 4, 529.
14. S.J. Chen, J.L. Hu, C.W.M. Yuen and L.K. Chan, *Materials Letters*, 2009, **63**, 17, 1462.
15. S.J. Chen, J.L. Hu, C.W.M. Yuen and L.K. Chan, *Polymer*, 2009, **50**, 19, 4424.
16. J.M. Lehn, *Science*, 1985, **227**, 4689, 849.
17. J.M. Lehn, *Chemical Society Reviews*, 2007, **36**, 2, 151.
18. J.M. Lehn, *Australian Journal of Chemistry*, 2010, **63**, 4, 611.
19. J.M. Lehn, *Progress in Polymer Science*, 2005, **30**, 8-9, 814.
20. J.M. Lehn, *Science*, 1993, **260**, 5115, 1762.
21. J.M. Lehn, *Proceedings of the National Academy of Sciences USA*, 2002, **99**, 8, 4763.
22. S. Ujiie and K. Iimura, *Macromolecules*, 1992, **25**, 12, 3174.
23. D. Braga, L. Maini, M. Polito and F. Grepioni, *Structure and Bonding*, 2004, **111**, 1.
24. I. Hyla-Kryspin, S. Grimme and J.P. Djukic, *Organometallics*, 2009, **28**, 4, 1001.
25. F. Cicoira, C. Santato and F. Rosei, *Topics in Current Chemistry*, 2008, **285**, 203.
26. A.J. Wilson, *Soft Matter*, 2007, **3**, 4, 409.
27. W. Shih, *Nature Materials*, 2008, **7**, 2, 98.

28. B.W. Pontius and P. Berg, *The Journal of Biological Chemistry*, 1992, **267**, 20, 13815.
29. L. Brunsveld, B.J.B. Folmer, E.W. Meijer and R.P. Sijbesma, *Chemical Reviews*, 2001, **101**, 12, 4071.
30. G. Armstrong and M. Buggy, *Journal of Materials Science*, 2005, **40**, 3, 547.
31. R.S. Neves, A.J. Motheo, R.P.S. Fartaria and F.M.S.S. Fernandes, *Journal of Electroanalytical Chemistry and Interfacial Electrochemistry*, 2008, **612**, 2, 179.
32. S. Chen, The Hong Kong Polytechnic University, 2009.
33. H.Y. Luo, Y. Liu, Z.J. Yu, S. Zhang and B.J. Li, *Biomacromolecules*, 2008, **9**, 10, 2573.
34. H.Y. Luo, M.M. Fan, Z.J. Yu, X.W. Meng, B.J. Li and S. Zhang, *Macromolecular Chemistry and Physics*, 2009, **210**, 8, 669.
35. M.M. Fan, Z.J. Yu, H.Y. Luo, Z. Sheng and B.J. Li, *Macromolecular Rapid Communications*, 2009, **30**, 11, 897.
36. H.X. Yang, Y.F. Li, J.G. Liu, S.Y. Yang, D.X. Yin, L.C. Zhou and L. Fan, *Journal of Applied Polymer Science*, 2004, **91**, 6, 3981.
37. E. Scortanu, C. Prisacariu, E.G. Hitruc and A.A. Caraculacu, *High Performance Polymers*, 2006, **18**, 6, 877.
38. O. Ihata, H. Yokota, K. Kanie, S. Ujiie and T. Kato, *Liquid Crystals*, 2000, **27**, 1, 69.
39. T. Kato, N. Mizoshita and K. Kishimoto, *Angewandte Chemie International Edition*, 2006, **45**, 1, 38.
40. D. Capitani, N. De Prisco, P. Laurienzo, M. Malinconico, N. Proietti and A. Roviello, *Polymer Journal*, 2001, **33**, 8, 575.
41. T. Kato and J.M.J. Frechet, *Journal of the American Chemical Society*, 1989, **111**, 22, 8533.
42. T. Gulikkrzywicki, C. Fouquey and J.M. Lehn, *Proceedings of the National Academy of Sciences USA*, 1993, **90**, 1, 163.

43. H. Kihara, T. Kato, T. Uryu and J.M.J. Frechet, *Chemical Materials*, 1996, 8, 4, 961.
44. H. Bernhardt, H. Kresse and W. Weissflog, *Molecular Crystals and Liquid Crystals Science and Technology*, 1997, 301, 25.
45. A. Sautter, C. Thalacker and F. Wurthner, *Angewandte Chemie International Edition*, 2001, 40, 23, 4425.
46. K.N. Koh, K. Araki, T. Komori and S. Shinkai, *Tetrahedron Letters*, 1995, 36, 29, 5191.
47. A. Kraft, A. Reichert and R. Kleppinger, *Chemical Communications*, 2000, 12, 1015.
48. T. Kato, H. Kihara, T. Uryu, A. Fujishima and J.M.J. Frechet, *Macromolecules*, 1992, 25, 25, 6836.
49. T. Kato, H. Kihara, S. Ujiie, T. Uryu and J.M.J. Frechet, *Macromolecules*, 1996, 29, 27, 8734.
50. T. Kato, M. Nakano, T. Moteki, T. Uryu and S. Ujiie, *Macromolecules*, 1995, 28, 26, 8875.
51. T. Kawakami and T. Kato, *Macromolecules*, 1998, 31, 14, 4475.
52. D. Stewart and C.T. Imrie, *Journal of Materials Chemistry*, 1995, 5, 2, 223.
53. K.I. Alder, D. Stewart and C.T. Imrie, *Journal of Materials Chemistry*, 1995, 5, 12, 2225.
54. C.M. Paleos and D. Tsiourvas, *Angewandte Chemie International Edition*, 1995, 34, 16, 1696.
55. T. Kato, O. Ihata, S. Ujiie, M. Tokita and J. Watanabe, *Macromolecules*, 1998, 31, 11, 3551.
56. G. Ambrozic, J. Mavri and M. Zigon, *Macromolecular Chemistry and Physics*, 2002, 203, 2, 439.
57. G. Ambrozic and M. Zigon, *Acta Chimica Slovenica*, 2005, 52, 3, 207.
58. G. Ambrozic and M. Zigon, *Polymer International*, 2005, 54, 3, 606.

59. A. Harada, Y. Takashima and H. Yamaguchi, *Chemical Society Reviews*, 2009, **38**, 4, 875.
60. H.H. Tønnesen, M. Másson and T. Loftsson, *International Journal of Pharmaceutics*, 2002, **244**, 1, 127.
61. H.-J. Buschmann, U. Denter, D. Knittel and E. Schollmeyer, *Journal of the Textile Institute*, 1998, **89**, 3, 554.
62. A. Miyawaki, Y. Takashima, H. Yamaguchi and A. Harada, *Tetrahedron*, 2008, **64**, 36, 8355.
63. S.A. Nepogodiev and J.F. Stoddart, *Chemical Reviews*, 1998, **98**, 5, 1959.
64. M. Nakahata, Y. Takashima, H. Yamaguchi and A. Harada, *Nature Communications*, 2011, **2**, 511.
65. X.J. Han, Z.Q. Dong, M.M. Fan, Y. Liu, Y.F. Wang, Q.J. Yuan, B.J. Li and S. Zhang, *Macromolecular Rapid Communications*, 2012, **33**, 12, 1055.
66. S. Tamesue, Y. Takashima, H. Yamaguchi, S. Shinkai and A. Harada, *Angewandte Chemie*, 2010, **122**, 41, 7623.
67. L. Huang and A.E. Tonelli, *Journal of Macromolecular Science-Reviews in Macromolecular Chemistry and Physics*, 1998, **C38**, 4, 781.
68. A. Harada, J. Li and M. Kamachi, *Macromolecules*, 1993, **26**, 21, 5698.
69. M. Ceccato, P. Lo Nostro and P. Baglioni, *Langmuir*, 1997, **13**, 9, 2436.
70. A. Harada, T. Nishiyama, Y. Kawaguchi, M. Okada and M. Kamachi, *Macromolecules*, 1997, **30**, 23, 7115.
71. Z.Q. Dong, Y. Cao, Q.J. Yuan, Y.F. Wang, J.H. Li, B. J. Li and S. Zhang, *Macromolecular Rapid Communications*, 2013, **34**, 10, 867.
72. I. Tomatsu, A. Hashidzume and A. Harada, *Macromolecules*, 2005, **38**, 12, 5223.
73. O. Peters and H. Ritter, *Angewandte Chemie International Edition*, 2013, **52**, 34, 8961.
74. S.J. Chen, J.L. Hu, H.T. Zhuo and Y. Zhu, *Materials Letters*, 2008, **62**, 25, 4088.

# 8

## Applications of Shape-memory Polymers

### 8.1 Introduction

Shape-memory polymers (SMP) have drawn wide attention due to their shape-moving functionality triggered by various stimuli, as well as their low cost, low weight, and easy manufacture. Recent developments include medical, spacecraft and textile applications. Several review articles have included the applications of SMP in various areas [1–4], particularly in biomedical fields [1].

In this chapter, we have selected and classified the applications of SMP into four major categories. The first are the applications of bulk SMP for realising different functions using different shape-memory effects (SME). The second are SMP applications for surface patterning and wrinkling. This is an emerging area of study and will be a promising direction of SMP applications because of their diversified functions and easy implementation. The third and fourth categories are textile and engineering applications.

### 8.2 Applications of Bulk Shape-memory Polymers

Figure 8.1 shows the response of a thermo-sensitive SMP to a typical thermo-mechanical cycle, which is represented as a three-dimensional (3D) plot of strain *versus* temperature and force. Beginning at zero strain, the SMP becomes soft, and deformation can be caused readily by application of a load at an elevated temperature (stage 1). Then, the shape can be ‘fixed’ during cooling and unloading at room temperature or cooler (stage 2). Thus, the work undertaken on the sample can be stored as the latent strain energy if recovery of the polymer chains is prohibited by vitrification, crystallisation or other means. Upon subsequent heating above the critical transition temperature ( $T_{trans}$ ), the glass transition temperature ( $T_g$ ) or melting temperature ( $T_m$ ), the stored strain energy can be released (stage 3). Different applications use different parts of the SME of an SMP in this cycle. Under high temperature in stage 1, the Young’s modulus is low, an effect that has been used for the deployment of airplane wings. The fixed shape (fixation) in stage 2 after removal of the external stimulus has many applications (e.g., orthopaedic devices). If the temperature increases, the shape

recovers (stage 3), a feature used for several purposes: (i) actuation; (ii) deployment; (iii) self-healing if the shape is compressed accidentally; and (iv) fitting if the original shape is stretched. In this section, we introduce examples of SMP as materials for different applications that are related directly to different stages in the SME cycle.

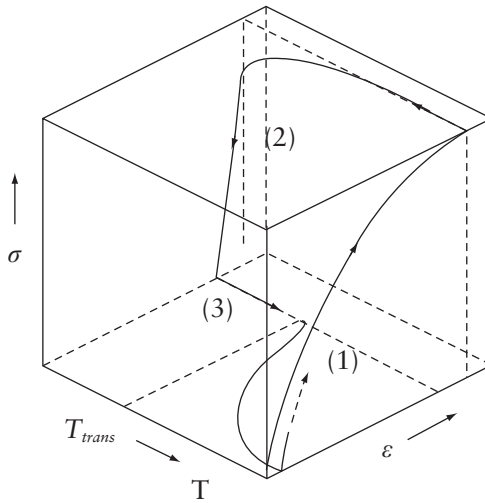


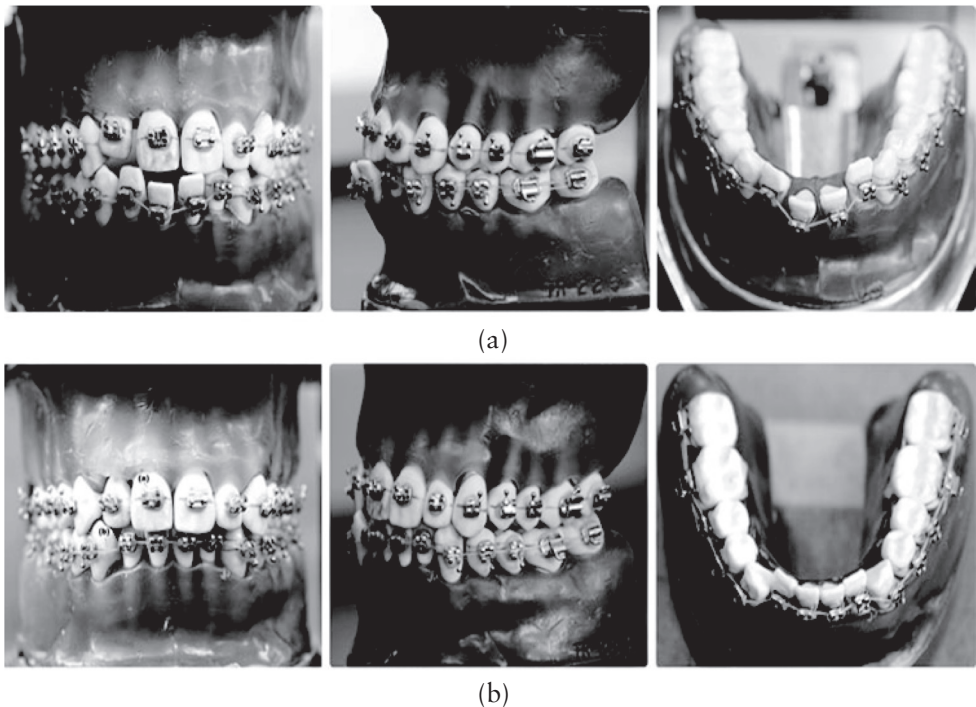
Figure 8.1 Typical thermo-mechanical cycle of a thermo-sensitive SMP.  $T_{trans}$ ; transition temperature. Reproduced with permission from Q. Meng, J. Hu, Y. Zhu, J. Lu and Y. Liu, *Journal of Applied Polymer Science*, 2007, 106, 2515. ©2007, John Wiley & Sons [2]

### 8.2.1 Fixation

Realisation of the fixation function is, in general, approached by releasing the stored stress upon removal of the external stimulus or by formation of a certain structure. After deformation at a high temperature, the shape is fixed if the temperature is decreased to a low temperature. Utilisation of this shape for specific functions has been widely accepted.

### 8.2.1.1 Orthodontic Wires

One application of SMP as fixation materials is their use in orthodontic wires. Traditional metallic orthodontic wires have superior properties: rigidity, flexibility, fatigue resistance, durability, and operability. However, their metallic colour poses aesthetic problems. Jung and Cho [3] reported on orthodontic wires made of shape-memory polyurethanes (SMPU) with poly( $\epsilon$ -caprolactone) (PCL) ( $M_n = 3,000$ ) as an alternative to metallic orthodontic wires. Their SMPU possessed many advantages: low density, high shape recovery, easy processing, transparency and aesthetically satisfactory appearance. Additionally, in contrast to the usual elastomers, it provided a constant shape recovery force to teeth over a long period of time (Figure 8.2). It was found that the shape recovery force reached a fixed level of 50 gf after certain reduction during the initial 2 h of application, and was then maintained for  $\approx 20$  days.



**Figure 8.2** Photographs of the PU wire-type orthodontic appliance (a) before and (b) after orthodontic treatment. PU: Polyurethanes. Reproduced with permission from Y.C. Jung and J.W. Cho, *Journal of Materials Science: Materials in Medicine*, 2010, 21, 10, 2881. ©2010, Springer [3]



### *8.2.1.2 Medical Casts*

Medical casts are commonly used to heal broken bones, tendon tears, and other injuries to limbs. Rousseau and co-workers [4] invented methods of applying a SMP with a larger diameter as a medical cast. After the material is fitted to the position of the injury and heated substantially to its  $T_{trans}$ , the primary temporary shape (i) attempts to revert to its permanent shape, and (ii) conforms to a secondary temporary shape with a diameter smaller than the diameter of the primary temporary shape and larger than that of the permanent shape, wherein the SMP in the secondary temporary shape conforms to the limb. Compared with traditional casting materials, the advantage of SMP is obvious because of their light weight, recyclability, permeability, ease of processing, X-ray transparency, and low cost.

## **8.2.2 Actuation**

Actuation entails the use of an actuator to move or control a mechanism or system as a type of motor. It is driven by a source of external energy, such as heating, electric current, radiation or air pressure. SMP as smart materials can ‘sense’ the specific external stimulus to automatically recover to their permanent shape from a programmed temporary shape. Therefore, they have already been provided with the capacity to release their entropic energy and to move a system upon triggering. Thus, actuation uses the recovery force from the thermo-mechanical SME cycle of a polymer as a motor. Diversified triggering patterns for actuation have been developed that use heating, electricity and alternating magnetic fields for the design of actuators. Some previously reported strategies are reviewed below.

### *8.2.2.1 Actuation Realised by Combining Shape-memory Polymers with Specific Structures*

In some specific actuator structures, the shape fixity of the SMP provides the advantages of fixing a rigid shape or stiffening a particular functional shape without the need for continuous control. In this case, actuation arises from the other driving part of the actuator structure, and SMP impart the controllable supporting force to achieve the designed function. The SMP-based McKibben artificial muscle was made by coating a SMP onto the braided mesh shell of a commercial McKibben artificial muscle [5]. If heated above the  $T_g$  of the SMP, it can be used as a conventional McKibben muscle. If the actuator reaches the desirable length, cooling to below the  $T_g$  can ‘freeze’ the structure into a rigid, actuated state without any air supply or control system. In this way, the SMP enhances the versatility of this type of artificial muscle (**Figure 8.3**). Likewise, in a nitinol-core/SMP-shell thermally activated endovascular thrombectomy

device, the SMP reaches its  $T_g$  and undergoes a reduction in its elastic modulus, allowing the micro-actuator to transform from a straight form for endovascular delivery to a pre-programmed corkscrew form for the clot retrieval (Figure 8.4). In this case, an electric current in the nitinol provides the electro-resistive (Joule) heat. If the current is turned off, the nitinol and SMP cool below the  $T_g$ , and the polymer returns to its glassy rigid state, ensuring enhanced stiffness to the corkscrew shape for removal of the clot or thrombus [6, 7].

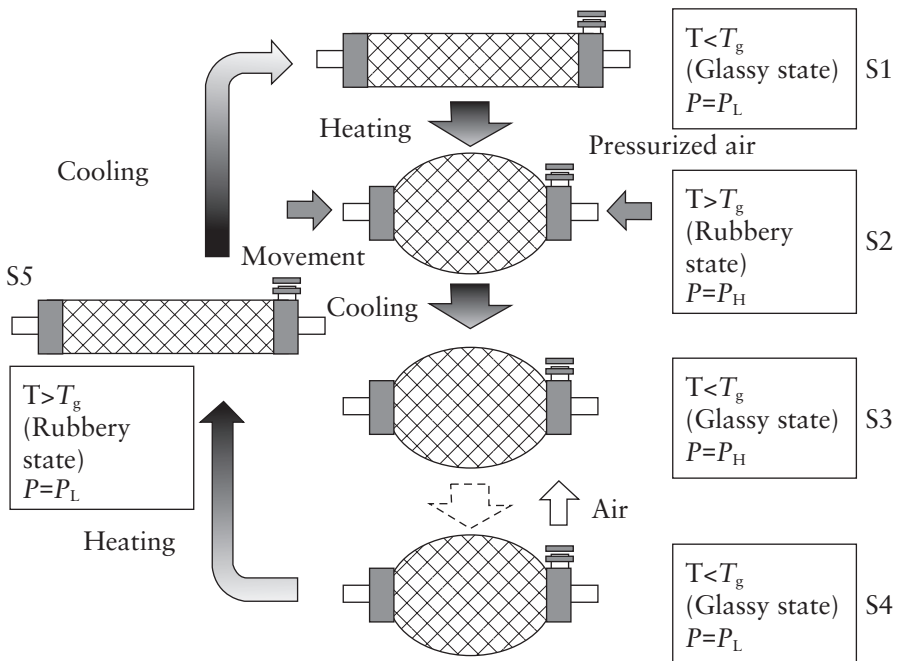
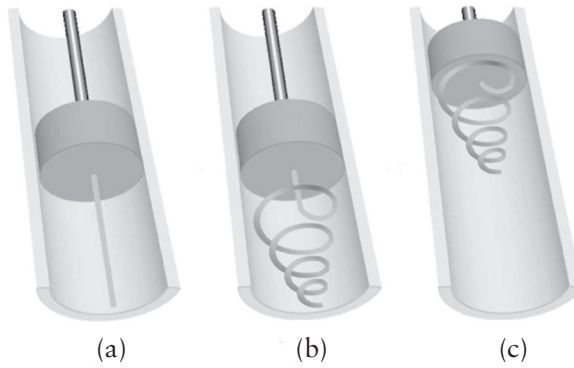


Figure 8.3 The McKibben artificial muscle, which uses SMP (schematic).  $P_H$ : high pressure and  $P_L$ : low pressure. Reproduced with permission from K. Takashima, J. Rossiter and T. Mukai, *Sensors and Actuators A: Physical*, 2010, 164, 1-2, 116. ©2010, Elsevier [5]



**Figure 8.4** Endovascular removal of a thrombus using a SMPU microactuator (schematic): (a) insertion of the microactuator as a straight rod (temporary shape) to the vascular occlusion, (b) triggering of the microactuator to obtain its primary corkscrew shape, and (c) retraction of the microactuator to remove the captured thrombus to restore blood flow. Reproduced with permission from W.I. Small, M.F. Metzger, T.S. Wilson and D.J. Maitland, *IEEE Journal of Selected Topics in Quantum Electronics*, 2005, 11, 4, 892. ©2005, IEEE [7]

### 8.2.2.2 Actuation arising from a Two-way Shape-memory Effect

Two-way SME have been reported in liquid-crystal elastomers (LCE) [8, 9],  $T_m$ -type SMP under constant stress [10], and laminated composites [11]. These systems are good candidates for achieving bending actuation. For example, the LCE systems developed by the Harris research team with a densely crosslinked and twisted configuration of azobenzene units demonstrated a high elastic modulus at room temperature ( $\approx 1$  GPa) [12]. Mechanical energy is related to the elastic modulus, so the systems are expected to provide great work output as light-driven actuator materials. Consequently, LCE with azobenzene units are intriguing smart actuator devices for the conversion of light energy into mechanical energy [13].

### 8.2.3 Deployment

In general, deployment implies moving a product from a temporary state to a permanent or desired state. To some extent, this concept corresponds to the definition of shape-memory function [14]. Hence, the temporary shape is determined by programming to store the entropic energy as a driving force to conduct the deployable

movement. The deployment arising from the shape-memory function of a SMP can be self-executable without a complicated system or mechanical structure. Recent advances in the self-deployable applications of SMP are reviewed in this section to provide insight into this promising area.

### ***8.2.3.1 Cold Hibernated Elastic Memory of Shape-memory Polymer Foams***

Because of their high shape-recovery ratio and compression ability ( $\leq 90\%$ ), SMP foams have attracted substantial interest in recent years. Their potential applications include micro-foldable vehicles, micro-tags and hearing aids [15, 16]. SMP foams can also be used for the embolic treatment of aneurysms [17]. SMP foam devices with a higher  $T_g$  can be delivered in a compressed state through a micro-catheter into the human body. Then, upon laser triggering, the SMP foam devices can expand in an aneurysm to provide successful treatment (Figure 8.5). The deployment time, maximum heating temperature, absorption of laser light by blood and tissue, as well as heat transfer from the device to blood and tissue require further engineering to avoid thermal damage to arterial tissue, but prototype SMP foam devices are an innovative treatment option [18].

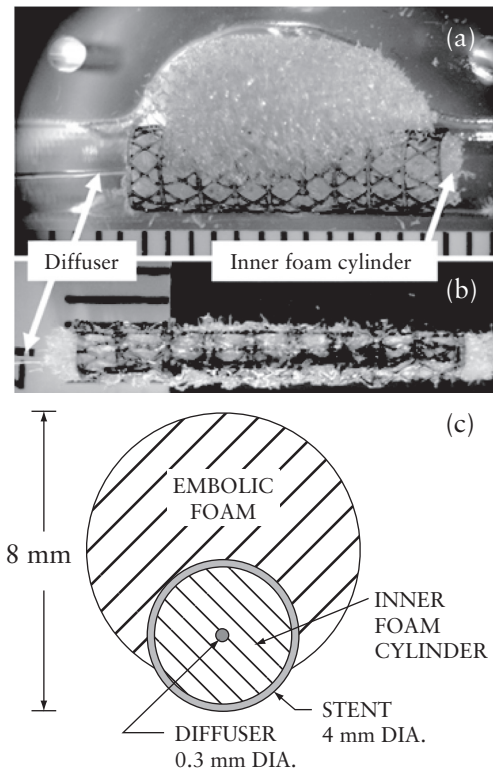
### ***8.2.3.2 Expandable Stents***

Interventions using SMP cardiovascular stents can reduce the catheter size for delivery and provide controlled deployment at body temperature. The recovery time and thermo-mechanical properties of stents have been shown to be controlled easily by the  $T_g$  and crosslink density for a tailor-made design, and are the target of further study (Figure 8.6) [19]. Hydration of polymers in the aqueous environment of vessels can also reversibly trigger the deployment of SMP stents with crosslinking structures from a clamped state to an expanded state [20]. Moreover, at 37 °C, the full collapse pressure of SMP stents is comparable with that of commercially available stents [21]. Expandable stents can also be used for drug-delivery applications because 35 wt% of a stent can be used to carry a high dose of an active agent [22].

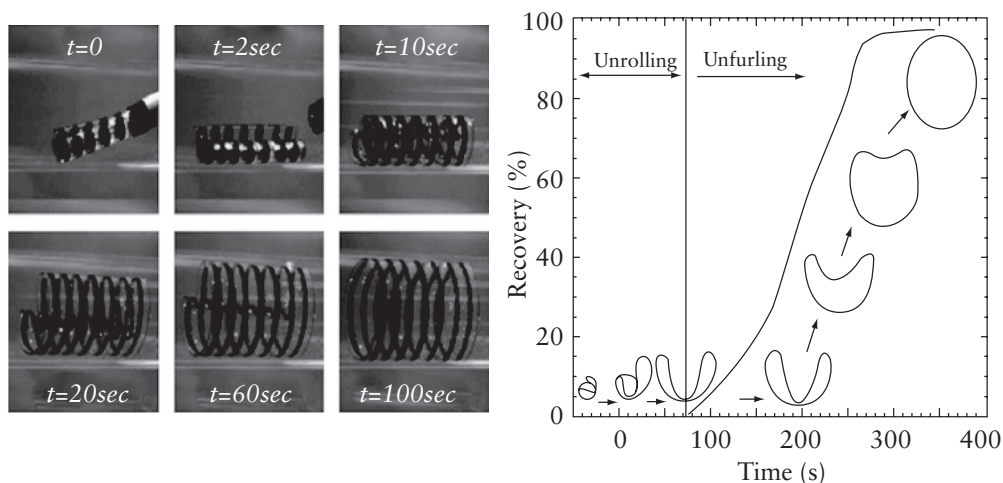
### ***8.2.3.3 Deployable Dialysis Needles, Coils and Neuronal Electrodes***

The other deployable application of SMP is in the design of adapters. These are deployed by a needle, warmed by blood flow, and expanded to their primary shape in a vessel to reduce the hemodynamic stress caused by impingement of flow of a dialysis needle within an arteriovenous graft [17]. Hampikian and co-workers [23] also reported that SMP coils with a  $T_g$  approximately at body temperature can be

used to treat intracranial aneurysms. In this capacity, a SMP coil with a temporary straightened shape can be deployed into an aneurysm cavity through simulated blood flow, and can subsequently recover its programmed coil shape to efficiently reduce flow velocity in the artificial aneurysm. In clinical practice, the deployed coil will lead to thrombus formation for aneurysm treatment. In the application of neuronal probes for long-term recording of brain activity and functional stimulation, existing metallic and ceramic probes cannot meet the requirement for long-term biocompatibility with brain tissue. Softer SMP probes not only enhance long-term biocompatibility but also provide self-implantation at suitably slow rates with sufficient insertion force to decrease the initial trauma caused by implantation [24].



**Figure 8.5** SMP stent-foam device with removable inner foam cylinder and laser light diffuser a) before and b) after collapsing for delivery, and c) cross-sectional diagram of the expanded device with a removable inner foam cylinder. Reproduced with permission from W. Small, P.R. Buckley, T.S. Wilson, W.J. Benett, J. Hartman, D. Saloner and D.J. Maitland, *IEEE Transactions on Biomedical Engineering*, 2007, 54, 6, 1157. ©2007, IEEE [17]



**Figure 8.6** Recovery of a 20 wt% crosslinked SMP stent with  $T_g = 52$  °C delivered via a 18-F catheter ( $\approx 6$  mm) into a 22-mm ID glass tube containing body-temperature water (37 °C). Reproduced with permission from C.M. Yakacki, R. Shandas, C. Lanning, B. Rech, A. Eckstein and K. Gall, *Biomaterials*, 2007, 28, 14, 2255. ©2007, Elsevier [19]

### 8.2.4 Self-healing

Self-healing in materials (in which damage is detected and repaired *in situ*) is the result of a new and innovative approach to the extension of material lifetime and reliability in use. The main self-healing mechanism is the incorporation of external healing agents. This approach is successful for healing damage at the micro-length scale. Compared with the method described above, SMP can be used to heal damage at the structural-length scale, and SMP outperform the self-healing schemes described above because they are driven by conformational entropy. Thus, the self-healing is controllable by programming and can be repeated. The reverse plasticity SME proposed by Xiao and co-workers [25] is the basis of the self-healing of polymers. Self-healing that uses the shape recovery of SMP under unconfined conditions is applicable to external scratches, surfaces and damage to thin materials, or to the internal cracks and flaws of an object under confined conditions.

In daily life, surface damage often occurs to plastic goods. Sliding friction and plowing can play important parts during damage and scratching of a surface. Rodriguez and co-workers [26] prepared a blend system consisting of a crosslinked PCL network

with linear PCL interpenetrating the network. This system exhibited a combination of shape-memory response from the network component and self-healing capacity from the linear component, which was termed ‘shape-memory assisted self-healing’ (SMASH). They found excellent self-healing effects of the films by the SMASH mechanism, which leads to nearly complete healing for linear PCL content >25 wt%.

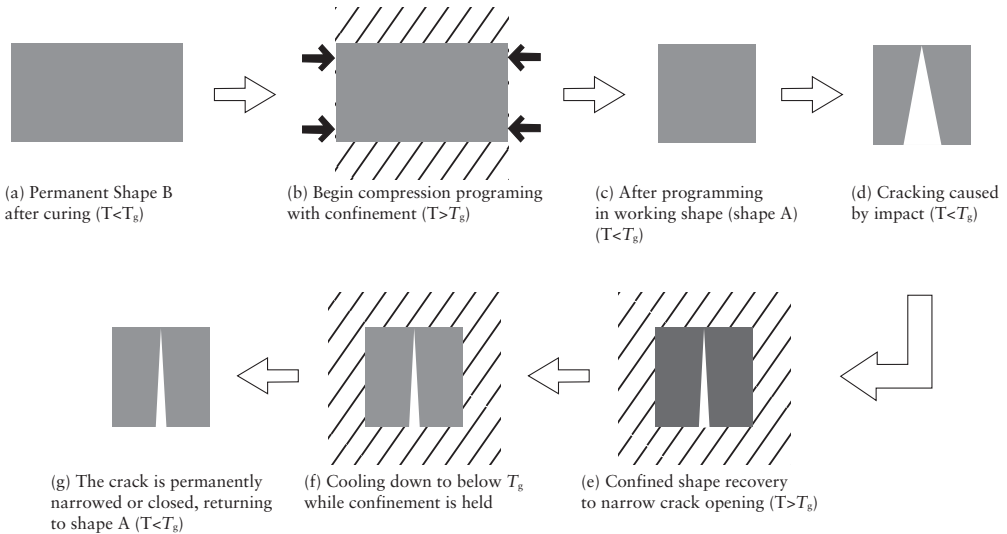
Xiao and co-workers [25] used free-standing nanolayered graphene as the filler to fabricate epoxy-based SMP composites. They found that the composites displayed significant property enhancement over unfilled SMP (including scratch resistance and thermal healing capabilities under stress-free conditions). Jorcin and co-workers [27] and Gonzalez-Garcia and co-workers [28] applied segmented block SMPU as a self-healing coating for the corrosion protection of pure aluminium and aluminium alloys. They found that the SMPU film recovered its shape after heat treatment, and could physically heal coating defects if damaged. In the proposed mechanism, an increase in temperature leads to relaxation of the soft segments, which fill the damaged area, whereas the hard segment preserves the mechanical properties of the film.

#### **8.2.4.1 Confined Shape-recovery Self-healing**

Because of the widespread use of thermoset polymers in structural applications, the self-healing of damage in thermosetting polymers has been a research focus for years. To mimic biological systems, Li and Nettles [29] believed that the self-healing of structural-scale damage could require multiple schemes or steps, and at least two steps must be considered: close then heal (CTH). They thought that SMP could be used to partially repair structural damage under confined shape recovery (first step of CTH). The self-healing mechanism is shown in **Figure 8.7**. They fabricated SMP-based syntactic foam by dispersing 40% by volume of hollow glass microspheres into the SMP resin. They found that 3D confined shape-recovery could fully close internal cracks. However, without external confinement, the SMP matrix would recover its original shape with little or no closure of internal cracks. Therefore, external confinement, along with compression programming, is the key to achieving self-closing. Nji and Li [30] proposed a 3D-woven fabric-reinforced SMP composite for impact mitigation using a three-step strain-controlled thermo-mechanical cycle at a pre-strain level of 5% and a one-dimensional confined shape-memory recovery. This composite had a self-healing capacity in addition to the various advantages associated with 3D-woven composites. Li and co-workers also published other articles to investigate the self-healing application of SMP and explain their proposed mechanism [31–33].

Development of self-healing SMP can compensate for the lack of non-destructive testing in offline and manual patching technology, and can repair damage to materials

quickly and spontaneously. The self-healing of SMP is in the preliminary exploration stage, but it is expected to solve key technology problems that cannot be solved by traditional methods. Therefore, self-healing of SMP has significant development prospects and value in some important engineering and advanced technological fields.



**Figure 8.7** Self-closing scheme of a proposed smart foam. Reproduced with permission from G.Q. Li and D. Nettles, *Polymer*, 2010, 51, 3, 755. ©2010, Elsevier [29]

### 8.2.5 Fitting

Application of SMP as packaging materials is well known in industrial settings, where they appear as heat-shrinkable films [34]. Their heat-shrinkage ability (or controlled shrinkage ability) is identical to thermally induced SME. Various polymer systems such as polyethylene (PE), polyethylene terephthalate and polyvinyl chloride (PVC) have been employed as thermal-shrinkage packaging materials. Their transparency, tightness, moisture resistance, processing simplicity, low cost, and diversity of packing have drawn significant industrial attention. Future development of these applications may lie in the development of more environmentally protective products and lower costs.



A classical application of SMP is heat-shrinkable tubing. Products with various diameters, transition conditions and other additional properties have been employed broadly in industry. Upon heating to their appropriate temperature, the tube shrinks to its original shape, thereby providing fixation, sealing, insulation, protection and other additional properties. Their typical application is as jackets for cables, which provide protection against abrasion from their surroundings and guarantee their insulation properties [35]. Polymer systems based on polytetrafluoroethylene, polyvinylidene fluoride, fluorinated ethylene propylene, PVC, and other similar materials are available commercially.

### **8.3 Applications in Surface Wrinkling and Patterning**

Wrinkling has been proven to be an effective method for the fabrication of patterned substrates. These periodic micro- or nano-sized surface patterns (wrinkling) can have many unusual properties: super hydrophobicity (wetting and spreading); self-cleaning ('lotus effect'); local structural colours; bonding and adhesion; friction, lubrication and surface roughness; drag and fluid flow. Accordingly, they have a wide range of applications in various fields: biological applications for modulating cellular-substrate interactions *via* dynamic nano-topography; nano-actuation applicable to stimuli-responsive polymer systems that exhibit nano-scale deformation under load; swimming suits and anti-reflection with sharkskin properties; biosensors; tribological uses; nano-metrology; stretchable electronics and nano-lithographic data storage capabilities (particularly in light of the ability to conceal stored data in a form of steganography) [36]. Therefore, these applications have enabled scientists to explore ways of creating surface wrinkling to achieve unusual physical properties, as mentioned above. Existing research shows that simple and cost-effective approaches can lead to surface patterning atop SMP.

#### **8.3.1 Principle of Surface Wrinkling**

In one of the physical mechanisms for wrinkle formation, if a rigid thin film supported on a soft substrate is compressed laterally beyond a critical strain, the mechanical instability leads to surface wrinkling. Because the moduli of SMP at higher temperature above the shape-memory  $T_{trans}$  are in line with those of elastomers, SMP are highly attractive materials as wrinkle substrates. Moreover, the strain fixing capability of SMP can be utilised to create localised indents [37]. The wrinkling of elastic gold thin SMP films atop different types of substrates has been investigated systematically under different conditions by Zhao and co-workers [38]. Different patterns of self-organised wrinkles (labyrinthine, striped, ring-shaped and radial) are obtained atop

polystyrene (PS)-based SMP (Figure 8.8). Depending on surface conditions, heating temperature and pre-straining, different patterns of micro- and nano-scaled wrinkles are produced. The authors demonstrated that the elastic buckling of the gold layer is the mechanism behind all types of wrinkles, and that SME and thermal expansion mismatches are the driving forces for the production of different patterns after heating to different temperatures.

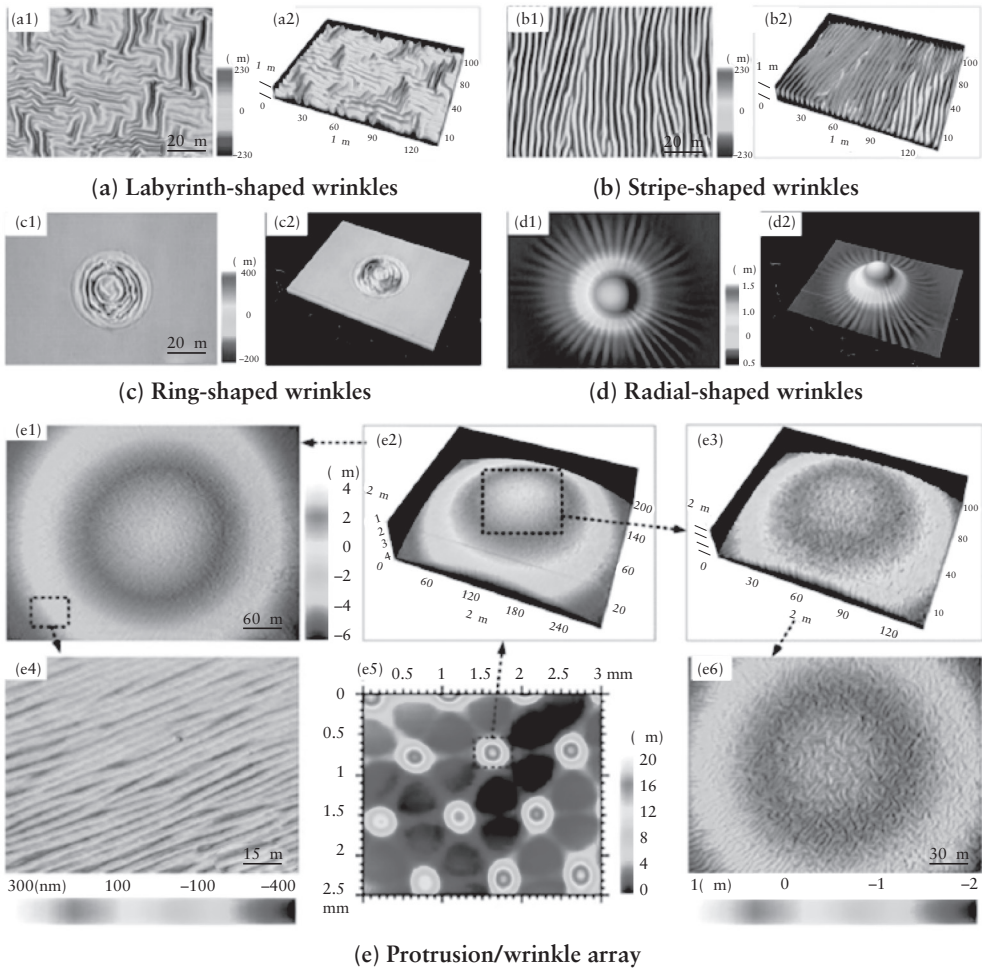


Figure 8.8 Wrinkle patterns. 1: two-dimensional (2D) top view; 2: 3D view. Reproduced with permission from Y. Zhao, W.M. Huang and Y.Q. Fu, *Journal of Micromechanics and Microengineering*, 2011, 21, 6. ©2011, IOP Science [38]

### **8.3.2 Wetting and Spreading**

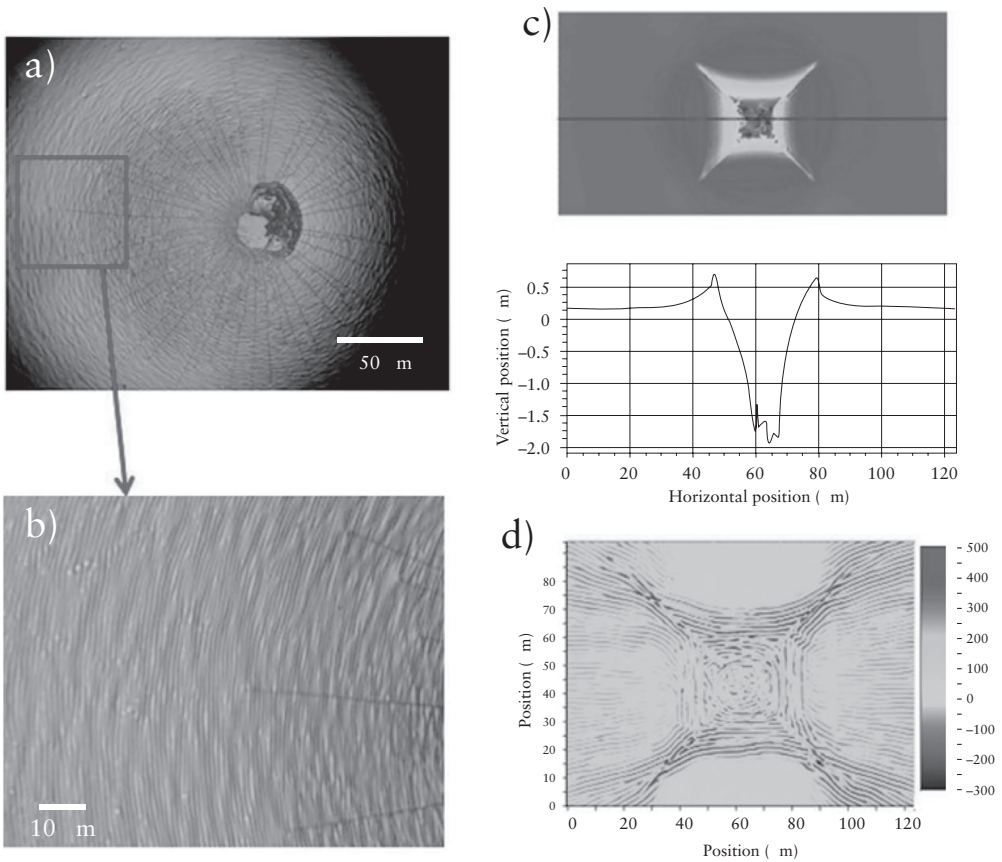
Sun and co-workers [39] reported that hydrophobicity can be a property of bio-inspired surface structures (e.g., lotus leaves or sharkskin) using periodic micro- or nano-sized patterns, which can offer significant commercial potential (e.g., swimming suits or antireflection coatings). For this purpose, they studied the spreading of water droplets atop smooth and patterned substrates using SMP. The influence of solid surface patterns and size of liquid droplets was investigated. Wetting anisotropy appeared if the droplets spread on the anisotropically patterned substrates. Static contact angles measured in the direction parallel to wrinkles were smaller than those measured in the direction perpendicular to wrinkles for the same droplet size, and the droplets elongated along wrinkles. The droplet size had an effect only on the anisotropically patterned substrates. Static contact angles increased and droplet elongation decreased as droplet size increased. Droplets were pinned at the edges of wrinkles if spreading perpendicular to them, showing a non-circular shape, and pinning was less obvious if the droplets were  $\leq 20 \mu\text{l}$ .

Xie and co-workers [40] described a highly versatile method using SMP to create localised structural colours by depositing a gold thin film on an epoxy SMP ( $T_{\text{trans}} \approx 40 \text{ }^\circ\text{C}$ ) to wrinkle the surface. The 3D appearance of their coloured logo originated from the light diffraction caused by the 2D wrinkle structure under regular fluorescent light while changing only the viewing angle ( $< 45 \text{ }^\circ\text{C}$ ) (**Figure 8.9**). The advantage of their method lies in its flexibility (i.e., an arbitrary structurally coloured image can be produced in most laboratories as long as the simple equipment needed for metal deposition is available). With a rigid thin film, the strain history at the local scale is captured by wrinkle-based colours, and spatially controlled wrinkles can be attractive for display. The fact that the wrinkles have been proven to be sensitive to the strain distribution at the microscopic scale may also be utilised for anti-counterfeiting purposes.

### **8.3.3 Adaptable Biological Devices for Modulating Cellular–substrate Interactions**

Nguyen and co-workers [41] fabricated tunable shrink-induced honeycomb microwell arrays for uniform embryoid bodies (EB) from a single-cell suspension. By printing various microwell patterns onto pre-stressed PS sheets and employing heat-induced shrinking, high aspect micro-moulds were generated. Notably, they achieved rounded-bottom polydimethylsiloxane wells, which are not easily achievable with standard micro-fabrication methods but are critical for the achievement of spherical EB using SMP. Furthermore, by controlling the size of the microwells and concentration of the cell suspension, they could control the initial size of the cell aggregate, thereby

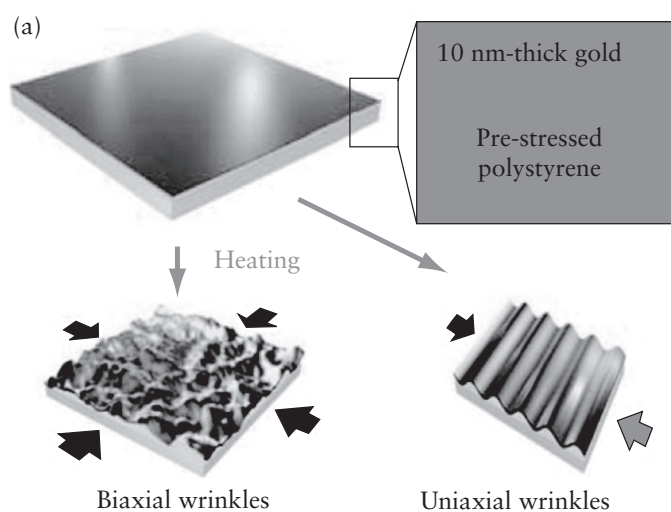
influencing the lineage commitment. In addition, these microwells are readily adaptable and scalable to most standard well plates, and are easily integrated into the handling of commercial liquids.



**Figure 8.9** Localised wrinkle formation at microscopic scales. Optical microscopic images of circularly distributed wrinkle structures created by a spherical indenter. a) low magnification; b) higher magnification); c) top and side view of the plastic deformed substrate using a Vickers indenter before wrinkling; and d) wrinkle structures created by the Vickers indent. Reproduced with permission from T. Xie, X.C. Xiao, J.J. Li and R.M. Wang, *Advanced Materials*, 2010, **22**, 39, 4390. ©2010, John Wiley & Sons [40]

### 8.3.4 Biosensor and Micro-systems

Fu and co-workers [42] presented a simple and ultra-rapid method to controllably create tunable nanometer-scale biaxial and uniaxial wrinkles on Shrinky-Dink sheets (PS-based SMP sheets) (Figure 8.10). They achieved tunable nano-wrinkles with broad tunable wavelength distributions (10–50 nm). Nanometer-scale wrinkles enable the use of these self-organised structures for surface plasmon resonance (SPR)-based sensing applications such as metal-enhanced fluorescence (MEF). Such flexibility and heterogeneity hold several advantages over single, homogeneous wavelength wrinkles. For instance, for further studies on multiple-probe MEF, these properties enable adjustment of broad SPR bands to overlap with the various absorption bands of fluorophores. A new approach was developed by Liu and co-workers [43] to fabricate various sidewall patterns *via* strain recovery deformations of a shape-memory (SM) PS film to overcome the limitations of the existing lithography for generating substrate sidewall patterns that can be used for vertical interconnects or electronic components in 3D circuits in microsystems. A  $50 \times 50 \mu\text{m}^2$  array of silver dots, 150- $\mu\text{m}$  wide lines and serpentine-shaped micro-resistors were generated on the top and side surfaces of PS blocks, followed by the characterisation of these products (including shrinking and pressing deformations, surface roughness, wrinkling deformations and resistance changes).



**Figure 8.10** Fabrication of biaxial (left) and uniaxial (right) wrinkles (schematic). Reproduced with permission from C.C. Fu, A. Grimes, M. Long, C.G.L. Ferri, B.D. Rich, S. Ghosh, S. Ghosh, L.P. Lee, A. Gopinathan and M. Khine, *Advanced Materials*, 2009, 21, 44, 4472. ©2009, John Wiley & Sons [42]

### **8.3.5 Programmable Surface Pattern**

The pattern memory effect is driven by the phase transformation of shape-memory polymers. Memorisation by a reversible pattern surface is formatted by two types of methods: the programmable pattern memorising surface and the non-reprogramming reversible deformation surface. Wang and co-workers [44] demonstrated the successful programming and recovery of a range of lithographically fabricated dense SMP patterns *via* nano-imprint lithography (NIL). There are two types of NIL processes: thermal embossing nano-imprint lithography (TE-NIL) and step-and-flash nano-imprint lithography (SF-NIL). TE-NIL is essentially a combination of the programming and fixing steps in a typical shape-memory cycle, but it occurs at much smaller length scales. In comparison, SF-NIL is mostly carried out at room temperature with ultraviolet (UV) radiation, which crosslinks the reactive monomers to replicate the mould. This study reported SMP with the novel ability to memorise and recover their lithographically fabricated nano-scale surface patterns. The successful pattern memory cycle proved replicable for multiple pattern heights with 100% recovery using an acrylate-based SMP.

### **8.3.6 No-programming Reversible Shape-memory Surface Patterns**

Higgins and co-workers [45] introduced a new shape-memory functionality for stimuli-responsive polymers. The shape-memory process is unique in that it utilises electrochemical control of the polymer redox state to conceal and temporarily store preformed nano-scale surface patterns. Unlike classical thermoset and thermoplastic SMP, electrochemical control does not completely perturb the low entropy state of the deformed polymer chains, thereby enabling reversible transition between permanent and temporary shapes. Their results revealed that cation/solvent exchange with the electrolyte and its effect on reconfiguration of the film structure is the mechanism behind the process (Figure 8.11).

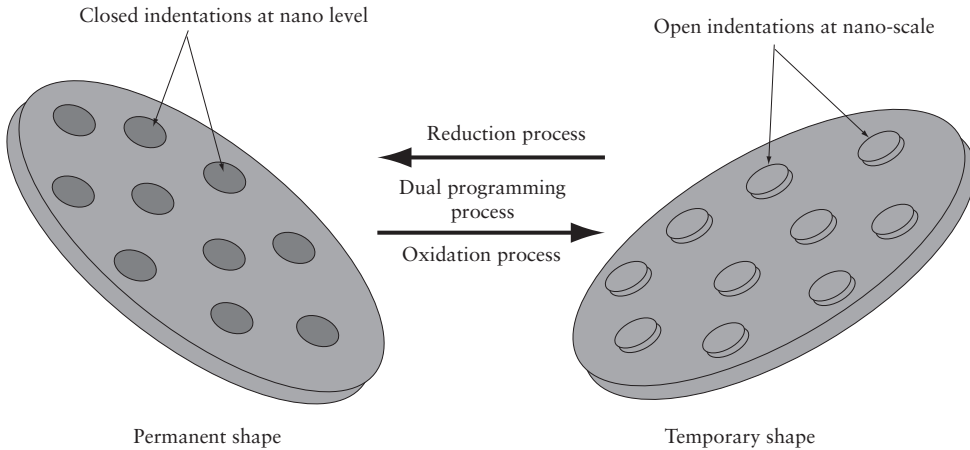
## **8.4 Applications in Textiles**

### **8.4.1 Shape-memory Polymer Fibres**

SMP to textile fibres through common spinning methods reflects significant progress. Making a polymer fibre is easy as long as the polymer has sufficient molecular weight, viscosity or suitable melting point, but making a fibre for textiles is difficult. Tenacity, elongation, hand-feeling and process ability are the main factors that influence final



end uses. The success of shape-memory fibres (SMF) has created a fibre type in the textiles industry.

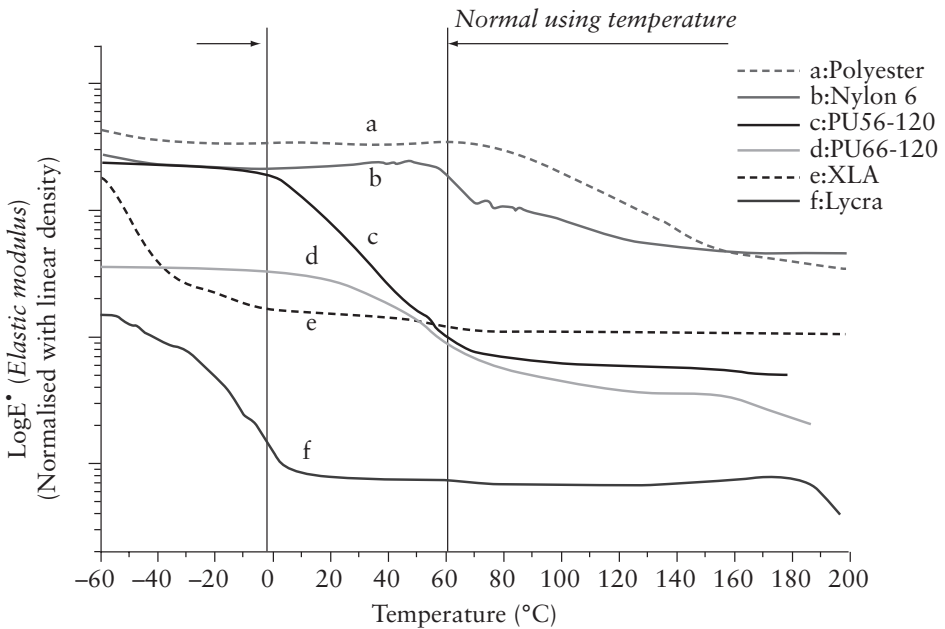


**Figure 8.11** Mechanism of reversible shape-memory surface patterns

SMF can be made by wet, melt and dry spinning methods [46]. Compared with other traditional man-made materials, SMF are unique because their elastic modulus changes within a specified utilisation temperature range and their recovery ability changes with an external stimulus [47]. The molecular orientation, recovery stress, hard segment micro-domains and post-treatments have also been studied [47]. **Figure 8.12** reveals the comparison between modulus change under increasing temperature: SMF is superior with an excellent temperature-response performance than spandex, nylon and X-linked agammaglobulinemia (olefinic-based fibre product of Dow company) [47].

Wet-spun SMF are good starts for application in textiles, and provide theoretical and practical research directions, such as the relationship between spinning parameters and fibre properties, and utilisation of SMF in textiles and garments. Melt spinning SMF were developed later to overcome the disadvantages of wet spinning fibres such as environmental pollution, lower manufacturing efficiency, and limited elasticity. The first melt-spun SMF began from commercially available SMPU (MM-4510) thanks to the work of Kaurisoin and Agrawal. They investigated the effect of drawing and heat-setting operations [48]. Melt spinning does not involve solvents, so bulk polymerisation provides a clean method for SMP resins of high molecular weight. In 2007, Meng and co-workers [49] obtained high-strength SMF with melt spinning. In

comparison with wet-spun SMF, melt-spun SMF have higher tenacity, controllable elongation, linear density, shape fixity, elasticity and switch temperature. Shape recovery is higher than for wet spun SMF due to formation of higher micro-phase separation during melt spinning. Similar to wet-spun SMF, thermal treatment could also help melt-spun SMF obtain excellent properties.



**Figure 8.12** Comparison of the elastic modulus between SMPU fibre and existing man-made fibres within normal temperature range (0-60 °C). Reproduced with permission from J.L. Hu, Y. Zhu, H.H. Huang and J. Lu, *Progress in Polymer Science*, 2012, 37, 12, 1720. ©2012, Elsevier [36]

Melt spinning also provides an efficient method to prepare various functional fibres. Meng and co-workers prepared a SMPU hollow filament with a thermally sensitive internal diameter *via* melt spinning. Additionally, Meng and co-workers [50] also prepared electro-active SMF by incorporating multiwalled carbon nanotubes (MWCNT) and temperature-regulating fibres made of polyethylene glycol (PEG)-based smart copolymers [51]. These studies on melt-spun SMF enable the actual commercial applications to be more versatile. However, in addition to the special requirements of melt-spinning technology, an SMP resin system with high molecular



weight, good resistance to hydrogenation, and good rheological properties are prerequisites.

A series of SMF has been developed with an optional mechanical property range, shape-memory fixity, recovery and switch temperature range, which allows for diversified textile designs (Table 8.1). Considering textile processing technology such as dyeing, finishing, and heat setting, SMF should have anti-oxidant, anti-thermal, chlorine-resistant and anti-aging properties, which are challenges for making commercially viable SMF.

<b>Table 8.1 Textile applications of SMP fibres</b>		
<b>Applications</b>	<b>Advantages</b>	<b>Products</b>
High-pressure garments/accessories	<ul style="list-style-type: none"> <li>• Application convenience: Easy to wear and easy removal</li> <li>• Durability</li> <li>• No slack</li> </ul>	Medical garments (burn-cure garments, compression stockings for varicose veins), pressure sportswear
Comfort garments/accessories	<ul style="list-style-type: none"> <li>• Low pressure</li> <li>• Size change with body figure</li> <li>• Thermo-wet control</li> <li>• No slack</li> </ul>	Underwear, socks, nappy welt, waistband, sportswear
Shape-retention garments/accessories	<ul style="list-style-type: none"> <li>• Flat appearance</li> <li>• Crease retention</li> <li>• Bagging recovery</li> <li>• Wrinkle recovery</li> </ul>	Shirts, trousers, dresses, bed sheets
Fashion design	Style change 3D effects	Dresses, skirts

#### **8.4.2 Shape-memory Polymer Yarns and Fabrics**

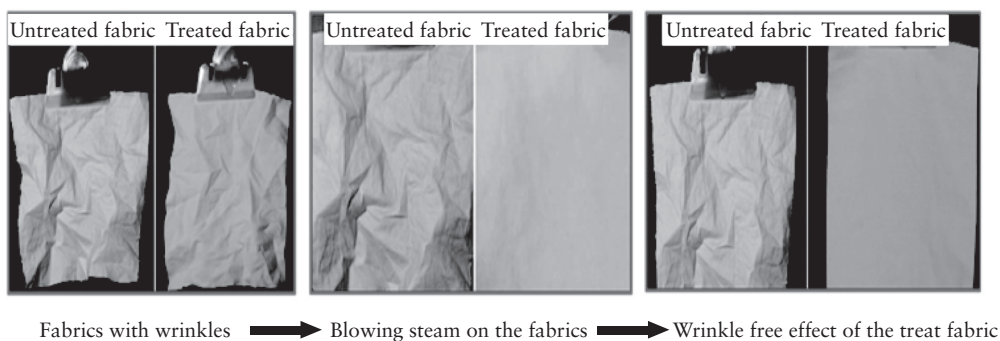
Application of SMF in textiles involves their shape fixity and recovery along the fibre length accompanied by stress changes. A comparison between Lycra and SMF knitted fabrics was also made to validate the SME of SMPU knitted fabrics [52]. Results showed that SME can be improved with increasing content of SMPU fibres.

Lu and Hu [53] studied core-spun yarns with SMF and cotton developed using a ring-spinning frame and friction-spinning machine. Shape-memory fabrics were woven from two types of shape-memory core-spun yarns. The mechanical and shape-memory properties of these yarns and fabrics were examined. The yarns had good weave-ability, and both yarns and fabrics had good shape-memory fixity and recovery properties. Shape-memory core-spun yarns have as good SME as pure SMF. Fabrics with shape-memory yarns as weft have better SME in the filling-direction but, in the warp-direction without shape-memory, yarns also show SME due to the force transfer from interlacing points of woven structures. From the information given above, it is clear that SMF, yarns and fabrics have good SME.

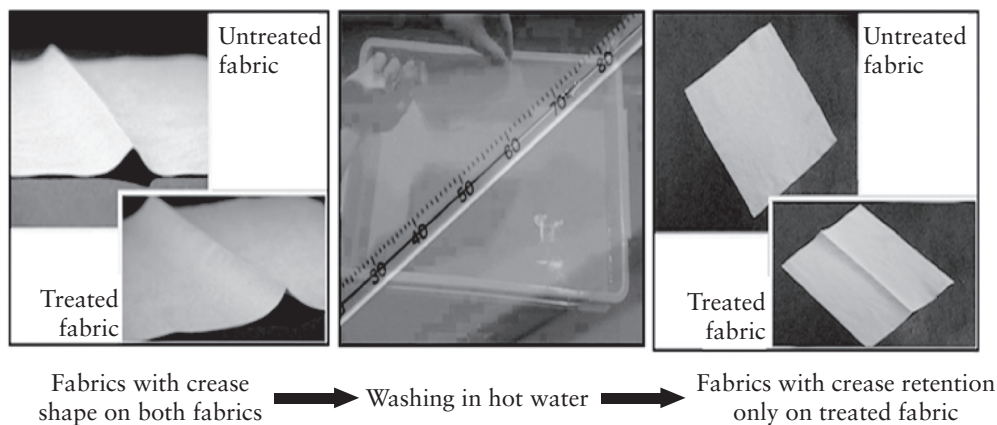
#### **8.4.3 Shape-memory Polymer Solutions for Finishing Fabrics**

SMP solutions are used directly as finishing agents to obtain valuable properties in different types of textile fabrics such as cotton or wool [54, 55]. It is another method for producing shape-memory fabrics by shape-memory finishing, which is a process that transfers the shape-memory properties from polymers to fabrics [56]. Cotton wrinkles easily and is difficult to set if creases are required, such as pleated skirts. Liu and co-workers [54] first reported a chemical-modification method for cotton through shape-memory finishing and investigated the resultant cotton fabric with Fourier-transform infrared spectroscopy and X-ray photoelectron spectroscopy. The results revealed that, if SMPU are grafted onto the surface of cotton, high washability and enduring anti-creasing of the treated cotton can be achieved. Hu and co-workers studied the wrinkle recovery, crease retention and pattern-retention properties of different shape-memory fabrics by coating them with SMP (Figures 8.13–8.15), and developed corresponding testing methods for shape-memory fabrics treated with shape-memory finishing and knitted by SMF, respectively [57, 58]. Furthermore, Hu and her research team developed SMP finishing agents for wool [55, 59]. The thermal and hygrothermal effects of wool fabrics were investigated through shape-memory finishing with SMPU [60, 61]. The results suggested that synthetic SMP influence the thermal and hygrothermal behaviours of wool fabrics.

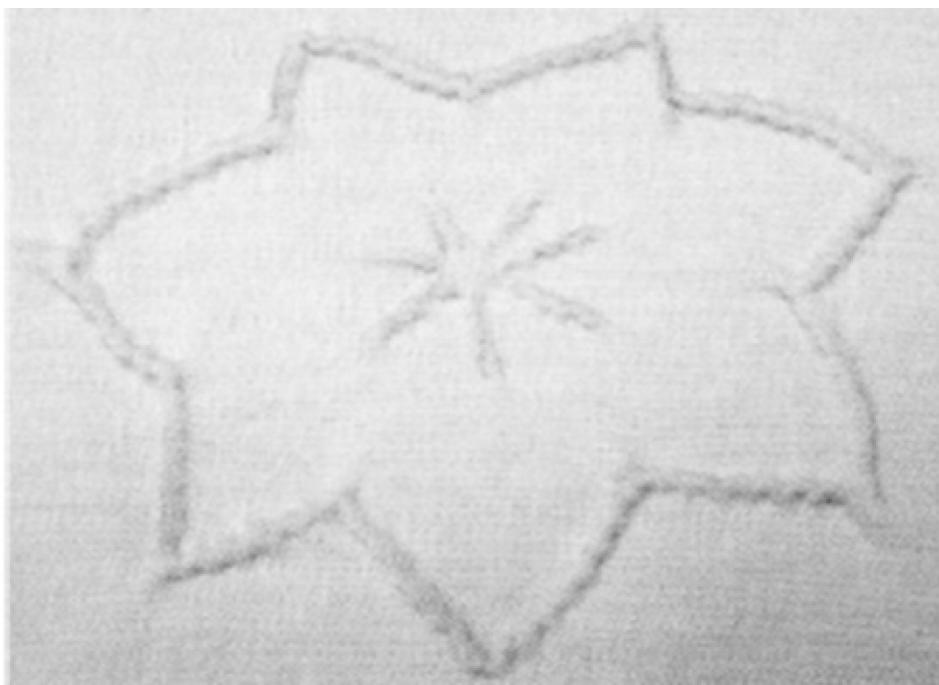
As compared with the shape-memory fabrics knitted or woven with SMF, a small content of SMP is sufficient to transfer SME to the fabric in shape-memory finishing. This process is highly efficient. Many interesting functionalities can be achieved in a fabric treated by shape-memory finishing: anti-pilling; flexibility/strength protection; dimensional stability; shrink proofing; good flat appearance; crease retention; ease of 3D pattern design; bulging recovery.



**Figure 8.13** Wrinkle-free effect of fabric treated with waterborne SMPU in comparison with that of fabric not treated with SMPU. Reproduced with permission from J.L. Hu and S.J. Chen, *Journal of Materials Chemistry*, 2010, 20, 17, 3346. ©2010, RSC Publishing [14]



**Figure 8.14** Crease retention of a fabric treated with SMP compared with that of a fabric not treated with SMP (crease shape was produced by ironing). Reproduced with permission from J.L. Hu and S.J. Chen, *Journal of Materials Chemistry*, 2010, 20, 17, 3346. ©2010, RSC Publishing [14]



**Figure 8.15** Pattern retention of a knitted fabric finished with SMPU after two washes. The untreated wool fabric shrinks severely while the treated fabric does not. Reproduced with permission from J.L. Hu and S.J. Chen, *Journal of Materials Chemistry*, 2010, 20, 17, 3346. ©2010, RSC Publishing [14]

#### **8.4.4 Shape-memory Polymer Nanofibres and their Nonwovens**

Compared with their bulk counterparts, SMP electrospun microfibre and nanofibre non-woven structures have advanced unique properties: quicker response to the external stimuli; larger recovery stress; quicker recovery rate; enhanced functionalities (e.g., anti-bacterial and water vapour permeability). Nanofibres have been electrospun from SMPU solutions by different research teams [62–66]. The resultant structures had ultrafine diameters in the range of 50 nm to 2  $\mu\text{m}$ . Uniform nanofibres can be prepared by adjusting the applied voltage, concentration and feeding rate. The concentration has a key role in controlling these diameters [62].

The thermal properties of SMPU nanofibrous nonwoven materials were investigated by Zhuo and co-workers. They were found to be influenced greatly by electrospinning and

recrystallisation conditions. Temperature-dependent strain recovery curves suggested that the SMPU nanofibre tended to have a lower recovery temperature as compared with SMPU bulk film due to their ultrafine diameter [67]. Another interesting work was by Ozin. The electroactuation of polymer microfibrils was realised from an ethoxysilane derivative of redox-active polyferrocenylmethylvinylsilane (PFMVS). Crosslinked fibres of average diameter 2  $\mu\text{m}$  were fabricated by electrospinning high-molecular-weight polymer solutions of PFMVS (ratio of ethoxysilane versus active PFMVS (m/n) = 0.1–1.0) after initiating the acid-catalysed condensation of ethoxysilane. In cases of low crosslink density, the resultant fibres responded rapidly (<100 ms) to electrical stimuli applied *via* an electrode or by titration with redox-active compounds. Large strains occurred within 10 ms if fibres were oxidised electrochemically on an electrode surface submerged in a supporting electrolyte. Such structures were predicted to rival existing bilayer actuators in strength but maintain rapid response times because of significantly larger ratios of surface area to volume, and smaller ion diffusion length [68].

A novel type of SMPU nanofibres with core-shell nano-structures was fabricated using coaxial electrospinning by Hu and co-workers [69]. Nanofibres with core-shell structures or bead-on-string structures can be electrospun from the core solution of polycaprolactone-based SMPU (CLSMPU) and shell solution of pyridine containing SMPU (Py-SMPU). In addition, excellent SME and excellent antibacterial activity against Gram-negative and Gram-positive bacteria can be achieved in CLSMPU-Py-SMPU core-shell nanofibres. It has been proposed that the antibacterial mechanism results from Py-SMPU shell materials containing the amido group and the high surface area per unit mass of nanofibres. Thus, core shell nanofibres can be used as shape-memory and antibacterial nano-materials.

The essential properties of protective clothing are good transport of water vapour, increased fabric breathability, and enhanced toxic chemical resistance. Hence, electrospun SMP nanofibre membranes are good candidates for these applications. According to Zhuo, in addition to excellent SME, SMPU nanofibrous nonwovens have good properties in terms of transfer of liquid vapour and water vapour. Moreover, the water vapour permeability (WVP) of a nonwoven material is sensitive to changes in relative humidity and temperature ('twin-switch'). Scanning electron micrographs at higher temperatures suggest that porous nanofibrous nonwoven structures are the foundation of such unique WVP properties [70]. Similarly, Park and co-workers investigated the applicability of electrospun nanofibre webs as intelligent clothing materials using SMP [71]. The web, having high orientation due to elongation in the process of the electrospinning, showed improved shape-recovery and good permeability of moisture and air due to countless nano-sized pores. Therefore, the SMPU web had the potential for application as an intelligent clothing material [66].

A porous structure and large surface-area-to-volume ratio endow SMP with better sensitivity, smart temperature control and moisture control. Research in this area has just started to attract attention, but the outcomes are very inspiring. Because of the wide use of SMP in medical and protective textile materials, such structures could potentially rival existing materials and devices.

### **8.4.5 Shape-memory Polymer Film/Foam and Laminated Textiles**

The functions of SMP films applied to textiles include water-proofing, WVP, seam sewing, crease recoverability and crease fixing (Table 8.2). To optimise these effects, various properties of SMP films have been investigated, such as thermo-mechanical properties [72], different structural factors affecting physical and water-vapour transport properties [73–75], molecular weight [76], effects of crystal melting [75] and influence of different processing temperatures [77].

Shapes	Functions	Products	Process methods
Film	<ul style="list-style-type: none"> <li>• Control of water vapour permeability</li> <li>• Water-proofing</li> <li>• Seamless sewing</li> </ul>	<ul style="list-style-type: none"> <li>• Waterproof and vapour-permeable apparel</li> <li>• Seamless sewing of underwear</li> </ul>	Laminating, coating, and melt sticking
Foam	<ul style="list-style-type: none"> <li>• Damping</li> <li>• Body figure fit</li> </ul>	<ul style="list-style-type: none"> <li>• Cushions on special garments such as motorcycle clothing</li> <li>• Brassieres</li> </ul>	Laminating and sewing
Nano-SM fibre film/nonwoven	<ul style="list-style-type: none"> <li>• WVP control</li> <li>• Multiple function of shape-memory and antibacterial properties, biodegradable properties</li> </ul>	<ul style="list-style-type: none"> <li>• Waterproof and vapour-permeable apparel</li> <li>• Medical apparel</li> </ul>	Laminating

WVP is a significant adaptive parameter of thermally induced SMP films that enables broad applications (including in textiles). SMPU have become good candidates in breathable laminated nonporous fabrics due to the relationship between WVP

sensitivity and temperature and humidity. In 2000, Cho and co-workers and Jeong and co-workers investigated the WVP properties of SMPU with an amorphous reversible phase, and water-vapour permeable fabrics were prepared by coating SMPU membranes to a fabric substrate [74]. Similarly, smart WVP was observed around the  $T_m$  in SMPU with semi-crystalline reversible phases [78]. This WVP property that is adaptable to environmental conditions can be beneficial for breathable textiles, biomedical, and many other industrial applications [79].

In addition to controlling WVP by adjusting temperature, Chen and co-workers attempted to adjust the size and shape of the free-volume holes found in membrane materials [80]. Huang and co-workers also investigated the influence of hard-segment content on temperature-sensitive WVP [81]. The influence of hydrophilic groups and crystalline soft segments on the WVP of SMPU film [82, 83] was studied by Mondal and Hu [79]. It was reported that WVP increased with increase in PEG content due to enhanced hydrophilicity. However, polycaprolactone glycol reduces WVP in polytetramethylene glycol-based SMPU due to increased interaction among the polymer chains [82].

Mondal and Hu tested SMPU-coated fabrics with a tailored transition temperature ( $T_r$ ), i.e., room temperature, and investigated their WVP properties [82]. The SMPU-coated fabrics showed an abrupt increase in WVP if the temperature reached the  $T_r$ . These results confirmed the need for breathable textiles to have a high WVP at higher temperatures and a low WVP at lower temperatures. Additionally, using SMPU comprising a small percentage of MWCNT, Mondal and Hu reported cotton fabric with excellent UV protection, along with a desirable WVP and wearing comfort [84]. SMP-laminated fabrics provide better comfort in cold and warm climates [84]. A Japanese company, Mitsubishi Heavy Industries, has developed outerwear ‘smart fabrics’ that use SMP membranes. The resulting Diaplex™ fabrics show excellent waterproof features and breathability with water pressure resistance of 20,000–40,000 mm H<sub>2</sub>O and moisture permeability of 8,000–12,000 g/m<sup>2</sup>/24 h. Such properties provide the resultant garments with high performance and enable wearers to be comfortable in various conditions. In addition, Toray Industries and Marmot Mountain Works have developed a PU film, MemBrain®. Fabrics laminated with MemBrain® provide a breathable clothing system. By combining the excellent WVP of SMP with the micro-porous coating and laminated technology of garments, SMP coatings and laminates may find wide applications in textile/garment fields (e.g., sportswear, footwear, gloves and socks).

SMP are used from emulsion/solution to bulk film, from wet-spun macro-SMF to microfibrils and nanofibrils, and from finishing of garments to laminated textiles. Among them, shape-memory finishing provides an easy and highly efficient process to achieve shape-memory function in common fabrics including cotton, wool and other



fabrics. Utilisation of SMP in laminated textiles is an easy way to fabricate various smart textiles. Successful preparation of SMF has made it possible to manufacture various shape-memory fabrics through weaving or knitting.

## **8.5 Engineering Applications**

### **8.5.1 Transportation**

SMP used for transportation are for energy absorption [85, 86], insulation, self-deployment and self-healing [87]. The energy-absorbing property is also good for packaging [85]. Apart from energy absorption, another application of SMP in packaging involves shape fixity and recovery in that the film can remember a specific basic shape and take on a second shape as desired [88]. SMP can be used to make floating boats using shape fixity and recovery. The floating boat can be folded for storage and be recovered for use with sufficient rigidity [89, 90].

Besides the applications described above, SMP are applied for other end uses. They can be used as insulators and sound or energy absorbers in foam. SMPU foams used in the aerospace field have three main advantages: (i) higher reliability of self-deployable structure; (ii) simplicity over expandable/deployable structures; and (iii) low density. SMPU foams have been anticipated to be used in space robotics and other support structures (e.g, telecommunication, power, sensing, thermal control, impact and radiation protection subsystems [91]). Recently, various feasibility studies and preliminary investigations have reported on the potential space applications of SMPU foams. Sokolowski and co-workers [92] produced a small model proof-of-concept for precision soft-lander and sensor delivery systems, as well as horn antennae and radar antennae using SMPU foams. Upon integration with nanorover, wheels has been induced and demonstrated in a laboratory experiment.

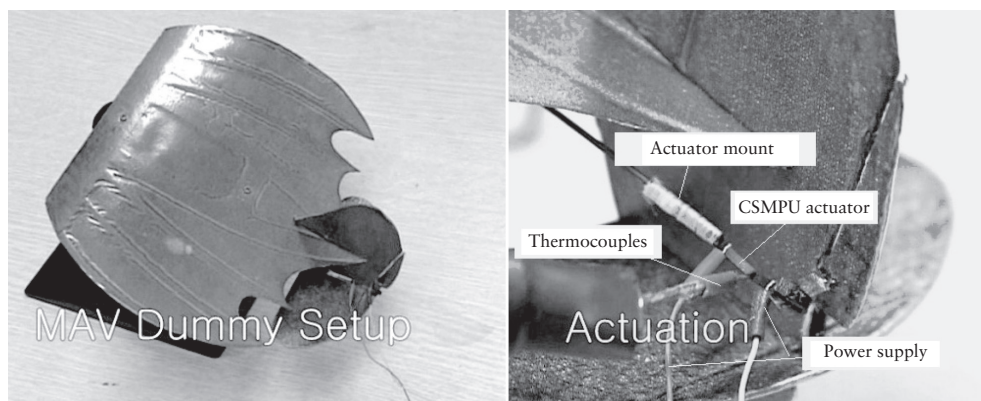
### **8.5.2 Sensors and Actuators**

Temperature-sensitive shape-memory function is the most common investigation of SMP. To meet the special need for sensors or actuators of biomedical devices and other devices, Zhang and co-workers [93] improved shape-memory recovery speed by electrospinning with the fibre diameter of 200 nm to 1  $\mu\text{m}$  instead of changing the chemical composition. The quicker shape-memory behaviour compared with bulk film is attributed to the higher surface area for quicker heating/cooling and quicker moisture diffusion. Besides, Cho and his research team demonstrated conducting



SMPU composites, electro-active shape-memory SMP for application as actuators using polyurethane block copolymer and conducting polypyrrole as well as MWCNT [94, 95]. Both conducting shape-memory composites gave desirable shape-recovery if an electric field of 40 V was applied.

Furthermore, Paik described a method to improve dispersion by *in situ* polymerisation [96, 97]. More importantly, they described actuation performance experiments, actuation displacement *versus* actuation force, and initial elongation force in the break-in procedure. SMP are lighter than shape-memory alloys, so they can be used in lightweight applications such as micro-aerial vehicles. **Figure 8.16** demonstrates application of an SMP actuator for the control surface of a micro-air vehicle. The SMP installed on the micro-aerial vehicle (MAV) enabled production of an actuation angle of 30° as a flight control.



**Figure 8.16** a) MAV ('Batwing') dummy set-up for an application test. b) Magnified view of a linkage for a control surface actuator. Reproduced with permission from I.H. Paik, N.S. Goo, Y.C. Jung and J.W. Cho, *Smart Materials and Structures*, 2006, 15, 5, 1476. ©2006, IOP Science [98]

SMP are also found in minimally invasive tools (see Section 5.2.2) because SMP offer the chance to insert a compact, temporary shaped device through a small incision in the body that can be recovered to a bulky shape inside the body by specific triggering. Corkscrew-type wires were proposed to remove blood clots out of a vein of a stroke patient [7]. To maximise the use of shape-memory stents, Wache combined a polymer stent with a drug-delivery system as additional therapy by injection moulding and

dip coating [99]. The loaded shape-memory stent gave continuous release over a long period of time. Ahmad [100] studied the feasibility of SMPU bandages as pressure actuators for the treatment of leg ulcers. His study showed that SMPU bandages can be used to solve the problem of pressure reduction during usage because the pressure provided by SMPU could be readjusted by heating.

### **8.5.3 Filtration**

SMPU foam is applied to deploy and expand to recovered geometric positions at or near its original geometric position to enable filtration, isolation, control or other functions for wellbore and downhole sand control filtration devices [101, 102]. Leo and co-workers [103] invented a sleeve-like primary air filter element cut from a block of resilient PU materials. Besides the improvement in the shape of the filter to enhance filtration, auxiliary functions were added to the polyurethane filter (e.g., antibacterial property). Prashant and co-workers [104] prepared silver nanoparticle-coated polyurethane foam which could be used as a drinking-water filter if bacterial contamination of surface water is a health risk. Elke and co-workers [105] used electrospun SMPU fibres for the absorption of volatile organic compounds from air. They found the sorption capacity of polyurethane fibre meshes to be similar to that of activated carbon designed specifically for vapour absorption. Because of the high affinity between polyurethane and toluene, chloroform displayed good absorption of the two volatile organic compounds. Wu and co-workers [106] reported that SMPU foam was used to isolate and differentiate human adipose-derived stem cells in <30 mins, whereas traditional methods require 5–12 days.

### **8.5.4 Insulation**

Conventional insulators are used in as-moulded shapes. Most of them are plastic foams containing a large amount of air, so are very bulky for their weight. Therefore, packing and transporting a large quantity of them simultaneously is difficult. Their bulkiness makes their storage inconvenient. In addition, conventional insulators need complex working if they are attached to pipes and tubes or odd-shaped containers. SMPU can be used as-moulded shapes convenient for packing, transportation, storage, and mounting. Additionally, SMPU hollow fibre has been found to be a promising material for textile insulation [71]. The diameter of the hollow fibre can recover to its original size if flattened and under ambient temperature above the switch temperature. The insulation property of textiles filled with common hollow fibre decreases after a long time. SMPU can also be used for adjusting insulation textiles by coating. With the shape recovery of SMPU, the fabric deforms or becomes a bulking layer. This type of thermally insulating textile provides a variable degree of thermal insulation

dependent upon ambient temperature. The textile comprises a laminate of two fabric layers having interposed a bulking layer which may comprise one or more fabric layers deposited on SMP, SMPU strips or fibres. As the temperature of the textile varies from the predetermined temperature towards a higher temperature, the SMPU bulking layer puckers to increase the gap between the two fabric layers.

## **8.6 Conclusions**

SMP provide enormous opportunities in many applications. Using SMP, we can obtain novel functional products with profoundly significant properties in industrial, biological, textile, consumer, transport, actuation, and filtration areas. This chapter provided brief descriptions of the possible applications of SMP. In addition to shape change and recovery properties, stimuli-responsive polymers can offer a deformation force that can be employed in medical applications. SMP which can change volume and shape could also be used in transportation, filtration, textiles, as well as in skincare products with controllable release of perfume, nutrition, and drugs. With rapid development of SMP and novel strategies for their applications, it is anticipated that research with SMP will grow in multiple dimensions.

## **References**

1. M. Behl and A. Lendlein, *Journal of Materials Chemistry*, 2010, **20**, 17, 3335.
2. Q. Meng, J. Hu, Y. Zhu, J. Lu and Y. Liu, *Journal of Applied Polymer Science*, 2007, **106**, 2515.
3. Y.C. Jung and J.W. Cho, *Journal of Materials Science: Materials in Medicine*, 2010, **21**, 10, 2881.
4. I.A. Rousseau, E. Berger, J. Owens and H. Kia, inventors; GM Global Technology Operations LLC, assignee; US 8100843 B2, 2012.
5. K. Takashima, J. Rossiter and T. Mukai, *Sensors and Actuators A: Physical*, 2010, **164**, 1-2, 116.
6. W. Small, T.S. Wilson, P.R. Buckley, W.J. Benett, J.A. Loge, J. Hartman and D.J. Maitland, *IEEE Transactions on Biomedical Engineering*, 2007, **54**, 9, 1657.

7. W.I. Small, M.F. Metzger, T.S. Wilson and D.J. Maitland, *IEEE Journal of Selected Topics in Quantum Electronics*, 2005, **11**, 4, 892.
8. S.V. Ahir, A.R. Tajbakhsh and E.M. Terentjev, *Advanced Functional Materials*, 2006, **16**, 4, 556.
9. S.K. Ahn, P. Deshmukh, M. Gopinadhan, C.O. Osuji and R.M. Kasi, *ACS Nano*, 2011, **5**, 4, 3085.
10. K.K. Westbrook, P.T. Mather, V. Parakh, M.L. Dunn, Q. Ge, B.M. Lee and H.J. Qi, *Smart Materials and Structures*, 2011, **20**, 6.
11. S.J. Chen, J.L. Hu, H.T. Zhuo and Y. Zhu, *Materials Letters*, 2008, **62**, 25, 4088.
12. K.D. Harris, R. Cuypers, P. Scheibe, C.L. van Oosten, C.W.M. Bastiaansen, J. Lub and D.J. Broer, *Journal of Materials Chemistry*, 2005, **15**, 47, 5043.
13. T. Ikeda and T. Ube, *Materials Today*, 2011, **14**, 10, 480.
14. J.L. Hu and S.J. Chen, *Journal of Materials Chemistry*, 2010, **20**, 17, 3346.
15. W.M. Huang, C.W. Lee and H.P. Teo, *Journal of Intelligent Material Systems and Structures*, 2006, **17**, 8-9, 753.
16. S.M. Kang, S.J. Lee and B.K. Kim, *eXPRESS Polymer Letters*, 2012, **6**, 1, 63.
17. W. Small, P.R. Buckley, T.S. Wilson, W.J. Benett, J. Hartman, D. Saloner and D.J. Maitland, *IEEE Transactions on Biomedical Engineering*, 2007, **54**, 6, 1157.
18. M.C. Chen, H.W. Tsai, Y. Chang, W.Y. Lai, F.L. Mi, C.T. Liu, H.S. Wong and H.W. Sung, *Biomacromolecules*, 2007, **8**, 9, 2774.
19. C.M. Yakacki, R. Shandas, C. Lanning, B. Rech, A. Eckstein and K. Gall, *Biomaterials*, 2007, **28**, 14, 2255.
20. G.M. Baer, T.S. Wilson, W. Small, J. Hartman, W.J. Benett, D.L. Matthews and D.J. Maitland, *Journal of Biomedical Materials Research Part B: Applied Biomaterials*, 2009, **90B**, 1, 421.
21. H.M. Wache, D.J. Tartakowska, A. Hentrich and M.H. Wagner, *Journal of Materials Science: Materials in Medicine*, 2003, **14**, 2, 109.

22. J.M. Ortega, W. Small, T.S. Wilson, W.J. Benett, J.M. Loge and D.J. Maitland, *IEEE Transactions on Biomedical Engineering*, 2007, **54**, 9, 1722.
23. J.M. Hampikian, B.C. Heaton, F.C. Tong, Z.Q. Zhang and C.P. Wong, *Materials Science and Engineering C: Materials for Biological Applications*, 2006, **26**, 8, 1373.
24. A.A. Sharp, H.V. Panchawagh, A. Ortega, R. Artale, S. Richardson-Burns, D.S. Finch, K. Gall, R.L. Mahajan and D. Restrepo, *Journal of Neural Engineering*, 2006, **3**, 4, L23.
25. X.C. Xiao, T. Xie and Y.T. Cheng, *Journal of Materials Chemistry*, 2010, **20**, 17, 3508.
26. E.D. Rodriguez, X.F. Luo and P.T. Mather, *ACS Applied Materials & Interfaces*, 2011, **3**, 2, 152.
27. J.B. Jorcin, G. Scheltjens, Y. Van Ingelgem, E. Tourwe, G. Van Assche, I. De Graeve, B. Van Mele, H. Terryn and A. Hubin, *Electrochimica Acta*, 2010, **55**, 21, 6195.
28. Y. Gonzalez-Garcia, J.M.C. Mol, T. Muselle, I. De Graeve, G. Van Assche, G. Scheltjens, B. Van Mele and H. Terryn, *Electrochemistry Communications*, 2011, **13**, 2, 169.
29. G.Q. Li and D. Nettles, *Polymer*, 2010, **51**, 3, 755.
30. J. Nji and G.Q. Li, *Smart Materials and Structures*, 2010, **19**, 3.
31. G.Q. Li and M. John, *Composites Science and Technology*, 2008, **68**, 15-16, 3337.
32. M. John and G.Q. Li, *Smart Materials and Structures*, 2010, **19**, 7.
33. G.G. Li and N. Uppu, *Composites Science and Technology*, 2010, **70**, 9, 1419.
34. N.T. Suzuka and A.T. Suzuka, inventors; Asahi Kasei Kabushiki Kaisha, assignee; US 7182998, 2007.
35. T. Saito, inventor; Yazaki Corp., assignee; US 6531659, 2003.

36. J.L. Hu, Y. Zhu, H.H. Huang and J. Lu, *Progress in Polymer Science*, 2012, 37, 12, 1720.
37. J.J. Li, Y.H. An, R. Huang, H.Q. Jiang and T. Xie, *ACS Applied Materials & Interfaces*, 2012, 4, 2, 598.
38. Y. Zhao, W.M. Huang and Y.Q. Fu, *Journal of Micromechanics and Microengineering*, 2011, 21, 6.
39. L. Sun, Y. Zhao, W.M. Huang and T.H. Tong, *Surface Review and Letters*, 2009, 16, 6, 929.
40. T. Xie, X.C. Xiao, J.J. Li and R.M. Wang, *Advanced Materials*, 2010, 22, 39, 4390.
41. D. Nguyen, S. Sa, J.D. Pegan, B. Rich, G.X. Xiang, K.E. McCloskey, J.O. Manilay and M. Khine, *Lab on a Chip*, 2009, 9, 23, 3338.
42. C.C. Fu, A. Grimes, M. Long, C.G.L. Ferri, B.D. Rich, S. Ghosh, S. Ghosh, L.P. Lee, A. Gopinathan and M. Khine, *Advanced Materials*, 2009, 21, 44, 4472.
43. X.C. Liu, A. Chakraborty and C. Luo, *Journal of Micromechanics and Microengineering*, 2010, 20, 9.
44. Z. Wang, C. Hansen, Q. Ge, S.H. Maruf, D.U. Ahn, H.J. Qi and Y.F. Ding, *Advanced Materials*, 2011, 23, 32, 3669.
45. M.J. Higgins, W. Grosse, K. Wagner, P.J. Molino and G.G. Wallace, *Journal of Physical Chemistry B*, 2011, 115, 13, 3371.
46. J. Hu in *Shape-Memory Polymers and Multifunctional Composites*, CRC Press, Taylor & Francis Group, London, UK, 2010, p.293.
47. Y. Zhu, J.L. Hu, L.Y. Yeung, Y. Liu, F.L. Ji and K.W. Yeung, *Smart Materials and Structures*, 2006, 15, 5, 1385.
48. J. Kaursoin and A.K. Agrawal, *Journal of Applied Polymer Science*, 2007, 103, 4, 2172.
49. Q.H. Meng, J.L. Hu, Y. Zhu, J. Lu and Y. Liu, *Smart Materials and Structures*, 2007, 16, 4, 1192.
50. Q.H. Meng, J.L. Hu and L. Yeung, *Smart Materials and Structures*, 2007, 16, 3, 830.

51. Q.H. Meng and J.L. Hu, *Solar Energy Materials and Solar Cells*, 2008, **92**, 10, 1245.
52. S.J. Chen, J.L. Hu, Y.Q. Liu, H.M. Liem, Y. Zhu and Y.J. Liu, *Journal of Polymer Science, Part B: Polymer Physics Edition*, 2007, **45**, 4, 444.
53. L. Jing and J.L. Hu, *Fibres & Textiles in Eastern Europe*, 2010, **18**, 4, 39.
54. L. Ye Qiu, H. Jin Lian, Z. Yong and Y. Zhuo Hong, *Carbohydrate Polymers*, 2005, **61**, 3, 276.
55. Y. Liu, Y.J. Zheng and J.L. Hu, inventors; no assignee; CN 1818198 A, 2006.
56. H. Liem, L.Y. Yeung and J.L. Hu, *Smart Materials and Structures*, 2007, **16**, 3, 748.
57. Y.K. Li, Hong Kong Polytechnic University, Hong Kong, China, 2007. {Dissertations}
58. Y. Liu, A. Chung, J.L. Hu and J. Lu, *Journal of Zhejiang University - Science A*, 2007, **8**, 5, 830.
59. J.L. Hu, Y.J. Liu, Q.M. Wang, Y. Liu and J. Lu, inventors; no assignee; CN 101994254 A, 2009.
60. J.L. Hu, Z.E. Dong, Y. Liu and Y.J. Liu, *Advances in Science and Technology*, 2008, **60**.
61. Z.E. Dong, J.L. Hu, Y. Liu, Y. Liu and L.K. Chan, *International Journal of Sheep and Wool Science*, 2008, **56**.
62. H.T. Zhuo, J.L. Hu and S.J. Chen, *Materials Letters*, 2008, **62**, 14, 2074.
63. H.T. Zhuo, J.L. Hu, S.J. Chen and L.Y. Yeung, *Journal of Applied Polymer Science*, 2008, **109**, 1, 406.
64. Y.C. Jung, J.W. Kim, B.C. Chun, Y.C. Chung and J.W. Cho, *Quality Textiles for Quality Life*, 2004, 1-4, 43.
65. D.I. Cha, H.Y. Kim, K.H. Lee, Y.C. Jung, J.W. Cho and B.C. Chun, *Journal of Applied Polymer Science*, 2005, **96**, 2, 460.
66. S.E. Chung, C.H. Park, W-R. Yu and T.J. Kang, *Journal of Applied Polymer Science*, 2011, **120**, 1, 492.

67. H. Zhuo, J. Hu and S. Chen, *Journal of Materials Science*, 2011, **46**, 3464.
68. J.J. McDowell, N.S. Zacharia, D. Puzzo, I. Manners and G.A. Ozin, *Journal of the American Chemical Society*, 2010, **132**, 10, 3236.
69. H.T. Zhuo, J.L. Hu and S.J. Chen, *eXPRESS Polymer Letters*, 2011, **5**, 2, 182.
70. H. Zhuo, J. Hu and S. Chen, *Textile Research Journal*, 2011 **81**, 9, 883.
71. J.L. Hu, H.P. Meng, G.Q. Li and S.I. Ibekwe, *Smart Materials and Structures*, 2012, **21**, 5.
72. H. Tobushi, H. Hara, E. Yamada and S. Hayashi, *Smart Materials and Structures*, 1996, **5**, 483.
73. J.W. Cho, Y.C. Jung, B.C. Chun and Y.C. Chung, *Journal of Applied Polymer Science*, 2004, **92**, 5, 2812.
74. H.M. Jeong, B.K. Ahn, S.M. Cho and B.K. Kim, *Journal of Polymer Science, Part B: Polymer Physics Edition*, 2000, **38**, 23, 3009.
75. X.M. Ding, J.L. Hu and X.M. Tao, *Textile Research Journal*, 2004, **74**, 1, 39.
76. S.J. Chen, J.L. Hu, Y.Q. Liu, H.M. Liem, Y. Zhu and Q.H. Meng, *Polymer International*, 2007, **56**, 9, 1128.
77. J.L. Hu, Y.M. Zeng and H.J. Yan, *Textile Research Journal*, 2003, **73**, 2, 172.
78. X.M. Ding, J.L. Hu and X.A. Tao, *Textile Research Journal*, 2004, **74**, 1, 39.
79. S. Mondal and J.L. Hu, *Designed Monomers and Polymers*, 2006, **9**, 6, 527.
80. Y. Chen, Y. Liu, H. J. Fan, H. Li, B. Shi, H. Zhou and B.Y. Peng, *Journal of Membrane Science*, 2007, **287**, 2, 192.
81. H. Huang, D. Zhang, T.J. Wang, Z.P. Mao, W.D. Yu and H.J. Yan in *Proceedings of the 2007 International Conference on Advanced Fibers and Polymer Materials*, Volumes 1 and 2, Shanghai, China, State Key Laboratory for Modification of Chemical Fibers and Polymer Materials, 2007, p.546.
82. S. Mondal and J.L. Hu, *Carbohydrate Polymers*, 2007, **67**, 3, 282.
83. S. Mondal, J.L. Hu and Z. Yong, *Journal of Membrane Science*, 2006, **280**, 1-2, 427.



84. S. Mondal and J.L. Hu, *Journal of Applied Polymer Science*, 2007, **103**, 5, 3370.
85. G.J. Bleys and S.E.L. Helsemans, inventors; Imperial Chemical Industries Plc, assignee; EP 0608626 B1, 1997.
86. W. Barvosa-Carter, N.L. Johnson, A.L. Browne, G.A. Herrera, G.P.M. Knight, A.J. Jacobsen and C. Massey, inventors; GM Global Technology Operations Inc., assignee; US 7350851 B2, 2008.
87. P.J. Hood, S. Garrigan and F. Auffinger, inventors; Cornerstone Research Group Inc., assignee; US 7981229 B2, 2011.
88. S. Hayashi, H. Fujimura and M. Shimuzu, inventors; Mitsubishi Jukogyo Kabushiki Kaisha, assignee; EP 0363919 B1, 1996.
89. T. Horie and H. Fujimura, inventors; Mitsubishi Heavy Ind Ltd., assignee; JP1990000150539, 1992.
90. T. Horie and H. Fujimura, inventors; Mitsubishi Heavy Ind Ltd., assignee; JP1990000147060, 1992.
91. W. Sokolowski in *Shape-Memory Polymers and Multifunctional Composites*, CRC Press, Taylor & Francis Group, London, UK, 2010, p.267.
92. W. Sokolowski, S. Tan, P. Willis and M. Pryor in *Proceedings of SPIE*, Bellingham WA, USA, 2008, 7267.
93. J-N. Zhang, Y-M. Ma, J-J. Zhang, D. Xu, Q-L. Yang, J-G. Guan, X-Y. Cao and L. Jiang, *Materials Letters*, 2011, **65**, 23–24, 3639.
94. N.G. Sahoo, Y.C. Jung, N.S. Goo and J.W. Cho, *Macromolecular Materials and Engineering*, 2005, **290**, 11, 1049.
95. J.W. Cho, J.W. Kim, Y.C. Jung and N.S. Goo, *Macromolecular Rapid Communications*, 2005, **26**, 5, 412.
96. H. Jin Yoo, Y. Chae Jung, N. Gopal Sahoo and J. Whan Cho, *Journal of Macromolecular Science: Part B*, 2006, **45**, 4, 441.
97. I.H. Paik, N.S. Goo, Y.C. Jung and J.W. Cho, *Smart Materials and Structures*, 2006, **15**, 5, 1476.

98. I.H. Paik, N.S. Goo, Y.C. Jung and J.W. Cho, *Smart Materials and Structures*, 2006, **15**, 5, 1476.
99. H.M. Wache, D.J. Tartakowska, A. Hentrich and M.H. Wagner, *Journal of Materials Science: Materials in Medicine*, 2003, **14**, 109-112.
100. M. Ahmad, J. Luo and M. Miraftab, *Science and Technology of Advanced Materials*, 2012, **13**, 1, 015006.
101. N. Carrejo and M.H. Johnson, inventors; Baker Hughes Inc., assignee; US 20120193019, 2012.
102. P. Duan and P. McElfresh, inventors; Baker Hughes Inc., assignee; US 7926565, 2011.
103. J.L. Leo, G. Elm and W. Wsuwatosa, inventors; Briggs & Stratton Corp, assignee; US 3766629, 1971.
104. P. Jain and T. Pradeep, *Biotechnology and Bioengineering*, 2005, **90**, 1, 59.
105. E. Scholten, L. Bromberg, G.C. Rutledge and T.A. Hatton, *ACS Applied Materials & Interfaces*, 2011, **3**, 10, 3902.
106. C.H. Wu, F.K. Lee, S. Kumar, Q.D. Ling, Y. Chang, Y. Chang, H.C. Wang, H. Chen, D.C. Chen, S.T. Hsu and A. Higuchi, *Biomaterials*, 2012, **33**, 33, 8228.



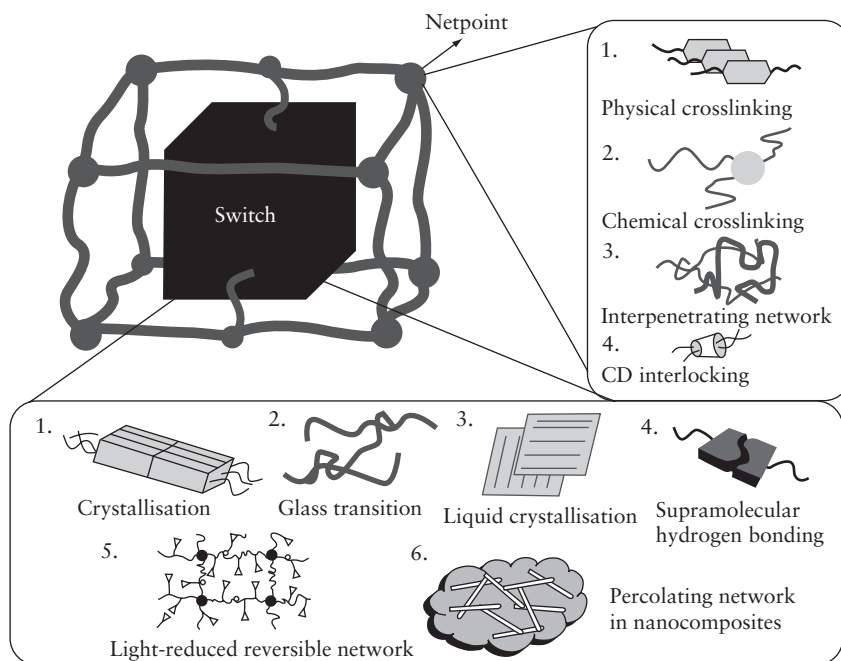
# 9 Future Outlook

## 9.1 Introduction

Shape-memory polymers (SMP) have been studied for half a century. Their applications have been explored in some areas, and a relatively complete research framework has been established in these areas, i.e., basic structures, mechanisms and principles, feasible stimuli, useful functions and application-related issues. The number of publications on SMP has increased dramatically in the last 5 years. According to the Science Citation Index, compared with 2005, the number of articles published in 2010 reflects a threefold increase, and presently this represents more than 20% of the total number of publications in the past 5 years [1]. This trend clearly shows that SMP research is becoming increasingly popular, and has gained considerable attention in academic and practical arenas. We believe that a more comprehensive and complete system can develop only from fundamental understanding, effective applications, and integration of methodologies and principles. The next 5 years will see an explosion of growth of research activities in many areas, which will hopefully include breakthroughs in applications. This outlook calls for exploration in the areas detailed in the sections detailed below.

## 9.2 New Shape-memory Polymers with Novel Structures and Diversified Functionalities

The discovery of novel SMP with different shape-memory effects (SME) will play a significant part as the capabilities of materials are pushed into new territories and create potential impacts in different application fields. Practically, the three-dimensional (3D) molecular model based on netpoints and switches proposed by Hu [1] (**Figure 9.1**) is an insightful structural framework of a SMP. This model can be enriched by adding more types of switches and netpoints to develop more varieties of SMP with various SME.



**Figure 9.1** Overall architecture of SMP. CD: cyclodextrins. Reproduced with permission from J.L. Hu, Y. Zhu, H.H. Huang and J. Lu, *Progress in Polymer Science*, 2012, 37, 12, 1720. ©2012, Elsevier [2]

### 9.2.1 New Stimulus Switches

Several SMP stimuli types have been devised, but the use of other switches in the place of existing ones (particularly glass transition or melting crystals) would be interesting. A promising switch structure may come from supramolecular entities containing donors and acceptors [3–6]. Special new molecular switches that would break ground for new SMP designs could produce many unexpected properties, as well as new functionalities (e.g., molecular switches including reversible molecular units activated upon the presence or removal of a certain voice or wavelength).

### 9.2.2 Intrinsic Athermal Switches

Further study is needed to develop intrinsic athermal switching SMP materials that can respond to different parameters of their applied environments. Currently, photo-

sensitivity and water response using cellulose nanowhiskers (CNW) and -SH are genuine non-thermal switches [7–10]. All other types of stimuli-responsive switches, such as electrically sensitive SMP, use heating as a trigger. Thus, the so-called ‘athermal switches’ are actually indirect thermal switches [11–14]. It is not known if genuine athermal switches are possible, for example, an electrically sensitive switch that does not heat the polymer but instead switches on and off upon electrical signals. If switches can be genuinely athermal in this way, the SME of SMP could be even more attractive. For example, if there are electrical switches in an elastomer, the recovery time of the strain could be extremely short, and the control could be more accurate because heating takes time in thermally responsive SMP, whereas the electrical signal could be instant. All other properties of such SMP could also be different, for example, cold drawing and reversible plasticity may not exist. Molecular imprinting polymers may play a part in this aspect. This method creates memory for template molecules within the flexible structure of a polymer.

### **9.2.3 Multi-responsive and Multi-functional Switches**

SMP are expected to be capable of providing more complex actuation events, and they have potential applications in sensors, actuators, biomedical devices and deployable structures. Thus, further studies on multi-step, multi-shape, multi-sensitive, multi-function and two-way SME are of interest. In particular, studies are moving rapidly toward combining different technologies for multi-functional and multi-sensitive SMP. Utilisation of supramolecular switches in SMP shows cross-disciplinary features that focus on functional polymers with supramolecular chemistry. Triple and multiple SME can be operated entirely using different mechanisms, such as combined switches activated by water as well as thermal and electrical stimuli [15–18]. In addition, special functions of SMP (other than simple SME) would be desirable to enhance their performance and tailor their properties for different applications. In addition to those illustrated by Behl and co-workers [18], special functions could include (but would not be limited to) antibacterial properties, ultraviolet resistance, thermal resistance and chemical resistance.

## **9.3 Development Trends of Shape-memory Polymer Composites and Blends**

SMP composites and blends are promising for achieving multi-responsive and multi-functional properties. SMP composites can exhibit novel properties that are significantly different from their ‘pure’ counterparts and are particularly powerful for materials that lead to new as well as multi-responsive and functional SME [2].

We can obtain SME by constructing composites that are not only triggered by heat but also by light, electricity, infrared radiation, magnetic fields and even moisture or chemical solvents individually, collectively and collaboratively. It would be even more attractive if we could use two independent, abundantly available materials, such as an elastomer as a matrix and particularly natural materials such as collagen, chitosan and CNW to produce SME of their composites. This could add new switches to the existing framework for novel SME, and could provide natural materials with new opportunities, as well as new materials for wide areas of applications. The use of CNW for shape-memory switches has led to the design of SMP with two totally non-shape-memory (SM) materials, i.e., an elastomer as a matrix or network and CNW as a switch. This could lead to thermal and moisture triggering (twin-switches), thereby renewing research interest in building multi-sensitive SMP.

### **9.3.1 Electric-Sensitive Shape-memory Effect**

A certain level of electrical conductivity of SMP can be reached by incorporating electrically conductive ingredients into thermally active SMP. If a current passes through the conductive ingredient network within a SMP the induced Joule heating can increase the internal temperature to above the switch transition temperature to trigger shape-recovery [14, 19–22]. During an electric-active shape-memory process, a SMP is subject to large variations in temperature and deformation. Temperature and strain have significant influences on the electrical resistivity of filled SMP. Gunes and co-workers [23] studied the relationship between the electrical resistivity and sample temperature and deformed strain of shape-memory polyurethanes (SMPU) filled with carbon nanofibres (CNF), oxidised-CNF, and carbon black (CB). It was found that CB-filled SMPU showed a pronounced positive temperature coefficient (PTC) of resistivity, which is related to non-linear thermal expansion during heating of the composites. Imposed deformation could increase the resistivity of the CB-filled composites by several orders of magnitude. CNF and oxidised-CNF-filled SMPU had no PTC effect, which the authors ascribed to low soft segment crystallinity. Strain also did not significantly affect the resistivity of the CNF and oxidised-CNF-filled SMPU. Another aspect that needs to be taken into consideration for electro-active SMP composites is the influence of conductive fillers on the deformability of SMP. Although fibrous conductive fillers can more significantly improve the electrical conductivity and enhance the stiffness and strength of SMP than CB, they cause lower maximum bending strain in comparison with conductive particles. Normally, the recoverable strain of pure SMP is  $\leq 100\%$  whereas that of fibrous filler-reinforced SMP is only a few percent, so deformation incompatibility occurs. For specific applications, there may be a best balance among the filler content, filler type, mechanical properties, and shape-memory properties.

### **9.3.2 Light-Sensitive Shape-memory Effect**

Light can also increase SMP temperature to above the switch transition temperature to trigger shape-recovery. The heat absorbance of SMP can be enhanced by incorporating fillers such as CB and CNT [11, 24–26]. These materials may be used for an intravascular laser-activated therapeutic device that can mechanically retrieve thrombi and restore blood flow [27]. There are other types of light-active SME that can be induced by photo-isomerisation (e.g., azobenzenes [28]), photo-induced ionic dissociation (e.g., triphenylmethane leuco derivatives [29]) or photo-reactive molecules (e.g., cinnamates [30]). It is believed that research of such novel SMP will increase in the near future.

### **9.3.3 Magnetic-Sensitive Shape-memory Effect**

By using ferromagnetic fillers, magnetic-sensitive SMP composites have been prepared. Several researchers using magnetic fields have enabled remote actuation of SMP composites by incorporating nano-iron (II,III) oxide nanoparticles into thermoplastics and thermoset SMP [11, 16, 31, 32]. Compared with conventional methods of shape-recovery triggering by direct heating, magnetic-active SME have five main advantages. Firstly, by selecting a ferromagnetic particle material with a Curie temperature within safe medical limits, Curie thermoregulation eliminates the danger of overheating. Secondly, power transmission lines leading to a SMP device are eliminated. Thirdly, more complex device shapes can be activated because consistent heating is expected to be achieved for any type of device geometry. Fourthly, selective heating of specific device areas is possible. Finally, remote actuation allows for the possibility of embedded devices that can be actuated later by an externally applied magnetic field [32, 33]. These advantages make magnetic-sensitive shape-memory materials promising materials for biomedical applications.

### **9.3.4 Water/Solvent-Sensitive Shape-memory Effect**

The glass transition temperature ( $T_g$ ) of SMPU (glass transition as the switch) drops if SMPU are exposed to a high-humidity environment/solution after a certain period of time because water molecules have a plasticising effect on polymeric materials, and can then increase the flexibility of the macromolecular chains. The two functions mentioned above lead to the shape-recovery of deformed SMP [34]. It was found that high CB content decreases the moisture sensitivity of composites [35]. Another method to obtain moisture/water-active SME is by using a hydrophilic or water-soluble ingredient in SMP [36]. A water-sensitive biodegradable stent made of chitosan films crosslinked with an epoxy compound is prepared following the strategy by Chen



and co-workers [37]. The raw materials (chitosan and polyethylene glycol-400) used in the fabrication of the developed stent are relatively hydrophilic. The degradable stent has been proposed to be used as an alternative to metallic stents and for local drug delivery. It is estimated that development of water/solvent-sensitive SMP will accelerate further for many application fields requiring non-thermal transitions.

### **9.3.5 Shape-memory Effect based on Non-thermal Phase Transitions**

In general, for most of the SMP and SMP composites reported, the switches to fix or recover the shapes of SMP are a  $T_g$  or melting transition temperature ( $T_m$ ). Researchers are trying to find other switches in place of glass transition or melting transition as shape-memory switches. A successful structure as the shape-memory switch is the transition between the isotropic phase to the nematic phase of a liquid-crystal phase [38]. Another promising switch structure may arise from supermolecular structures containing donors and acceptors [39]. Other structures that can be used as switches for SMP are thermally reversible covalent reactions such as thermo-reversible Diels–Alder chemistry [40], photo-reversible olefin cyclo-additions [41], thiol-driven reversible sulfide coupling [42], and thermally cleavable alkoxyamines [43]. Though these structures as the switch of SME are not necessarily to be achieved first in SMP composites or blends, such structures inspire researchers to study the possibility of developing SMP composites and blends using the transitions mentioned above as switches.

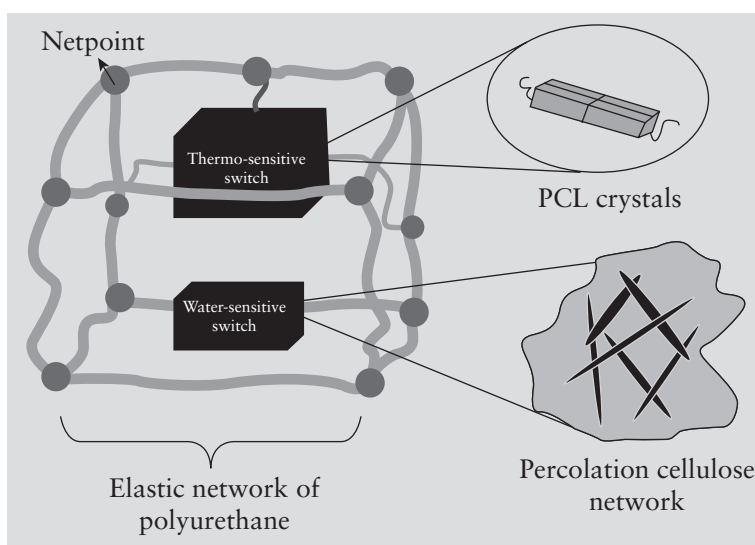
## **9.4 Versatile Shape-memory Effects by Novel Programming Protocols**

One of the most beautiful features of SMP is their versatile programmability. Xie [44] made an analogy of the programming of SMP to the programming of computer software. This analogy vividly describes the nature of the capacity of SMP. The types of software for SMP will become more versatile and readily available over the next 5 year as SMP are studied with a greater understanding of their programming principles. Thus, discovery of novel SME and protocols by programming are equally important to new SMP structures because they have potential impacts on real-world applications in terms of choices during device design.

### **9.4.1 Programmability**

The discovery of programming principles is required. The temperature-memory

effect [45] is an interesting example useful for designing new types of shape-memory functionalities. Combination of SME among one-way, two-way and triple SME and the temperature memory effect are good examples to inspire novel programming principles in the years to come. Another example is twin-switch SMP. Hu and co-workers [46–48] reported that CNW/elastomer and CNW/SMPU nanocomposites show novel water sensitivity due to reversible hydrogen bonding among the  $-OH$  groups of CNW. They proposed a CNW/SMPU nanocomposite with heterogeneous twin-switches (**Figure 9.2**). Interestingly, they found that the resultant CNW/SMPU exhibited triple SME upon exposure to sequential thermal and water stimuli [46].



**Figure 9.2** Structure of CNW/SMPU nanocomposites with twin-switches. PCL: poly( $\epsilon$ -caprolactone). Reproduced with permission from H.S. Luo, J.L. Hu and Y. Zhu, *Macromolecular Chemistry and Physics*, 2011, 212, 18, 1981. ©2011, John Wiley & Sons [46]

#### 9.4.2 Imperfection or a New Shape-memory Effect

The following enlightening experience is related to programmability. Cold drawing during shape-memory programming was observed years ago by different researchers (including our research team) and perceived as a defect, such as the ease of deformation

under normal temperatures in many applications. Although cold drawing does not cause ‘true’ plastic deformation [49], this means that SMP cannot be particularly controllable or not ‘smart’ enough because they change their shape beyond their switching temperature range without opening the switch structure. During cold drawing, through reversible rearrangement of the entangled molecular chains, devices made of such SMP can be more easily deformed than others. Thus, the advantages of SME by controlling shape change by switches cannot be realised before their shortcomings affect their use. To overcome this problem, our research team spent years trying to find the solution. The eventual solution was to make an ‘imperfect’ SMP that has only 50% fixity (or a compromised SME) with part elasticity. However, Xie [44] used a new concept of reversible plasticity and described some applications that elevate it to a new SME for SMP.

## **9.5 Fundamental Understanding**

Because of the nature of the wide range of transitional glassy and crystal structures, SMP have some unstable and less defined properties (if they are considered from a negative point of view) or highly flexible properties (from a positive point of view), which can be programmed to become new functions for various applications in actual case design and application methods. In reality, as we talk about SMP, there are always many advantages, but we frequently encounter co-existing limitations for their implementation in applications. Thus, despite the current prosperity of newly discovered SME, new structures and new applications of SMP, our understanding of the fundamentals, in general, remain superficial. The positive aspects of the inherent features of SMP require extensive search of smart, innovative and practical applications, as well as in-depth understanding of polymer physics.

## **9.6 Comprehensive Study of Structure–property Relationships**

A precise SME for a specific application should include: (a) the most effective triggering media, heat, water, infrared (IR) light, or electricity; (b) optimal triggering conditions, temperature, and starting/ending times; (c) controllable recovery speed, time and dependency; (d) fixity level (perfect or compromised); (e) recovery level; (f) exact recovery shape; and (g) engineered recovery force at different steps. Although research activities have covered these aims, this field has reached a full level of understanding and accurate design of a polymer system. Specific application situations pose specific requirements on the overall properties of a SMP. Extensive and intensive studies are required on the relationship between the structure of a SMP, the properties of the material, and the requirements of the specific application. Depending on polymer

physics, more precise programming and detailed control of different parameters, the conflicting properties for a certain application may be resolved, which can lead to smart, broad, meaningful and practical applications as a result of a more thorough understanding of SMP.

The study of composites includes their interfacial behaviour, dispersion efficiency, mechanisms of SME transfer by different stimuli, optimisation of structure and properties, and structural analyses within components, as well as the discovery of new phenomena within different shape-memory composite systems.

## **9.7 Modelling**

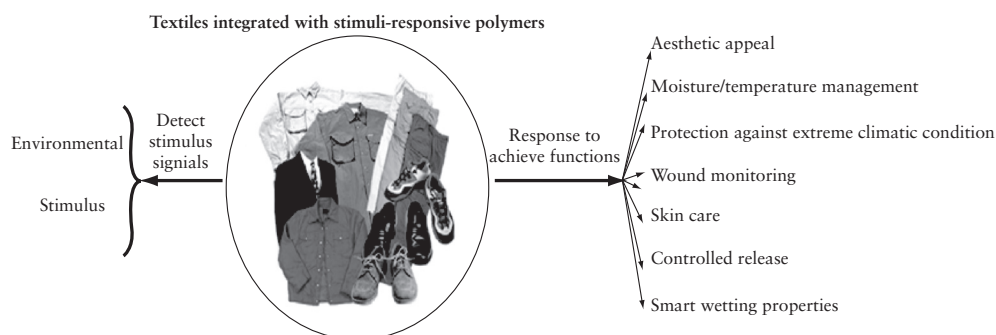
Several methods have been used to model the constitutive relationships at different structural levels of SMP. Each of them is applicable to a particular set of SME parameters and a particular polymer system, such as thermally induced amorphous copolymers. More models are needed for different polymer systems, including those responsive to stimuli other than heat and light, such as water-sensitive composites. More generalised models would also be useful because they are more universally applicable to different polymer systems, particularly heterogeneous systems. From this perspective, the multiple natural configurations framework devised by Rao and co-workers [50–53] could unify some of the polymer systems.

Modelling results have important implications for future research efforts and emerging applications. As applications of SMP enter the stage of more accurate engineering and more practical design of devices, advanced numerical modelling will be extremely important. Constitutive models of SMP incorporated into finite element software can predict their mechanical behaviour in applications with different environments. A good example by Oh and co-workers [54] represents the arrival of this era, in which mechanical modelling of SMPU braided stents was carried out to assess their mechanical performance and to investigate the feasibility of developing smart and thermo-responsive stents. Obstacles must be overcome for user-friendly models by the modelling community, including over-complicated modelling processes, limitations in the small strain domain, isotropic properties, and over-simplifications of some assumptions. In reality, shape-memory (recovery) occurs under complicated environmental constraints (e.g., surrounding tissues in biomedical applications). All of these considerations must be addressed in the future.

## **9.8 Application in Textiles**

SMP provide potential and enormous current opportunities in the textile industry.

By integrating SMP into textile structures, we can obtain novel functional textiles with profoundly significant properties, in areas such as: moisture/temperature management; protection against extreme climatic conditions; textile soft displays; wound monitoring; skin care; fantasy design with colour changes; controlled release; and smart wetting properties on textile surfaces (**Figure 9.3**). Textiles with SMP can move or change their shapes, achieving different 3D forms in garments, thereby enhancing their aesthetic appeal. Window curtains or screens with surface plasmon resonance (SPR) can open and close intelligently under environmental stimulation. The microstructure or macrostructure changes in smart clothing in response to stimuli are a good means for achieving heat and moisture management of human bodies with feelings of comfort. The change in fabric configuration can also be used for protection against extreme environments.



**Figure 9.3** Textiles integrated with SPR can achieve many novel functions

Light as a stimulus for textile applications is particularly attractive because it is convenient and environmentally friendly. Many light-active polymers have been developed, such as azobenzene-based crystalline elastomers, anthracene-based polymers and coumarin-based polymers. However, research in the application of light-active polymers in textiles is limited, though some light-active threads and nanofibres have been reported [55, 56]. One of the reasons is that most light-active polymers need light of a particular wavelength, which constrains their practical applications in garments.

In addition to shape change and recovery properties, stimuli-responsive textiles can offer a deformation force that can be employed in medical applications. Orthopaedic smart textiles can be applied in corrective aids. Furthermore, the textile products developed could be used in protective clothing to provide protection against hazardous

heat and light. Stimuli-responsive textiles with changes in volume and shape can also be used in skin-care products with controllable release of perfume, nutrition, and drugs. In addition to the applications mentioned above, stimuli-responsive textiles open up new opportunities for smart textiles in the fields of medicine, thereby widening their applications.

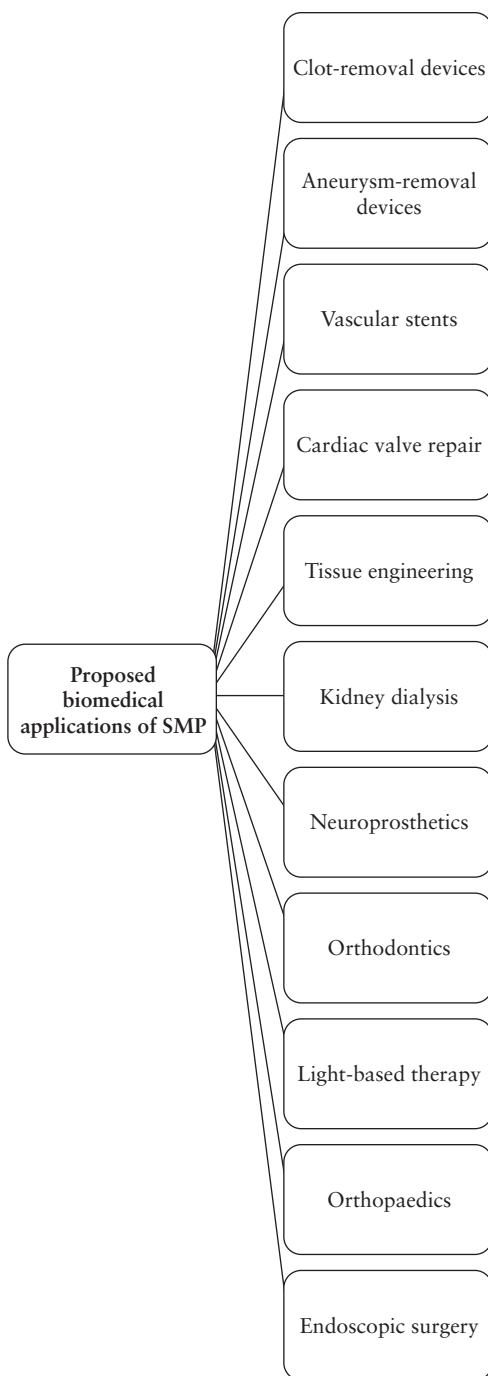
Use of SMP for textile applications is largely unexplored. Even though polymer materials can have good compatibility with textiles, textile applications impose strict requirements on the original properties of SMP such as safety, light weight, high stability, soft handle and good processability. Dyeing, washing and maintenance also need to be taken into consideration for most clothing applications. Much work needs to be carried out to investigate the properties of SPR in detail and then integrate these properties in textile products.

With rapid development of SMP and novel strategies for integrating SMP into textiles, it is anticipated that research into smart textiles with SPR will grow in multiple dimensions as a result of their promising potential applications. In the future, textiles may perform functions that are much more significant, far beyond what is being achieved at present.

## **9.9 Biomedical Applications**

SMP have advantages such as light weight, high strain/shape-recovery ability, easy processability, biocompatibility, and biodegradability that make them promising materials for biomedical applications. Several researchers have investigated the potential of SMP in many applications arenas, such as: drug-delivery systems; medical devices for minimally invasive surgery; micro-actuators for endovascular removal of thrombi; aneurysm occlusion; degradable sutures (**Figure 9.4**). Companies making SMP include DiAPLEX (thermoplastic and thermoset polyurethane), Cornerstone Research Group (Veriflex, Verilyte™, Veritex™: thermoset polystyrene), Lubrizol Advanced Materials (Tecoflex: aliphatic thermoplastic urethane), and Composite Technology Development, Inc. (TEMB: thermoset epoxy) [57].

There is a lot of scope for extending the applications of SMP in many other biomedical fields. For instance, the design of ‘growth’ stents [58] that could be deployed in infants whose blood vessels will grow after implantation could benefit from biodegradable SMP-based stents if designed as polymers that can be remodelled with surrounding tissue. Moreover, use of SMP in orthodontics could be explored further to provide lighter materials and more constant forces that may cause less pain to the patient, along with the aesthetic advantages that these materials offer (e.g., transparency, colourable, and/or stain resistant) [59].



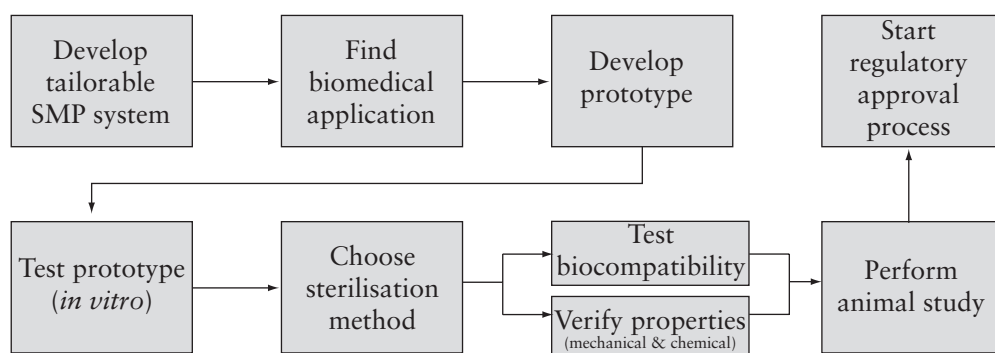
**Figure 9.4** Applications of SMP in biomedical fields

Recently developed SMP foams together with cold hibernated elastic memory (CHEM) processing further widen their potential biomedical applications [2, 60, 61]. CHEM foams can be miniaturised, deformed and inserted in the body through small catheters. Then, under body heat, they can self-deploy/recover precisely a much larger predetermined required shape in a satisfactory position. Several important CHEM applications are being considered for self-deployable vascular and coronary devices. One of these applications, endovascular treatment of aneurysms, was investigated experimentally with encouraging results. It is strongly believed that SMP materials and CHEM foams will significantly and positively impact the medical-device industry. It will open a door to designing and building novel, exciting and (often life-saving) medical products and devices.

The SMP that have been discovered so far have sufficient thermo-mechanical and shape-memory properties to succeed as medical devices. However, there is concern about how to improve stress recovery, produce better manufacturability, and modify chemistry remotely. For example, in the case of stenting, larger radial strength is necessary to withstand vessel pulsation pressure at 37 °C, as well as broader ranges of mechanical properties to completely fulfil vascular mechanical requirements [62]. Moreover, ageing after implantation should be considered carefully because it can increase switching temperatures by >10 °C [59, 63]. The complex tissue environment around SMP devices is an enormous challenge for their applications. Hence, constitutive modelling studies could facilitate implementation of this technology by predicting important limitations before clinical use.

Yackacki and Gall [64] proposed a pathway for the research and development of SMP biomedical devices (**Figure 9.5**). First, a tailor-able SMP system must be developed, such as a novel thermoset acrylate system or biodegradable multiblock copolymer [65]. Next, a biomedical application must be identified [66]. It is debatable whether the application should come before development of the SMP system. Thereafter, a prototype design must be developed to prove the capabilities of manufacturing the device [67]. Once proof-of-concept of the SMP device is established in an *in vitro* model, an appropriate method of sterilisation must be selected. Once the performance and biocompatibility of the device has been demonstrated in a reasonable fashion, a pilot animal study may be needed for class-II devices and upwards [68]. Furthermore, the costs and difficulty of these tasks increase along the projected pathway, ending with the regulatory approval process. All of the steps in the research and development pathway should be met before any steps in the regulatory approval can begin.





**Figure 9.5** Proposed research and development pathway for SMP biomedical devices. Reproduced with permission from C.M. Yakacki and K. Gall, *Advanced Polymer Science*, 2010, 226, 147. ©2010, Springer [64]

## 9.10 Applications toward Commercial Success

Applications are the ultimate goal of all fundamental investigations of SMP. SMP have a tremendous capacity for design (as demonstrated in the structure model proposed by Hu [1]), programmability (as described by Xie [44]), functionality (as realised by the triple and multiple shapes and choices of properties examined by Ji and co-workers [69]) and triggering stimuli (as summarised by Meng and Hu [11]). Thus, the application potential for SMP appears to be nearly unlimited, and we can reasonably predict that the applications of SMP to various areas will continue to prosper in the years to come.

### 9.10.1 Maturing and Broadening of Applications

#### 9.10.1.1 Existing Widely Researched Areas

Biomedical applications have been the most active area of research in the past decade, and will continue to be one of the most important area in the near future. Some devices may become mature technologies, and particular interest will be focused on tissue engineering, tissue repair, minimally invasive surgery, controllable drug delivery, as well as the biodegradability and biocompatibility of SMP. Textiles offer another direction of interest. SM fibres using different technologies have been developed and

some prototypes have been made in Hong Kong Polytechnic University by working with international companies for textiles, sportswear, intimate apparel and industrial applications. In the next 5 years, SMP may see considerable commercial success.

### **9.10.1.2 Broadening Areas**

In addition to medicine and textiles, broadening of the application range is important. This broadening is beginning to occur for SMP. From this perspective, another possible early successful application area could be deployable structures for aircraft and space industries, as well as military applications. In addition to their light weight, large volume change and flexibility, SMP can change in a gradual fashion (smooth and without shock), and they have well-controlled recovery. This control is important because an overly fast recovery can vibrate systems in space, which causes damage. Surface and thin-film applications should also be the subject of increased attention because the advantages of SMP can be more easily realised, such as their need for small recovery forces (a typical feature of SMP). Emerging areas also include energy harvesting from solar energy (light-responsive SMP), chemical energy (chemical-responsive SMP) and two-way SMP to achieve cyclical deformation in artificial muscles, as is the case for shape-memory alloys [70]. Because these areas offer high value and social importance, future effort may be drawn in these directions.

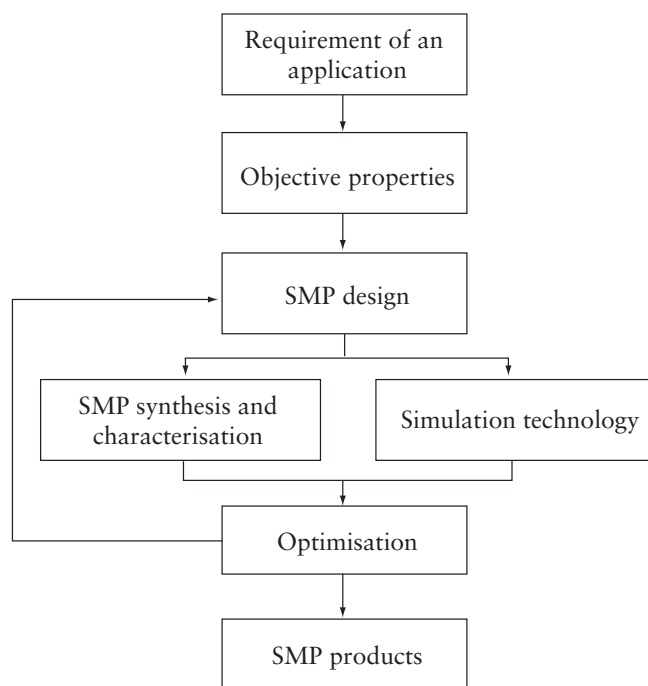
### **9.10.1.3 Untouched Areas**

Applications of SMP are limited mainly to one-way SMP. In future work, it would be interesting to explore the practical applications of two-way, triple and multi-shape SMP in innovative ways. Combination of all of these SME and the temperature-memory effect could generate highly attractive new shape-memory functionalities. Clearly, the future for SMP is bright: their scope of applications is broad and only limited by our imagination.

### **9.10.2 Integrated Approaches**

With the aim of developing SMP products for various applications, a useful strategy for related studies has been employed at the Shape-memory Textiles Center in Hong Kong Polytechnic University (**Figure 9.6**). First, with respect to SMP applications, users bring forward their requirements for a product. These requirements allow materials researchers to develop the objective properties of the SMP. These properties are the starting points for the synthesis and characterisation of SMP, as well as other basic studies. Meanwhile, simulation technologies, such as Materials Studio, Gauss

technology, and finite element packages, are used to facilitate polymer design and illustrate the mechanisms and relationships between the structure and properties. To achieve the desired properties for a certain application, there is a general need to optimise the structures and morphologies of SMP. These systematic studies produce desired outcomes and finally enhance SMP product design and performance. During this process, cross-disciplinary collaboration among chemists, material scientists and experts in highly specialised areas is necessary. Thus, new products can be more easily designed, and more innovative work will appear in the near future.



**Figure 9.6** Strategy for a SMP application study. Reproduced with permission from J.L. Hu, Y. Zhu, H.H. Huang and J. Lu, *Progress in Polymer Science*, 2012, 37, 12, 1720. ©2012, Elsevier [2]

### **9.10.3 Challenging Issues in Applications**

We have discussed the considerable potential of SMP for diverse applications in different arenas. Several application ideas, prototypes and initial commercial trials

have been proposed and implemented, but many conflicting issues remain to be resolved. Normally, specific application situations pose special requirements on the overall properties of SMP. For example, for biomedical applications, challenges exist with incorporation of SME to fulfil the multi-dimensional requirements of the: modulus; triggering/fixing conditions; degree and rate of fixing/recovery; level of recovery force; biocompatibility; rate of biodegradability and drug elution; release kinetics. The other key issue may lie in control of SME inside the human body, where the material must interact with flexible mechanical constraints such as tissue surroundings and daily motion, biological metabolism and complicated chemical environments (e.g., acids, salts and alkalis). For textile applications, difficulties lie in meeting the stringent requirements for all aspects of appearance. These include colour, dimensional stability, comfort and tactile properties, washability, strength, flexibility, stretchability and shape-memory, as well as compatibility with many other chemical, mechanical and thermal processing requirements and low-cost production. For engineering applications, the low recovery stress of SMP and the fact that the materials become too soft above the switch temperature of the SMP composites remain major concerns that present difficult problems. Although the shape-recovery stress can be improved to a certain degree by compounding or blending with other materials, under most circumstances, this method causes problems with low shape-recovery ratios and low deformable strains.

### **9.11 Supramolecular Shape-memory Polymers**

Fabricating smart materials with supramolecular switches is an attractive research topic. The use of non-covalent interactions in supramolecular SMP can offer several improvements over existing materials. Research of supramolecular SMP is a new research direction for shape-memory materials (SMM). Furthermore, the unique feature of this new SMP endows smart materials with more attractive functions. It can further promote applications of SMP greatly. Research into pyridine-containing supramolecular SMP networks is just beginning. A wide range of future possibilities for new research and applications are expected, and some future works are suggested below.

Polymer blending is an easy method to fabricate more new types of SMP networks. For example, Zhang and co-workers [71] prepared a novel styrene-butadiene-triblock copolymer and PCL blend for utilisation of SMM. Pyridine-based polyurethanes (PUPy) can form miscible polymers blends with polymers containing methacrylic acid groups. Based on the supramolecular structure of a polymer network with the addition of PUPy, excellent SME are expected to be achieved in polymers possessing no SME before. Furthermore, other properties (e.g., mechanical and damping) can also be improved in the new polymer blends. Hence, preparation and characterisation

of SMP blends with PUPy are attractive. Investigation of the interaction of PUPy polymers blends is also interesting.

Being one type of important supramolecular polymer, supramolecular liquid-crystalline polymers (LCP) have been studied widely [38, 54, 72]. LCP can form regions of highly ordered structure, and many unique properties can be developed in liquid-crystal elastomers (LCE). For example, a mesomorphic structure is observed in flexible polymer–surfactant systems due to hydrogen bonds between poly(4-vinyl pyridine) and pentadecylphenol. In addition, two-way SME have also been reported in triblock LCE. Hence, study of LCP is a hot topic. LCP or LCE can provide a route to nano-scale research because they are good polymers for many functional materials. *N,N*-bis(2-hydroxyethyl)isonicotin (BINA)-SMPU contain a large-fraction pyridine ring, and there are strong hydrogen bonds among urethane groups. Therefore, a polymer complex can be formed in the pyridine ring with addition of 4-dodecylcoylbenzoic acid. Simultaneously, the hydrogen bonds present in the urethane group can provide the polymer networks for formation of the liquid crystal phase. The molecular structure of BINA-SMPU is very close to supramolecular LCE, so some unique properties in this system are expected. Conversely, SME are maintained in these supramolecular LCE. Liquid crystalline properties are combined with BINA-SMPU through this polymer complex. Therefore, investigation of supramolecular LCE will be attractive in future studies.

Thermally induced SME and moisture-sensitive SME are observed in BINA-SMPU [3–6, 73–76]. In this system, the non-covalent molecular switch controls the shape-recovery and shape fixation in thermally induced SME and moisture-sensitive SME. The dynamic feature of non-covalent bonds is responsive to the external stimulus. According to the principles of dynamic combinatorial chemistry or constitutional dynamic chemistry, non-covalent bonds such as hydrogen bonds will be replaced by more adaptive non-covalent bonds upon application of an external stimulus. It is known that the moisture is water vapour. Similarly, by applying a gas on BINA-SMPU, the new formed hydrogen bonds between the pyridine rings and gas (e.g., acetic acid vapour) will interrupt the original hydrogen bonds. Hence, gas-sensitive SME can be expected in BINA-SMPU. Acetic acid vapour-sensitive SME can be achieved in BINA-SMPU, so future study in this area will be very interesting.

According to the nature of netpoints, SMP are divided into physically crosslinked SMP and chemically crosslinked SMP. In general, chemically crosslinked SMP show high shape-recovery and higher recovery force. In addition to the synthesis of physically crosslinked SMP, many types of chemically crosslinked SMP have also been studied [77–79]. Although many unique properties have been developed in physically crosslinked PUPy, some properties need to be improved. For example, the final shape-recovery under higher moisture conditions or water conditions is not high. Shape-

recovery force is low in PUPy with higher *N*-bis(2-hydroxyethyl)isonicotinamine content. It is known that the rubber modulus can be improved significantly by chemical crosslinking. Hence, it is expected that the hard phase acting as netpoints is more stable in PUPy with chemical netpoints. Consequently, it is expected that water-driven shape recovery can be improved by chemical crosslinking. Studies on crosslinked PUPy have been interesting, so many new properties are expected to be developed in crosslinked PUPy.

It has been reported that the main-chain type of PUPy containing a pyridine ring on the backbone can be synthesised with 2,6-bis(hydroxymethyl) pyridine [80–82]. The polymer chain of the main chain-type of PUPy is more regular than that of the side chain-type of PUPy. Accordingly, the supramolecular structure and morphology will be quite different from the side chain-type of PUPy. Based on this fact, other unique properties or better SME are expected. Therefore, the synthesis and characterisation of supramolecular SMP is another interesting area. Investigation of their properties will reinforce understanding of supramolecular SMP. In future studies, some unique properties and new applications are expected in this new type of main-chain type PUPy.

## 9.12 Conclusions

Significant progress has been made in enabling SMP technologies such as materials, processes, and methods, but these successes of application remain limited. Innovating the integration of all or major functions in practice is worth concerted effort. With respect to distinctive weak points, such as low recovery stress, we must look for new technologies to produce more powerful materials. We should be reasonable in our expectations for the near future, but existing problems can be overcome by finding more innovative applications that exploit the existing features and capacity of SMP. This goal requires tremendous creativity and sharp vision as well as financial investment.

## References

1. J.L. Hu and S.J. Chen, *Journal of Materials Chemistry*, 2010, **20**, 17, 3346.
2. J.L. Hu, Y. Zhu, H.H. Huang and J. Lu, *Progress in Polymer Science*, 2012, **37**, 12, 1720.
3. S.J. Chen, J.L. Hu, S.G. Chen and C.L. Zhang, *Smart Materials and Structures*, 2011, **20**, 6.

4. S.J. Chen, J.L. Hu, H.T. Zhuo, C.W.M. Yuen and L.K. Chan, *Polymer*, 2010, **51**, 1, 240.
5. S.J. Chen, J.L. Hu, C.W.M. Yuen and L.K. Chan, *Polymer International*, 2010, **59**, 4, 529.
6. S.J. Chen, J.L. Hu, C.W.M. Yuen and L.K. Chan, *Materials Letters*, 2009, **63**, 17, 1462.
7. N. Ljungberg, J.Y. Cavaille and L. Heux, *Polymer*, 2006, **47**, 18, 6285.
8. N.L.G. de Rodriguez, W. Thielemans and A. Dufresne, *Cellulose*, 2006, **13**, 3, 261.
9. D. Bondeson, I. Kvien and K. Oksman, *ACS Symposium Series*, 2006, **938**, 10.
10. A. Dufresne, J.Y. Cavaille and W. Helbert, *Polymer Composites*, 1997, **18**, 2, 198.
11. H. Meng and J.L. Hu, *Journal of Intelligent Material Systems and Structures*, 2010, **21**, 9, 859.
12. X.F. Luo and P.T. Mather, *Soft Matter*, 2010, **6**, 10, 2146.
13. J.S. Leng, X. Lan, Y.J. Liu, S.Y. Du, W.M. Huang, N. Liu, S.J. Phee and Q. Yuan, *Applied Physics Letters*, 2008, **92**, 1.
14. V.A. Beloshenko, V.N. Varyukhin and Y.V. Voznyak, *Composites, Part A: Applied Science and Manufacturing*, 2005, **36**, 1, 65.
15. X.F. Luo and P.T. Mather, *Advanced Functional Materials*, 2010, **20**, 16, 2649.
16. U.N. Kumar, K. Kratz, M. Behl and A. Lendlein, *eXPRESS Polymer Letters*, 2012, **6**, 1, 26.
17. U.N. Kumar, K. Kratz, W. Wagermaier, M. Behl and A. Lendlein, *Journal of Materials Chemistry*, 2010, **20**, 17, 3404.
18. M. Behl and A. Lendlein, *Journal of Materials Chemistry*, 2010, **20**, 17, 3335.
19. Y.J. Liu, H.B. Lv, X. Lan, J.S. Leng and S.Y. Du, *Composites Science and Technology*, 2009, **69**, 13, 2064.

20. H.B. Lu, F. Liang and J.H. Gou, *Soft Matter*, 2011, 7, 16, 7416.
21. X. Lan, W.M. Huang, N. Liu, S.Y. Phee, J.S. Leng and S.Y. Du in *Proceedings of SPIE*, Bellingham WA, USA, 2008, 6927.
22. M.Y. Razzaq, M. Anhalt, L. Frormann and B. Weidenfeller, *Materials Science and Engineering: A*, 2007, 444, 1-2, 227.
23. I.S. Gunes, G.A. Jimenez and S.C. Jana, *Carbon*, 2009, 47, 4, 981.
24. F. El Feninat, G. Laroche, M. Fiset and D. Mantovani, *Advanced Engineering Materials*, 2002, 4, 3, 91.
25. J.S. Leng, D.W. Zhang, Y. Liu, K. Yu and X. Lan, *Applied Physics Letters*, 2010, 96, 11.
26. J.S. Leng, X.L. Wu and Y.J. Liu, *Journal of Applied Polymer Science*, 2009, 114, 4, 2455.
27. W.I. Small, M.F. Metzger, T.S. Wilson and D.J. Maitland, *IEEE Journal of Selected Topics in Quantum Electronics*, 2005, 11, 4, 892.
28. Y.L. Yu, M. Nakano and T. Ikeda, *Nature*, 2003, 425, 6954, 145.
29. A. Mamada, T. Tanaka, D. Kungwachakun and M. Irie, *Macromolecules*, 1990, 23, 5, 1517.
30. A. Lendlein, H.Y. Jiang, O. Junger and R. Langer, *Nature*, 2005, 434, 7035, 879.
31. D.W. Zhang, Y.J. Liu and J.S. Leng, *Multi-Functional Materials and Structures III*, 2010, 123-125, 995.
32. Q.H. Meng and J.L. Hu, *Composites Part A: Applied Science and Manufacturing*, 2009, 40, 11, 1661.
33. M.Y. Razzaq, M. Anhalt, L. Frormann and B. Weidenfeller, *Materials Science and Engineering: A*, 2007, 471, 1-2, 57.
34. H.B. Lv, J.S. Leng, Y.J. Liu and S.Y. Du, *Advanced Engineering Materials*, 2008, 10, 6, 592.
35. B. Yang, W.M. Huang, C. Li, L. Li and J.H. Chor, *Scripta Materialia*, 2005, 53, 1, 105.



36. Y.C. Jung, H.H. So and J.W. Cho, *Journal of Macromolecular Science Part B*, 2006, **45**, 4, 453.
37. M.C. Chen, H.W. Tsai, Y. Chang, W.Y. Lai, F.L. Mi, C.T. Liu, H.S. Wong and H.W. Sung, *Biomacromolecules*, 2007, **8**, 9, 2774.
38. I.A. Rousseau and P.T. Mather, *Journal of the American Chemical Society*, 2003, **125**, 50, 15300.
39. J.H. Li, J.A. Viveros, M.H. Wrue and M. Anthamatten, *Advanced Materials*, 2007, **19**, 19, 2851.
40. X.X. Chen, M.A. Dam, K. Ono, A. Mal, H.B. Shen, S.R. Nutt, K. Sheran and F. Wudl, *Science*, 2002, **295**, 5560, 1698.
41. Y. Chen and K.H. Chen, *Journal of Polymer Science, Part A: Polymer Chemistry Edition*, 1997, **35**, 4, 613.
42. Y. Furusho, T. Oku, T. Hasegawa, A. Tsuboi, N. Kihara and T. Takata, *Chemistry: A European Journal*, 2003, **9**, 12, 2895.
43. E. Themistou and C.S. Patrickios, *Macromolecules*, 2006, **39**, 1, 73.
44. T. Xie, *Polymer*, 2011, **52**, 22, 4985.
45. T. Xie, *Nature*, 2010, **464**, 7286, 267.
46. H.S. Luo, J.L. Hu and Y. Zhu, *Macromolecular Chemistry and Physics*, 2011, **212**, 18, 1981.
47. H.S. Luo, J.L. Hu and Y. Zhu, *Materials Letters*, 2012, **89**, 172.
48. H.S. Luo, J.L. Hu, Y. Zhu, S. Zhang, Y. Fan and G.D. Ye, *Journal of Applied Polymer Science*, 2012, **125**, 1, 657.
49. J. Karger-Kocsis and E.J. Moskala, *Polymer*, 2000, **41**, 16, 6301.
50. J.S. Sodhi and I.J. Rao, *International Journal of Engineering Science*, 2010, **48**, 11, 1576.
51. G. Barot, I.J. Rao and K.R. Rajagopal, *International Journal of Engineering Science*, 2008, **46**, 4, 325.
52. G. Barot and I.J. Rao, *Journal of Applied Mathematics and Physics (ZAMP)*, 2006, **57**, 4, 652.

53. I. Rao in *Proceedings of the SPE-ANTEC Conference*, San Francisco, CA, USA, 2002. 2002.
54. Y.T. Oh, W.J. Kim, S.H. Seo and J.Y. Chang, *Macromolecular Research*, 2009, **17**, 2, 84.
55. T. Yoshino, M. Kondo, J. Mamiya, M. Kinoshita, Y.L. Yu and T. Ikeda, *Advanced Materials*, 2010, **22**, 12, 1361.
56. M. Kondo, T. Matsuda, R. Fukae and N. Kawatsuki, *Chemistry Letters*, 2010, **39**, 3, 234.
57. W. Small, P. Singhal, T.S. Wilson and D.J. Maitland, *Journal of Materials Chemistry*, 2010, **20**, 17, 3356.
58. P. Ewert, E. Riesenkampff, M. Neuss, O. Kretschmar, N. Nagdyman and P.E. Lange, *Catheterization and Cardiovascular Interventions*, 2004, **62**, 4, 506.
59. M.C. Serrano and G.A. Ameer, *Macromolecular Bioscience*, 2012, **12**, 9, 1156.
60. W. Sokolowski, A. Metcalfe, S. Hayashi, L. Yahia and J. Raymond, *Biomedical Materials*, 2007, **2**, 1, S23.
61. W.M. Sokolowski, A.B. Chmielewski, S. Hayashi and T. Yamada, *Smart Materials and Structures*, 1999, **3669**, 179.
62. M.C. Serrano, E.J. Chung and G.A. Ameer, *Advanced Functional Materials*, 2010, **20**, 2, 192.
63. V. Lorenzo, A. Diaz-Lantada, P. Lafont, H. Lorenzo-Yustos, C. Fonseca and J. Acosta, *Materials & Design*, 2009, **30**, 7, 2431.
64. C.M. Yakacki and K. Gall, *Advanced Polymer Science*, 2010, **226**, 147.
65. A. Lendlein, A.M. Schmidt and R. Langer, *Proceedings of the National Academy of Sciences*, 2001, **98**, 3, 842.
66. H.M. Wache, D.J. Tartakowska, A. Hentrich and M.H. Wagner, *Journal of Materials Science: Materials in Medicine*, 2003, **14**, 2, 109.
67. W. Small, T.S. Wilson, P.R. Buckley, W.J. Bennett, J.A. Loge, J. Hartman and D.J. Maitland, *IEEE Transactions on Biomedical Engineering*, 2007, **54**, 9, 1657.

68. A. Metcalfe, A.C. Desfaits, I. Salazkin, L. Yahia, W.M. Sokolowski and J. Raymond, *Biomaterials*, 2003, **24**, 3, 491.
69. F.L. Ji, J.L. Hu, T.C. Li and Y.W. Wong, *Polymer*, 2007, **48**, 17, 5133.
70. B. Zhou and Y.J. Liu, *International Journal of Modern Physics B*, 2009, **23**, 6-7, 1248.
71. H. Zhang, H.T. Wang, W. Zhong and Q.G. Du, *Polymer*, 2009, **50**, 6, 1596.
72. S.K. Ahn, P. Deshmukh, M. Gopinadhan, C.O. Osuji and R.M. Kasi, *ACS Nano*, 2011, **5**, 4, 3085.
73. S.J. Chen, J.L. Hu and S.G. Chen, *Polymer International*, 2012, **61**, 2, 314.
74. S.J. Chen, J.L. Hu, H.T. Zhuo and S.G. Chen, *Journal of Materials Science*, 2011, **46**, 15, 5294.
75. S.J. Chen, J.L. Hu and H.T. Zhuo, *Journal of Materials Science*, 2011, **46**, 20, 6581.
76. S.J. Chen, J.L. Hu, C.W.M. Yuen and L.K. Chan, *Polymer*, 2009, **50**, 19, 4424.
77. D.L. Safranski and K. Gall, *Polymer*, 2008, **49**, 20, 4446.
78. M. Kamenjicki and S.A. Asher, *Macromolecules*, 2004, **37**, 22, 8293.
79. C.D. Liu, S.B. Chun, P.T. Mather, L. Zheng, E.H. Haley and E.B. Coughlin, *Macromolecules*, 2002, **35**, 27, 9868.
80. G. Ambrozic, J. Mavri and M. Zigon, *Macromolecular Chemistry and Physics*, 2002, **203**, 2, 439.
81. G. Ambrozic and M. Zigon, *Acta Chimica Slovenica*, 2005, **52**, 3, 207.
82. G. Ambrozic and M. Zigon, *Polym International*, 2005, **54**, 3, 606.

# Abbreviations

1,4-BD	1,4-Butanediol
2D	Two-dimensional
3D	Three-dimensional
3M4F	3 Multi-maleimide 4 multi-furan
ACP	Acrylic copolymer
Alg	Alginate
BF	Bisfuranic
BINA	<i>N,N-bis</i> (2-hydroxyethyl) isonicotinamide
CA	Cinnamic acid
CA-MA	Crosslinkable mercapto group
CB	Carbon black
CD	Cyclodextrins
CG	Coarse-grained molecular
CHEM	Cold hibernated elastic memory
CIE	Crystallisation-induced elongation
CLEG	Molecular network consisting of polyethylene glycol and poly( $\epsilon$ -caprolactone)
CLSMPU	Core solution of polycaprolactone based shape-memory polyurethanes

*Shape Memory Polymers: Fundamentals, Advances and Applications*

CNF	Carbon nanofibres
CNT	Carbon nanotube(s)
CNW	Cellulose nano-whiskers
COMPASS	Condensed-phase optimised molecular potentials for atomistic simulation studies
CS	Chitosan
CTH	Close then heal
DA	Diels-Alder
DETA	Diethylenetriamine
dl-PLA	Poly(D,L-lactic acid)
DMA	Dynamic mechanical analysis
DMF	Dimethylformamide
DNA	Deoxyribonucleic acid
DPD	Dissipative particle dynamics
DSC	Differential scanning calorimetry
EB	Embryoid bodies
EBAGMA	Ethylene-butyl acrylate-glycidyl methacrylate terpolymer
EMC	Elastic memory composites
EMISE	Electromagnetic interference shielding effectiveness
ENR	Epoxidised natural rubber
EOC	Two ethylene-1-octene copolymers
F	Fabric
Fc-PEI	Ferrocene modified branched ethyleneimine polymner

FEM	Finite element method
F <sub>o</sub>	Uncoated fabric
FTIR	Fourier-Transform infrared
GOD	Glucose oxidase
HDI	1,6-Hexamethylene diisocyanate
HDPE	High-density polyethylene
HS	Hard segment
HSC	Hard-segment content
IC	Inclusion complexes
IPDI	Isophorone diisocyanate
IPN	Interpenetrating polymer networks
IR	Infrared
LC	Liquid-crystalline
LCE	Liquid-crystalline elastomers
LCP	Liquid-crystalline polymers
$L_{\text{high}}$	Length at high-temperature
LLDPE	Linear low-density polyethylene
$L_{\text{low}}$	Length of the sample at low temperature
l-PCL	Linear poly( $\epsilon$ -caprolactone)
LSMP	Light-sensitive shape-memory polymers
MACL	Molecular network consisting of poly( $\epsilon$ -caprolactone)
MAI	Macroazoinitiator
MAV	Micro-aerial vehicle

MC	Monte Carlo
MCC	Microcrystalline cellulose
MD	Molecular dynamics
MDI	4,4-Diphenylmethane diisocyanate
MDTO	2-Methyl-7-methylene-1,5-dithiacyclooctane
MDTVE	2-Methylenepropane-1,3-di(thioethyl vinyl ether)
MEF	Metal-enhanced fluorescence
MEO <sub>2</sub> MA	2-(2-Methoxyethoxy)ethyl methacrylate
MIC	Melting-induced contraction
MWCNT	Multi-walled carbon nanotubes
Na-MMT	Sodium montmorillonite
NdFeB	Neo magnet
NIL	Nano-imprint lithography
Niti	Nickel-titanium
n-PCL	Crosslinked poly( $\epsilon$ -caprolactone) network
OEGMA	Oligo(ethylene glycol) methacrylate
PA	Polyamide
PA6	Nylon 6
PB	Polybenzoxazine
PBA	Polybutylene adipate
PBPSF2	Poly(1,4-butylene succinate-co-1,3-propylene succinate) prepolymer
PBS	Phosphate-buffered saline
PCHMA	Polycyclohexyl methacrylate

PCL	Poly( $\epsilon$ -caprolactone)
PCLA	Poly( $\epsilon$ -caprolactone- <i>co</i> -lactide)
PCN	Percolation cellulose network
PCO	Polycyclooctene
PDCL	Poly( $\epsilon$ -caprolactone) dimethacrylate
PDLLA	Poly(D,L-lactide)
PDMS	Polydimethyl siloxane
PEA	Polyester acrylate
PE	Polyethylene
PE-G	Maleated polyethylene
PEG	Polyethylene glycol
PEGDA	Polyethylene glycol diacrylate
PEGDMA	Polyethylene glycol dimethacrylate
PEO	Polyethylene oxide
PET	Polyethylene terephthalate
PETMP	Pentaerythritol- <i>tetra</i> -(3-mercaptopropionate)
PFMVS	Polyferrocenylmethylvinylsilane
PFSA	Perfluorosulfonic acid
P <sub>H</sub>	High-pressure
P <sub>L</sub>	Low-pressure
PLA	Poly lactide
PLGA	Poly(lactide- <i>co</i> -glycolide)
PLLA	Poly(L-lactide)



*Shape Memory Polymers: Fundamentals, Advances and Applications*

PMA	Polymethyl acrylate
PMMA	Polymethyl methacrylate
PMMA- <i>co</i> -VP	Polymer polymethyl methacrylate- <i>co</i> -(vinyl-2-pyrrolidone)
PMVS	Polymethyl vinyl siloxane
PNIPAAm	Poly( <i>N</i> -isopropylacrylamide)
POE	Polyoxyethylene
POE- <i>g</i> -MAH	Ethylene-octane copolymer graft maleic anhydride
Poly(LA- <i>co</i> -CL)	Poly(lactide- <i>co</i> - $\epsilon$ -caprolactone)
POSS	Polyhedral oligomeric silsesquioxanes
PP	Polypropylene
PPD	Poly( $\omega$ -pentadecalactone)
PPDO	Poly( <i>p</i> -dioxanone)
PPy	Polypyrrole
PS	Polystyrene
PTC	Positive temperature coefficient
PTMEG	Polytetramethylene ether glycol
PTMG	Polytertramethylene ether glycol
PU	Polyurethanes
PUPy	Moisture-active shape-memory polyurethanes
PUU	Polyurethane urea
PVA	Polyvinyl alcohol
PVAc	Polyvinyl acetate
PVC	Polyvinyl chloride

PVDF	Polyvinylidene fluoride
PVP	Polyvinyl pyrrolidone
Py-SMPU	Pyridine derivative shape-memory polyurethanes
$R_{act}$	Actuation magnitude
$R_f$	Fixity ratio
RH	Relative humidity
$R_r$	Recovery ratio
SBS	Styrene-butadiene-styrene
SCF	Short carbon fibres
SCLCN	Side-chain liquid crystalline network
SF-NIL	Step-and-flash nano-imprint lithography
SEM	Scanning electron microscopy
sG	Sulfonated graphene
SM	Shape-memory
SMA	Shape-memory alloys
SMASH	Shape-memory assisted self-healing
SMC	Shape-memory ceramics
SME	Shape-memory effects
SMEC	Shape-memory elastomeric composites
SMF	Shape-memory fibres
SMM	Shape-memory materials
SMP	Shape-memory polymers
SMPU	Shape-memory polyurethanes

SP	Soybean protein
SPR	Surface plasmon resonance
SWCNT	Single-walled carbon nanotubes
$T_{ah}$	Temperature at melting or solution state of <i>N,N</i> -bis(2-hydroxyethyl) isonicotinamide-shape-memory polyurethanes
$T_{al}$	Lower temperature when all hydrogen bonds are present in <i>N,N</i> -bis(2-hydroxyethyl) isonicotinamide-shape-memory polyurethanes
TCP	Triple-shape creation procedure
TE-NIL	Thermal embossing nano-imprint lithography
$T_g$	Glass transition temperature
$T_h$	High temperature
$T_{high}$	Higher order transition temperature
$T_i$	Isotropic temperature
$T_l$	Low temperature
$T_{low}$	Lower order transition temperature
$T_m$	Melting temperature
$T_{m,p}$	Temperature at which primary crystallites melts
$T_{m,s}$	Temperature at which secondary crystallites melts
TPCO	<i>Trans</i> -polycyclooctene
TPU	Thermoplastic polyurethane
$T_r$	Tailored transition temperature
TSPC	Triple-shape polymeric composites
$T_{sw}$	Switching temperature

$T_{trans}$	Transition temperature
UPF	Ultraviolet protection factor
UPy	Ureidopyridinone
UV	Ultraviolet
UVA	Ultraviolet A
UVB	Ultraviolet B
VGCF	Vapour grown carbon fibre
VIS	Visible
$w_{sp}$	Weight percentage of soybean protein in polyurethane/soybean protein blend
WVP	Water vapour permeability
x-PMMA	Crosslinked polymethyl methacrylate



# Index

1,4-Butanediol, 119, 123, 143, 197  
1,6-Hexamethylene diisocyanate, 119, 143, 175, 197-199  
2-(2-Methoxyethoxy)ethyl methacrylate, 131  
2-Methyl-7-methylene-1,5-dithiacyclooctane, 134, 136  
2-Methylenepropene-1,3-di(thioethyl vinyl ether), 134, 136  
3 Multi-maleimide 4 multi-furan, 123  
4,4-Diphenylmethane diisocyanate, 119, 197, 203

## A

Abrasion property, 234  
Absorption characteristics, 73, 213  
    Moisture absorption on shape-memory, 142-144, 206-207, 265  
    Filtration application, 251  
    Energy Absorption, 79, 120, 139, 249, 251  
Acceptor functionalities, 106, 192, 196-198  
    Hydrogen acceptor, 29, 123, 194, 198  
Activation, 27, 172  
    Remote activation, 26-27, 70, 228, 249  
Actuation magnitude, 126  
Adhesion, 100, 103, 234  
    Structure-property relation, 100, 103  
    Application, 60, 234  
Adsorption, 173-175, 178  
Agent, 94, 243  
    Self-healing, 94, 231  
    Finishing, 243  
Aggregation, 69, 176  
Alginate, 212-213  
Alignment, 41, 132, 146  
    Liquid crystalline elastomer, 41-42  
    Importance of fillers alignment, 71, 146  
Amorphous, 10, 14-15, 24, 89-90, 95, 118

- Phase, 15, 24, 170
  - Modelling of amorphous region, 170, 177
- Anisotropy property, 236
- Antibacterial, 216, 246-247, 251
- Appearance and aesthetics, 225, 242-243
- Application, 121, 148, 157, 170, 173, 215-217, 223-251, 269-279
  - Biomedical, 120-121, 223-230
  - Self-healing, 94, 231
  - Surface wrinkling and patterning, 234-239
  - Textiles, 239-248
  - Transportation, 249
  - Sensors and Actuators, 249
  - Filtration and Insulation, 251
- Applied stress, 35, 127, 165
- Aspect ratio, 62
- Atomic force microscopy, 103

## **B**

- Bimodal actuation, 129
- Binary blends, 90-91, 112
  - Biocompatible/biodegradable polymer, 27, 110, 144
- Biomaterial, 78
- Biomedical applications, 225-232, 271-273
  - Actuators, 228
  - Aneurysms treatment, 229
  - Cast, 226
  - Dialysis needles, 229
  - Drug-delivery, 229, 250
  - Orthodontic wires, 225
  - Muscle, 227
  - Stent, 228-230
- Biomimetic, 29, 117
- Bisfuranic, 37
- Blending in shape-memory polymer, 89-110
  - blending with fillers, 69, 74
  - crosslinked blends, 108-109
  - immiscible blends, 97-104
  - miscible blends, 90-93
  - blending in supermolecular shape-memory polymers, 277
- Block copolymer, 3, 10, 12, 97, 125
- Branched polymer, 3, 12, 129, 211

Building, 94

Bulk application, 223-233

## C

Carbon as filler material, 67, 120, 127

black, 120-121, 264-265

nanofibre(s), 65-68, 74-75

nanotube(s), 65-71

powder, 68, 146

Casting application, 226

Casting process, 197, 209-210

Cellulose nano-whiskers, 61-65, 263-264

Chemical stability, 148, 194-195

Chitosan, 211-212, 264-266

Chromophore, 13, 138

Classification of shape-memory polymer, 15-17

Close then heal, 232

Coarse-grained molecular, 173-174

Coating application, 226, 247-248

textile, 247-248

insulation, 251

medical, 226, 232

wetting, 236

Coil, 120-121

Cold drawing, 263, 267-268

Cold hibernated elastic memory, 229, 273

Condensed-phase optimised molecular potentials for atomistic simulation studies  
(COMPASS), 173-174, 176-177

Conformational, 175, 231

Corrosion protection, 232

Crack healing, 232-233

Crosslink polymers, 93-94, 108, 123-124, 210-212

Crystallisation-induced elongation, 42-43, 45

Cyclodextrin(s), 208-214

## D

Damping application, 129, 247

Degradable sutures, 271

Degree of crosslinking, 108, 111

Degree of crystallinity, 95, 146



Degree of swelling, 131  
Deployable system, 129, 228-230  
Diels-Alder reaction, 37  
Differential scanning calorimetry, 67, 202  
Dissipative particle dynamics, 157, 169  
Drug delivery, 138-139, 229  
Dual-shape memory effect, 31-34, 39

## **E**

Elastic memory composites, 71  
Elastomer, 97-98, 263-264  
Electrically induced shape-memory effect, 75, 144-147, 226-227  
    black, 120-121  
    nanofibre(s), 65-68, 74-75  
    carbon nanotube(s), 65-71  
    electromagnetic fillers, 75, 140  
Electromagnetic shielding effectiveness, 79  
Embryoid bodies, 236  
Epoxidised natural rubber, 111  
Epoxy, 44, 73-75  
Expandable system, 229, 249

## **F**

Fabric, 243-246  
Fatigue resistance, 42, 225  
Fibre, 239-242  
Filler in shape-memory polymer, 78-79  
    cellulose nanowhiskers, 62  
    Fe<sub>3</sub>O<sub>4</sub> particles, 139  
    graphene, 232  
    inorganic filler, 78  
    organic filler, 78  
    metal oxide, 75  
    nanofiller, 60  
    nanofiber/nanotube, 66  
Film(s), 232-234, 236, 238-239  
Filtration, 173, 251-252  
Finishing, 242-243, 248  
Finite element method modelling, 178-179  
Fixity ratio, 212

Foam, 229-230, 232-233  
cold hibernated elastic foam, 229

## G

Gel(s), 140-141, 213  
Gelation, 110, 178  
Glass fibre, 73  
Glass transition temperature, 15, 118-119  
Gold depositing for patterning, 234-236  
Grafting, 78, 194

## H

Hard segment, 5, 90-91, 173-175  
content, 39-41  
Hardening, 165  
Healing, 231-233  
High-density polyethylene, 101-102  
Homopolymerisation, 106  
Hydrogel, 137-138  
Hydrolysis, 61, 211  
Hysteresis, 162, 171

## I

Immiscible polymer blends, 97-98  
Impact application, 226, 249  
*In situ*, 66, 250  
application, 231, 249-350  
polymerisation, 66  
Inclusion complexes characteristics for supramolecular shape-memory polymer,  
208-213  
Incompatibility requirement for shape-memory effect, 10, 101  
Indentation, 240  
Induced stress, 180  
Injection moulding, 250  
Inorganic fillers, 78  
Insulation applications, 251  
Intelligent textiles using shape-memory polymer, 217  
Interpenetrating polymer network(s), 106-109  
Intravascular therapeutic device, 120, 138, 265  
Isotactic polypropylene, 62

Isotropic temperature, 24, 26

## **L**

Lamellae, 92

Laminated, 132, 228

composites, 215, 228

films, 132

Textiles, 247

Laser actuated, 120, 229-230, 265

Layered structure, 69

Ligand, 195

Light sensitive shape-memory polymer, 26-27, 70

Liquid crystalline elastomers, 41

Liquid crystalline polymers, 196-197, 278

Low density polyethylene, 101

Lower order transition temperature, 33, 128

## **M**

Macroazoinitiator, 76, 78

Magnetic fillers, 75-76, 139

Magnetic shape-memory effect, 139-140

Maleated polyethylene, 101-102

Melting induced contraction, 42-43, 45

Membrane, 87-88, 248, 257

Metal-enhanced fluorescence, 238

Metallic, 225, 230, 266

Micro-aerial vehicle, 250

Modeling of shape-memory polymers, 157-182

Interactions effects, 176

Mechanical properties, 177

Physical properties, 173-174, 178

Structure, 174-175

Modeling types for shape-memory polymers, 158,

Constitutive modelling, 158-159

Finite element, 178

Mesoscale modelling, 166-168

Microscale modelling, 170-172

Molecular dynamics/Monte Carlo, 173

Multi-scale modelling, 182

Moisture-active shape-memory polyurethane(s), 197-199, 201-203, 205-206

Moisture responsive shape-memory effect, 143, 206  
Molecular dynamics, 173-174, 176-177  
Monte Carlo, 157, 173-175  
Montmorillonite, 76  
Moulding, 9, 111, 250  
Multifunctional switches, 263  
Multi shape-memory effect, 16, 65  
    Mechanism, 65  
    Multi switch, 64, 267  
Multi-walled carbon nanotube(s), 71-72, 79-80, 105, 127, 145

## **N**

Nano-imprint lithography, 239  
Nanoclay, 76-77  
Nanocomposite shape-memory, 59-60, 68-69  
    Carbon based, 65-67  
    Electric/magnetic sensitive, 68, 75-76  
    Light sensitive, 70  
    Special function(s), 79  
Nanofiber as fillers, 65-68, 74-75  
Nanoscale indentation/wrinkling, 235  
Nanotubes as fillers, 65-71  
Natural rubber, 111  
Neo magnet, 60, 75  
Neuronal electrode, 24, 130, 229  
Nickel-titanium shape-memory alloy, 8-9  
Nickel powder, 71, 75  
Non-linear, 161, 264  
Non-polar, 25  
Non-toxic, 139

## **O**

Oligo(ethylene glycol) methacrylate, 131  
One-step programming, 32, 38  
Optical/light actuation, 14-129  
Order-disorder transition, 106  
Ordering in liquid crystalline, 41-42, 125  
Organic fillers, 78-79  
Organic solvents as stimuli, 25  
Organoclay, 77

## **P**

- Packaging application, 233, 249
- Patterning, 234-239
- Pentaerythritol-*tetra*-(3-mercaptopropionate), 134, 136
- Percolation cellulose network, 62
- Perfluorosulfonic acid, 38, 46-47
- Permeability, 79, 226, 245-248
- Permeation, 216
- Peroxide, 112, 126
- Phase separation, 10, 25-26, 175-176
- Phase transition, 41-42, 131, 193
  - Non-thermal, 266
  - Thermal, 24, 131
  - Liquid crystalline phase transition, 26, 28, 41
    - Anisotropic-isotropic, 41
    - Modelling, 170
- Phosphate buffered saline, 144
- Physicochemical properties, 176
- Plasticiser, 25
- Poly( $\epsilon$ -caprolactone), 31-35, 43-46, 90-94, 97-100, 231-232
- Poly(1,4-butylene succinate-*co*-1,3-propylene succinate) prepolymer, 28
- Polyacrylic acid, 131, 196
- Polyamide, 101-102
- Polybenzoxazine, 93
- Polybutylene adipate, 25, 46
- Polycondensation, 106
- Polycyclohexyl methacrylate, 32-34, 44, 76
- Polycyclooctene, 2, 11, 43, 126
- Polydimethyl siloxane, 169, 236
- Poly(D,L-lactic acid), 98
- Poly(D,L-lactide), 78
- Polyether ether ketone, 24
- Polyferrocenylmethylvinylsilane, 246
- Polyhedral oligomeric silsesquioxanes, 43, 46, 78-79, 144-145
- Polyisoprene, 25, 177
- Poly lactide, 95, 98, 100, 109
  - co*- $\epsilon$ -caprolactone, 109
  - co*-glycolide), 24, 107
- Poly(L-lactide), 103

- Polymethyl acrylate, 110-111, 189
- Polymethyl methacrylate, 47, 95, 106-108, 189
- Polymethyl vinyl siloxane, 110
- Poly(*N*-isopropylacrylamide), 131, 137-138
- Polyolefin(s), 25
- Polyoxyethylene, 100-103
- Poly(*p*-dioxanone), 37, 91, 119
- Polypropylene, 26, 62, 80, 100, 102-104
  - glycol, 100
- Polypyrrole, 103-105, 120, 146-147, 250
- Polystyrene, 3, 9, 235-236, 238, 271
- Polytetrafluoroethylene, 197, 234
- Polytetramethylene ether glycol, 25, 46, 119
- Polytetramethylene glycol, 248
- Polyurethane(s), 118-119
  - foam, 251
  - urea, 174
  - fiber, 240-241
  - finishing, 243-244
- Polyvinyl acetate, 62, 95
- Polyvinyl alcohol, 25, 66-67, 71
- Polyvinyl chloride, 90-91, 233-234
- Polyvinyl pyrrolidone, 106
- Polyvinylidene fluoride, 95-97, 234
- Poly( $\omega$ -pentadecalactone), 38, 44-45
- Porous nanofibrous, 246-248
- Positive temperature coefficient, 264
- Powder, 75, 197
- Prediction of properties of shape-memory, 161-165
- Prepolymer, 28, 93
- Probes for biomedical application, 230, 238
- Properties of shape-memory polymers, 160-177
  - Interaction, 176
  - Mechanical, 177
  - Physical, 173-174
  - Stress-strain characteristics, 160
  - Structural, 174
- Protection features, 79-80, 232, 270
  - Corrosion protection, 232
  - Impact protection, 229, 249

- UV protection, 79-80, 248
- Protein blend, 91
- Pyridine derivative shape-memory polyurethane(s), 30, 246

## **R**

- Recrystallisation, 122, 246
- Reinforcement, 57, 59, 62, 64, 73
- Reliability, 231, 249
- Remote actuation, 122, 265
- Response surface, 178
- Reversible phase transformation, 8
- Reversible order–disorder transition, 106
- Rigidity, 225, 249
- Ring opening polymerisation, 17
- Rotational, 182
- Roughness, 234, 238

## **S**

- Segmented polyurethane, 2, 119
- Self-healing, 231-232
- Semi-crystalline, 10-11, 23-25, 42-43
- Sensor, 129, 139, 249
- Shape fixity/recovery, 6-7
- Shape-memory effect(s), 38-48
  - One-way, 38-40
    - Thermally reversible reaction, 122
  - Multiple, 44-47, 128-130
  - Supramolecular, 123-124
  - Temperature memory, 48
  - Two-way, 40-44, 126
- Shape-memory function types, 16
- Shape-memory structure types, 16
- Shape memory materials, 1-2
  - Shape-memory alloy, 7-9
  - Shape-memory ceramics, 1-2
  - Shape-memory elastomeric composite(s), 99
  - Shape-memory fibres, 239-242
  - Shape-memory foam, 229
  - Shape-memory polymers, 3
  - Shape-memory polyurethane(s), 118-119

- Shape-memory mechanism,
  - of supramolecular, 190
  - of pyridine based shape-memory polymer, 204-207
  - of thermally induced, 11
  - of light-induced, 14, 129
  - of magnetic-induced, 140
  - of moisture-induced, 14, 64
  - of multiple shape-memory effect, 65
  - of elastomer/switch polymer blends, 98
  - of two-way shape memory effect, 128
- Short carbon fibres, 120-121
- Silicon, 74
- Single-walled carbon nanotubes, 69
- Smart textiles, 131, 249, 270-271
- Soft segment(s), 5, 31, 66-67, 118-119
- Softening, 30, 162
- Soybean protein, 91-93
- Spectroscopy, 243
- Spinning, 125, 239-241, 243
- Stent, 130, 144, 179, 229
- Step-and-flash nano-imprint lithography, 239
- Step growth, 118, 178
- Sterilisation, 273-274
- Stress-strain characteristics, 160-162
- Stimulus types, 16
- Stress-strain temperature relationship, 224
- Stroke treatment, 121, 250
- Structural modelling, 178-179
- Stimuli-responsive polymers, 117-147
  - Electric, 144-146
  - Heat, 117-120
  - Light, 132-133
  - Magnetic, 139-140
  - Water/solvent, 141-142
- Sulfonated graphene, 70
- Surface plasmon resonance, 238, 270-271
- Surface patterning, 234-236
- Surfactant, 67, 278
- Switching temperature, 31, 90-91
- Synergistic, 46, 71, 74



Synthesis, 108-109, 136, 143, 178, 195

## T

Targeted drug release, 130

Temperature memory effect, 48

Temperature sensors, 249-250

Tensile properties, 66, 102

Tensile strength, 104

Tensile stress, 170

Tensile testing, 71

Tetrahydrofuran, 3

Thermal analysis, 186

Thermal conductivity, 30, 57, 74, 81

Thermal control, 249

Thermal embossing nano-imprint lithography, 239

Thermal properties, 62, 66, 245

Thermal resistance, 263

Thermal stability, 79, 148

Thermal treatment, 37, 177, 241

Thermocouples, 250

Thermo-mechanical testing, 223-224

Thermoplastic elastomer, 97

Thermoplastic polyurethane(s), 62-65, 90

Thermoset shape-memory polymer, 73

Thin film application of shape-memory polymer in patterning, 234-236

Tissue engineering application, 229-230

    polymer used, 78

    hydrogel, 131

Transformation in shape-memory alloy, 8-9

Transition effect, 5-6

    Transition temperature, 5-6, 89

        in liquid crystalline elastomers, 26, 41, 46

Transparent shape-memory polymer, 69, 225

Transportation application, 249, 251-252

Treated clay, 76-77

Triple-shape memory, 16, 44-46

    Three way shape, 35-36, 39

    Triple-shape creation procedure, 77

    Triple-shape polymeric composites, 100

## U

- Ultrasonic, 61, 66
- Ultraviolet, 14, 27, 29, 42, 94, 108-109, 132, 134-137, 239
  - A, 80
  - absorption, 79
  - B, 80
  - protection factor, 79-80, 248
- Uni-axial tensile testing, 223-224
- Ureidopyridinone, 29, 45, 123-124, 189, 193-194

## V

- Vapour, 79, 245-248, 251
- Vapour grown carbon fibre, 79
- Velocity, 173
- Vertical, 237-238
- Vibration, 71, 73, 139, 199
- Vinyl pyridine, 278
- Viscoelasticity, 158, 161
- Viscosity, 100-101, 159, 197, 165-166
  - melt viscosity, 100-101, 103
  - coefficient of viscosity, 159
- Visible, 28-29, 132, 137
- Vitrification, 32, 223
- Voltage induced shape-memory effect, 69, 73, 104, 146
- Volume, 80, 166, 174, 232, 246-248, 275
  - volume change upon triggering, 4, 80, 232, 271, 275
  - fraction, 168, 170
  - surface area to volume ratio, 247
  - free-volume in WVP, 248

## W

- Wash fastness, 244
- Water actuation, 13-14, 141-143
- Water in supramolecular, 190-193, 206-207
- Water in shape-memory polyurethane, 30, 68, 142-143, 206-207
- Water vapour permeability, 79, 245-248
- Wavelength, 28, 131-132, 238, 262
  - for light-induced actuation, 28, 131-132
  - for patterning, 238
- Whiskers, 61

- property, 61
- as fillers in shape-memory polymer, 60, 62
- two way shape-memory effect, 14, 64
- twin-switch shape-memory effect, 267
- Wires for orthodontic application, 225
- Wrinkling, 234-237
  - principle, 234-235
  - wetting and spreading, 236
  - biological devices, 236
  - micro-system, 238
- Wetting, 234, 236, 270

## **X**

- X-ray diffraction, 43

## **Y**

- Young's modulus, 9, 29, 166-167, 182



Published by Smithers Rapra Technology Ltd, 2014

Shape-memory polymers (SMP) are a unique branch of the smart-materials family that can change shape upon exposure to an external stimulus. Discovery of SMP has been a significant breakthrough in the development of novel smart materials for various engineering applications, has superseded traditional materials, and influenced current methods of product design. This book is extremely useful for any academic, R&D manager, research scientist or engineer involved in SMP research.

The first objective of this book is to provide the latest advanced research information on SMP. This will enlighten readers to the achievements and tremendous potentials of SMP. The second objective is to provide readers with the basic fundamentals of SMP (including the mechanisms of shape-memory). This will help readers to become familiar with SMP to guide them in undertaking independent research on SMP. The third objective is to describe the challenges and application problems associated with SMP. This could help them to focus on these issues and exploit their knowledge to look for innovative solutions. The final objective of this book is to detail the future outlook of SMP research, which could further promote the applications of these novel materials.



Shawbury, Shrewsbury, Shropshire, SY4 4NR, UK  
Telephone: +44 (0)1939 250383  
Fax: +44 (0)1939 251118  
Web: [www.polymer-books.com](http://www.polymer-books.com)